CDF Study Report

XEUS

X-ray Evolving-Universe Spectroscopy

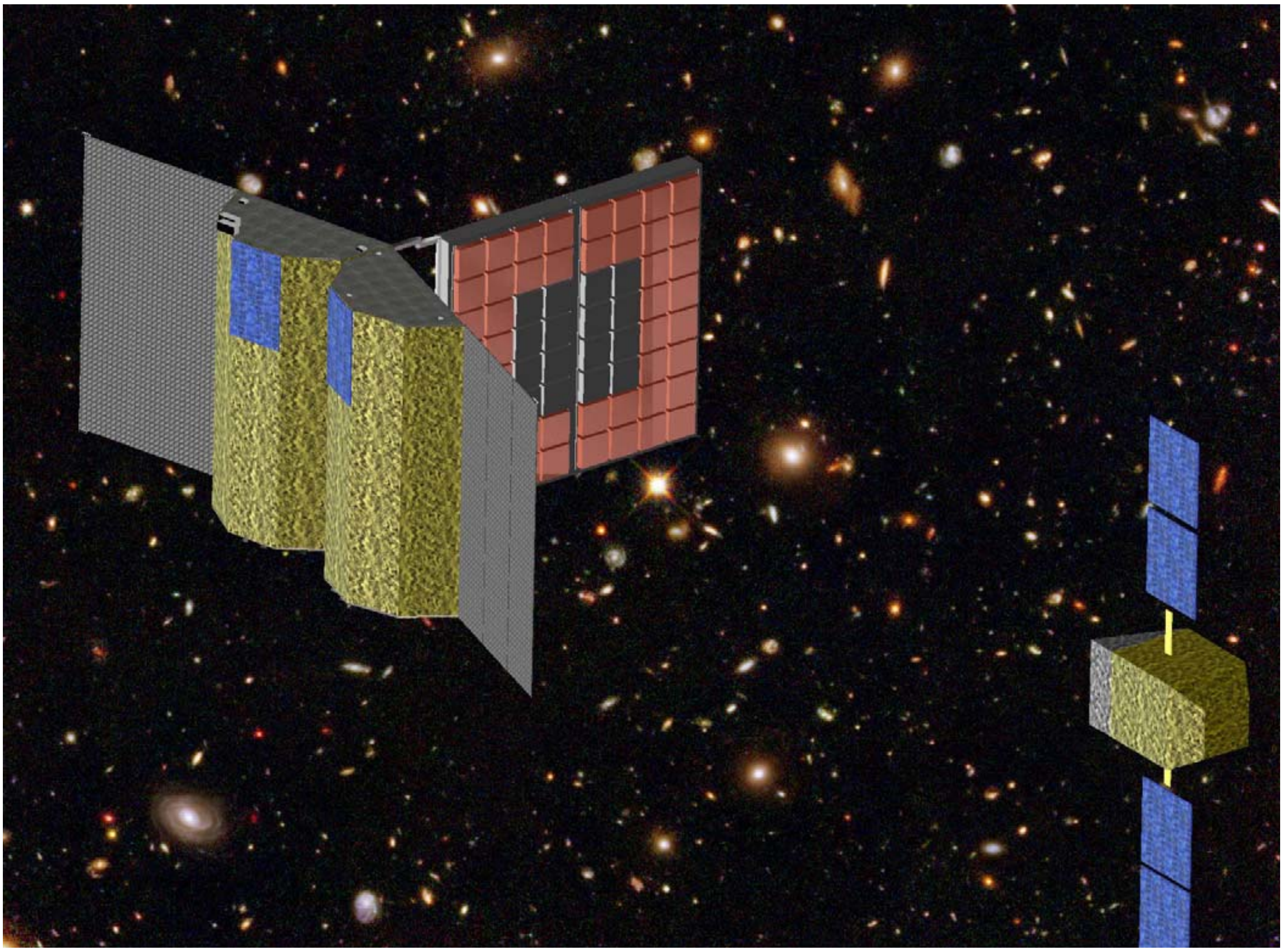

CDF-31(A)
October 2004

This page intentionally left blank

CDF STUDY REPORT

XEUS

X-RAY EVOLVING-UNIVERSE SPECTROSCOPY

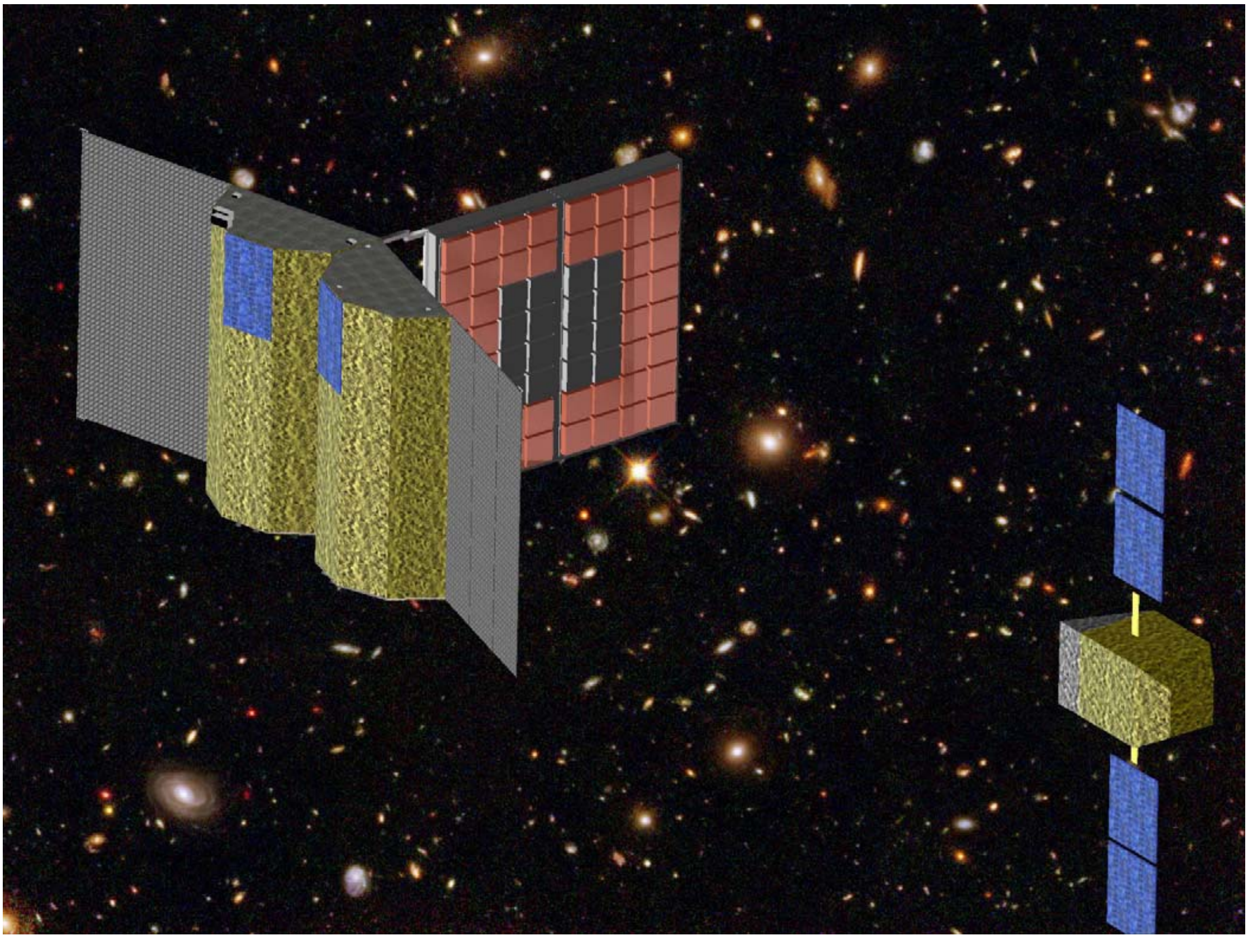

FRONT COVER

XEUS mirror spacecraft (left) flying in formation with the
detector spacecraft (right)
Image background courtesy of the Hubble Space Telescope

STUDY TEAM

This Study was performed in the ESTEC Concurrent Design Facility (CDF) by the following interdisciplinary team:

TEAM LEADER	L. Gerlach, TEC-EPG		
SYSTEMS	T. van der Laan, SCI-PTS R. Biesbroek, TEC-ACD S. Bayon, TEC-ACD	MECHANISMS	L. Gaillard, TEC-MMM
OPTICS	K. Wallace, TEC-MMO	MISSION	G. Janin, OPS-GA
AOCS	B. Udrea, TEC-ECN A. Martinez, TEC-ECM G. Ortega, TEC-ECN	POWER	S. Zimmermann, TEC-EPS
PROPULSION	N. Kutufa, TEC-MP N. Boman, TEC-MPC	PROGRAMMATICS/ AIV	J-P. Vessaz, TEC-MTC D. Hagelschuer, TEC-MTC
COMMUNICATIONS	J. Perello, TEC-ETT		
CONFIGURATION	S. Mangunsong, TEC-MCS	RISK	F. Restagno, TEC-QQD
COST	P. Ponzio, TEC-ICE	STRUCTURES	C. Bonelli, TEC-MCS
DATA HANDLING	G. Furano, TEC-EDD	THERMAL	J. Barbe, TEC-MCT
GROUND SEGMENT AND OPERATIONS	K. Nergaard, OPS-OSF		

Under the responsibility of:
M. Bavdaz, SCI-AT

with the scientific leadership of:
D. Lumb, SCI-AT

Visiting guests or consultants:
J. Grady, NASA GSFC
B. Savage, NASA GSFC
J. Bookbinder, Harvard Center for Astrophysics
K. Flanagan, MIT
W. Cash, Boulder CASA

The editing and compilation of this report has been provided by:
M. Kruk-Strzelecki, TEC-ACD
D.M. van Eck, TEC-ACD

Further information and/or additional copies of the report are available from:
M. Bavdaz
ESA/ESTEC/SCI-AT
Postbus 299
2200 AG Noordwijk
The Netherlands
Tel: +31-(0)71-5654933
Fax: +31-(0)71-5654690
Marcos.Bavdaz@esa.int

For further information on the Concurrent Design Facility please contact:
M. Bandecchi
ESA/ESTEC/TEC-ACD
Postbus 299
2200 AG Noordwijk
The Netherlands
Tel: +31-(0)71-5653701
Fax: +31-(0)71-5656024
Massimo.Bandecchi@esa.int

TABLE OF CONTENTS

1. INTRODUCTION

1.1 Background

A proposal was made by D/SCI-A to use the ESTEC Concurrent Design Facility (CDF) methodology for the conceptual design of an X-ray Evolving Universe Spectroscopy mission deployed at L2 and implemented as a formation flight (FF) of a mirror spacecraft (MSC) and detector spacecraft (DSC). This study focused on MSC design and FF aspects and package. The scientific requirements provided the main study inputs (RD[1]). The XEUS mission was originally considered as part of ESA's Horizon 2000 plus programme within the context of the International Space Station (ISS).

1.2 Scope

The objectives of the study were to perform a system conceptual design and trades, prepare a preliminary system design including budgets and subsystem designs with required performance, show science requirements compliance, define critical design issues requiring further analysis and assess and analyse programme, risk and costs. Further the constraints imposed by the chosen design were analysed and described, where appropriate. This document reports on the analysis performed and conclusions drawn for an X-ray Evolving Universe Spectroscopy conceptual design.

The CDF activities have accommodated the study of a number of different options. Initially the study was devoted to the lowest-cost feasible mission scenario, based on the launch of the MSC and DSC each on a Soyuz-Fregat. The clear disadvantage of that case is that the limited mass capability of the launcher does not allow a MSC with sufficient telescope collecting area to match the basic science requirements. Further complications arise from the required sequencing of the two launches.

Subsequently the studies concentrated on heavier launchers (Ariane-5 and Delta IV Heavy), substantially increasing the telescope's available effective area. However, launch mass constraints still require a considerable reduction in effective mirror area when considering the accommodation of possible additions to the instrumentation, such as a grating spectrometer proposed by NASA or a dedicated high-energy telescope.

1.3 Document structure

The first chapter comprises an Executive Summary describing the science requirements, instrument design and budgets, critical issues and the proposed mission and platform design and budgets. Subsequent chapters provide detailed system information with mission and platform design results for each domain addressed in the study. Latter chapters summarise outputs from the programmatics and test analysis and risk assessment tasks, the overall conclusions and the reduced science option obtained with the Soyuz-Fregat launcher.

The cost assessment and assumptions made and performed as an integral part of the concurrent engineering used for this CDF study will be published as a separate document (CDF-31(B)).

1.3.1 Miscellaneous

The *X*-ray *E*volving *U*niverse *S*pectroscopy XEUS mission represents a potential follow-on mission to the ESA XMM-Newton cornerstone observatory currently in orbit. XEUS can be considered as the next logical step forward in X-ray astrophysics after the current set of great observatories, XMM-Newton and Chandra, have completed their operational lives. The scientific objectives of XEUS are, however, so demanding that the mission will clearly represent a major technological challenge compared to past astrophysics missions. The development and ultimate success relies on the capability to achieve a key breakthrough in the size of an optic capable of entering orbit.

The primary aim of XEUS is to study the astrophysics of some of the most distant and hence youngest known discrete objects in the Universe. The specific scientific issues, which XEUS aims to address, are to:

- Measure the spectra of objects with a redshift z >4 at flux levels below 10^{-18} erg cm^{-2} s^{-1}. Note this is 1000 times fainter than XMM-Newton, the agency's most recent astrophysics mission launched into orbit.
- Determine from the X-ray spectral lines the redshift and thus age of these very faint objects that may not have easily identified optical counterparts.
- Establish the cosmological evolution of matter in the early Universe through the very clear means of the study of heavy element abundances as a function of redshift, i.e. the role of element evolution as the Universe aged through galaxy formation in the associated early stellar processes.

Based on these themes, specific requirements for instrument performance were developed. The angular density of objects at high redshift drives the necessity for angular resolution of ~2 arcsec (HEW). The potential rarity of the exceptional high-z objects further requires a maximisation of field of view coverage. The phenomenon of star-forming galaxies particularly motivates good low energy response. Conversely the measurement of low-z obscured AGN with peaked spectral distributions at 20-50 keV demand an extension to *higher* energies. Such a baseline design of the XEUS mirror system provides for a large collection area and outstanding angular resolution, so that all fields of X-ray astronomy will be advanced by observations made by this observatory.

The mission scenario envisages the deployment of a telescope with 10 m^2 area (at 1 keV) into an L2 observing orbit. This is the fundamental requirement that drives the current study activities. However there are many technical aspects of the instruments, and even the system design that must be considered to ensure all important science requirements are met:

1. Effective area
2. Energy range
3. Angular resolution
4. Field of view
5. Spectral resolution
6. Sensitivity
7. Time resolution

8. Count rate capability
9. Observing duration without interruption
10. Sky accessibility

The science community has been involved in the mission definition, for example as an Instrument Working Group in the selection of the baseline instrument package for the Detector Spacecraft, establishing the performance of selected detectors and providing resource estimates as inputs to the current activities.

1.3.1.1 Mirrors

The requirements for XEUS are not expected to be met with some simple further development of the XMM replication technology, due to the extreme requirements of XEUS. To accommodate a launchable mass, the XEUS optics require a reduction of the specific mass (normalised to the area) by a factor 10, and a reduction of the specific volume by a factor of 3 but without a loss in resolution or effective area. To achieve this, a mirror material is needed that is both thinner and less dense. The stiffness must be increased and hence a monolithic structure is implied. These simply posed modifications demand a pore structure, which then enables a significant reduction in mirror length to be achieved while using the conical approximation. Figure 1-1 shows the required structure, and Figure 1-2 shows that the conical approximation is facilitated by the choice of a 50-m focal length for XEUS.

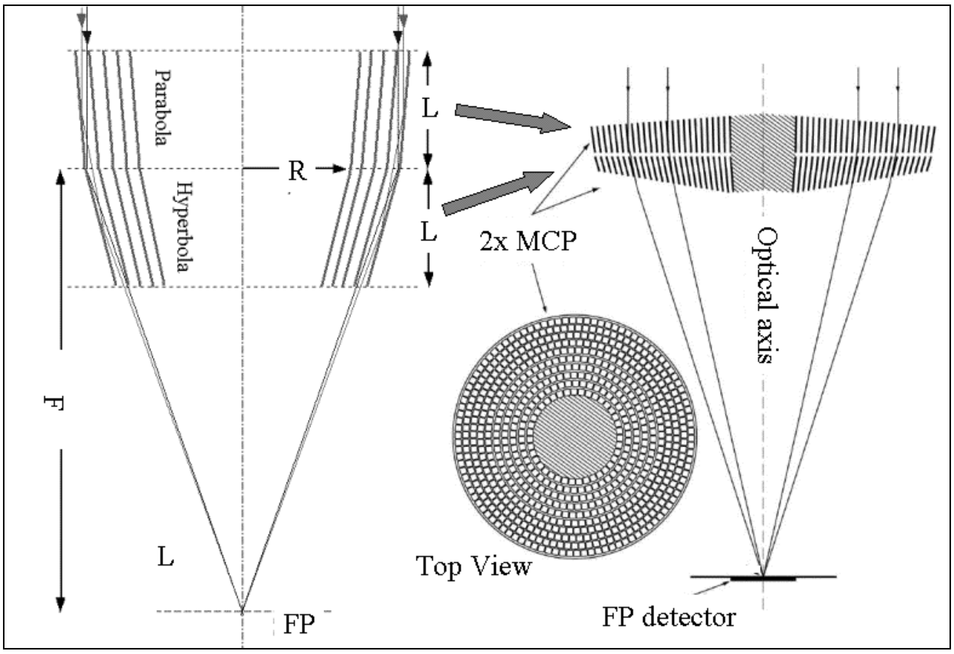

Figure 1-1: Normal Wolter and pore-structured optics

The Wolter design employs pairs of hyperbolae and parabolae to obtain a real image of the sky in the focal plane. Reduction of the length of shells and introduction of a long focal length (see below) allows two sets of pores to be placed back to back to replace the shell structures.

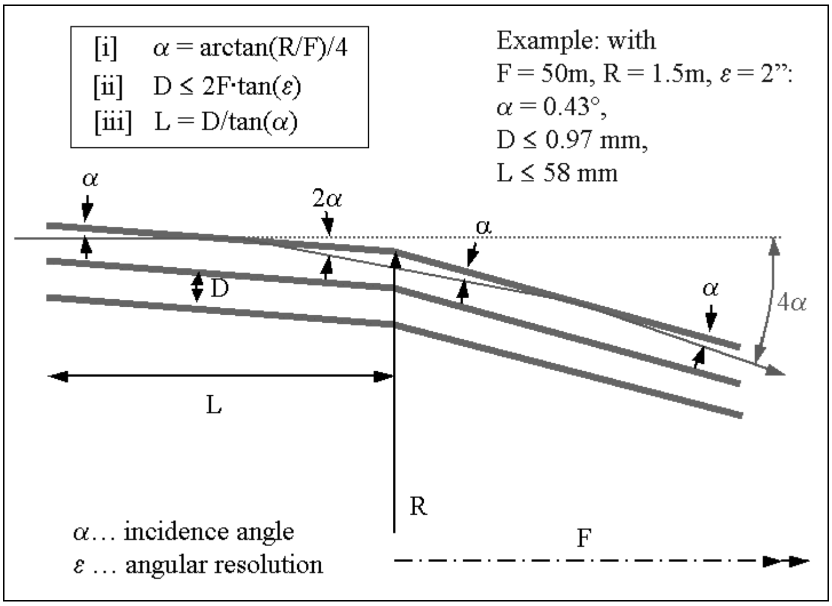

Figure 1-2: Required conditions for replacement of the parabolic and hyperbolic surfaces

The required conditions for replacement of the parabolic and hyperbolic surfaces of a Wolter-I system by simple conical surfaces are shown in Figure 1-2. The dimensions given represent an average shell of the XEUS mirror system.

Fortunately, silicon wafers can be used as the thin low-density starting material to produce mirror shells, having a density nearly four times less than nickel. Huge investments in silicon wafer technology have accrued in the electronics industry over many years, including large volume processes for surface chemo-mechanical polishing which can provide the low surface nm scale roughness required for specular X-ray reflection. Compact chip and sensor design have forced the development of attachment techniques to build up three-dimensional structures, and the commercial requirements of the microelectronics industry have forced wafer manufacturers to fabricate atomically flat (<1 micron over 30 cm) and very smooth surfaces (sub-nm), and finally silicon is a good thermal conductor. Some details of the fabrication steps are outlined briefly here.

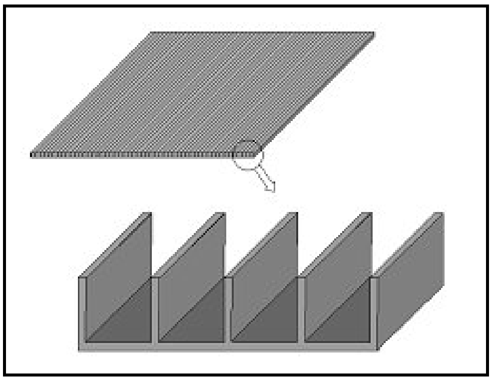

Figure 1-3: Silicon ribbed plates where the ribs and reflecting plate are only ~200 µm thick

The current generation 300 mm size of silicon wafers do not limit telescope size, since a large telescope would be assembled in modules based on very thin mirror plates (~250 microns). The modular fabrication of a pore optic is then hierarchical, and requires only very compact equipment to produce high resolution mirror units, less than one litre in volume. The build-up of such a module starting from a single silicon wafer is shown in Figure 1-3. Production begins with ribbed plates that have very high-quality surfaces on both sides.

Processed silicon wafer components are then stacked onto a precision Si mandrel, requiring only a single curvature (for the conic surface). Several plates are stacked on top of each other while being curved in the azimuthal direction to form a single monolithic unit that is intrinsically very stiff, as well as possessing a very good temperature stability without differential expansion problems (see Figure 1-4). The optics module can be completed by retaining the mandrel as support (losing area) or detaching from the mandrel (which is preferred).

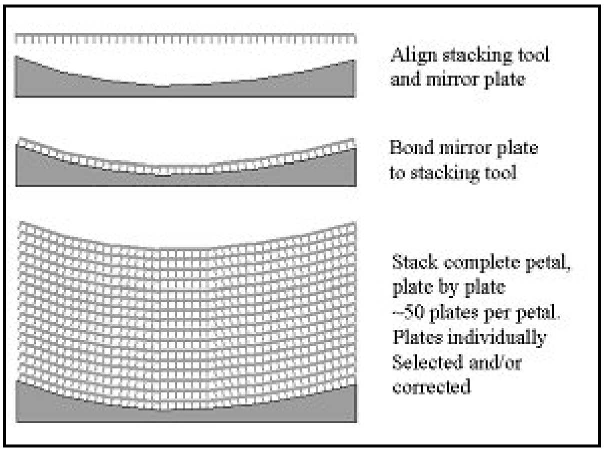

Figure 1-4: Stacking of many silicon ribbed plates onto a mandrel

A number of these "sub-petal" units are integrated, aligned and fixed to form the major component of the mirror petal. Two such modules are stacked in series (precision alignment required), forming the conical approximations of the parabola and hyperbola of a Wolter-I optics. Such twin modules (p+h) are then integrated on ground onto the petals, qualified and calibrated. Such units are small enough to allow simple handling, but large enough to simplify the SC integration and in-orbit maintenance (e.g. alignments in orbit, if necessary, are done on the petal level). See Figure 1-5.

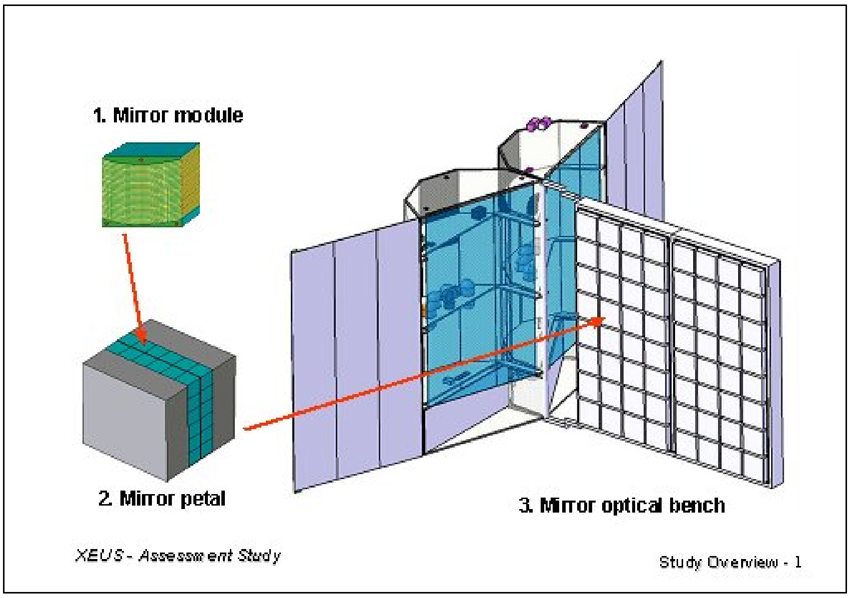

Figure 1-5: The hierarchy for fabrication of the complete mirror assembly

The hierarchy for fabrication of the complete mirror assembly, starting from a module of mirror plates, built into a petal containing many modules of mirror pairs and pre- and post-collimators. Finally several petals are combined into the optics of desired area.

The basic sub-petal elements of a XEUS optic have been fabricated. The plates were produced from the latest generation of wafers having the properties of extreme low surface roughness (measured to be <0.3 nm rms) and high flatness (~1 μm). The X-ray performance of the sub-petal prototype optics was measured using a synchrotron radiation facility.

In tests at a synchrotron facility, the wafers provided locally sub-arcsecond imaging quality while single pores were found to have an angular resolution of 3 arcseconds Half Energy Width, (HEW). Pencil-beam scanning of a 2 cm^2 area demonstrated a resolution of 6 arcseconds HEW. The quality of subsections of the sub-petal stack are significantly better than the full stack (Figure 1-6), providing confidence that controlled alignment of mirror plates will allow the 5 arcseconds HEW requirement to be met by actively aligning each element individually to its correct position. In demonstrating the basic silicon wafer technology that will eventually achieve our resolution goal, a completed stack assembly has been fabricated that matches the resolution of XMM but with vastly superior Area/Mass factor (~15).

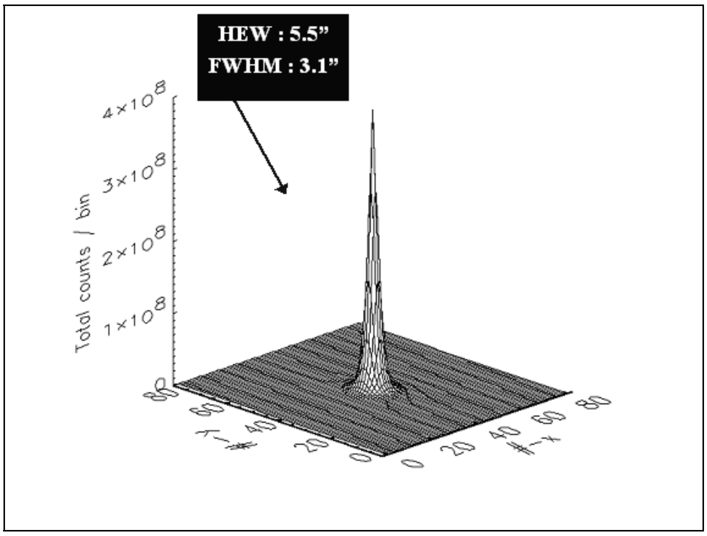

Figure 1-6: FWHM resolution of mirror optics measured over 2 cm^2 representative area

1.3.1.2 Detectors

Based on the broad technical and science requirements outlined above, a three-instrument focal plane package was originally considered:

A wide-field, broad-band imaging solid-state camera (WFI) covering the field of view and energy range, while adequately sampling the mirror PSF. This instrument combines a high imaging sensitivity with modest broadband spectral resolution. This instrument is primarily used to make extremely deep surveys (~10^{-18} erg cm^{-2} s^{-1}) thereby positioning sources and measuring their broadband medium resolution spectra, or at least give an estimate of their colour index.

There are two narrow-field high-resolution imaging spectrometers (NFI1/2) that focus on the soft and medium X-ray bands, respectively, and are used as follow-up spectrometers on specific sources. Two types of NFI detectors are considered here and are based on rather different technologies: the superconducting tunnel junction (STJ) and the transition edge sensor (TES). Given the large dynamic energy range required for the XEUS science, two NFIs are considered necessary to meet the few eV energy resolution requirement with high efficiency over the complete energy band. NFI1, based on STJ technology, will be optimised below 2 keV. The NFI2, based on TES technology, will be optimised above 1 keV, so that significant overlap in the intermediate energy range will occur.

The overall characteristics of these instruments are summarised in Table 1-1:

Parameter	WFI	NFI1	NFI2
Detector Type	Active Pixel DEPFET	STJ	TES
Field Coverage	5 arcminutes	30 arcseconds	32 arcseconds
Number of pixels	1000x1000	48x48	32x32
Pixel size	0.3 arcseconds	0.6 arcseconds	1 arcseconds
Energy resolution	125eV at 6 keV	<2 eV at 1 keV	5eV at 8keV
Detection efficiency	100% at 1 – 6 keV	90% at 1keV	90% at 6keV
Time resolution	< 5 ms	<5μs	< 1 ms
Count rate limit	200-1000 Hz / psf	25000 Hz / psf	250 Hz / psf
Operating temperature	180 K	300 mK	35 mK

Table 1-1: Major characteristics of baseline instruments for XEUS

The basic strategy to ensure the study of the XEUS core science is that the narrow field instruments are used to obtain follow-up high-resolution spectra of objects detected by the wide field instrument. The energy resolutions for the narrow field instruments is a few eV while the field of view is restricted to ~30 arc seconds. The WFI instrument should, from its broadband spectra or colour indices, allow XEUS to identify those candidates that may be at high red shift.

1.3.1.2.1 WFI

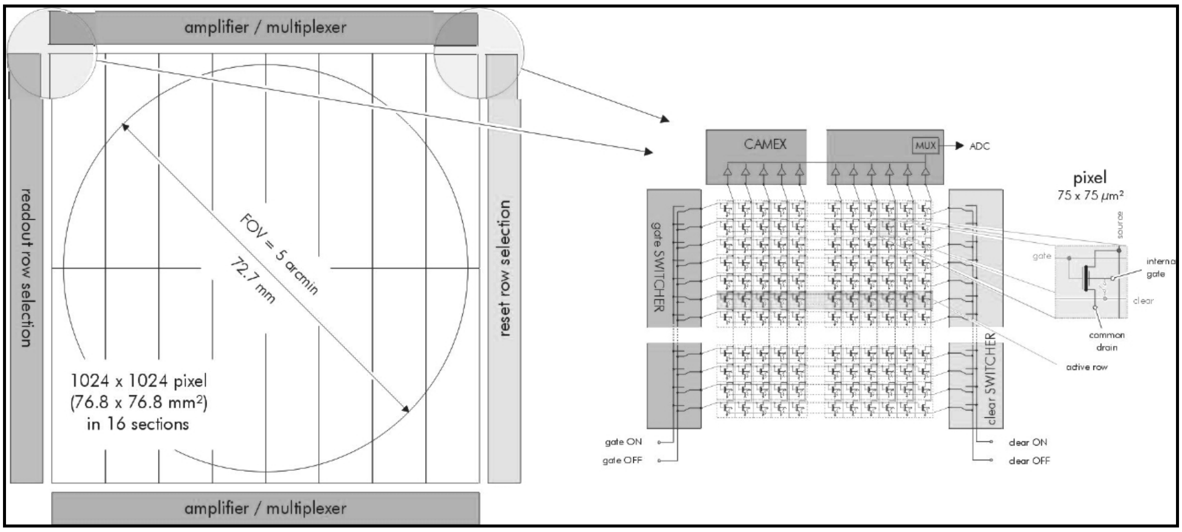

Figure 1-7: WFI layout

Figure 1-7 shows the WFI layout, with the coverage of focal plane with multiple sections on the left and an expanded view of individual pixel readout cells on the right

As the collecting area of XEUS is a factor of 100 larger than XMM-Newton it is clear that, rather than improving the existing CCD schemes, a new device concept is needed. The p-channel Depleted Field Effect Transistor (DEPFET) type of Active Pixel Sensor allows measurement of position, arrival time and energy with sufficiently high detection efficiency in the range from 0.1

to 30 keV. Every pixel has its own amplifier and can be addressed individually by external means. This results in a high degree of operational freedom and performance advantages:

Operation with high spectroscopic resolution at temperatures as high as -50°C, keeping the total readout noise below 5 electrons (rms). The charge does not need to be transferred parallel to the wafer surface over long distances. That makes the devices very radiation hard, because trapping, the major reason for degrading the charge transfer efficiency, is avoided. The ratio between photon integration time and read out time can be made as large as 1000:1 for a full frame mode, that means that the so called out-of-time events are suppressed. As the integration time per event will be in the order of 1 ms and the read out time per line about 1 µs, more than 1000 counts per second per HEW (2~arcsec, i.e. 7x7 pixels) can be detected with a pile-up below 6%.

Any kind of windowing and sparse readout can be applied easily, different operation modes can be realised simultaneously. The device properties are summarised in Table 1-2:

Parameter	Value
Integration + Readout read time per row (128 channels)	2.5 µs
Total read time	1.25 ms
Integration : read time	800:1
Window Mode	160 µs for 128 x 128 pixels
Response to Radiation	
QE at 110 eV	85%
QE at 2 keV	100%
QE at 8.05 keV	100%
QE at 10 keV	96%
QE at 20 keV	45%
Depletion depth	500 µm
Rejection efficiency of MIPs	~100%
Spectroscopy	
System noise	3 - 5 e^- (rms)
^{55}Fe resolution	125 eV
C Kα resolution	50 eV
Radiation Hardness (at 260 K)	No change up to10^{10} p per cm^2
Focal Plane Geometries	
Device size	75 x 75 mm
Device format	1000x1000
Pixel size	75x75 μm^2
Position resolution	30 µm
Operating temperature	220K

Table 1-2: Summary characteristics of WFI instrument for XEUS

1.3.1.2.2 NFI 1

The Narrow Field Imager 1 is optimised for the 0.07-3 keV energy band (>70% efficiency). This soft X-ray range is especially suited to the study of objects at high redshift, since below 2 keV the mirror effective area is very large. NFI1 is based on the superconducting tunnel junction, which is available in small array formats, but considerable development is required to meet the demanding requirements of XEUS. The NFI1 will only cover a small part of the field of view (0.5 arcminutes i.e. ~7~ mm in extent).

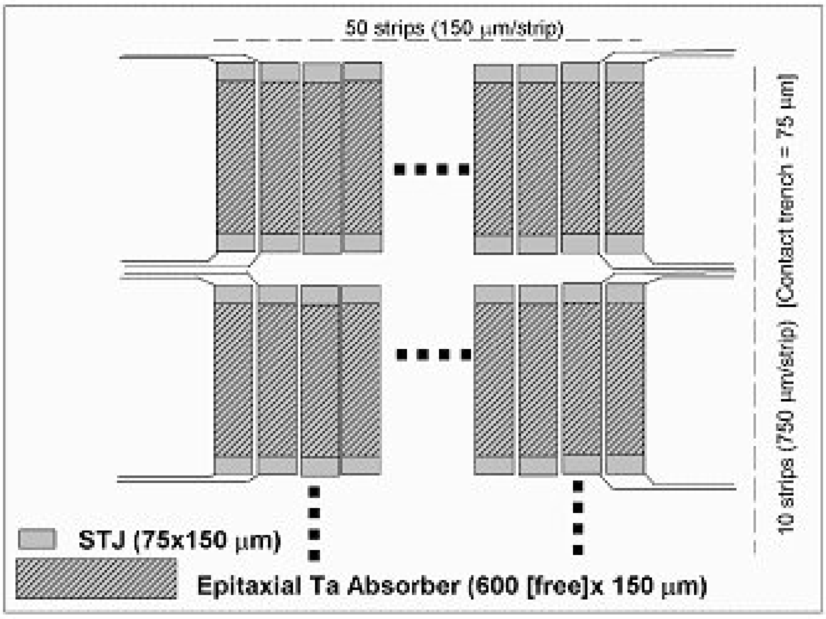

Figure 1-8: Organisation of 1-D strip DROIDs for the XEUS NFI1

Characteristic	Requirement (Goal)
Field of view	30x30 arcseconds (1arcminute x 1 arcminute)
Pixel size/resolution	0.6 arcminute (150 μm)
Number of pixels and format	50x10 (DROID)
Operating temperature (mK)	350 (Hf/Mo > 30 mK)
Low temperature stage	He3 Sorption pump (Hf/Mo ADR)
High-low temperature stage (2K)	Mechanical cooler
Energy range: (10% efficiency) (80% efficiency)	 50 - 7000 eV 100 - 2300 eV
Energy resolution	<2eV at 500 eV (goal 1 eV)
Time resolution	5 μs

Table 1-3: Summary characteristics of NFI1 instrument for XEUS

For XEUS, a possible configuration is the distributed readout imaging devices (DROIDs) in which photons are absorbed in an epitaxial superconducting film, or *absorber*, such as tantalum of large dimension, and the resultant charge detected by STJs that are located at the corners of either a 2-D absorber or at the ends of a 1-D strip of absorber. The 1-D DROID, while not providing the largest possible reduction in read-out connections, might be able to maintain the required energy simultaneously with the spatial resolution and while handling reasonably high count rates, (see Figure 1-8). The device properties are summarised in Table 3-3. Good spectroscopic performance has been demonstrated with a small 1-D prototype DROID (10x200 μm, including two 20x20 μm readout STJ at the end). See Figure 1-9, for which resolution ~2.4 eV FWHM at 500 eV, was achieved. A tantalum 1-D DROID would operate at a temperature of ~350 mK, to be provided by a sorption cooler pre-cooled by a Joule-Thomson/Stirling cooler combination.

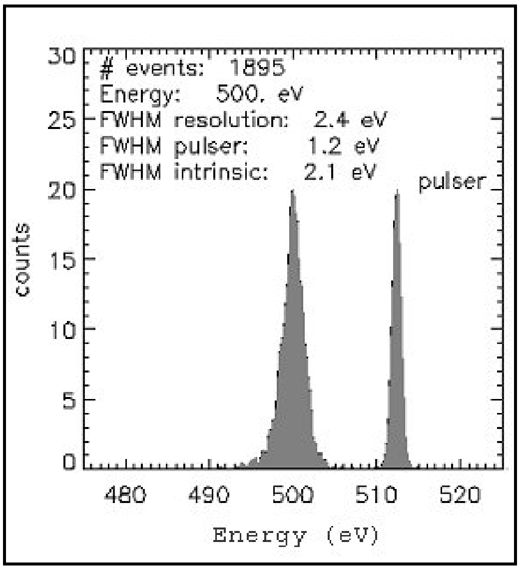

Figure 1-9: Demonstrated energy resolution of 1-D strip DROIDs for the XEUS NFI1

1.3.1.2.3 NFI2

The second Narrow Field Imager, NFI2, is optimised for the 0.5-7 keV energy band. Up to intermediate red shifts (z <3) this energy range contains the majority of diagnostic X-ray lines, which can be observed largely unabsorbed by the interstellar medium of our own galaxy. At larger red shifts most of the lines move to energies below 1~keV, which makes NFI1 more suited for the deepest observations. Within the above energy range, micro-calorimeters equipped with a normal to super-conducting phase-transition thermometer, usually called transition edge sensors (TES), have recently shown excellent performance. Currently results on single pixel devices have mostly been obtained, but multiplex readouts are available. Although some initial designs for imaging arrays have been published, very considerable developments, both with regard to the sensor itself as well as with regard to the read-out electronics, are required to create the 32 x 32 pixel imager required for XEUS.

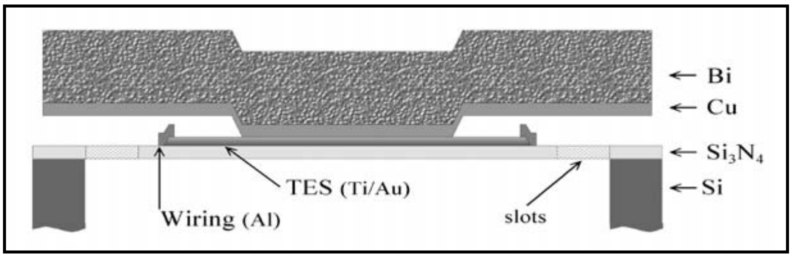

Figure 1-10: Single TES calorimeter, with a 100 µm square Bi/Cu mushroom absorber and Ti/Au TES sensor

Figure 1-10 shows a pulse height spectrum measured at SRON for 5.9 and 6.4 keV X-rays with a microcalorimeter consisting of a 310 x 310 µm^2 Ti/Au thermometer. Small arrays with energy resolution ~2.5eV FWHM have since been demonstrated. The device properties are summarised in Table 1-4.

The operating temperature of the NFI2 would be ~30mK, requiring a cryostat technology based around an ADR (Adiabatic Demagnetisation Refrigerator), which are being developed and space-qualified for other ESA missions (for example, Herschel/Planck).

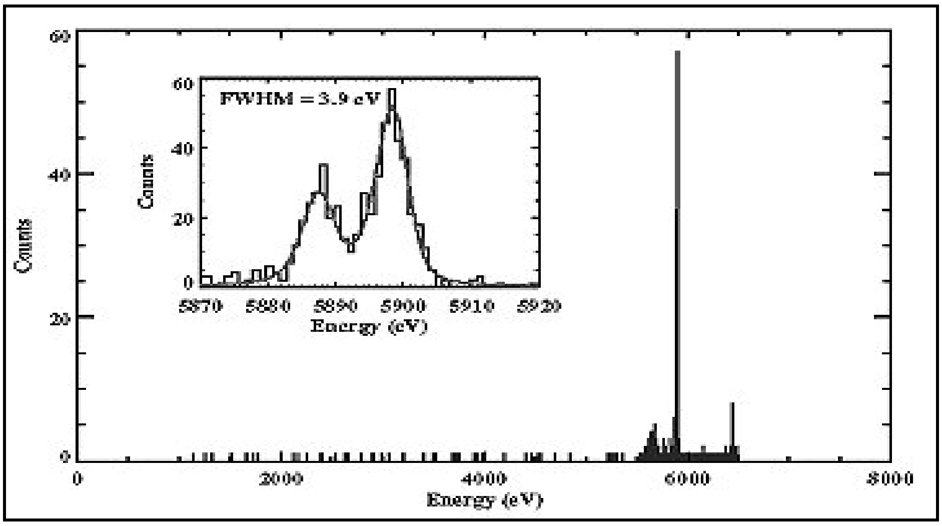

Figure 1-11: Energy response of a prototype TES calorimeter for NFI2

Spatial resolution element - pixel size	1 arcsec - 240 µm
Field of view - array size	0.5 arcmin - 32 × 32 resolution elements
Energy range - Detection efficiency	0.5 - 15 keV - >90% for 1-7 keV
FWHM energy resolution	2 eV at 1 keV and 5 eV at 7 keV
Countrate - Effective time constant	> 250 c/s/pixel - 100 µs
Background rejection	> 95% (minimum ionising) particles

Table 1-4: Summary characteristics of NFI2 instrument for XEUS

1.4 Ancillary instruments

The instrument complement that has been considered to address important ancillary science goals include:

A fast timing instrument based on a silicon drift detector to provide spectrally resolved counting information for point sources, at Megacount/sec rates. This instrument will enable tests of general relativity in the strong field regime through observations of the brightest X-ray sources in the sky (e.g. X-ray transients and bursts).

A hard X-ray detector co-axially aligned with the on-axis imaging instrument. This should offer a modest spectral resolution over the core of the field of view to support the identification and analysis of extremely obscured or hard spectral objects, identify the sources contributing to the peak of the cosmic diffuse background spectral power, and measure spectral features such as cyclotron lines. It would be implemented as compound semiconductor detector pixel-array located behind the Wide Field Imager.

An enhanced wide-field instrument, that increases the field of view of the baseline imager to maximise the survey potential for locating the most extreme objects in the high red-shift Universe. An increase of a factor of two in sources detectable at high redshift is anticipated using an array of more conventional CCDs located around the on-axis imager.

A polarisation-sensitive detector is considered, comprising a micro-well gas electron multiplier that senses the photoelectric polarisation effect. Polarisation measurements represent the last of the traditional astronomical tools, which heretofore has not been significantly employed in X-ray astronomy.

1.5 Conclusions

Option 1	**Ariane-5 single launch of MSC +DSC**
	Mirror area at 1keV ~ 7 sq m, but soft response as inner petals are missing
	DSC contains baseline of WFI, NFI1 and NFI2
Option 2	**Ariane-5 launch of MSC and Soyuz launch of DSC**
	Mirror area at 1 keV ~ 11 sq m, but the high energy response as in baseline
	DSC can probably include also the Hard X-ray camera, High Time Resolution Spectrometer etc.
Option 3	**Delta IV Heavy (a)**
	Mirror area 11 sq m, but the high energy response as baseline
	DSC can probably include also the Hard X-ray camera, High Time Resolution Spectrometer etc.
Option 4	**Delta IV Heavy (b)**
	Mirror area ~9 sq m at 1 keV, and grating provides 0.2 sq m TBC at

	500 eV (mirror response as hard as baseline)
	DSC contains baseline of WFI, NFI1 and NFI2 + grating readout
Option 5	**Delta IV Heavy (c)**
	Grating on DSC - Area ~0.3 sq m at ~500eVin combination with. Mirror area for NFI2 ~ 6 m^2 Mirror area 11 sq m at 1 keV for WFI and NFI1
	DSC contains baseline of WFI, NFI1 and NFI2 + grating readout

Table 1-5: Trade-offs for launch options

2. EXECUTIVE SUMMARY

2.1 Study flow

A feasibility study for the XEUS mission using the ESA Concurrent Design Facility was requested by ESA/ESTEC/SCI-A in early 2004. The study began with a kick-off on 26th May 2004 and finished with an Internal Final Presentation on 18th June 2004. It consisted of eight technical half-day sessions of the interdisciplinary study team. For this initial study, Soyuz-Fregat launches from Kourou were requested (MSC and DSC launched separately into L2) and optimistic mirror mass assumptions were provided. The CDF team presented a viable solution for this scenario of which a summary is given in Appendix A, Reduced Science Option (XEUS 1). After review of the design and its scientific return, it was concluded that the effective collecting mirror area does not fulfill the scientific challenges and it was decided to perform a second study concentrating on an accommodation on a larger launcher, with the Ariane-5 as baseline and some consideration given to a Delta IV Heavy, and focusing on some key technical areas, including the thermal design of the MSC. This second part of the XEUS feasibility study started with a kick-off on 5th October 2004 and finished with an Internal Final Presentation on 28th October 2004. It consisted of eight technical half-day sessions. A team of NASA (GSFC), MIT, Harvard Center for Astrophysics and Boulder CASA participated part time in the study as observers and payload experts.

The objectives of XEUS part 2 were to:

- Perform a feasibility study for the XEUS mission by using a 'Design-to-Mass/Volume' approach compatible with a single Ariane-5 (baseline) launch and Delta IV H as option:
- DSC to be considered as "black box" based on JAXA configuration input (1753 kg with baseline instrument package)
- Consider direct injection into L2 orbit
- Demonstrate technical feasibility including:
    - Mission architecture (DSC and MSC)
    - System and subsystem conceptual design for the MSC
    - Mirror petal accommodation
    - Optimal MSC spacecraft configuration (including thermal design)
    - Formation flying package (accommodation on DSC and MSC)
    - Technical risk assessment
    - Programmatics
    - Costing
- Propose a formation flying approach for the DSC and MSC and present a baseline design
- Propose a MSC configuration and mass budget for a 50-m grating option
- Propose a conceptual design for the 10-m grating option on the DSC
- Propose a configuration for the high-energy telescope

The mission objectives for the XEUS (X-ray Evolving-Universe Spectroscopy) mission encompass the long-term data collection of consistent quality and in particular to the:

- Detection of massive black holes in earliest active galaxy nuclei

- Study of the formation of first gravitationally bound
- Study of evolution of metal synthesis
- Characterisation of intergalactic medium

The proposed payload consists of three X-ray primary imaging spectrometers on DSC (for details see XEUS Payload Definition Document):

- WFI (Wide Field Imager)
- NFI2 (Narrow Field Imager 2)
- NFI1 (Narrow Field Imager 1) for low energy range (0.1 – 2 keV) with an energy resolution of E/dE of ~ 500
- Payload options (see Figure 2-1 and Figure 2-2) are a dispersive spectrometer (grating) allowing for higher resolutions E/dE of 1000 - 5000 range with two configurations identified

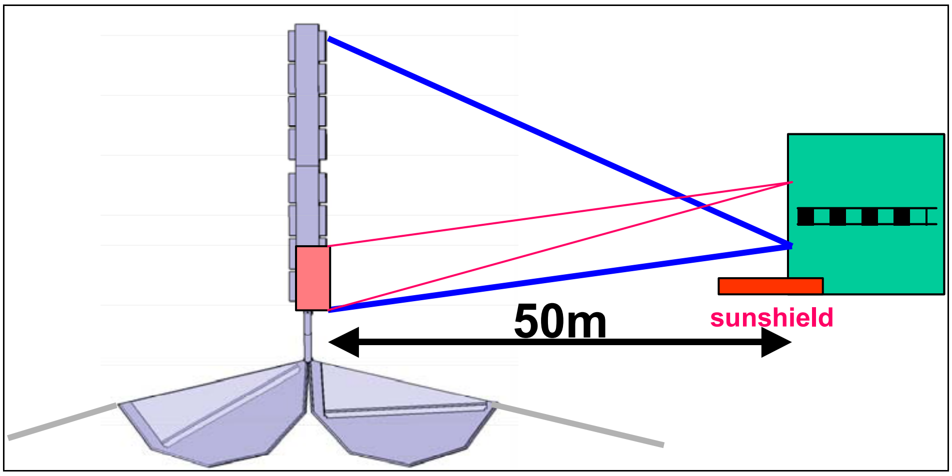

Figure 2-1: Configuration concept for grating option 1 (MSC left, DSC right)

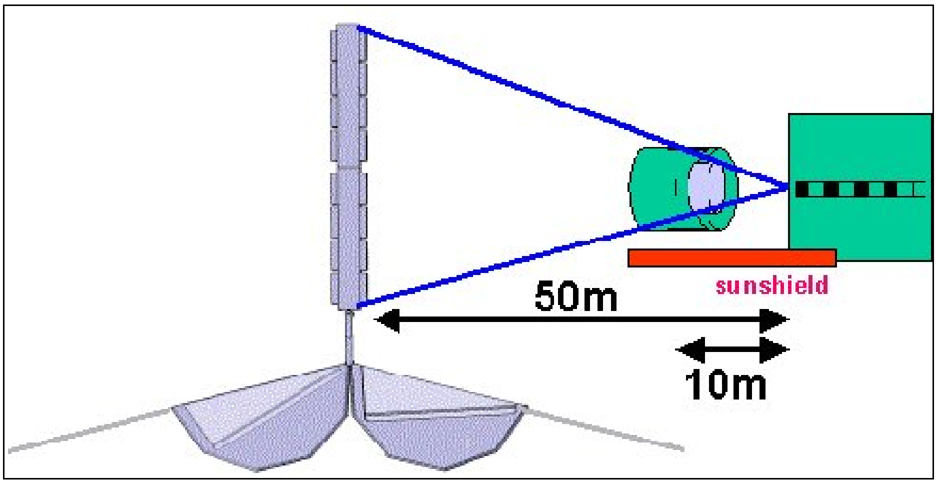

Figure 2-2: Configuration concept for grating option 2 (MSC left, DSC right)

2.2 Requirements and design drivers

The system requirements for the XEUS mission are listed below (see also Figure 4-1):

- The system comprises two spacecraft flying in formation:
  - Mirror spacecraft–MSC (Provided by ESA)
  - Detector spacecraft – DSC (Concept presented by JAXA)
  - MSC-DSC separation distance 50 metres
  - MSC life time: 15 years + 5 years extension
  - DSC life time about 5 years (replaceable at EOL and/or if more sophisticated detectors become available)
  - XEUS telescope requirement:
    - Pointing direction = centre of detector to centre of optics
    - Mainly affected by DSC to MSC position error: +/-1 mm max (allowed formation flying error sideways to optical axis)
    - Focal depth is +/-5 mm (allowed formation flying error along optical axis)
    - The difference between the inertial attitudes of the DSC and the MSC shall be less than 1 arcsecond per axis
- Launch:
  - Launch date: 2015
  - MSC and DSC to be launched as a stack
  - Using Ariane-5 launcher. Alternatively Delta IV-H
- Operational Orbit: L2
- Typical observation time: $3x10^5$ s (about 3.5 days)

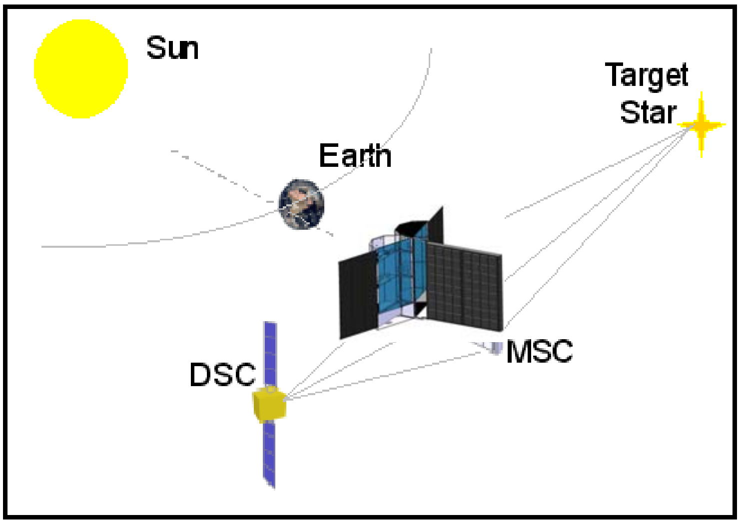

Figure 2-3: XEUS spacecraft elements configuration in target orbit at L2

The CDF study showed that the following issues drive the design of the mission:

- Formation Flying and Rendezvous:
  - Major issue for DSC AOCS: required relative range error during nominal formation keeping imposes autonomous control system
  - Ranging accuracy from ground segment → operations and rendezvous strategies

- MSC lifetime:
  - Imposes very low consumables, simple and reliable design for the SVM of MSC
- Launch vehicle, cruise phase and injection strategy:
  - Drives the maximum launch mass (available mirror surface), cost, programmatic
  - Composite launch has direct impact on cruise phase (BBQ mode, MSC design)
- Petal mass:
  - Petal mass is strongly dependant on:
    - Petal location
    - Petal size
    - Number of petals
    - Concept how mirror is populated with petals
  - Total mirror performance (science output) depends strongly on above boundary conditions. Large contribution to overall MSC wet mass.
- Petal interface:
  - Requires a large number of actuators on MSC and optical detection system to compensate for initial mirror misalignment
  - Petals locking during launch
- Temperature gradients in mirror plane:
  - Direct impact on MSC configuration. Hot Sun shield flaps and cold spacecraft closure panels to be implemented
- Temperature gradients within mirror petals in optical axis:
  - Off-normal Sun angle to be limited to about 5°
- Mirror contamination prevention:
  - Specific strategies to avoid contamination. Stay in launch configuration (BBQ mode) until outgassing procedure is executed and completed
  - Configuration: protect mirror during outgassing, protect from exhaust-plume impingement on mirror surface
  - Propulsion: choice of non-contaminating propellant. Hydrazine used during cruise and could be burnt off if necessary. Cold gas used for AOCS manoeuvres.

2.3 Mission and MSC design

Table 2-1 shows a summary of the XEUS mission and MSC main characteristics. The MSC baseline configuration and major hardware definitions are shown in Figure 2-4.

Scientific objectives	• Detection of massive black holes in earliest active galaxy nuclei • Study of the formation of first gravitationally bound • Study of evolution of metal synthesis • Characterisation of intergalactic medium
Payload	• MSC: o Two deployable mirror leaves with in total 8 x 8 segments of which 48 are populated with mirror petals. The 16 centre segments are equipped with light tight covers due to mass constraints o Petal dimension: length 70 cm, width 70 cm, height 80 cm o Average petal mass: 61 kg/m2

<table>
<tr><td></td><td>DSC:
WFI (Wide Field Imager)
NFI2 (Narrow Field Imager 2)
NFI1 (Narrow Field Imager 1) for low energy range (0.1 – 2 keV) with an energy resolution of E/dE of ~ 500
Payload options are a dispersive spectrometer (grating) allowing for higher resolutions E/dE of 1000 - 5000 range with two configurations identified</td></tr>
<tr><td>Launcher</td><td>Ariane-5 launch from Kourou carrying both MSC and DSC (launcher performance for direct injection into L2 is 6800 kg).</td></tr>
<tr><td>Spacecraft</td><td>MSC nominal mission = 15 yrs, extended mission up to 20 yrs (Note: DSC is expected to be designed for 5 years and planned to be replaced when required)
Dry mass = 4586 kg. Propellant mass 294 kg.
Main S/C bus: octagonal cylinder 4100 mm x 6910 mm (stowed configuration).
Three-axis stabilised (cold gas system to prevent mirror contamination)
Reaction wheels for re-pointing to acquire new target
No formation keeping (only orbit correction & maintenance)
Payload: matrix of petals that constitute the mirror (» 1434 kg for Ariane-5, » 2610 kg for Delta IV)
Absolute point error 60 arcsec (X & Y-axes), 3600 arcsec on Z-axis
Absolute measurement error 1 arcsec (X & Y-axes), 300 arcsec on Z-axis
Two body-mounted solar arrays of 9.5 m^2 using triple junction cells with 28% BOL efficiency
Two switchable X-band LGAs, omni coverage
S-band inter S/C RF link
17 different types of mechanism
Greater than 72 hrs full autonomy</td></tr>
<tr><td>Cruise Phase and XEUS deployment</td><td>Duration: 90 to 160 days
Direct injection:
Launcher's dispersion correction required, $\Delta V < 25$ m/s, to be performed with AOCS not later than 2 days after injection
Trimming manoeuvre: < 2 m/s at day 10
Mid-course manoeuvre: < 1 m/s at day 50
MSC - DSC separation after day 50
No ΔV required for L2 halo orbit insertion
The proposed XEUS deployment scenario is as follows:
During the initial part of the cruise phase MSC and DSC remain in launch configuration and are spin stabilised (hydrazine thrusters)
During the attached mode the stack is controlled by the MSC (i.e trajectory corrections and AOCS) and DSC is passenger
MSC and DSC commissioning commences after stack separation and could be completed prior to target orbit (L2) being reached</td></tr>
<tr><td>Nominal</td><td>Duration: 15 + 5 years</td></tr>
</table>

Mission Phase	• Final orbit: L2 halo orbit:
	  o Quasi-periodic: Every 20 days, small orbit maintenance manoeuvres needed (~ 5 cm/s)
	  o Orbit maintenance budget: 1-2 m/s per year
	  o No eclipses
	  o Amplitude: > 670 000 km
	  o Orbit period: 6 months
	  o No insertion ΔV when using optimal transfer trajectory
	• Typical observation time: 3×10^5 s (about 3.5 days)

Formation Flying Package	• Formation set-up and precision formation flying control performed by the DSC (MSC is free-flyer, DSC is follower). The same applies when slewing to a new target:
	  o Both S/C move in purely inertial space
	  o Both S/C perform absolute pointing control
	  o Only the DSC performs relative distance control
	• DSC – MSC distance during science operations shall be 50 m:
	  o Allowed formation flying error along optical axis: +/- 5 mm
	  o Allowed formation flying error sideways to optical axis: +/- 1 mm
	• Metrology approach:
	  o Inter S/C distance <30 000 km: RF metrology (S-band)
	    - Precision at 120 m: elevation: ±12 cm, azimuth: ± 6 cm, Range: ± 0.52 cm
	    - Six LGA antennas on MSC, six on DSC
	  o Inter S/C distance <120 m: Optical metrology:
	    - Four corner cube reflectors on MSC mirror
	    - Laser rangefinder with absolute distance meter (submillimetric accuracy) on DSC
	    - Dual λ interferometer (±3.5 μm range resolution)
	    - 12 optical heads, max. ~2.5 m baseline:
	      • Pulses sequenced to each head
	      • Multilateration
	• During cruise after S/C separation loose formation (RF metrology)
	• Inter S/C link (S-band) allows data transfer (housekeeping) in case one of the two spacecraft has lost communication with ground segment

Operations	• Only MSC housekeeping (per day: 0.3 hrs at 95 kbps) • LEOP performed by ESA LEOP network stations Kourou, Vilspa & Perth/New Norcia • Routine operations using the Perth 35-m ground station linked to XEUS mission control centre
Program-matics	• Model philosophy: STM, ATB & PFM • System Simulation Facility • Formation flying test bed

Table 2-1: Summary of XEUS mission and MSC characteristics

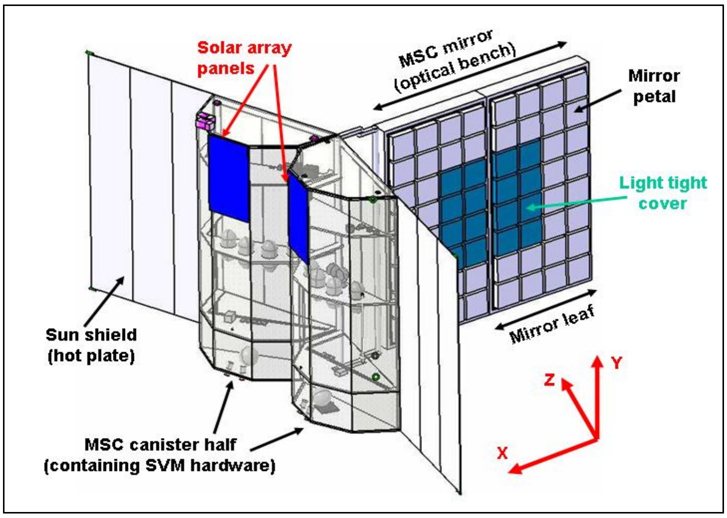

Figure 2-4: MSC configuration and definitions

2.4 Technical conclusions and options

2.4.1 Technical conclusions

The technical conclusions from the XEUS feasibility study are summarised in this chapter. They have been organised in three categories.

2.4.1.1 General

- Based on the actual boundary conditions (i.e. relatively early stage of technology developments and formation flying etc.) the XEUS mission is judged to be feasible from technical, programmatic and cost point of view
- No obvious "showstoppers" have been identified

2.4.1.2 Design-related

The biggest challenge during the study was the optimisation of the thermal design for the MSC. Detailed trades revealed the following solution:

- Passive mirror temperature control (due to large mirror area & its open structure)
    - Temperature variation across mirror is 42.8°
    - Worst case between petals 7.1°
    - Petal temperature variation along optical axis (worst case):
        - At 0° Sun angle: negligible
        - At 5° Sun angle: about 3°
        - At 10° Sun angle: 5 - 7°
        - At 15° Sun angle: 8 - 11°
    - Actual lowest absolute temperature –161°C

2.4.1.3 Critical areas

The following key critical areas require more detailed assessment:

- Mirror temperature level and distribution:

  - o Although an acceptable mirror gradient could be achieved it is recognised that the gradients are critical and a detailed thermal model of the mirror petals is required and additional thermal design at system level is essential.
- Stray light analysis:
  - o Stray light is recognised to be critical. No detailed analysis has been done during this study.
  - o Acceptable solutions exist but it is essential that a detailed stray light analysis is performed to confirm impacts
- Mirror design:
  - o As the largest single payload mass component, suitable investments into the mirror technology are essential to keep the mass under control
  - o The proposed baseline considers that each mirror petal is equipped with three actuators to allow for a potentially required mirror alignment
  - o The optical bench design and its behaviour during launch and in the space environment (such as moisture loss) might allow the omission of the petal actuation systems
  - o Detailed design of the actuator concept and mirror petal locking during launch has to be performed

2.4.1.4 Recommendation for the next steps

- NASA study/design of DSC considering MSC design and formation flying package as studied by XEUS CDF study team:
  - o Consideration of Baseline Mission Architecture
  - o Updates of the 10 m and 50-m grating option considering actual MSC design
  - o ESA appreciates further joint activity via participation in NASA's Con-X IMDC design study (observer / consulting)
- Requirement of 10 m^2 total effective mirror area is a severe system driver (even to level of launcher selection). This is aggravated by the RGA and HXT mass/area requirements. Need to confirm science requirements and invest in mirror technology
- Further design consolidation is suggested once payload requirements have been decided

2.4.2 Launcher options

The science requirements and resulting mirror design is a strong design driver for the XEUS mission, having direct influence on the launch mass and consequently on the launcher selection. The options presented below will help assess the consequences of alternative payload requirements:

Ariane-5 compatible solutions (6800 kg, direct injection into L2 - based on JWST project data):

- Single launch (MSC + DSC), baseline architecture:
  - o MSC with 64 (8x8) element mirror frame in with only outer ring populated with mirror petals (in total 48 petals of each 70 cm x 70 cm, total mirror area 23.5 m^2 effective mirror area area about 7- 8 m^2 at 1 keV) and DSC of 1753 kg (including 20% system margin).
  - o Acceptable solutions exist but these options require further studies, as described above.
- Dual launch (MSC with Ariane-5 and DSC with Soyuz-Fregat from Kourou):

- MSC with 64 (8x8) petals of 75 cm x 75 cm (effective mirror area about 11 to 12 m^2)
- Dual launch is required, with associated cost and logistic/operational impacts
- Allows wide range of flexibility in DSC design:
  - Direct injection (max. 2050 kg) impractical (launch window 1 day per 6 month)
  - Trajectory via L1 to L2 (max. 2050 kg), cruise time ca. 6 months:
    - Compatible with DSC baseline design and reduced configuration from JAXA
  - Via two intermediate HEO to L2 (2200 kg S/C payload mass, including propellant for AOCS):
    - Compatible with all DSC design options (incl. extended IWG Report configuration)
    - Compatible with DSC baseline design plus 10-m grating option

Delta IV H-compatible solutions (9300 kg, direct injection into L2, based on Boeing handbook):

- MSC with 64 (8x8) petals of 75 cm x 75 cm (effective mirror area about 11 - 12 m^2 TBC)
  - Compatible with all DSC design options (incl. IWG Report configuration)
  - Compatible with DSC Baseline design plus 10-m grating option
- Compatible with MSC 64 petal + DSC baseline design (JAXA) plus 50 m US grating option if grating instrument contribution is less than 550 kg (MSC and DSC contributions)

2.4.3 Payload options

Delta IV H-compatible solutions (9300 kg, direct injection into L2, based on Boeing handbook)

2.4.3.1 Grating option 1 (50-m configuration)

- Eight mirror petals are replaced by special grating petals
- The grating instruments drive the formation flying
- For a single launch Delta IV H is required:
  - With fully equipped 64 (75 cm x 75 cm) petal mirror 550 kg can be allocated to the grating option (delta for petal mass on MSC and grating detector on DSC)
  - Any additional mass to be recovered by removal of additional petals
  - Note core payload not served by grating petals (0.17 m^2 / petal)

2.4.3.2 Grating option 2 (10-m configuration)

- At a distance of 10 m from the focal plane of the DSC a grating system is mounted on a deployable hexapod construction
- A thermal shield is protecting the grating configuration from direct Sun illumination
- A focal plane area of 2 m x 2 m (initial JAXA configuration) is not sufficient to carry all required detector units, but can be enlarged
- Conflicting baffle accommodation (each instrument + metrology) on DSC needs investigating

2.4.3.3 High-Energy Telescope (HET) option

- Due to mass constraints the HET options is only attractive for a Delta IV launch option

- Depending on the number of telescopes requested the corresponding number of mirror petals have to be replaced
- The envisaged telescope design is assumed to be fully compatible with the mirror petal interfaces

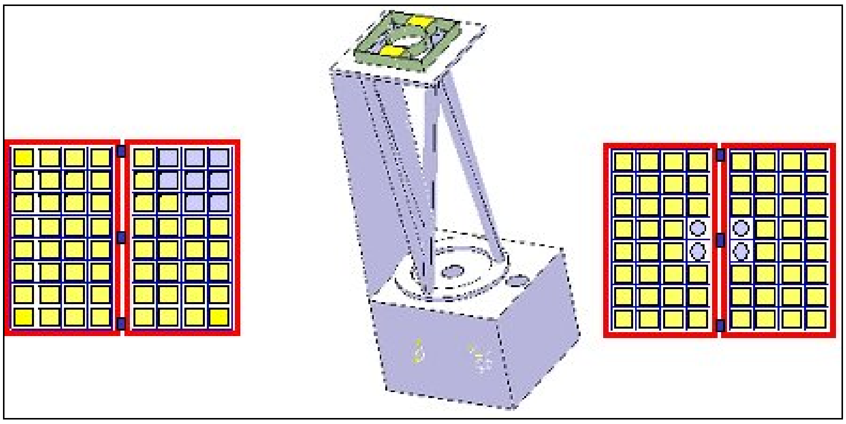

Figure 2-5: Payload options (left to right: 50-m grating, 10-m grating, HET)

3. MISSION ANALYSIS

3.1 Requirements and selection of the orbit

Initially foreseen to be located on a low Earth orbit so as to be serviceable by the International Space Station (RD[1]), the X-ray Evolving-Universe Spectroscopy dual spacecraft is now to be located in an orbit better suited for satisfying the scientific requirements, namely:

- Perturbations as little as possible ("quiet" orbit)
- Stable thermal environment
- No eclipses during the total mission lifetime (20 years)
- A large portion of the sky reachable at any time
- Any direction in the sky reachable within one year

Such requirements are rather common for modern space astronomy missions and the best location celestial mechanics can offer for orbits satisfying these requirements is around Sun-Earth libration points L_1 or L_2 (Figure 3-1). L_2, behind the Earth on the Sun-Earth line, is particularly suitable for space observatories. Orbits around libration points are called *Lissajous* orbits. Some large amplitude orbits are contained in a tube and never pass close to the Sun-Earth line: these orbits are called *halo* orbits and they are never in eclipse. Such a halo orbit is selected for XEUS.

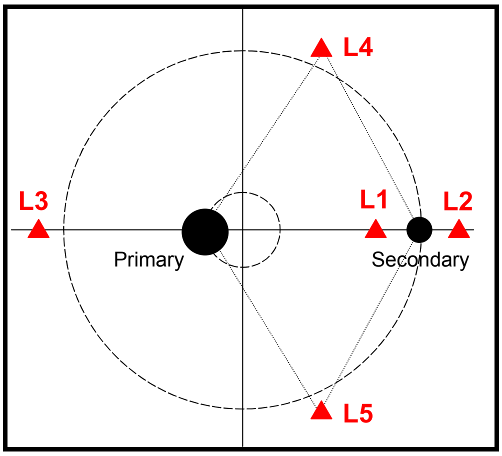

Figure 3-1: Libration points around the primary (Sun) and secondary (Earth)

Past and future ESA missions in halo or Lissajous orbits are recalled for information here:

- Halo orbit around L_1:
  - SOHO (Solar Heliospheric Observatory) launched in 1995, still in operation
  - SMART-2 (LISA Pathfinder), technology demonstration for LISA, launch planned in June 2007 with Rockod (LISA: Laser Interferometer Space Antenna, in collaboration with NASA, gravitational waves detection, launch planned in 2012 by a Delta IV on a 20° Earth trailing orbit)
- Lissajous orbit around L_2:
  - Herschel, far infrared astronomy, launch planned in February 2007
  - Planck, cosmic background measurement, dual launch planned in February 2007 by Ariane-5 with Herschel
  - GAIA (Global Astrometric Interferometer for Astrophysics), launch planned in June 2011 by Soyuz + Fregat
  - JWST (James Webb Space Telescope), launch planned in August 2011 by Ariane-5
  - Darwin, infrared space interferometry for Earth-like planet search, launch planned in 2014
  - Eddington, star seismology, project in stand-by

3.2 Halo orbits

3.2.1 Characteristics

Halo orbits around Sun-Earth L_1 or L_2 have amplitudes larger than 670 000 km and a period of 6-months. Such an orbit around L_2, proposed for XEUS, is shown in the synodic space (rotating coordinate system centred on the Earth) on Figure 3-2 (*x*-*y* ecliptic projection), Figure 3-3 (projection on the *x*-*z* plane) and Figure 3-4 (projection on the *y*-*z* plane). As seen, such an orbit is never in the shadow of the Earth.

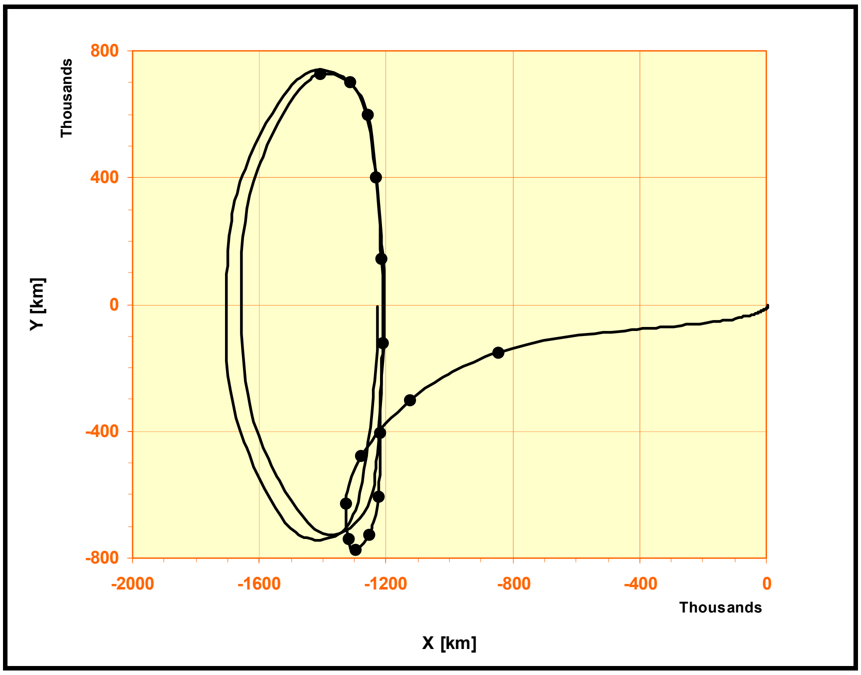

Figure 3-2: Halo orbit around L_2 in synodic space: ecliptic projection, Earth at coordinate (0, 0) and Sun along positive *x*-axis

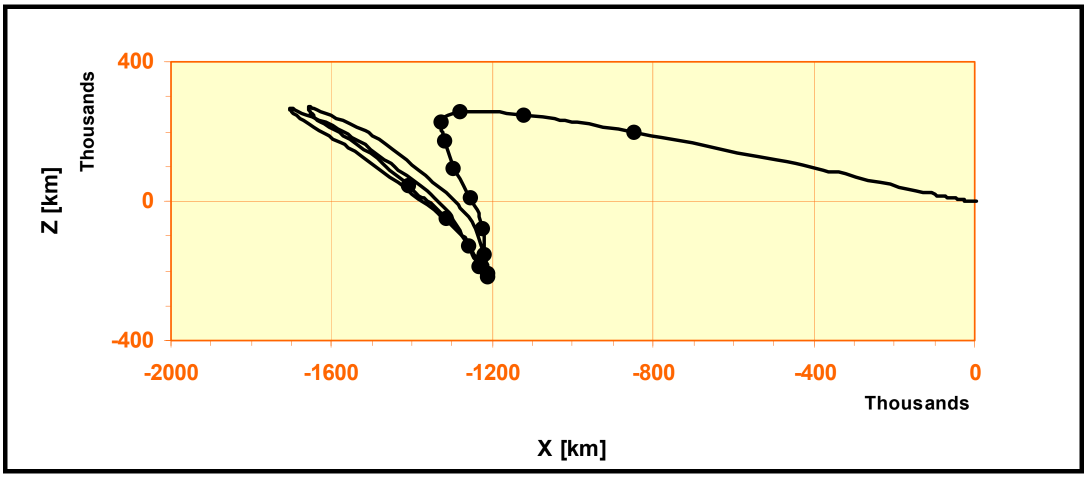

Figure 3-3: Halo orbit around L_2 in synodic space: x-z projection, Earth at coordinate (0, 0) and Sun along positive *x*-axis

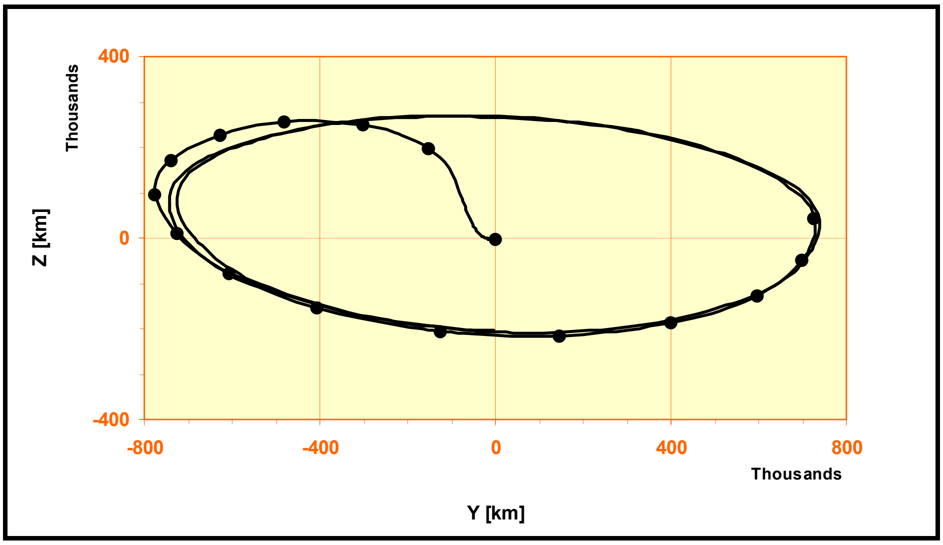

Figure 3-4: Halo orbit around L_2 in synodic space: y-z projection, Earth and Sun in the (0, 0) coordinate point

There are two types of halo orbits (Figure 3-5):

- Type 1: northern part tilted toward the Earth, southern part tilted away from the Earth
- Type 2: galactic mirror image of type 1

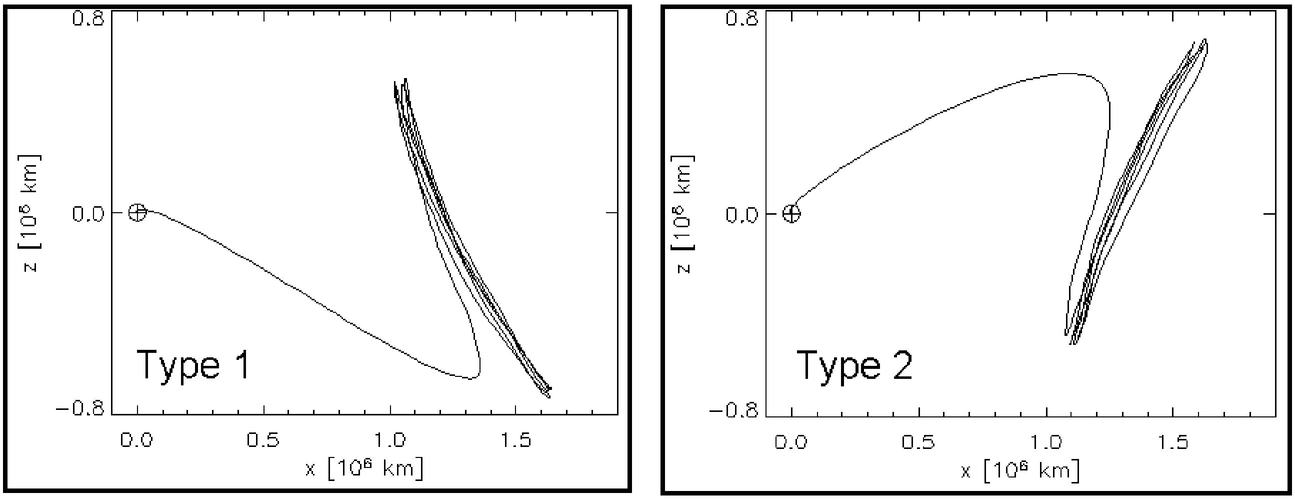

Figure 3-5: Type 1 and 2 halo orbits

The XEUS halo orbit shown in Figure 3-3 is of type 2.

3.2.2 Halo orbit maintenance

Halo orbits are unstable and maintenance is needed for staying in them. This is accomplished by performing a maintenance manoeuvre of about 5 cm/s every 20th day, resulting in a yearly ΔV usage of no more than 1 m/s. These manoeuvres are targeted to remove the unstable part of the motion (the so-called *escape direction*) and are aligned along a line 28° away from the Earth-Sun line (Figure 3-6, RD[2]).

Due to satellite attitude constraint, it may not be possible to perform this manoeuvre optimally. For example, if the thrust direction is oriented normal to the Sun direction, the efficiency of the manoeuvre is reduced by a factor 1/sin(28°) = 2.1. It turns out that the component of the manoeuvre along the non-escape direction does not harm orbit stability, therefore the only drawback is a doubling of the yearly ΔV usage.

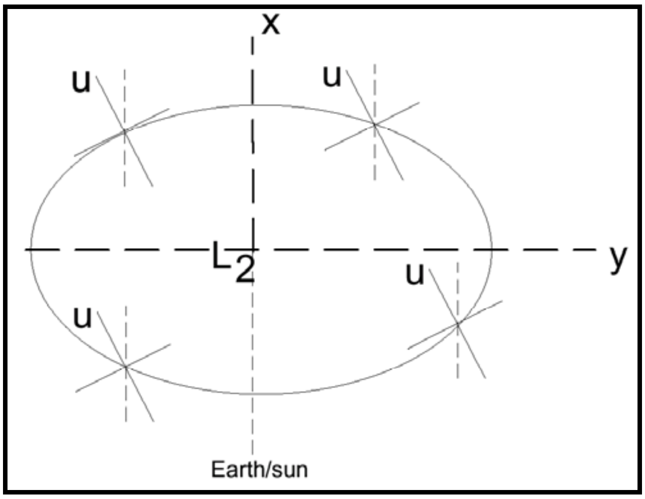

Figure 3-6: Escape (u) and non-escape direction in a libration point orbit

3.2.3 Formation flying maintenance manoeuvres for gravity gradient correction

The gravitational gradient in libration point orbits is very low: of the order of 10^{-13} s^{-2}. This explains why these orbits are preferred for missions sensitive to gravity gradient, such as interferometry in space. Indeed, the thrusting effort needed for gravity gradient compensation when several spacecraft are flying in formation is negligible compared to compensation of other perturbations such as solar radiation pressure or attitude manoeuvres.

3.2.4 Mission parameters

XEUS's distance from the Earth during the mission is shown in Figure 3-7 while the angle Sun-Spacecraft-Earth is shown in Figure 3-8.

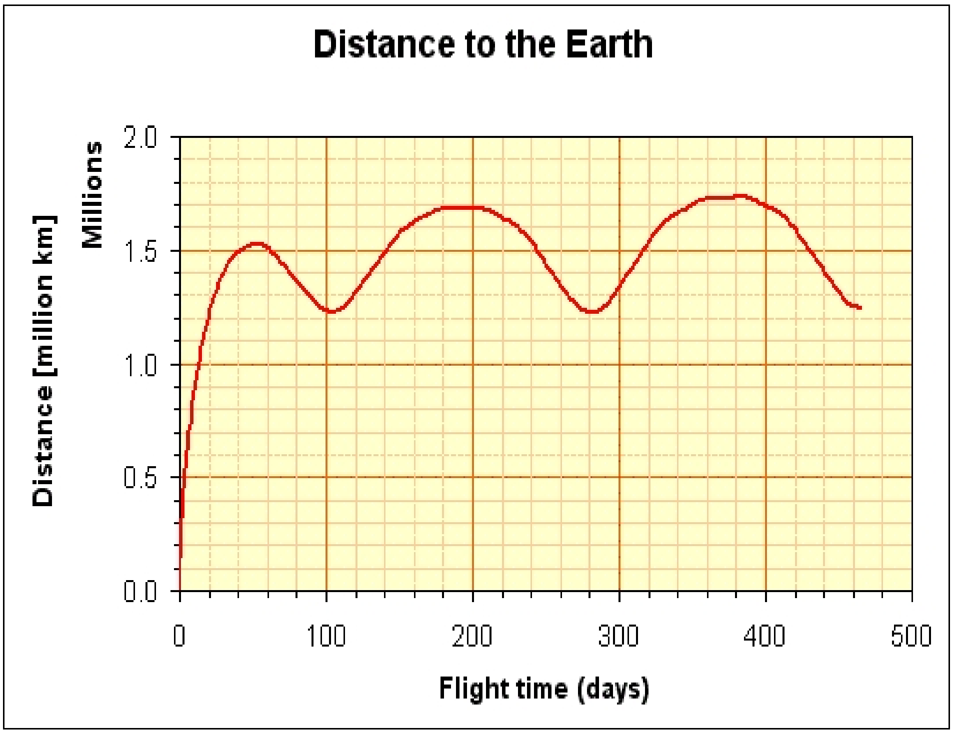

Figure 3-7: XEUS's distance from the Earth

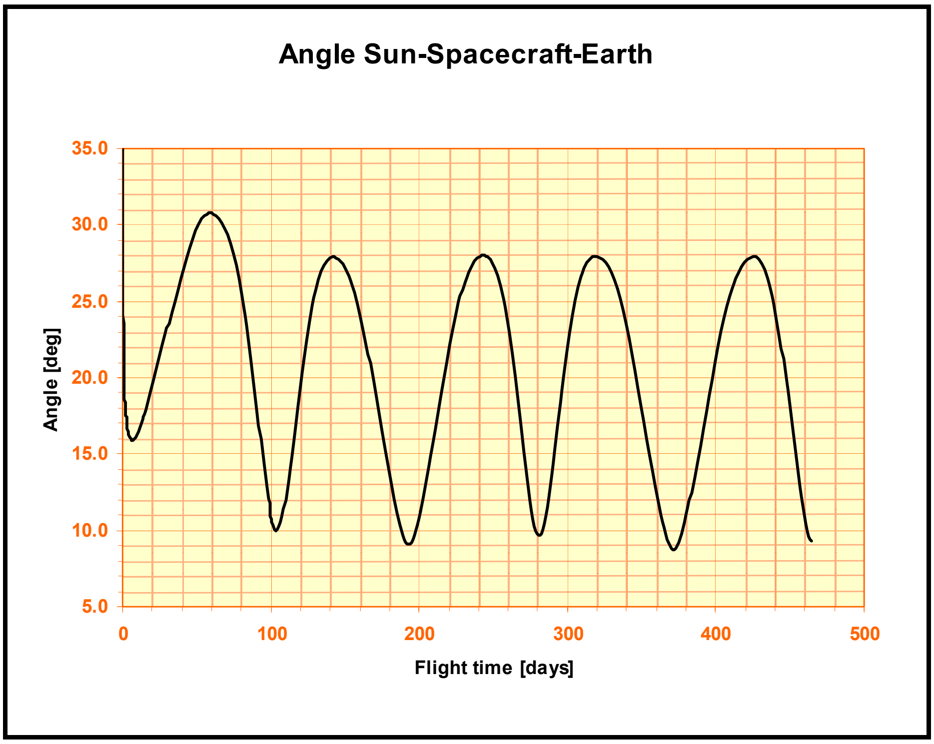

Figure 3-8: Angle Sun-spacecraft-Earth

Ground Station coverage with a minimum elevation of 10° from New Norcia (latitude 30.97° S) and Cebreros (lat. 40.45° N) is shown in Figure 3-9.

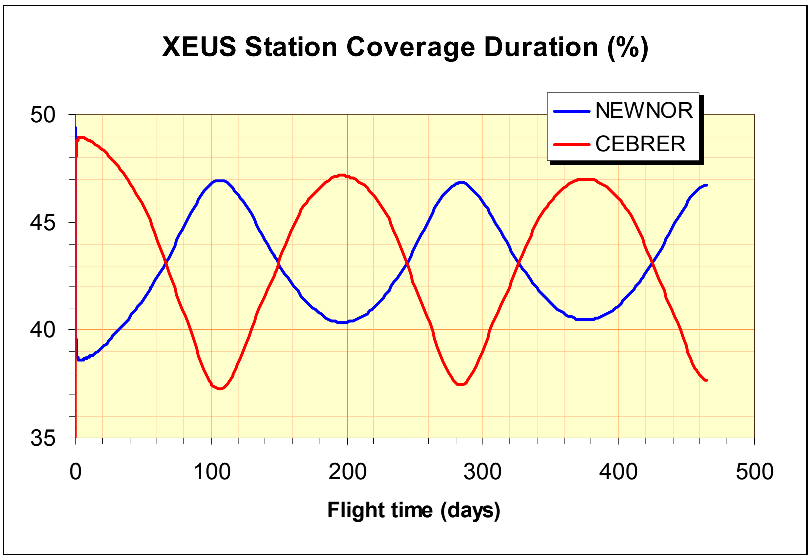

Figure 3-9: Coverage duration in % from New Norcia and Cebreros

For Cebreros, having a relatively high latitude, minimum coverage depends on the phase of the spacecraft on its halo orbit and the season. If the phase is unfavourable, there may be periods without coverage. This can be prevented by imposing a seasonal launch window leading to a favourable phase in the halo orbit.

3.3 Transfer to halo orbit

3.3.1 Insertion into halo orbit

If the insertion into a halo orbit is performed along an escape direction, there is no insertion manoeuvre as such. It turns out that if the insertion point is located at the point of maximum out-of-plane amplitude above (below) the ecliptic for halo orbit of type 1(2), the escape direction leads to a trajectory reaching the vicinity of the Earth, as shown in Figure 3-2 to Figure 3-5, where dots along the transfer trajectory represent 10-day time interval. This means that, for any launch date, there is a transfer orbit from Earth allowing inserting into a halo orbit without ΔV. Consequently, a halo orbit can be reached by a spacecraft having no propulsion unit (unavoidable correction manoeuvres can be performed with the AOCS). The departure leg of the transfer orbit may be in eclipse during a maximum duration of 75 minutes.

3.3.2 Manoeuvres during transfer orbit

For every Earth departure day the transfer orbit is different, with a transfer duration between 3 and 5 months. The launch energy needed at Earth departure is near parabolic. Inclination of the departure orbit can be as high as 63°. Typically, for a launcher equipped with a modern liquid upper stage, correction of the launcher dispersion is less than 25 m/s to be performed not later than 2 days after launch. Apart from this, a trimming manoeuvre of less than 2 m/s is to be performed about 8 days later and a mid-course manoeuvre of less than 1 m/s is required about 50 days after launch (RD[3]). From that time on no more major manoeuvres are scheduled, therefore scientific operations can start.

3.3.3 Alternate transfer orbits

The transfer trajectory leaves the Earth along a direction opposite to the Sun (see Figure 3-2 and Figure 3-3). This can be achieved with a dedicated launch. If the spacecraft is to be launched in a dual-launch configuration with a co-passenger requiring another launch direction, an alternate transfer trajectory has to be used. Such alternate transfer trajectories are complex to generate and make use of acrobatics in the Weak Stability Boundary region. Transfer duration can reach 6 months but there is no large ΔV penalty associated with such a long transfer. An example of a transfer from GTO to an L_2 orbit is shown in Figure 3-10:

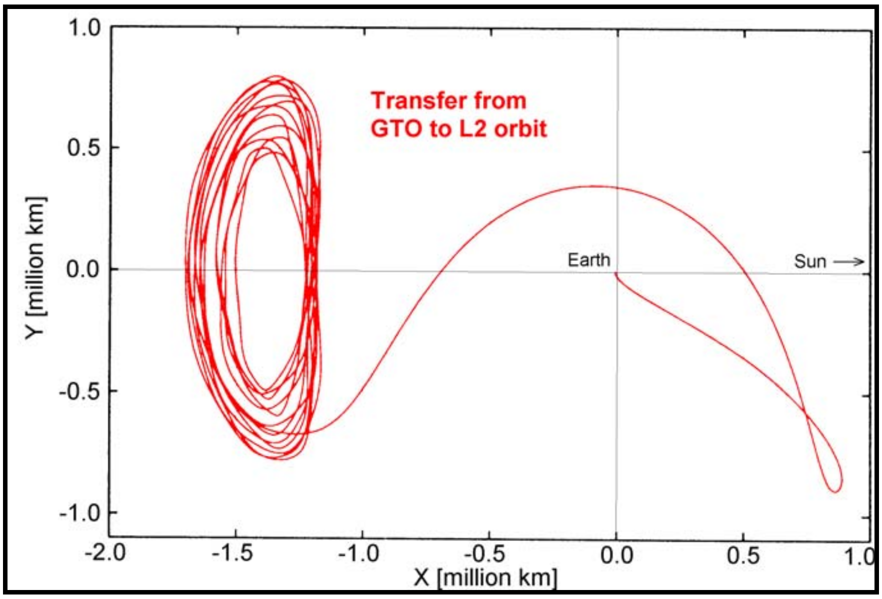

Figure 3-10: Transfer from GTO to an L_2 orbit

3.4 Launch

Three launchers are contemplated for the XEUS mission: Ariane-5 ECA, Delta IV Heavy and, for a descoped mission, Soyuz-ST 2.1b + Fregat.

3.4.1 Ariane-5 launcher

3.4.1.1.1 Direct launch

An Ariane-5 ECA is assumed here, with an assumed performance for near-parabolic orbit of 6800 kg for a low inclination orbit (performance figure adopted for the launch of JWST). By launching into a HEO and using an extra stage for going into near-parabolic orbit, this performance can be increased.

3.4.1.1.2 HEO launch

As mentioned in section 3.3.1 the spacecraft, once delivered by the launcher on the transfer orbit, does not need a dedicated propulsion unit for insertion into halo orbit. However, if the spacecraft does possess a propulsion unit, the launcher can inject the spacecraft into a lower energy HEO and, after separation from the launcher, the spacecraft itself completes the velocity increment to reach parabolic speed. This staging allows increasing payload mass. Before performing its manoeuvre at perigee, the spacecraft may stay one or several revolutions in the HEO for performing tasks such as orbit determination and thruster calibration. This HEO phase can also be used to extend the launch window. The advantages and disadvantages of a direct versus HEO launch are listed in Table 3-1.

	Direct	HEO
Payload mass	Given	Higher
Propulsion unit	No	Yes
Launch window (for Detector S/C)	Twice a year	As large as desired
Radiation dose	Low	High if many HEO revolutions
Gravity loss	No	High
Injection dispersion correction	Marginally possible with AOCS	Comfortable with propulsion unit
LEOP duration	A few days	+ time in HEO
Eclipses	Short (75 mn)	Several hours
Mission complexity	Simple	Extra manoeuvres
Mission risk	Minimum	Additional risk attached to propulsion unit

Table 3-1: Advantages and disadvantages of direct versus HEO launch

The selection of the optimum HEO apogee height is the result of an optimisation taking into account:

- Launch performance
- Spacecraft propulsion unit characteristics (mass, specific impulse)
- Gravity loss

Two options are possible for a HEO launch with Ariane-5 ECA, depending on the type of stage selected for XEUS:

1. *Use of a solid stage*. To have a substantial performance increase, a large stage is needed, such as the largest stage of the Thiokol Star family: the Star 75 (empty mass: 565 kg, maximum propellant load: 7503 kg, specific impulse: 288 s). Optimum HEO altitude for the target Ariane HEO is estimated to be 9000 km with a corresponding performance of 16170 kg (TBC). LEOP duration (between launch and correction of launcher's dispersion) is 2 days. The payload mass gain on near-parabolic orbit compared to a direct launch is about 800 kg. Such a large solid stage will introduce extra constraints on spacecraft design and accommodation under the fairing.
2. *Use of a bi-propellant stage*. The only bi-propellant motor available in Europe for integration into a spacecraft has a thrust of 400 N. At the time of XEUS launch it can be assumed that the thrust will reach 500 N with a specific impulse of 320 s. However, considering the high mass of the spacecraft, a large gravity loss is to be expected. There are two possible ways for reducing gravity loss: 1) combine several propulsion units in a cluster; 2) perform the manoeuvre in several steps. Due to the complexity of the development of a

cluster of engines (some of them have to be gimballed), only the second way is contemplated here. If the manoeuvre is performed in six steps, starting from an Ariane HEO with an apogee of 30 000 km (corresponding Ariane performance: 10770 kg, TBC), the gravity loss can be maintained around 15% and the mass gain in near-parabolic orbit is about 600 kg compared to a direct launch. Note that a six-step injection will lead to a quite complex LEOP with a duration of at least 10 days.

3.4.2 Delta IV Heavy launcher

The best performing launcher of the Boeing Delta IV family is the Delta IV Heavy. Its performance for near-parabolic orbit of inclination up to 28.5° is 9300 kg (RD[4]). The mass of the Payload Attach Fitting (PAF) is 520 kg.

3.4.3 Soyuz launcher

3.4.3.1.1 Direct launch

Performance of the Soyuz-ST 2.1b + Fregat launched from Kourou for near-parabolic orbit is 2050 kg for an inclination < 28.5° and decreases to 1846 kg for 63° inclination (RD[5]).

3.4.3.1.2 HEO Soyuz performance

The Soyuz-ST + Fregat performance from Kourou for a launch on a GTO is 3050 kg. Using this figure and a recent performance estimation (RD[6]) allows, by extrapolation, building a performance table in terms of apogee height (for a perigee height of 180 km) and four values of inclination illustrated in Figure 3-11:

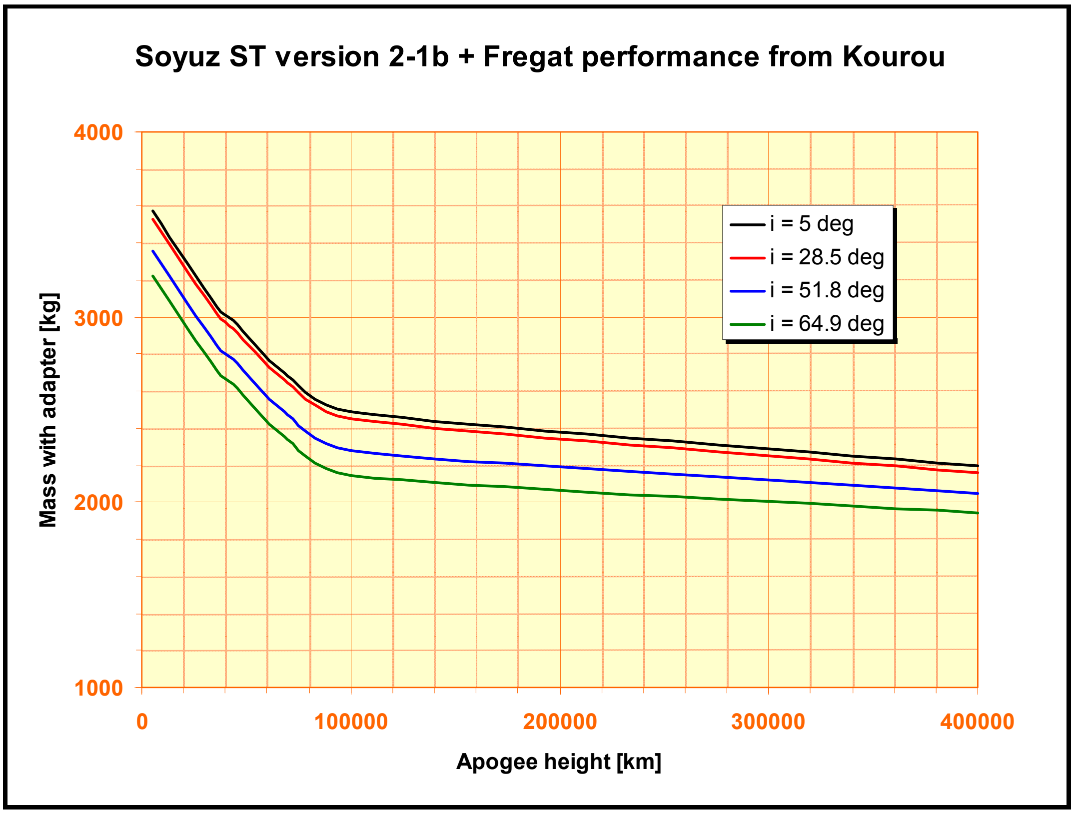

Figure 3-11: Soyuz performance for HEO in terms of apogee height (perigee height 180 km)

3.4.3.1.3 Characteristics of propulsion unit

A standard bi-liquid European propulsion unit is proposed with the following characteristics with a thrust of 500 N and specific impulse 320 s.

3.4.3.1.4 Selection of the optimum apogee height

By assuming an impulsive perigee manoeuvre the optimum apogee height can be assumed to be about 40 000 km. In this case, the velocity increment the spacecraft has to communicate by a perigee manoeuvre to reach parabolic orbit is 706 m/s. This leads to figures for Soyuz performance, spacecraft propellant and dry mass listed in Table 3-2. A spacecraft propulsion unit is used for injection into a parabolic orbit. The bottom line shows the mass gain (including the mass of the propulsion unit) compared to a direct launch.

Inclination	5.2°	63°
Soyuz performance [kg]	2944	2619
Propellant mass [kg]	593	527
Spacecraft dry mass [kg]	2351	2092
Gain in mass [kg]	371	316

Table 3-2: Mass budgets for a Soyuz launch on a 180×40 000 km HEO

3.4.3.1.5 Gravity loss

The perigee manoeuvre is subjected to a gravity loss of 26%. This can be reduced by performing the perigee manoeuvre in two or more steps, namely by introducing several HEOs of increasing apogee height. Table 3-3 describes the situation for direct launch (0 perigee manoeuvre, column 3), one HEO (1 perigee manoeuvre, column 4) or two HEOs for inclinations not exceeding 28.5°. By performing the perigee thrust in two steps, the gravity loss is reduced from 26% to 7% and spacecraft dry mass can reach 2350 kg, including propulsion unit. Assuming an integrated propulsion system of mass motor + tanks + structure to be 15% of propellant mass, payload mass on near-parabolic orbit is 76 kg (1 HEO) or 178 kg (2 HEO) higher than for a direct launch.

	Number of manoeuvres:	0	1	2
HEO 1	Apogee height [km]	-	40000	40000
	Orbit period [h]	-	11.9	11.9
	S/C dry mass [kg]	-	2974	2974
HEO 2	Apogee height [km]	-	-	90000
	Orbit period [h]	-	-	32.3
	Gravity loss [%]	-	-	7.2
	Propellant mass [kg]	-	-	340
	S/C dry mass [kg]	-	-	2634
HALO	Apogee height [km]	1500000	1500000	1500000
	Gravity loss [%]	-	25.8	7.2
	Propellant mass [kg]	-	711	283
	S/C dry mass [kg]	2080	2263	2351
	Motor + tanks + structure	0	107	93
	Payload mass [kg]	2080	2156	2258

Table 3-3: Summary table for direct or HEO (with one or two perigee manoeuvres) launch into parabolic orbit of inclination < 28.5°

3.4.3.1.6 LEOP and eclipse duration

LEOP is a period defined here between launch and time of correction of injection dispersion. For the case of a HEO launch, one revolution on each HEO is assumed. Table 3-4 lists LEOP duration. Eclipse duration for a direct launch does not exceed 75 minutes. In a HEO, when the Sun has the most unfavourable direction, eclipse duration can reach several hours, as shown in Table 3-4. By restricting the launch date in suitable periods, maximal eclipse duration can be reduced.

Number of manoeuvres	0	1	2
LEOP duration [h]	48	61	91
Maximum eclipse duration [h]	1.3	2.5	3.5

Table 3-4: LEOP and maximal eclipse duration for a direct or a HEO launch

3.4.3.1.7 Maintenance manoeuvres in HEO

Should the spacecraft stay several revolutions on HEO, luni-solar perturbations may change the orbit eccentricity and may cause the perigee height to decrease. This has to be counteracted by a perigee raise apogee manoeuvre. For the contemplated HEOs, corresponding ΔV for such maintenance manoeuvres does not exceed 4 m/s per week.

4. SYSTEMS

4.1 XEUS system requirements and design drivers

The system requirements for the XEUS mission are listed below (see also Figure 4-1):

- The system comprises two spacecraft flying in formation:
  - Mirror spacecraft–MSC (Provided by ESA)
  - Detector spacecraft – DSC (Concept presented by JAXA)
  - MSC-DSC separation distance 50 metres
  - MSC life time: 15 years + 5 years extension
  - DSC life times about 5 years (replaceable at EOL and/or if more sophisticated detectors become available)
- Launch:
  - Launch date: 2015
  - MSC and DSC to be launched as a stack
  - Using Ariane-5 launcher. Alternatively Delta IV-H
- Operational Orbit: L2
- Typical observation time: $3x10^5$ s (about 3.5 days)

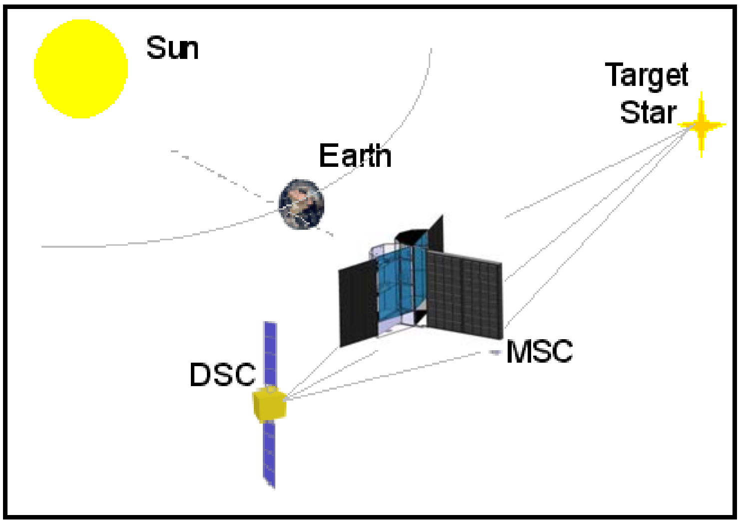

Figure 4-1: XEUS spacecraft elements configuration in target orbit at L2

The CDF study showed that the following issues drive the design of the mission:

- Formation Flying and Rendezvous:
  - Major issue for DSC AOCS: required relative range error during nominal formation keeping imposes autonomous control system
  - Ranging accuracy from ground segment → operations and rendezvous strategies
- MSC lifetime:
  - Imposes very low consumables, simple and reliable design for the SVM of MSC
- Launch vehicle, cruise phase and injection strategy:
  - Drives the maximum launch mass (available mirror surface), cost, programmatics

  - Composite launch has direct impact on cruise phase (BBQ mode, MSC design)
- Petal mass:
  - Petal mass is strongly dependant on:
    - Petal location
    - Petal size
    - Number of petals
    - Concept how mirror is populated with petals
  - Total mirror performance (science output) depends strongly on above boundary conditions.
  - Large contribution to overall MSC wet mass
- Petal interface:
  - Requires a large number of actuators on MSC and optical detection system to compensate for initial mirror misalignment
  - Petals locking during launch
- Temperature gradients in mirror plane:
  - Direct impact on MSC configuration. Hot Sun shield flaps and cold spacecraft closure panels to be implemented
- Temperature gradients within mirror petals in optical axis:
  - Off-normal Sun angle to be limited to about 5°
- Mirror contamination prevention:
  - Specific strategies to avoid contamination. Stay in launch configuration (BBQ mode) until outgassing procedure is executed and completed
  - Configuration: protect mirror during outgassing, protect from exhaust-plume impingement on mirror surface
  - Propulsion: choice of non-contaminating propellant. Hydrazine used during cruise and could be burnt off if necessary. Cold gas used for AOCS manoeuvres.

4.2 MSC requirements

A set of requirements was derived for the mirror spacecraft (see Figure 2-4), which is to be provided by ESA:

- Lifetime = 15 years, extended lifetime = + 5 years
- No formation keeping (only orbit correction and maintenance)
- Three-axis stabilised
- Payload: matrix of petals that constitute the mirror (≈1434 kg for Ariane-5, ≈2610 kg for Delta IV-H)
- Mirror petals shall be kept clean from contamination
- Absolute pointing error 60 arcsec (X and Y-axes), 3600 arcsec on Z-axis
- Absolute measurement error 10 arcsec (X and Y-axes), 300 arcsec on Z-axis

4.3 DSC requirements

No system requirements were derived for the detector spacecraft. However as both spacecraft have to fly in formation, formation flying-related requirements on the DSC have been derived:

- Lifetime: 5 years , extended lifetime = + 2 years (it can be replaced at EOL and/or if more sophisticated detectors become available)
- The DSC performs the initial formation set-up, the formation keeping and reorientation (as flyer, chaser spacecraft)
- The DSC – MSC distance shall be 50 m
- Absolute pointing error 60 arcsec (X and Y-axes), 3600 arcsec on Z-axis
- Absolute measurement error 10 arcsec (X and Y-axes), 300 arcsec on Z-axis

4.4 XEUS telescope requirements

The telescope requirements were found to be the following:

- Pointing direction = centre of detector to centre of optics
- Mainly affected by DSC to MSC position error: +/-1 mm max (allowed formation flying error sideways to optical axis)
- Focal depth is +/-5 mm (allowed formation flying error along optical axis)
- The difference between the inertial attitudes of the DSC and the MSC shall be less than 1 arcsec per axis

4.5 System trade-offs

Four options were evaluated at system level:

1. Large mirror area with only outer ring populated with mirror petals (48 out of 64 possible mirror petals installed. Average petal mass of 61 kg/m^2)
2. Fully populated mirror option (8x8 petals of 75x75 cm and average mirror petal mass of 72.5 kg/m^2)
3. Fully populated mirror option with 50-m grating
4. Fully populated mirror option with 10-m grating

For each system option, four launch options were evaluated:

1. "Ariane-5-direct": an Ariane-5 ECA launches the MSC-DSC stack directly into L2.
2. "Ariane-5-HEO": an Ariane-5 ECA launches the MSC-DSC stack into a High Elliptic Orbit (HEO). The stack then uses its own propulsion module for the HEO to L2 transfer.
3. "Ariane-5-LEO": an Ariane-5 ECA launches the MSC-DSC stack into LEO. The stack then uses a Star 75 solid stage for the LEO to L2 transfer.
4. "Delta IV-H": a Delta IV-H launches the MSC-DSC stack directly into L2.

As the performance of the Delta IV-H was sufficient to launch all system options, the three Ariane launch strategies were traded for system options 1 and 2. They are shown in Table 4-1.

Trade-key:	A	Injection orbit trade-off								
System Option:		1			2			3		
Name		Ariane-direct			Ariane-HEO			Ariane-LEO+STAR75		
Notes										
Parameter	Weights	Option	Ranking	Value	Option	Ranking	Value	Option	Ranking	Value
Launch costs	3.00		0	9.00		0	9.00	Added STAR75	-	6.00
MSC wet mass	1.00	4887	0	3.00	5492	+	4.00	5687	++	5.00
DSC wet mass	0.50	1753	0	1.50	1753	0	1.50	1753	0	1.50
S/C cost	3.00		0	9.00	Added prop. System	--	3.00	More complex AOCS design, higher structure mass	-	6.00
Complexity	1.00		0	3.00	Added prop. System	--	1.00	Different moments of inertia, interface, spin-stabilised during burn	--	1.00
criticality	1.00	No large burns	0	3.00	2 large burns	--	1.00	1 large burn	-	2.00
redesign of MSC	1.00		0	3.00	Added prop. System	-	2.00	redesign structure & aocs & interface	-	2.00
Total Score:				31.5			21.5			23.5

Table 4-1: Ariane launch trade-off table

Since one of the system requirements given for the study was to launch the MSC-DSC stack using the Ariane-5 launcher, launch option 1 was selected as the baseline. However, a more detailed design of this direct injection option showed that the Ariane-5 performance (6800 kg to L2) was not sufficient for a single launch (MSC+DSC) with the fully equipped mirror (2610 kg). For this reason, variations of this option were looked into to study if a sufficient performance improvement could be achieved by injecting into L2 via either HEO or LEO (options 2 and 3, respectively).

In launch option 2 the performance improvement was found to be still small (7405 kg by means of six perigee burns) with the added disadvantages that a large propulsion system is needed for the transfer from a HEO to the L2 halo transfer orbit, added risk due to the need of large perigee burns, and added cost for the added propulsion system and added critical operations cost. For these reasons, this option was ruled out and not studied in further details.

Launch option 3 showed that the performance improvement achieved with the strategy of injecting into L2 via LEO was still not enough to launch the stack with the fully populated mirror (7600 kg which is an improvement of 11.8%). Moreover, this option requires an expensive Star 75 solid stage for the transfer from LEO to the L2 halo transfer orbit, plus a complete re-design of the AOCS system (which needs to be compatible with a spin-stabilised spacecraft during the solid stage burn), and added risk due to a large perigee burn. Option 3 was therefore ruled out and not studied in more detail.

After the analysis in launch options 1, 2 and 3, it appeared to be clear that using Ariane-5 would not allow a single launch of the stack with the fully equipped mirror of 2610 kg. However, due to the programmatic advantages of launch option 1, it was decided to still keep it as the baseline featuring a de-scoped, lighter mirror (first system option) while selecting Delta IV-H for all other system options. Therefore, in this baseline option the mirror mass came as an output, rather than an input, to size the spacecraft so that a single Ariane-5 direct launch would be possible.

For the sake of completeness, and to study an option in which the full 2610 kg mirror is feasible, a direct launch with Delta IV-H (9200 kg to L2) was studied in detail. The mass budgets for this option can be seen in the following sections. Also in further sections, more details are included for the cases of a Delta IV-H launch including the 50-m and 10-m grating options proposed by the United States.

Figure 4-2 shows an overview of the selected system options:

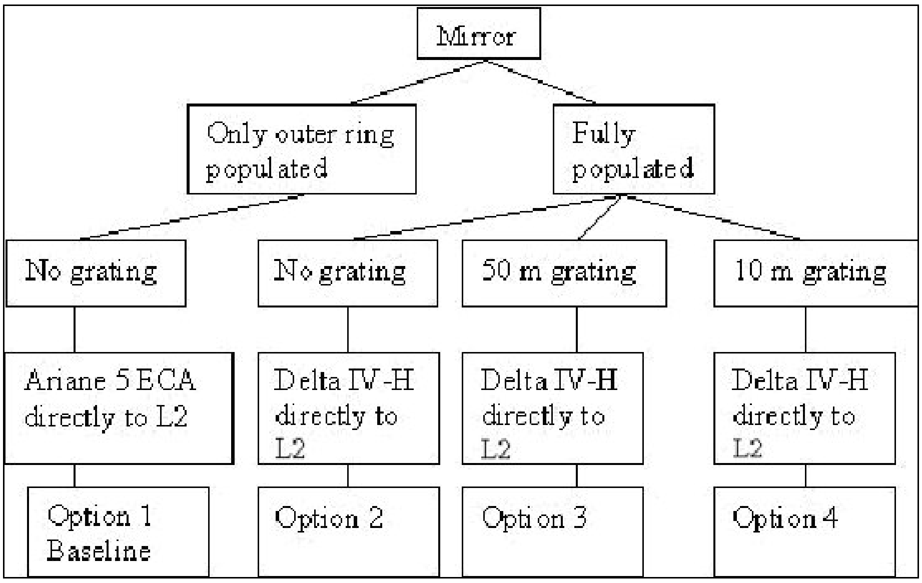

Figure 4-2: Overview of system and launch options

4.6 MSC configuration trades

Two configurations were studied for the design of the MSC. Concept A presented an optimum temperature gradient across the mirror but a too cold absolute temperature (-250°C to -230°C range). For this reason, hot sunshield flaps and cold spacecraft closure panels were implemented resulting in Concept B, which was selected as the baseline. This concept provides acceptable temperature gradients across the mirror of about 42.8°C and a worst case between petals of 7.1°C, being the gradient within one petal of about 1°C. It has a lowest absolute temperature of 161°C, which is acceptable for the mirror design and suitable for ground testing using LN_2. Besides, the choice of cold gas as the propulsion system for AOCS manoeuvres prevents mirror contamination. Concepts A and B (baseline) are shown in Figure 4-3.

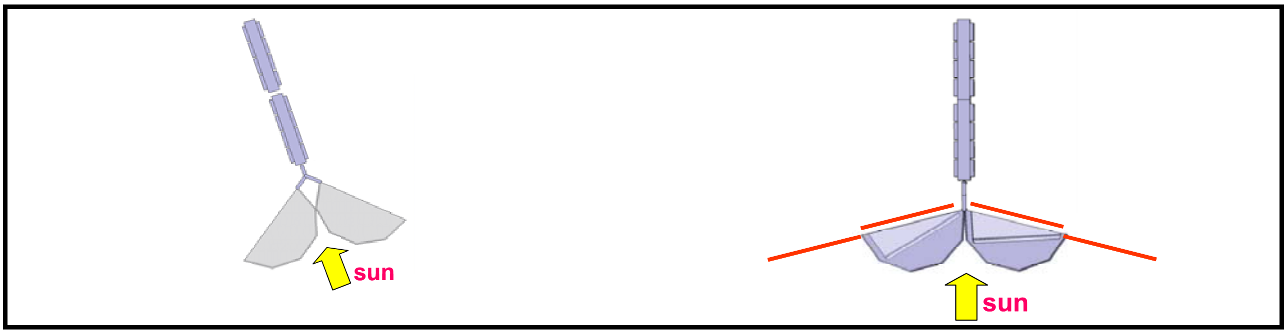

Figure 4-3: MSC concepts A (left) and B (right)

4.7 Baseline design

The baseline design (System Option 1) features the MSC-DSC stack launched in 2015, using a direct injection to L2 with Ariane-5. The DSC separates after two conditions are met:

- Once the hydrazine propulsion system is no longer required
- The MSC outgassing procedure is completed

The launch configuration and definition of the coordinate system are shown in Figure 4-4:

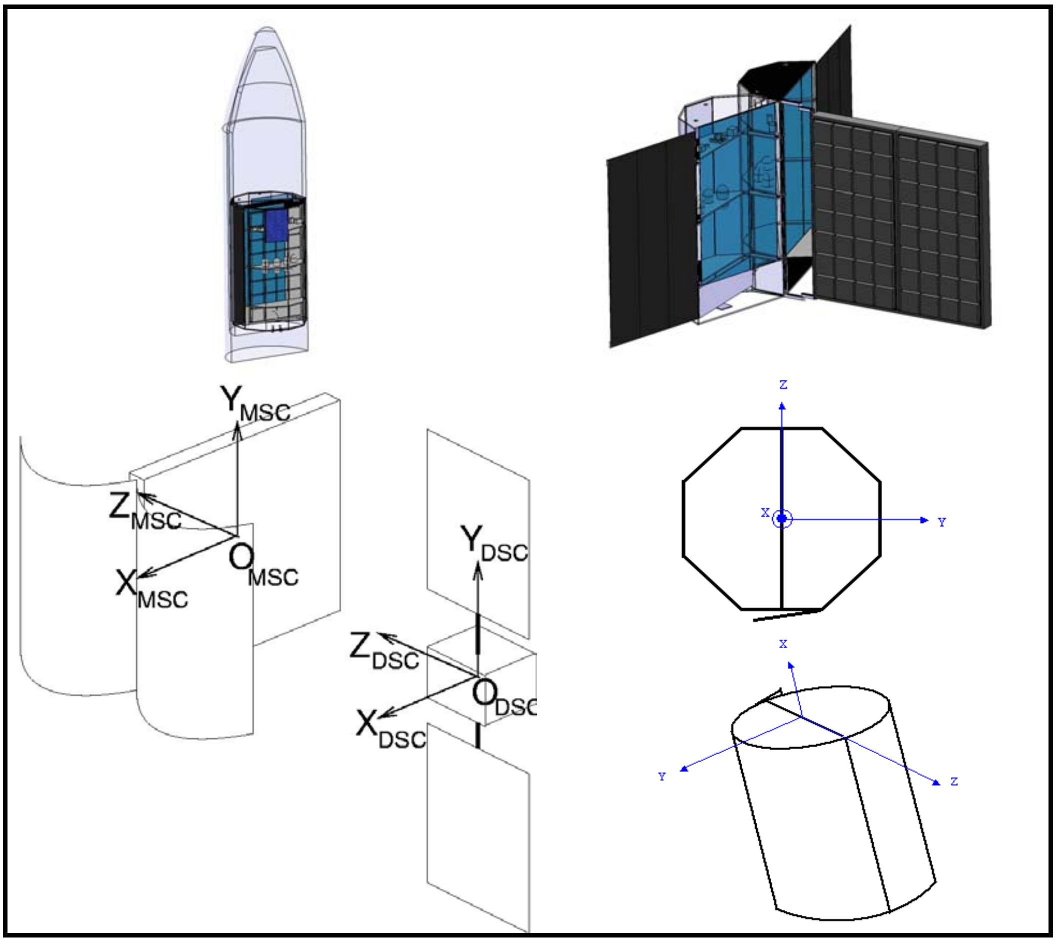

Figure 4-4: XEUS launch configuration and definition of coordinate system

Some special strategies had to be determined to prevent petal contamination: BBQ mode is used during initialisation to allow outgassing in stowed configuration. Monopropellant (hydrazine) thrusters are used only in stowed configuration.

Therefore two propulsion systems are needed. The correction of launcher dispersion (25 m/s) and cruise manoeuvres (5 m/s) are performed by hydrazine engines, whereas cold gas thrusters are used for remaining orbit corrections and attitude control to protect petals from plume impingement.

The MSC-Sun incidence angles for the chosen configuration are shown in Figure 4-5.

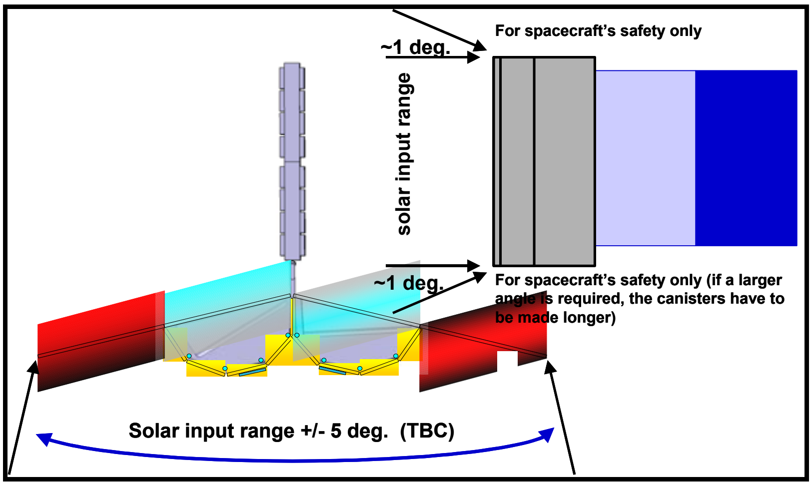

Figure 4-5: MSC-Sun incidence angles

Figure 4-6 gives an overview of the XEUS system. The modes of operations are defined in Chapter 8, AOCS.

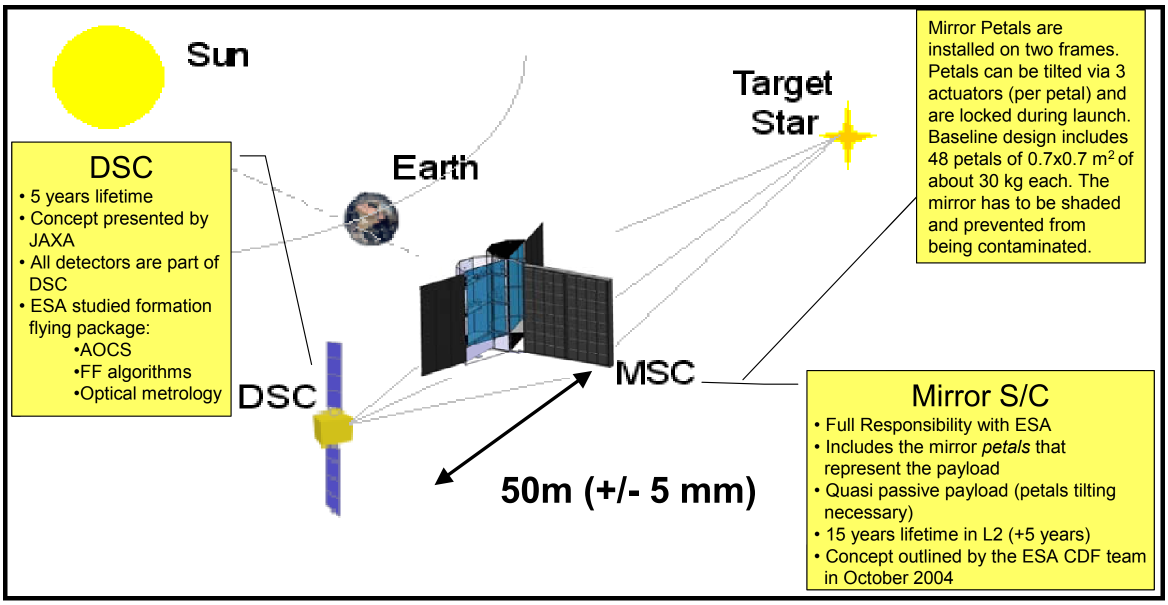

Figure 4-6: XEUS system overview

The DSC element has not been designed in this study, and the suggested configuration of DSC presented by JAXA (input of May 2004 [RD4]) has been adopted as the baseline. See Figure 4-7 for more details on this configuration.

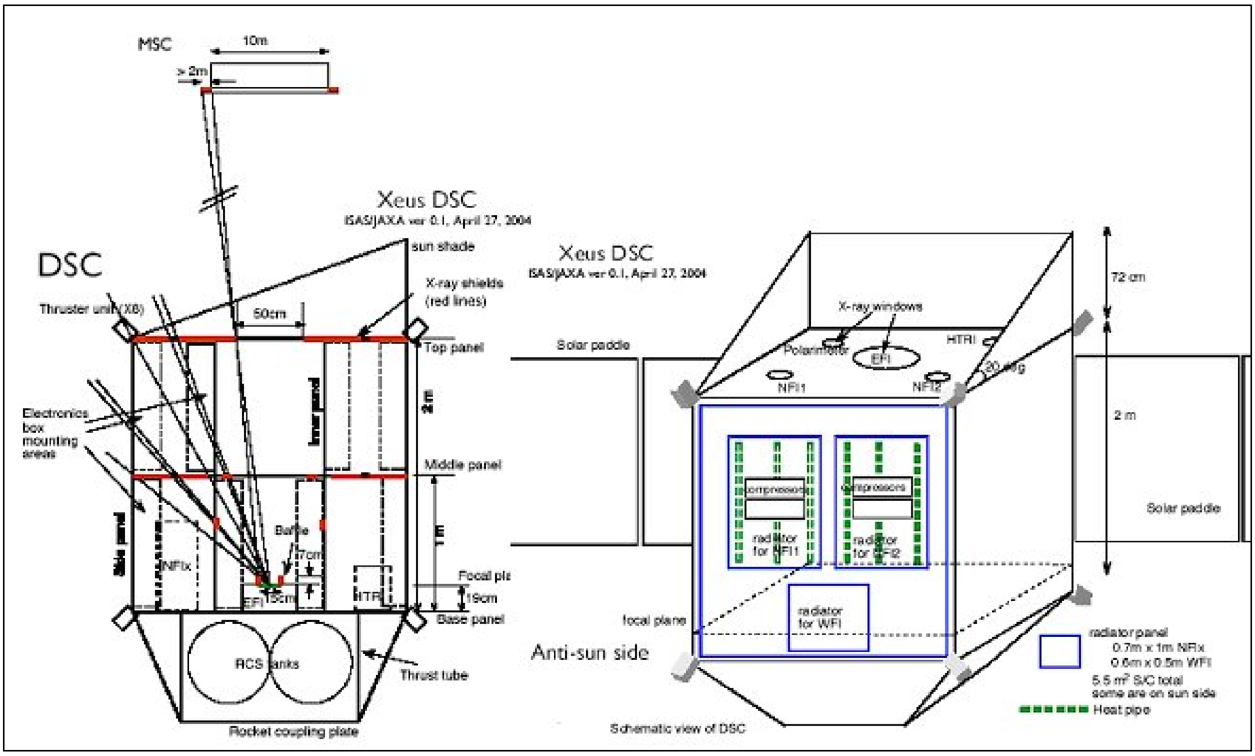

Figure 4-7: DSC system overview

Note that in all mass calculations it has been assumed that the DSC separation mechanism is included in the DSC equipment and not included in the mass budget of the MSC.

The mirror petal arrangement is shown in Figure 4-8:

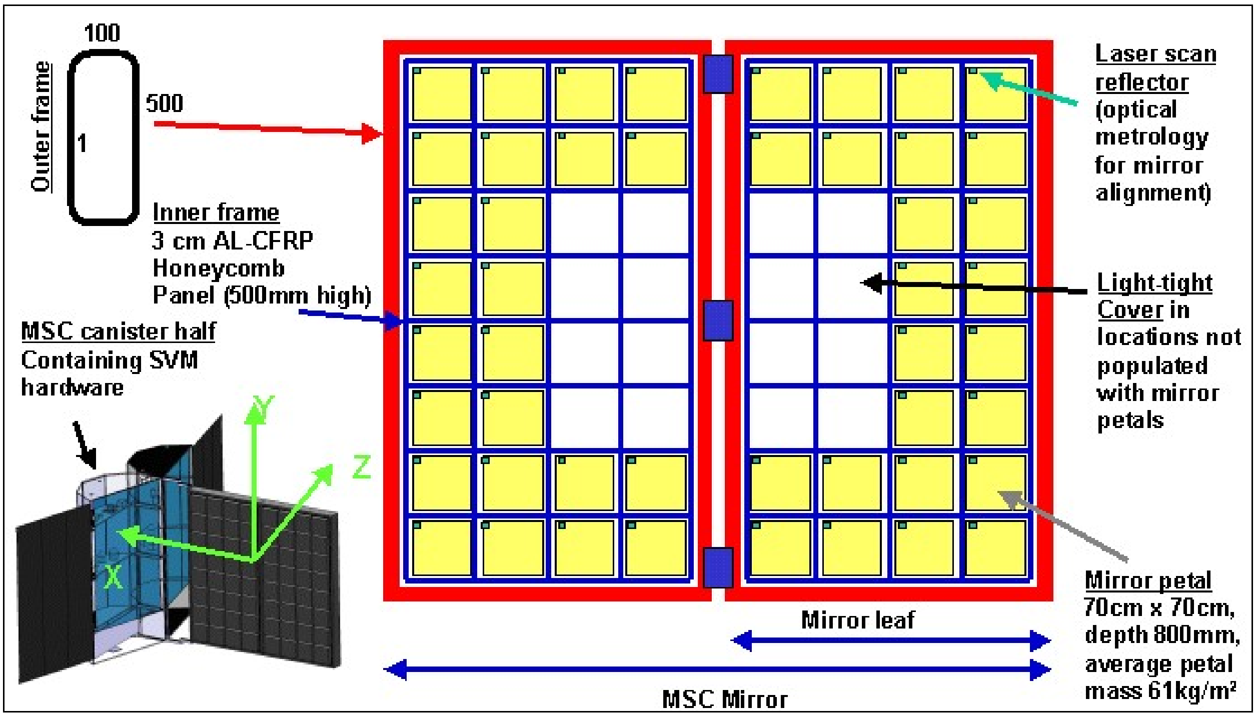

Figure 4-8: Baseline mirror petal arrangement

4.7.1 Budgets

The mass budget for the Ariane-5 baseline design is shown in Table 4-2 and Table 4-3. The instrument mass is based on a large mirror area with only outer ring populated with mirror petals (48 out of 64 possible mirror petals installed with an average petal mass of 61 kg/m^2). This mirror configuration fits within the Ariane-5 performance of 6800 kg to L2.

Mirror S/C					
		Target Spacecraft Mass at Launch		4887.00	kg
		Below Mass Target by:		4.46	kg
	Without Margin	Margin		Total	% of Total
Dry mass contributions		%	kg	kg	
Structure	1431.01 kg	10.00	143.10	1574.11	32.24
Thermal Control	124.92 kg	20.00	24.98	149.90	3.07
Mechanisms	203.20 kg	15.00	30.48	233.68	4.79
Pyrotechnics	10.00 kg	0.00	0.00	10.00	0.20
Communications	18.74 kg	12.21	2.29	21.03	0.43
Data Handling	9.30 kg	20.00	1.86	11.16	0.23
AOCS	35.19 kg	5.43	1.91	37.10	0.76
Propulsion	180.68 kg	9.00	16.27	196.95	4.03
Power	60.60 kg	12.80	7.76	68.36	1.40
Harness	81.19 kg	0.00	0.00	81.19	1.66
Instruments	1434.72 kg	0.00	0.00	1434.72	29.38
Optics	5.00 kg	5.00	0.25	5.25	0.11
Total Dry(excl.adapter)	3594.55			3823.45 kg	
System margin (excl.adapter)		20.00 %		764.69 kg	
Total Dry with margin (excl.adapter)				4588.14 kg	
Propellant	294.40 kg	0.00	0.00	294.40	6.03
Launch mass (including adapter)				4882.54 kg	

Table 4-2: XEUS MSC mass summary

Mirror S/C		
Total Dry(excl.adapter)		3823.45 kg
System margin (excl.adapter)	20.00 %	764.69 kg
Total Dry with margin (excl.adapter)		4588.14 kg
Propellant		294.40
Adapter mass (including sep. mech.), kg		0.00
Element 1 Launch mass (including adapter)		4882.54 kg
Detector S/C		
Total Dry(excl.adapter)		1164.00 kg
System margin (excl.adapter)	20.00 %	232.80 kg
Total Dry with margin (excl.adapter)		1396.80 kg
Propellant		281.20
Adapter mass (including sep. mech.), kg		75.00
Element 2 Launch mass (including adapter)		1753.00 kg
Stack		
Total Dry Mass		5984.94
Total Wet Mass		6635.54
Adapter mass (including sep. mech.), kg		160.00
Total Launch mass		6795.54 kg
	Target Spacecraft Mass at Launch	6800.00 kg
	Below Mass Target by:	4.46 kg

Table 4-3: XEUS total mass budget

The power budgets are shown in Chapter 14, Power.

4.8 Options

4.8.1 Option 2: Fully populated mirror

The major differences with respect to the baseline are:

- Fully populated mirror: 64 petals instead of 48
- Launcher: Delta IV-H

Since this option was the only one allowing a single launch of the stack with the fully populated mirror, it was studied in detail and the budgets are presented in Table 4-4 and Table 4-5. The mirror featured in this case has an area of 36 m^2 (64 petals of 75 cm x 75 cm), with a density of 72.5 kg/m^2 and a dry mass of 2610 kg (without system margin). Note that 36 m^2 corresponds to an effective mirror area of about 11 m^2. For the DSC an overall mass of 1753 kg has been assumed.

Mirror S/C					
	Target Spacecraft Mass at Launch			7287.00	kg
	Below Mass Target by:			754.91	kg
	Without Margin	Margin		Total	% of Total
Dry mass contributions		%	kg	kg	
Structure	1538.02 kg	10.00	153.80	1691.83	25.90
Thermal Control	124.92 kg	20.00	24.98	149.90	2.29
Mechanisms	203.20 kg	15.00	30.48	233.68	3.58
Pyrotechnics	10.00 kg	0.00	0.00	10.00	0.15
Communications	18.74 kg	12.21	2.29	21.03	0.32
Data Handling	9.30 kg	20.00	1.86	11.16	0.17
AOCS	35.19 kg	5.43	1.91	37.10	0.57
Propulsion	197.21 kg	9.17	18.09	215.29	3.30
Power	60.60 kg	12.80	7.76	68.36	1.05
Harness	110.00 kg	0.00	0.00	110.00	1.68
Instruments	2610.00 kg	0.00	0.00	2610.00	39.96
Optics	5.00 kg	5.00	0.25	5.25	0.08
Total Dry(excl.adapter)	4922.18			5163.59 kg	
System margin (excl.adapter)		20.00	%	1032.72 kg	
Total Dry with margin (excl.adapter)				6196.31 kg	
Propellant	335.78 kg	0.00	0.00	335.78	5.14
Launch mass (including adapter)				6532.09 kg	

Table 4-4: MSC system mass for the Delta IV-H option

Mirror S/C			
Total Dry(excl.adapter)		5163.59	kg
System margin (excl.adapter)	20.00 %	1032.72	kg
Total Dry with margin (excl.adapter)		**6196.31**	**kg**
Propellant		335.78	
Adapter mass (including sep. mech.), kg		0.00	
Element 1 Launch mass (including adapter)		**6532.09**	**kg**
Detector S/C			
Total Dry(excl.adapter)		1164.00	kg
System margin (excl.adapter)	20.00 %	232.80	kg
Total Dry with margin (excl.adapter)		**1396.80**	**kg**
Propellant		281.20	
Adapter mass (including sep. mech.), kg		75.00	
Element 2 Launch mass (including adapter)		**1753.00**	**kg**
Stack			
Total Dry Mass		7593.11	
Total Wet Mass		8285.09	
Adapter mass (including sep. mech.), kg		260.00	
Total Launch mass		**8545.09**	**kg**
	Target Spacecraft Mass at Launch	9300.00	kg
	Below Mass Target by:	754.91	kg

Table 4-5: Total mass budget for the Delta IV-H option

Note that, as in all options, the 20% system margin is also applied to the mirror dry mass. This is justifiable given the maturity level of the petal technology but it is recommended to revisit this issue as it represents more than 500 kg.

The adapter to the Delta IV-H launcher has been assumed to have a mass of 260 kg (including the separation mechanism).

4.8.2 Grating options

Two grating options (10 m and 50 m) have been looked into, to accommodate the grating designs provided by NASA. Both cases have been studied as variations of the Delta IV-H option and, therefore, a 9300 kg into L2 performance has been assumed.

4.8.2.1 Option 3: 50-m grating

For this grating option, the Service Module (platform) design is identical to the one without grating presented above. The mirror is a fully populated one featuring 8x8 petals, eight of which have been replaced by specific grating petals. Moreover, the actuators proposed for locking during launch are compatible with heavier grating petals. The mass budget computed with these assumptions is shown in Table 4-6 and Table 4-7.

Mirror S/C					
		Target Spacecraft Mass at Launch		7287.00	kg
		Below Mass Target by:		38.05	kg
	Without Margin	Margin		Total	% of Total
Dry mass contributions		%	kg	kg	
Structure	1538.02 kg	10.00	153.80	1691.83	23.34
Thermal Control	124.92 kg	20.00	24.98	149.90	2.07
Mechanisms	203.20 kg	15.00	30.48	233.68	3.22
Pyrotechnics	10.00 kg	0.00	0.00	10.00	0.14
Communications	18.74 kg	12.21	2.29	21.03	0.29
Data Handling	9.30 kg	20.00	1.86	11.16	0.15
AOCS	35.19 kg	5.43	1.91	37.10	0.51
Propulsion	213.70 kg	9.26	19.79	233.49	3.22
Power	60.60 kg	12.80	7.76	68.36	0.94
Harness	110.00 kg	0.00	0.00	110.00	1.52
Instruments	2610.00 kg	0.00	0.00	2610.00	36.01
Optics	5.00 kg	5.00	0.25	5.25	0.07
Grating	550.00 kg	0.00	0.00	550.00	7.59
Total Dry(excl.adapter)	5488.67			5731.79 kg	
System margin (excl.adapter)		20.00 %		1146.36 kg	
Total Dry with margin (excl.adapter)				6878.15 kg	
Propellant	370.80 kg	0.00	0.00	370.80	5.12
Launch mass (including adapter)				7248.95 kg	

Table 4-6: MSC system mass for the 50-m grating option

Mirror S/C		
Total Dry(excl.adapter)		5731.79 kg
System margin (excl.adapter)	20.00 %	1146.36 kg
Total Dry with margin (excl.adapter)		**6878.15 kg**
Propellant		370.80
Adapter mass (including sep. mech.), kg		0.00
Element 1 Launch mass (including adapter)		**7248.95 kg**

Detector S/C		
Total Dry(excl.adapter)		1164.00 kg
System margin (excl.adapter)	20.00 %	232.80 kg
Total Dry with margin (excl.adapter)		**1396.80 kg**
Propellant		281.20
Adapter mass (including sep. mech.), kg		75.00
Element 2 Launch mass (including adapter)		**1753.00 kg**

Stack		
Total Dry Mass		8274.95
Total Wet Mass		9001.95
Adapter mass (including sep. mech.), kg		260.00
Total Launch mass		**9261.95 kg**
Target Spacecraft Mass at Launch	9300.00	kg
Below Mass Target by:	38.05	kg

Table 4-7: Total system mass for the 50-m grating option

These tables show that up to 550 kg (without 20% system margin) can be allocated to the 50-m grating. This mass includes both the difference in petal mass on MSC and grating detector mass on DSC. Note that the 50-m grating design provided by NASA does not reflect the actual mirror configuration and, therefore, it is recommended to revisit the 50-m grating option.

4.8.2.2 Option 4: 10-m grating

For this grating option, the Service Module (platform) design is again identical to the one without grating presented above. The mirror is also a fully populated one featuring 8x8 petals, eight of which have been replaced by specific grating petals. Moreover, the actuators proposed for locking during launch are compatible with heavier grating petals. As shown in Table 4-8 and Table 4-9 of the mass budgets for this option, a DSC of up to 2045 kg (dry mass including 20% system margin) can be accommodated.

Mirror S/C					
	Without Margin	Margin		Total	% of Total
Dry mass contributions		%	kg	kg	
Structure	1538.02 kg	10.00	153.80	1691.83	25.90
Thermal Control	124.92 kg	20.00	24.98	149.90	2.29
Mechanisms	203.20 kg	15.00	30.48	233.68	3.58
Pyrotechnics	10.00 kg	0.00	0.00	10.00	0.15
Communications	18.75 kg	12.21	2.29	21.04	0.32
Data Handling	9.30 kg	20.00	1.86	11.16	0.17
AOCS	35.19 kg	5.43	1.91	37.10	0.57
Propulsion	197.21 kg	9.17	18.08	215.29	3.30
Power	60.60 kg	12.80	7.76	68.36	1.05
Harness	110.00 kg	0.00	0.00	110.00	1.68
Instruments	2610.00 kg	0.00	0.00	2610.00	39.96
Optics	5.00 kg	5.00	0.25	5.25	0.08
Total Dry(excl.adapter)	**4922.19**			**5163.61 kg**	
System margin (excl.adapter)		**20.00**	**%**	**1032.72 kg**	
Total Dry with margin (excl.adapter)				**6196.33 kg**	
Other contributions					
Wet mass contributions					
Propellant	335.78 kg	0.00	0.00	335.78	5.14
dapter mass (including sep. mech.), kg	0.00 kg	0.00	0.00	0.00	0.00
Total wet mass (excl.adapter)				**6532.11 kg**	
Launch mass (including adapter)				**6532.11 kg**	

Table 4-8: MSC system mass for the 10-m grating option

Mirror S/C			
Total Dry(excl.adapter)		5163.61	kg
System margin (excl.adapter)	20.00 %	1032.72	kg
Total Dry with margin (excl.adapter)		**6196.33**	**kg**
Propellant		335.78	
Adapter mass (including sep. mech.), kg		0.00	
Element 1 Launch mass (including adapter)		**6532.11**	**kg**
Detector S/C			
Total Dry(excl.adapter)		1704.00	kg
System margin (excl.adapter)	20.00 %	340.80	kg
Total Dry with margin (excl.adapter)		**2044.80**	**kg**
Propellant		281.20	
Adapter mass (including sep. mech.), kg		75.00	
Element 2 Launch mass (including adapter)		**2401.00**	**kg**
Stack			
Total Dry Mass		8241.13	
Total Wet Mass		8933.11	
Adapter mass (including sep. mech.), kg		260.00	
Total Launch mass		**9193.11**	**kg**
	Target Spacecraft Mass at Launch	9300.00	kg
	Below Mass Target by:	106.89	kg

Table 4-9: Total system mass for the 10-m grating option

4.9 Summary

A detailed thermal parametric study and configuration trade was successful and the presented spacecraft design fulfils all payload and system specific requirements. Ariane-5's performance was found to be not sufficient for a single launch (MSC+DSC) with a fully equipped mirror. Only a 20% increase in mirror area with respect to the Soyuz-Fregat solution was achieved. A dual launch would also be feasible (MSC with Ariane-5 and DSC with Soyuz-Fregat) bringing the launch cost to a level comparable to Delta IV Heavy option.

With the United States 50-m grating option (baseline + 550 kg dry mass without margin), the stack mass is just within Delta IV Heavy performance (9300 kg to L2).

5. CONFIGURATION

The selected configuration concept for the mirror spacecraft of the XEUS mission is described in this chapter.

5.1 Requirements and design drivers

The main configuration requirement for the mirror spacecraft is the accommodation of the mirror element in the spacecraft and in the chosen launcher.

Design drivers for the configuration of the mirror spacecraft of the XEUS mission are:

- Available volume in the chosen fairing:
    - Baseline Ariane-5 long fairing (cylinder part d= 4.57 m, h=6.55 m)
    - Option Delta IV-H fairing (cylinder part d= 4.57 m, h=12.19 m)
- Deployment mechanism of the cylinder shell
- Deployment mechanism of the mirrors
- Structural - mechanical requirements of the spacecraft during mission lifetime
- Thermal requirement of the mirror elements and the spacecraft
- Pointing direction and field of view of the solar panel

5.2 Baseline design

The Ariane-5 launcher is chosen to be the baseline launcher for this XEUS mission. A type-long fairing of the launcher will be used to accommodate the spacecraft. A customised adapter needs to be designed for this mission.

5.2.1 Mirrors

The dimensions of the mirror petal used for the baseline are 700 mm by 700 mm by 800 mm. Each of the mirror leaves contains eight by eight petals. Figure 5-1 shows the overall configuration of the mirror leaves.

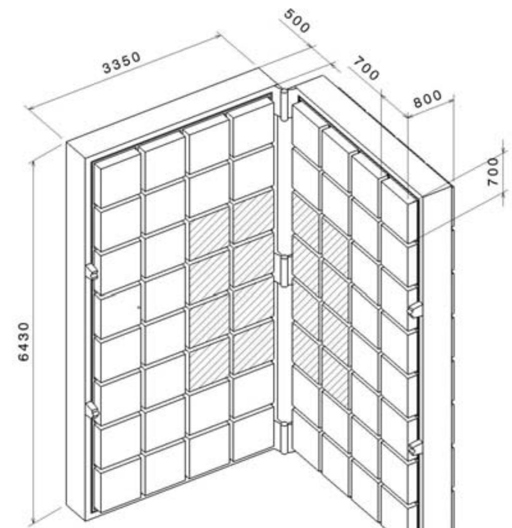

All dimension are in mm and valid for the baseline

Figure 5-1: Configuration of the mirror leaves

5.2.2 Mirror spacecraft

The folded mirror leaves, housekeeping equipments and propulsion tanks will be accommodated in a container, as shown in Figure 5-2:

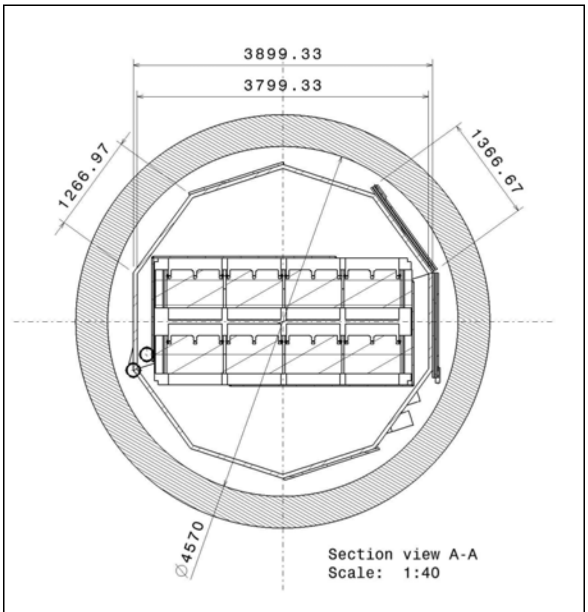

Figure 5-2: MSC inside Ariane-5

Some trade-offs have been performed between different polygonal shapes. An octagonal shaped box gives a minimum open area when the container is deployed and has an angle of 210 degrees between both plates as shown in Figure 5-3.

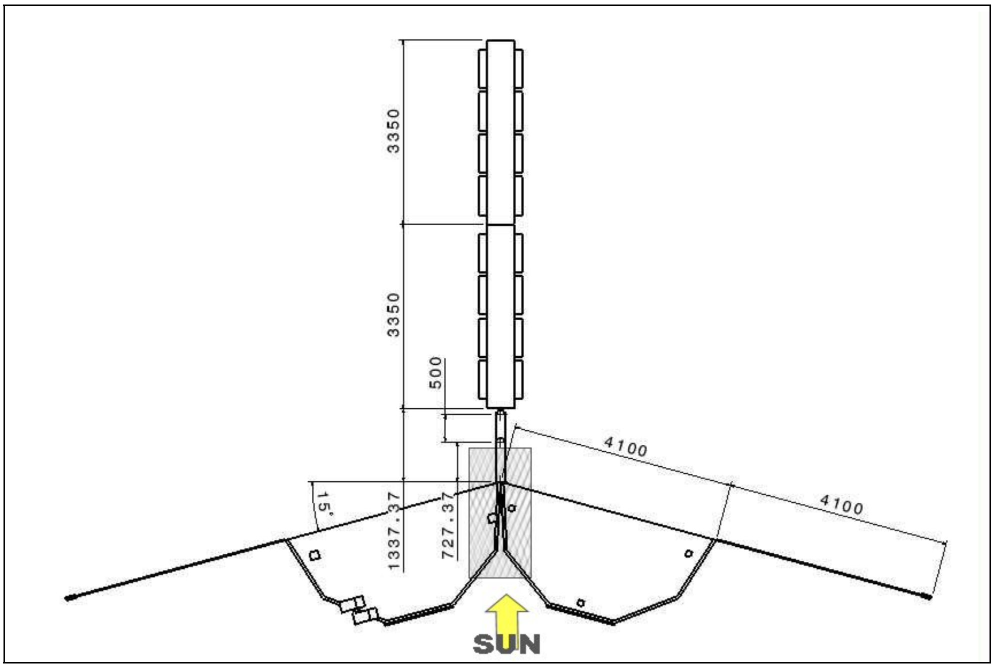

Figure 5-3: Top view of deployed MSC

5.2.3 External and internal accommodation

Figure 5-4 shows the external and internal accommodation of the units in the MSC. Detailed design of the units will not be shown in this phase of the study.

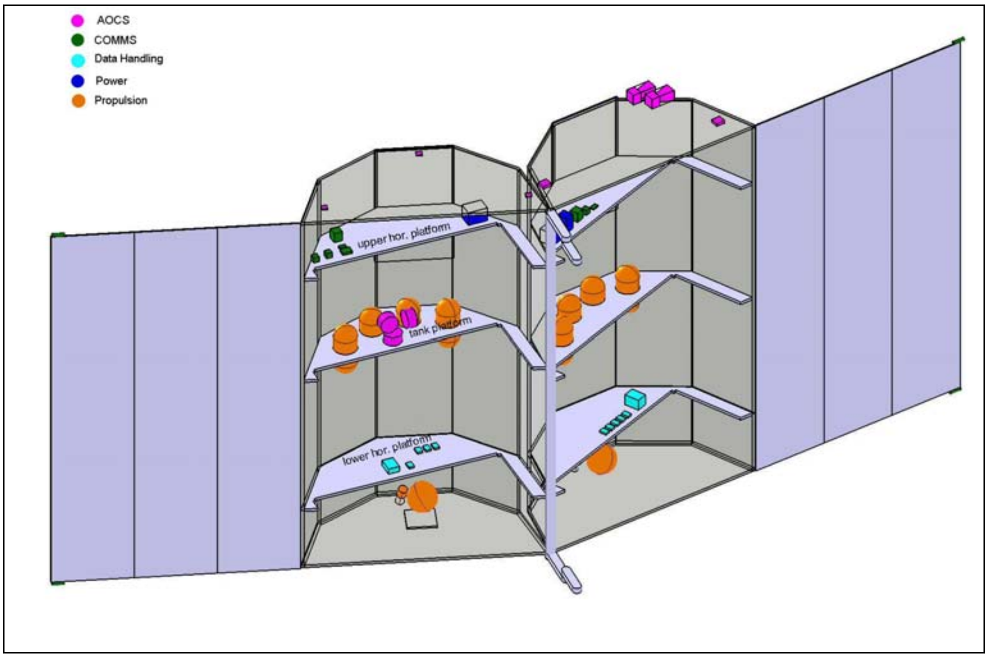

Figure 5-4: External and internal accommodation of MSC

External accommodation:

- Deployable panel – thermal flaps
- Top platform will accommodate the sun sensors and star trackers
- Cold gas and monopropellant thrusters (location of the thrusters will be further described in Chapter 7, Propulsion)
- Antennas for communications subsystem
- Solar panels (two panels mounted vertically and one mounted on the bottom panel of the container)

Internal accommodation:

- Deployable panel – thermal panels
- Upper horizontal platform will accommodate the power subsystem units: Battery, PCDU, PDU and Communication subsystem units: transponders, RFDUs
- Tank platforms will accommodate the propellant tanks (eight for cold gas and one for monopropellant) and the AOCS units: Reaction Wheels, Gyros
- Lower platform will accommodate DHS subsystem units: CDMU and command matrix units

The overall dimensions of the final configuration for the MSC baseline are shown in Figure 5-5 and Figure 5-6. Some detailed dimensions of the mirror parts are also shown in Figure 5-6.

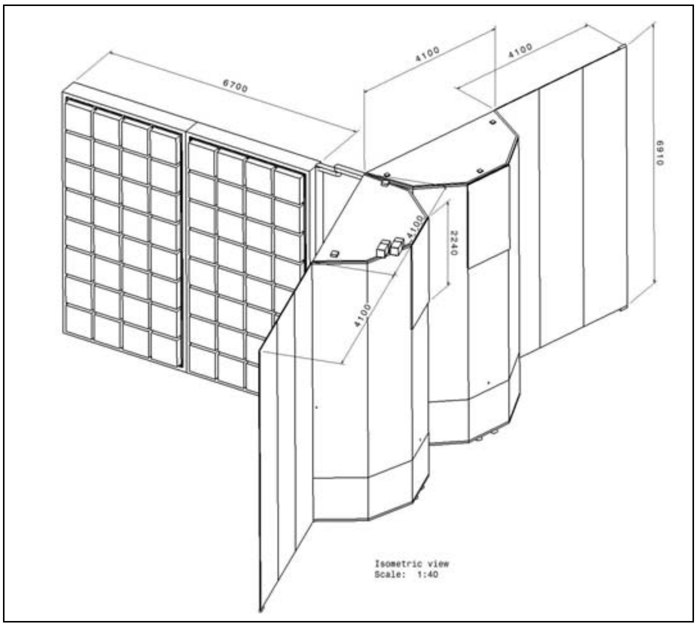

Figure 5-5: Deployed configuration of MSC

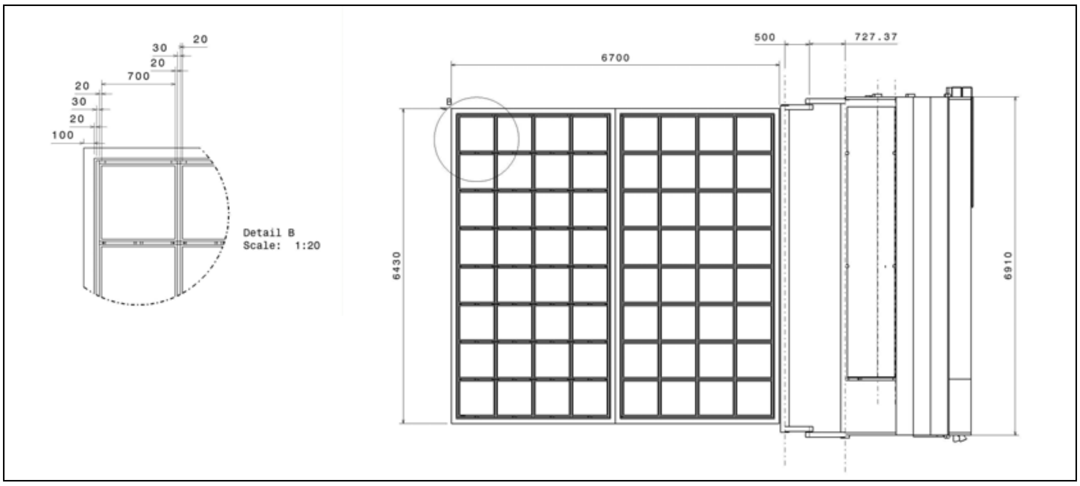

Figure 5-6: Overall mirror dimensions

The stowed configuration of the MSC stack with DSC in the long fairing of Ariane-5 is shown in Figure 5-7:

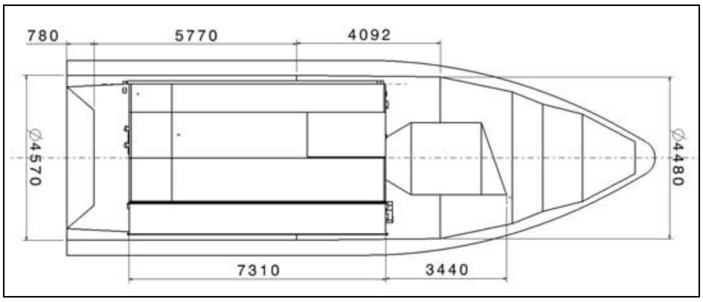

Figure 5-7: Launch configuration of the MSC-DSC stack in Ariane-5 long fairing

5.3 Options

The Delta IV-H launcher is chosen as alternative option to the baseline. The spacecraft's overall configuration is scaled up from the baseline design. The main difference is the mirror petal dimension 750 mm by 750 mm by 800 mm. The launch and deployed configuration for this option are shown in Figure 5-8 and Figure 5-9:

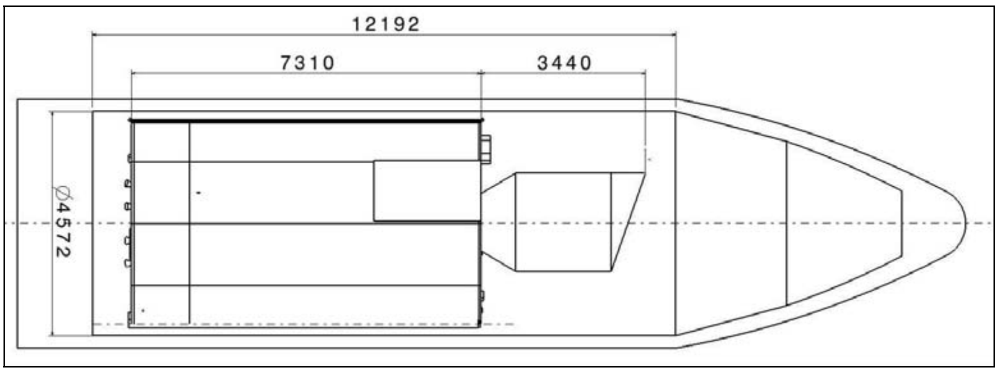

Figure 5-8: Launch configuration of the MSC-DSC stack in Delta IV-H fairing

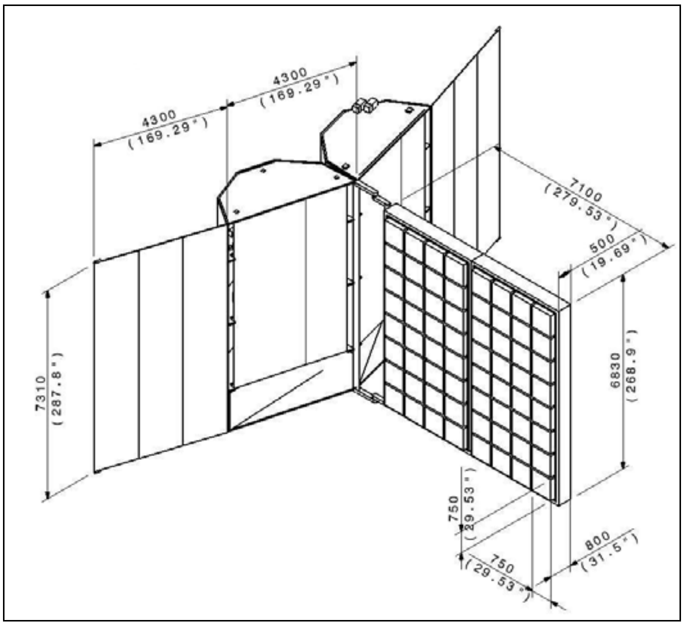

Figure 5-9: Deployed configuration of the MSC for Delta IV-H option

6. STRUCTURES

The objective of this chapter is to provide the relevant characteristics of the structures for the XEUS mission feasibility study, performed in the CDF at ESA/ESTEC. The focus in this chapter is on the MSC.

6.1 Requirements and design drivers

The main requirements and design drivers for the structural design of XEUS spacecraft derive from the compatibility with the chosen launcher, i.e. the payload has to fit inside the fairing and it has to be compatible statically and dynamically with the structural characteristics of the launcher. In particular, the Ariane-5 long fairing (see Figure 6-1) was considered for the single launch of the MSC-DSC stack.

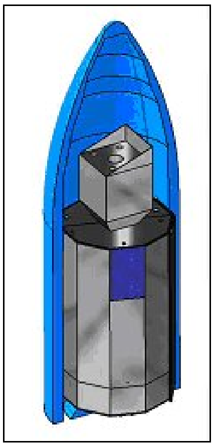

Figure 6-1: MSC and DSC stacked in the long fairing of Ariane-5

The first requirement is the maximum value for the spacecraft diameter, which has to be less than 4.57 m to fit in the Ariane-5 fairing; it was fixed to 4.3 m. Then the static compatibility with the launcher is ensured providing a custom adapter of about 160 kg and twelve bolted attachments between it and the MSC. There is also an interface between MSC and DSC to act during the launch phase (75 kg interface adapter).

The dynamic compatibility is reached when the spacecraft stiffness is sufficiently higher w.r.t. the launcher one. The first two structural frequencies (axial and lateral) of the MSC therefore have to be higher than the launcher ones. For the Ariane-5, these are 27 Hz and 10 Hz, respectively.

From a structural point of view, the main consideration is the design of the inner and the outer frames that support the core payload, the leaves of mirrors petals. The structural stability of these items is very important since the correct inclination of the mirrors is fundamental for the communication with the DSC. Therefore CFRP was chosen as material because of its thermal stability and GRP for elements in danger of thermal conduction.

6.2 Baseline design

The stowed MSC shape is a cylinder with a decagonal cross section of 4.3 m diameter and 7.31 m length. On the top, flat panels close it to avoid space contamination. A polygonal cross section for the cylinder was chosen because of production and mounting simplicity.

The deployed configuration sees the cylinder opening while rotating by means of a complicated hinge system composed of two couples of four hinges and two torsion bars, and then stretching out the frames of the two petals. Then, one petal rotates w.r.t. the common hinge and places itself parallel to the other one. For the initial stowed configuration and final result, see Figure 6-2 and Figure 6-3. In Figure 6-3, the structural and equipment walls and platforms are visible inside half of the cylinder. Note that in the final configuration the two halves of the cylinder, when completely deployed, have a relative angle higher than 180 degrees (210 degrees) because of thermal protection issues. For the same reason, deployed thermal protection panels are deployed inside and outside the cylinder.

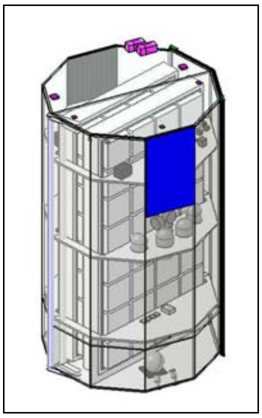

Figure 6-2: XEUS MSC in stowed configuration

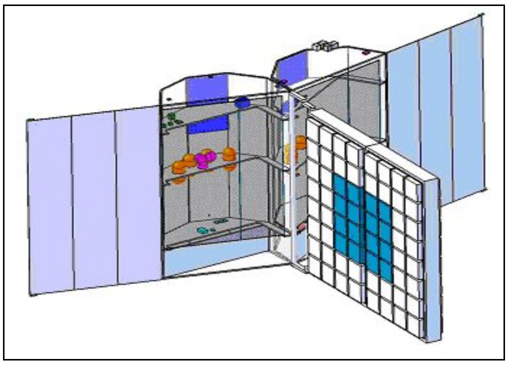

Figure 6-3: XEUS MSC in fully deployed configuration

The bottom part of the shells is reinforced with a bigger thickness of the walls because of the attachment to the adapter. There are twelve bolted attachments and therefore twelve “load paths” to the top of the spacecraft for the required stiffness during launch. Inside the cylinder there are several walls and platforms for structural purposes: two vertical panels in the bottom prevent the leaves from bending while stowed, while six horizontal platforms accommodate equipments and provide lateral stiffness.

The petals structure is connected to the cylinder by means of the outer frame that supports also the inner frame. This last item is a very important issue since the mirrors and the mechanisms to move them are attached to its structure. Particular care is needed when developing this part. Note that in Figure 6-4 the blue mirror petals are only covers, they do not constitute working mirrors. Every structural item except for the hinge system is in CFRP (with different surface density) because of its high thermal stability. Since solar panels are located on the external walls of the shell, the hinge system is in GRP to avoid thermal conduction toward the mirrors.

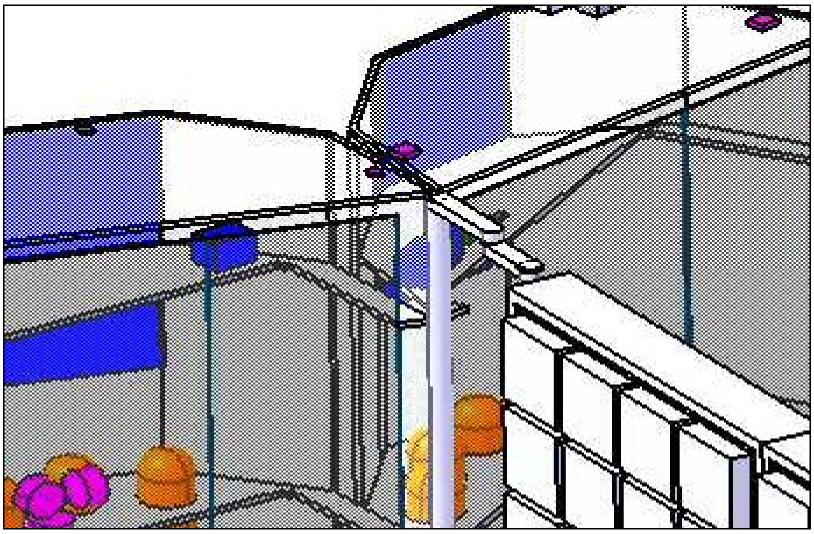

Figure 6-4: Deployed XEUS MSC in which the hinge system is shown

6.3 Budget

The mass budget for the structures in the baseline of the MSC is shown in Table 6-1:

Item	No.	Material			Unit mass without margin (Kg)	Unit mass with margin (Kg)	Total mass with margin (+ 10%) (Kg)
		Type	Skin thickness (mm)	Panel density (Kg/m2)			
Inner frames	2	CFRP	1	4.459	133.47	146.81	293.62
Outer frames	2	CFRP	1	4.459	111.08	122.19	244.38
Top shell	2	CFRP	1	4.459	156.05	171.66	343.31
Bottom shell	2	CFRP	1.75	6.94	48.6	53.46	106.92
Horizontal platforms	4	CFRP	1	4.459	13.48	14.83	59.31
Tank platforms	2	CFRP	1	4.459	11.17	12.29	24.57
Closure panels	4	CFRP	1	4.459	27.53	30.28	121.13
Bottom support panels	2	CFRP	1	4.459	17.30	19.03	38.06
Thermal panels	2	CFRP	0.75	3.151	76.5	84.15	168.3
Thermal flaps	2	CFRP	0.75	3.151	94.85	104.34	208.67
Torsion bars	2	GRP	-	-	13.82	15.2	30.4
TOTAL					**1431.01**	**1574.11**	

Table 6-1: Mass budget for the baseline

6.4 Options

6.4.1 Delta IV Heavy

The first option to the baseline arises from using Delta IV-H as alternative launcher. In this case, the required stiffness comes from Delta IV-H typical frequencies: axial min. 30 Hz and lateral min. 8 Hz, with a minimum payload mass of 6577 kg.

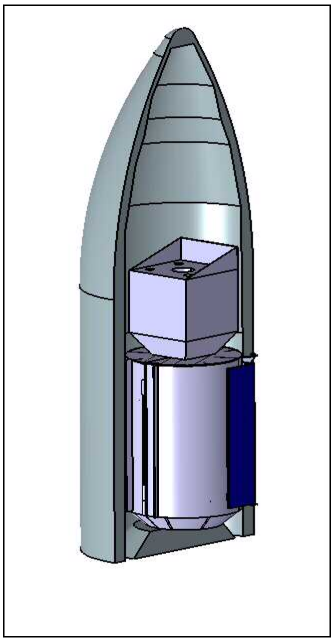

Figure 6-5: MSC and DSC stowed in Delta IV-H fairing

Table 6-2 shows the mass budget for the Delta IV H option. Comparing with the baseline budget note that when using Delta IV H there an increase of mass of 7.38 % with respect to the use of Ariane-5.

Item	No.	Material			Unit mass without margin (Kg)	Unit mass with margin (Kg)	Total mass with margin (+ 10%) (Kg)
		Type	Skin thickness (mm)	Panel density (Kg/m2)			
Inner frames	2	CFRP	1	4.459	133.47	146.81	293.62
Outer frames	2	CFRP	1	4.459	111.08	122.19	244.38
Top shell	2	CFRP	1	4.459	168.8	185.68	371.36
Bottom shell	2	CFRP	1.75	6.94	52.55	57.81	115.61
Horizontal platforms	4	CFRP	1	4.459	14.43	15.87	63.49
Tank platforms	2	CFRP	1	4.459	11.65	12.82	25.63
Closure panels	4	CFRP	1	4.459	28.71	31.58	126.32
Bottom support panels	2	CFRP	1	4.459	19.31	21.24	42.48
Thermal panels	2	CFRP	0.75	3.151	76.5	84.15	168.3
Thermal flaps	2	CFRP	0.75	3.151	94.85	104.34	208.67
Torsion bars	2	GRP	-	-	14.54	16	32
TOTAL					**1538.02**	**1691.83**	

Table 6-2: Mass budget for Delta IV-H option

7. PROPULSION

The objective of this chapter is to provide the relevant propulsion subsystem characteristics for the XEUS mission feasibility study performed in the CDF at ESA/ESTEC. The baseline launcher for the study is Ariane-5 but nevertheless, the United States launcher Delta IV-H is also considered and budgets for both launchers are presented in this chapter.

The propulsion subsystem of the XEUS mirror spacecraft (MSC) comprises a combination of two complete separate (stand alone) monopropellant hydrazine systems and two complete separate (stand alone) cold gas systems using nitrogen gas. Figure 7-1 shows the MSC in folded (launch configuration) and in unfolded configuration (on-station mode).

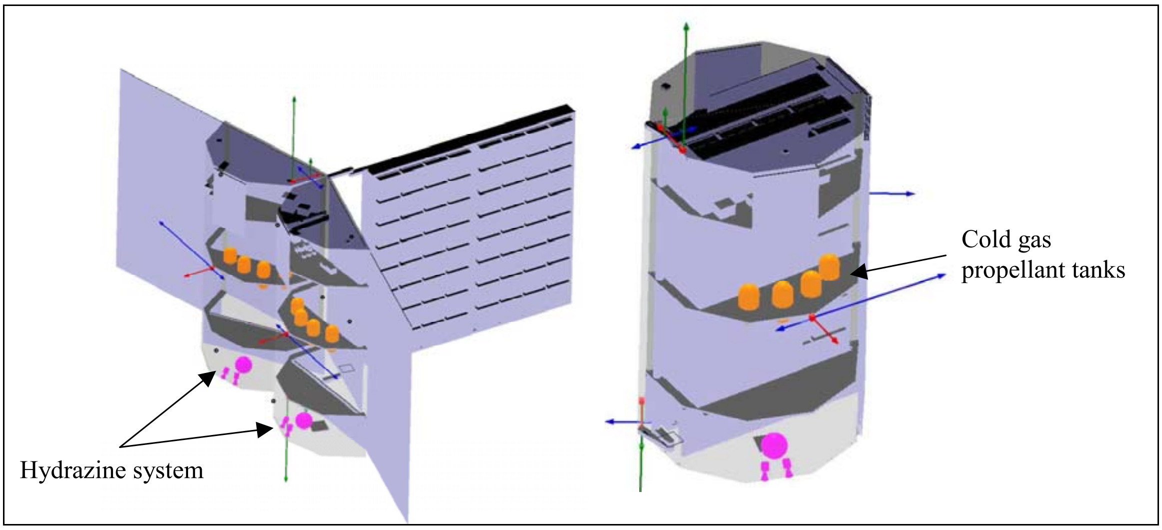

Figure 7-1: Overview of the MSC propulsion subsystems

The purpose of the XEUS propulsion subsystem is to provide adequate forces and torques during the mission lifetime (15 years) and to complete the following manoeuvres:

- Correct launcher dispersions
- Mid-course manoeuvres
- Trimming manoeuvres
- Halo orbit maintenance manoeuvres
- Off-load RWs and perform attitude control

Three propulsion phases are defined for the XEUS mission:

1. LEOP phase
2. Mid-cruise phase
3. On-station phase

The operation of the hydrazine propulsion subsystem is limited to phase 1 and phase 2 due to an upper level requirement, see PROREQ-01 in section 7.1, i.e. to avoid mirror contamination. When phase 1 and phase 2 are completed, closing the normally open latch valves isolates the hydrazine propulsion subsystem to minimise possible leakage and hence preventing payload/spacecraft contamination. The hydrazine propulsion subsystem comprises four 5 N thrusters in blow down mode using a diaphragm tank to minimise sloshing. To prevent the latch valve and FCV from clogging a 15-micron filter is placed downstream the propellant tank.

The main function of the cold gas propulsion system is to provide forces and torques to perform halo orbit maintenance, off-load reaction wheels and to perform attitude control. The cold gas propulsion subsystem comprises 28 thrusters (55mN) in two separate systems. Each system comprises seven thrusters in two branches. The reason for the high number of attitude control thrusters is due to the mission scenario (folded and deployed spacecraft) and the “unusual shape” of the spacecraft. Note that AOCS requires full attitude control during the complete mission and therefore a large number of thrusters are necessary.

Eight 89.5-litre nitrogen tanks provide the required propellant to the thruster assembly to complete the mission.

7.1 Requirements and design drivers

The following section outlines the system level requirements and design drivers for the propulsion subsystem for the baseline design i.e. direct injection into L2 using the European Ariane-5 launcher.

The main requirements (PROREQ) placed on the propulsion subsystem are:

PROREQ-01: The characteristics of the thrusters and their accommodation on the MSC shall not cause any adverse effects on either the satellite or the payload.

Discussion: A monopropellant and bipropellant system is ruled out due to contamination reasons. It cannot be fully established how a monopropellant/bipropellant system would impact the payload in terms of contamination. However, when using a monopropellant/bipropellant system, unburned propellant will probably come through the nozzle. This phenomenon typically occurs when the thrusters operate in pulse mode. Ion/Hall-Effect thrusters are ruled out due to the fact it is believed that charged particles can impinge or cause sputtering on the payload. Therefore, an inert cold gas propulsion system seems most feasible for attitude control and orbit correction when the MSC is fully deployed.

PROREQ-02: The propulsion system shall be as simple as possible and consume as little propellant as possible.

Discussion: In terms of performance, ion/Hall-Effect thrusters have far better specific impulse compared to chemical propulsion systems. Cold gas systems have the lowest performance.

PROREQ-03: The propulsion system used on station shall be able to produce 55 mN – 3N of thrust.

Discussion: A monopropellant and bipropellant system is ruled out. These chemical systems cannot perform in the required thrust range. 1 N to 5 N monopropellant thrusters are available off the shelf (COTS). However bipropellant thrusters are not available in the defined thrust range. Ion/Hall-Effect thrusters are ruled out because the maximum thrust is in the range of 80 mN. Cold gas thrusters seem most feasible. The performance of cold gas thrusters is in the specified range and COTS hardware is in most cases available. Note that MEMS technology cannot yet provide the required thrust.

PROREQ-04: The propulsion system used during LEOP and midcourse manoeuvres shall be able to produce 5 N to 20 N of thrust BOL.

Discussion: Cold gas is ruled out. Ion/Hall-Effect thrusters are ruled out. A mono/bipropellant seem feasible. See also above discussion.

7.2 Assumptions and trade-offs

According to the discussion in section 7.1, a monopropellant propulsion system is selected for the LEOP and mid-cruise phase to perform launcher dispersion, trimming and mid-cruise manoeuvres.

Moreover, a trade-off between an ion propulsion system and cold gas propulsion system shows that a cold gas propulsion system seems more favorable compared to ion engines. A number of characteristics/features of the two systems were marked from 1 to 5 where 5 is the best score (see Table 7-1). The marking of the different propulsion system features are discussed below.

Specific impulse: The performance of an ion engine is superior compared to a cold gas system. The specific impulse for a typical cold gas system using nitrogen gas as propellant is between 60 – 70 seconds depending on the thruster design, temperature and duty cycle, while the specific impulse for a typical ion engine is ~1500 seconds.

System / Feature	Cold gas	Ion
Specific Impulse	2	5
Thrust level (55mN – 3N)	3	1
Contamination	4	2
System complexity	*5*	*1*
Maturity level	5	5
Dry mass	2	4
Power demand	*5*	*1*
Cost	*4*	*1*
Availability in Europe	5	5
TOTAL SCORE =	**35**	**25**

Table 7-1: Trade-off between cold gas thrusters and ion engines

Thrust level: The required thrust level to provide the adequate torques and forces are between 55 mN and 3 N (defined by AOCS subsystem). The maximum thrust of the selected ion engine is approximately 80 mN while a typical cold gas system can provide the adequate forces in the defined thrust range.

Contamination: A cold gas nitrogen system is considered as inert and the contamination of the expelled nitrogen on the mirrors is considered negligible. However, an ion engine is considered to have a contamination effect on the mirrors in terms of sputtering and impingement with charged particles.

System complexity: In terms of system complexity it is clear that the ion propulsion system is much more complex compared to a simple cold gas system. Therefore, the cold gas marking is superior compared to the marking for the ion engine.

Maturity level: The technology readiness level for ion engines and cold gas propulsion system is believed to be 8 or 9. Therefore, the marking is equal to 5 for both options.

Dry mass: The dry mass of a propulsion system comprising 28 ion engines is lower compared to the total dry mass of a equivalent cold gas system (see Table 7-2). Therefore, the marking of the ion propulsion system is higher compared to the cold gas system.

XEUS Hall thrusters	PPS 1350 Dry mass			
	unit mass (kg)	n items	Total mass	
Thruster	4.0	28	112.0	kg
Neutraliser	0.5	28	14.0	kg
Low Pressure Flow Control Unit	0.4	28	11.2	kg
Low Pressure regulators and Pre card	4.0	2	8.0	kg
Power Supply and Control Unit (600 W)	8.0	14	112.0	kg
Switching Unit	0.5	8	4.0	kg
Filter Unit	0.5	28	14.0	kg
Harness &Tubing	1.0	28	28.0	kg
Orientation mechanisms	5.0	0	0.0	kg
Supporting Structure	1.0	28	28.0	kg
Tanks+structure	1.5	2	3.0	kg
TOTAL			334.2	kg

Table 7-2: Mass budget of an ion engine ACS using PPS 1350

Power demand: The cold gas system is superior to the ion engine in terms of required power. The cold gas system requires only a few watts. However, an ion engine of type PPS 1350 requires 600W.

Cost: It is believed that a cold gas system using COTS hardware is far cheaper compared to an ion engine system using COTS hardware and therefore the marking is higher for the cold gas system. Development cost is not taken into account here.

Availability in Europe: The technology for both options are available in Europe and therefore the marking is equal.

7.3 Baseline design

The baseline design of the monopropellant hydrazine system and the cold gas system is described in this section. The function as well as architecture is discussed.

7.3.1 Monopropellant hydrazine subsystem

The monopropellant propulsion system comprises two complete separate hydrazine subsystems due to the design of the MSC. In particular, the main reason for having two separate systems is due to the fact the propellant lines can not be drawn over hinges (see Figure 7-1).

Both hydrazine systems are identical and therefore only one of them is described hereafter. The hydrazine system operates in blow down mode with a propellant tank BOL pressure of 24.6 bar. The blow down ratio is here 4, which implies that the propellant tank EOL pressure is approximately 6.2 bar. The mean specific impulse is assumed to be 220 seconds because the thruster mainly operates in steady state firing (SSF) mode. Each thruster is capable of producing 5 N of thrust at BOL.

The propellant tank is equipped with (minimum) 1 pressure transducer and (minimum) 1 thermocouple/thermistor. The thermistor/thermocouple and pressure transducer serves two functions:

1. Health keeping and monitoring
2. Monitoring the propellant load in the tank using the PVT method

A 15-micron filter is placed downstream of the propellant tank to prevent clogging and mail function of the latch valve and FCV. The bi-stable latch valve is closed during launch, but nevertheless, propellant is present at the FCV inlet. A telemetry command opens the latch valve in the initial LEOP.

The FCV is a dual seat solenoid valve whose purpose is to supply the thruster with propellant. The FCV is mechanically and electrically redundant. Figure 7-2 shows an overview of the XEUS MSC hydrazine system.

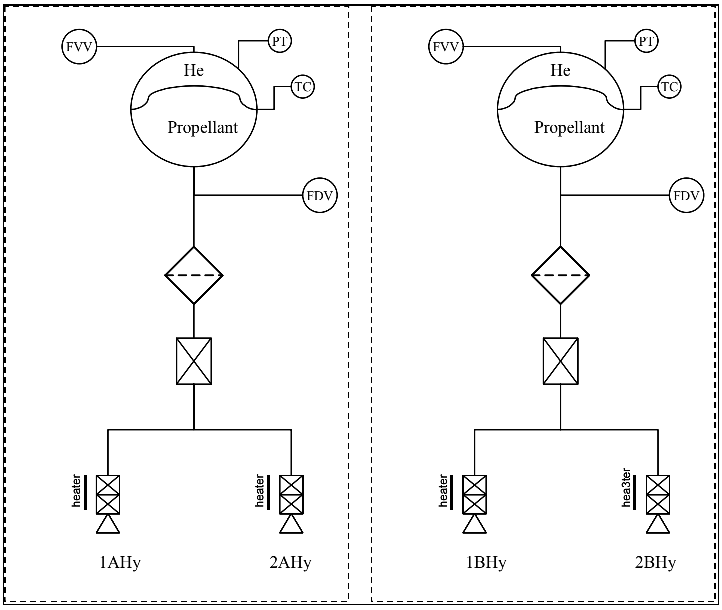

Figure 7-2: Hydrazine propulsion subsystem schematic

Most components are off the shelf (COTS hardware) and are available in Europe (EADS, SNECMA, RTG, Bradford etc).

7.3.2 Cold gas subsystem

The cold gas propulsion system comprises two complete separate cold gas systems: one in each cylinder half. The main reason for having two separate systems is because the propellant lines can not be drawn over hinges (see Figure 7-1).

Cold gas systems are basically solenoid or piezo valves operating at low pressure with a De Laval nozzle down stream. The system requires pressure regulators, pressure transducers, latch valves and heaters to maintain the gas in the operating range to not decrease the Isp too much.

The cold gas subsystem comprises four tanks (eight in total) filled with nitrogen gas at a pressure of 280 bar BOL. The propellant tanks are equipped with pressure transducers and thermocouples to serve two functions:

1. Health keeping and monitoring
2. Monitoring the propellant load in the tank using the PVT method

An overview of the cold gas subsystem is shown in Figure 7-3. Note that the subsystem comprises two branches, each branch equipped with seven thrusters. Two pressure regulators, adjust the up stream pressure to 2 bar, which is enough to feed the thrusters so that the chamber pressure is approximately 1.1 bar. Each branch of thrusters can be isolated using the upstream bi-stable latch valve.

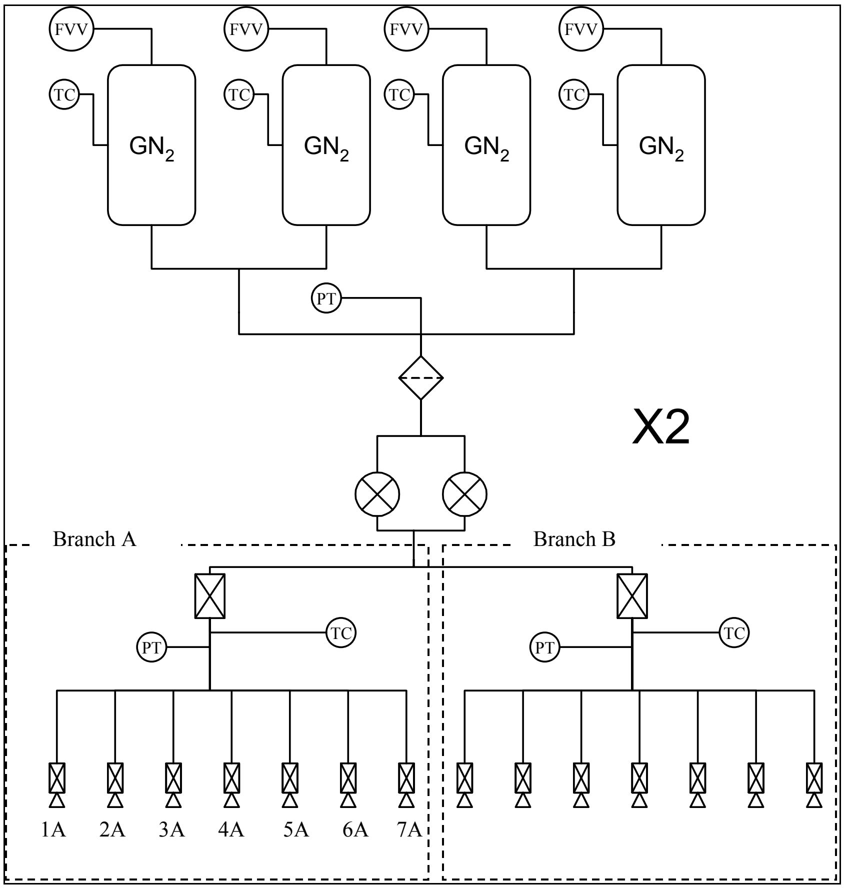

Figure 7-3: Cold gas propulsion subsystem schematic

The AOCS requires 28 cold gas thrusters in total, to be able to perform torques and forces in all six degrees of freedom. The current design encompass two "sets" of cold gas thrusters: one set is used to perform AOC (attitude and orbit control) during LEOP and mid-cruise and when the MSC is folded (see right-hand side of Figure 7-4). The second set of cold gas thrusters are used to perform AOC during on-station i.e. mirror unfolded (see left-hand side of Figure 7-4).

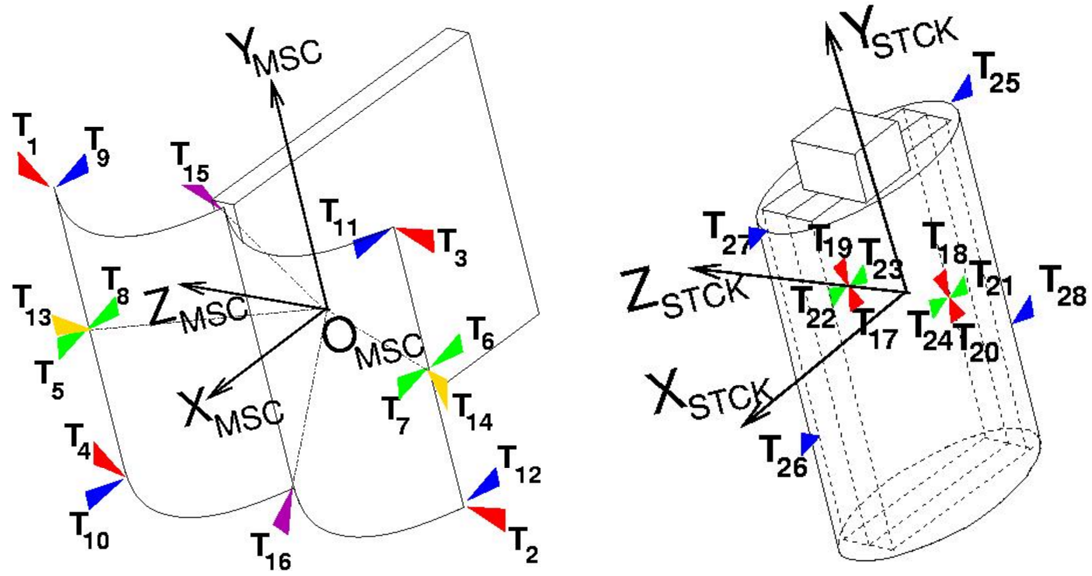

Figure 7-4: MSC cold gas thruster locations

Cold gas systems have been developed mainly in the United States. European expertise however exists (for example, Polyflex, Bradford, Laben). A 55 mN European cold gas thruster should however be developed.

7.4 Future developments

This section outlines future developments on cold gas generators and cold gas micro thrusters, i.e. MEMS technology.

7.4.1 Cold gas generator of nitrogen

Cold gas generators come from the airbag concept in which the gas is released at high pressure by ignition of a chemical reaction. The gas is stored in solid cartridges and then released in a small plenum.

The advantages compared to conventional nitrogen storage systems come from the reduction of the volume (20 < 50 %) and of the dry mass (20 < 50%) of the nitrogen-pressurised tank. The system has been developed by Bradford (NL) and will be tested in the PROBA 2 satellite (COGEX experiment).

7.4.2 Cold gas micro thrusters

Cold Gas Micro thrusters (CGMT) are under development by ACR Electronics at the Ångström Space Technology Center (ÅSTC) in Uppsala, Sweden. The micro thruster system is built using highly integrated MEMS technology; the internal structure of the thruster consists of four silicon wafer-stacks with different functions. The gas-handling module contains microstructures for all gas handling functions, including nozzles, channels, filters and valves. Analogue electronics and interconnections are located in the analogue module, while the processor module holds the micro controller chips and related circuits. The interface module includes filters, electrical I/F and other electronics. The gas handling wafers contain microstructures for all gas handling functions, including nozzles, channels, valves and pressure-sensors. A cross-section of the gas-handling unit is shown in Figure 7-5:

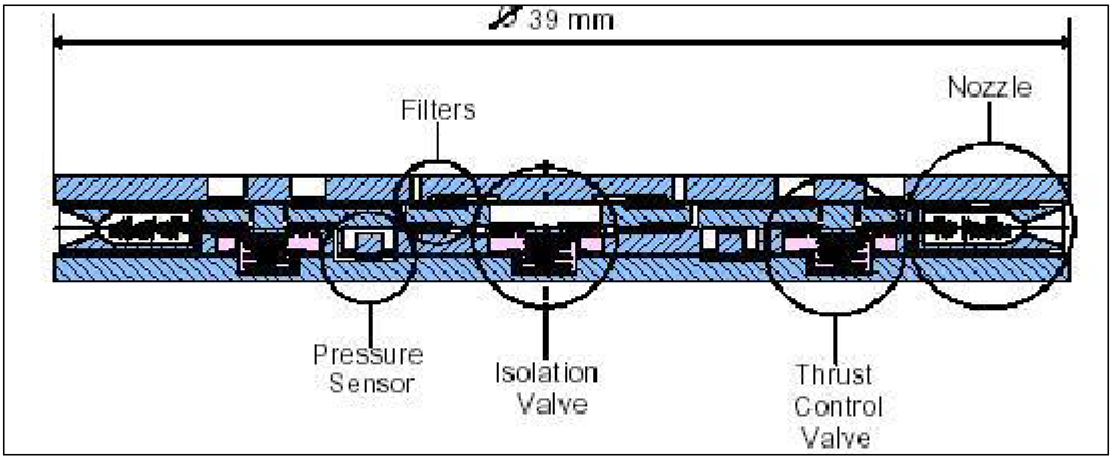

Figure 7-5: Cross-section of the gas handling unit

The CGMT thrust range is expected between 5 mN and 1 µN. The main advantage of the CGMT over conventional cold gas system is the specific impulse. The Isp of 110s (heated gas) is a major improvement compared to 60 seconds for conventional cold gas system technology.

7.4.3 Small electric propulsion thrusters

FEEP thrusters have not been taken into consideration due to the contamination concern of the caesium plume towards the mirrors of the MSC.

In the past, small xenon ion thrusters in the range of 0.5 –2 mN have been built at laboratory level (EADS) with a size 2- 4 cm of diameter. The Isp of these systems is 30 times higher (1500 s) than cold gas system (50 s). Moreover it is possible to throttle the thrust in the range with fine tuning.

Ion thruster technology is well known in Europe and Japan and flight HW is flown on board Artemis. For BepiColombo, ion thrusters are planned as baseline. Small xenon Hall Effect thrusters are now under development at ALTAS (I). The thrust range is between 1-4 mN. The power consumption is below 100W and the Isp is around 1000 s. Hall thruster technology is well known in Europe and flight HW is flown on SMART-1.

7.5 Budgets

This section outlines the various budgets for the XEUS MSC propulsion subsystems. The budgets presented are the ΔV budget; dry mass budget, propellant budget and finally an overall mass budget for the MSC.

7.5.1 ΔV budget

The following ΔV budget has been considered for the MSC. Table 7-3 shows a summary of the manoeuvres required by the XEUS MSC propulsion subsystems. The hydrazine propulsion subsystem performs the launcher dispersion, mid-cruise and trimming manoeuvres, in total 28 m/s, while the cold gas system is required to perform AOC and halo-orbit maintenance, in total 18 m/s. Moreover, the cold gas systems are also required to off-load reaction wheels and to perform attitude control during the mission. The required total impulse for these manoeuvres are ~ 38 kNs.

Mission phase	**ΔV (m/s) nominal**	**Required impulse (Ns)**	**Remark**
Launcher dispersions	25	-	Both A5 and Delta IV
Mid-course manoeuvres	1	-	
Trimming manoeuvre	2	-	
AOC (spin/de-spin etc)	3	-	
Halo orbit Maintenance	15	-	1 m/s per year
Off-load RWs and attitude control	-	38349	

Table 7-3: Summary of the ΔV budget

Note that it is assumed that the ΔV required for launcher dispersions is equal for both launchers, Ariane-5 and Delta IV.

7.5.2 Propellant budget

The hydrazine and nitrogen propellant budget is presented in this section. Table 7-4 and Table 7-5 show the baseline design for the Delta IV launcher and Ariane-5 launcher option.

7.5.3 Cold gas subsystem

The cold gas propellant budget for the Delta IV option is shown in Table 7-4. The major part of the nitrogen gas required comes from the ΔV manoeuvres (73.6%), while the remaining 26.4% represents the necessary nitrogen gas for the impulse requirement. In total, including a 5% propellant margin, 231.3 kg of nitrogen are required to complete the mission.

Propellant mass breakdown			
Impulse contribution	58.1 kg	=	26.4%
dV contribution	162.2 kg	=	73.6%
Margin	5%		
Total	**231.3 kg**		

Table 7-4: Cold gas subsystem propellant budget mass budget (Delta IV option)

The cold gas propellant budget for the baseline design (Ariane-5) is shown in Table 7-5. Again, the major part of the propellant budget comes from the ΔV manoeuvres (69.5%), while the remaining 30.5% comes from the impulse manoeuvres required by the cold gas system. In total, including a 10% margin, 205.8 kg of nitrogen is necessary to complete the mission.

Propellant mass breakdown			
Impulse contribution	58.1 kg	=	30.5%
dV contribution	132.6 kg	=	69.5%
Margin	10%		
Total	**205.8 kg**		

Table 7-5: Cold gas subsystem propellant budget mass budget (Ariane-5)

7.5.4 Hydrazine subsystem

The hydrazine propellant budget for the Delta IV option is shown in Table 7-6. The purpose of the hydrazine system is to provide adequate forces and ΔV for the LEOP and mid-cruise phase. Therefore, no impulse requirement is placed on the hydrazine system. The required propellant mass for the Delta IV option is 104.3 kg.

Propellant mass breakdown			
Impulse contribution	0.0 kg	=	0.0%
dV contribution	99.4 kg	=	100.0%
Margin	5%		
Total propellant mass=	**104.3 kg**		

Table 7-6: Hydrazine subsystem propellant budget mass budget (Delta IV option)

The hydrazine propellant budget for the baseline design (Ariane-5) is shown in Table 7-7. The total propellant mass required is 88.5 kg including a 5% margin.

Propellant mass breakdown			
Impulse contribution	0.0 kg	=	0.0%
dV contribution	85.4 kg	=	100.0%
Margin	5%		
Total propellant mass=	**88.5 kg**		

Table 7-7: Hydrazine subsystem propellant budget mass budget (Ariane-5)

7.5.5 Dry mass budget

In this section the dry mass budget for both the cold gas subsystem and the hydrazine subsystem is described.

7.5.5.1 Cold gas subsystem

The cold gas dry mass budget for the Delta IV option is shown in Table 7-8. Note that this budget corresponds to two identical cold gas systems. The major part of the total mass, 172 kg, is the massive propellant tanks. The mass of all eight tanks corresponds to 70.8% (121.8 kg) of the total mass.

Component mass breakdown					
	Units	mass/unit	Total mass		
Thruster (CG)	28	0.3	8.4	=	4.9%
Filter (CG)	2	0.3	0.6	=	0.3%
Latch Valve (CG)	4	0.5	2.0	=	1.2%
Pipe work (CG)	2	12.0	24.0	=	14.0%
HP regulator (CG)	4	1.5	6.0	=	3.5%
FVV (CG)	8	0.5	4.0	=	2.3%
TC (CG)	28	0.1	2.8	=	1.6%
PT(CG)	24	0.1	2.4	=	1.4%
Propellant Tank (CG)	8	15.2	121.8	=	70.8%
		Total drymass =	**172.0**	**kg**	

Table 7-8: Cold gas component mass budget (Delta IV option)

The cold gas dry mass budget for the baseline design (Ariane-5) is shown in Table 7-9. The major part of the total mass, 157.1 kg, is the massive propellant tanks. The mass of all eight tanks corresponds to 68.1% (106.9 kg) of the total mass.

Component mass breakdown					
	Units	mass/Unit	Total mass		
Thruster (CG)	28	0.3	8.4	=	5.3%
Filter (CG)	2	0.3	0.6	=	0.4%
Latch Valve (CG)	4	0.5	2.0	=	1.3%
Pipe work (CG)	2	12.0	24.0	=	15.3%
HP regulator (CG)	4	1.5	6.0	=	3.8%
FVV (CG)	8	0.5	4.0	=	2.5%
TC (CG)	28	0.1	2.8	=	1.8%
PT(CG)	24	0.1	2.4	=	1.5%
Propellant Tank (CG)	8	13.4	106.9	=	68.1%
		Total drymass =	**157.1**	**kg**	

Table 7-9: Cold gas subsystem component mass budget (Ariane-5)

7.5.5.2 Hydrazine subsystem

The hydrazine dry mass budget for the Delta IV option is shown in Table 7-10. The total dry mass for two systems is 25.2 kg. The propellant tanks dry mass adds up to 11.4 kg, which is equivalent to 45.4% of the total, dry mass.

Component mass breakdown	mass/Unit	Units	Total mass		
Thruster (MP)	0.2	4	0.9	=	3.5%
Filter (MP)	0.1	2	0.2	=	0.8%
Latch valve (MP)	0.5	2	1.0	=	4.0%
Pipe work (MP)	5.0	2	10.0	=	39.6%
FVV(MP)	0.1	2	0.2	=	0.8%
FDV(MP	0.2	2	0.3	=	1.2%
PT(MP)	0.1	6	0.6	=	2.4%
TC(MP)	0.1	6	0.6	=	2.4%
Propellant tank(MP)	5.7	2	11.4	=	45.4%
	Total dry mass =		**25.2**	**kg**	

Table 7-10: Hydrazine subsystem component mass budget (Delta IV option)

The hydrazine dry mass budget for the baseline design (Ariane-5) is shown in Table 7-11. The total dry mass is 23.6 kg including two propellant tanks of 4.9 kg each.

Component mass breakdown	mass/Unit	Units	Total mass		
Thruster (MP)	0.2	4	0.9	=	3.7%
Filter (MP)	0.1	2	0.2	=	0.8%
Latch valve (MP)	0.5	2	1.0	=	4.2%
Pipe work (MP)	5.0	2	10.0	=	42.5%
FVV(MP)	0.1	2	0.2	=	0.8%
FDV(MP	0.2	2	0.3	=	1.3%
PT(MP)	0.1	6	0.6	=	2.5%
TC(MP)	0.1	6	0.6	=	2.5%
Propellant tank(MP)	4.9	2	9.8	=	41.5%
	Total dry mass =		**23.6**	**kg**	

Table 7-11: Hydrazine subsystem component mass budget (Ariane-5)

7.5.6 Overall budget and summary

In this section the overall mass budget is described. The baseline design (Ariane-5) and the Delta IV option are presented.

7.5.6.1 Cold gas subsystem

The cold gas subsystem overall mass budget for the Delta IV option is shown in Table 7-12. The dry mass is 172 kg and the propellant mass is 403.3 kg.

Mass budget			
Dry mass =	172.0 kg	=	43%
Propellant mass =	231.3 kg	=	
Total wet mass =	**403.3 kg**		

Table 7-12: Cold gas subsystem total mass budget (Delta IV option)

The cold gas subsystem overall mass budget for the baseline design (Ariane-5) is shown in Table 7-13. The total wet mass is 362.9 kg and comprises 159.8 kg dry mass and 205.8 kg of nitrogen gas.

Mass budget			
Dry mass =	157.1 kg	=	43%
Propellant mass =	205.8 kg	=	57%
Total wet mass =	**362.9 kg**		

Table 7-13: Cold gas subsystem total mass budget (Ariane-5)

7.5.6.2 Hydrazine subsystem

The hydrazine subsystem overall mass budget for the Delta IV option is shown in Table 7-14. The total wet mass including 0.1 kg pressurant (helium) is 129.7 kg. The propellant mass required is 104.3 kg divided in two tanks.

Mass budget			
Dry mass =	25.2 kg	=	19.4%
Propellant mass =	104.3 kg	=	80.4%
Pressurant mass =	0.1 kg	=	0.1%
Total wet mass =	**129.7 kg**		

Table 7-14: Hydrazine subsystem total mass budget (Delta IV option)

The hydrazine subsystem overall mass budget for the baseline design is shown in Table 7-15. The total wet mass for the hydrazine subsystem is 112.2 kg including 0.1 kg of pressurant (helium).

Mass budget				
Dry mass =	23.6 kg		=	21.0%
Propellant mass =	88.5 kg		=	78.9%
Pressurant mass =	0.1 kg		=	0.1%
Total wet mass =	**112.2 kg**			

Table 7-15: Hydrazine subsystem total mass budget (Ariane-5)

7.6 List of equipment

The list of equipment for the cold gas subsystem as well as the hydrazine subsystem is described in section 7.5.5. Most components are off the shelf and but may need additional qualification testing for the XEUS mission scenario. However, new propellant tank development is probably needed for the cold gas system. Figure 7-6 shows off-the-shelf hardware in terms of hydrazine thrusters:

Figure 7-6: COTS hardware (EADS hydrazine thrusters)

Figure 7-7 shows a wide variety of off-the-shelf cold gas thrusters available in the United States. The thrust range here is between a few milli-Newtons to tens of milli-Newtons.

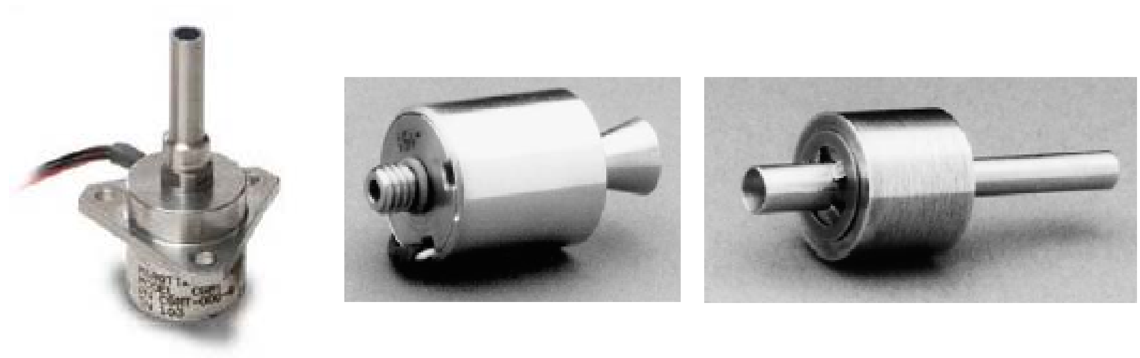

Figure 7-7: Off-the-shelf cold gas thrusters from Marotta (left), Moog (middle) and Moog (right)

7.7 Options

The design presented in this chapter is a preliminary baseline design of the propulsion subsystem for the XEUS mission MSC spacecraft. The design and choice of propulsion subsystem for this mission is still subject for change.

Currently, ESA and other space agencies around the world are investigating low-toxicity high-performance monopropellants. These monopropellants are expected to increase the specific impulse (240 seconds) and density (1300 kg/m^3) compared to conventional hydrazine systems. High-performance green monopropellants can therefore be considered as an option to the hydrazine system presented here.

Moreover, MEMS technology thrusters are now being developed in Sweden and in other countries. MEMS technology offers a significant increase in the specific impulse compared to conventional cold gas systems should therefore not be excluded as a possible attitude control system option.

8. AOCS

This section presents a preliminary MSC AOCS architecture. The assumptions made for the preliminary sizing calculations are given together with their justification.

8.1 Requirements and design drivers

The system level requirements are presented in section 4.1. The preliminary error budget allocations for the AOCS subsystems are given in section 8.3.3. The most important design driver for the MSC AOCS has been simplicity and commonality with “classical” AOCS.

8.2 Assumptions, features and trade-offs

The MSC AOCS has a “classical” AOCS architecture. The sensors on the MSC are six coarse Sun sensors (CSS), four gyros, and two star trackers (STR). The actuators are four reaction wheels (RW) and the thrusters of the reaction control systems (RCS).

8.3 Baseline design

8.3.1 Thruster placement

One peculiar design feature of the MSC is the dual RCS made of hydrazine and cold gas RCSs. The hydrazine RCS is used for launch dispersion corrections and cruise manoeuvres, while the cold gas RCS is used for RW angular momentum dumping and halo orbit maintenance. The dual hydrazine/cold gas RCS is justified by the requirement to avoid the contamination of the mirror petals with hydrazine.

Another peculiar design feature of the MSC arises from the fact that the spacecraft has an axisymmetrical shape in the stowed configuration, i.e. during the cruise, and a strongly asymmetrical shape in the deployed configuration, i.e. during the observation mode. This leads to a non-optimal placement of the thrusters, as shown in Figure 8-1. The thrusters’ placement can be improved so that a subset of thrusters is used in both modes. The hydrazine thrusters are not shown (see Figure 8-1).

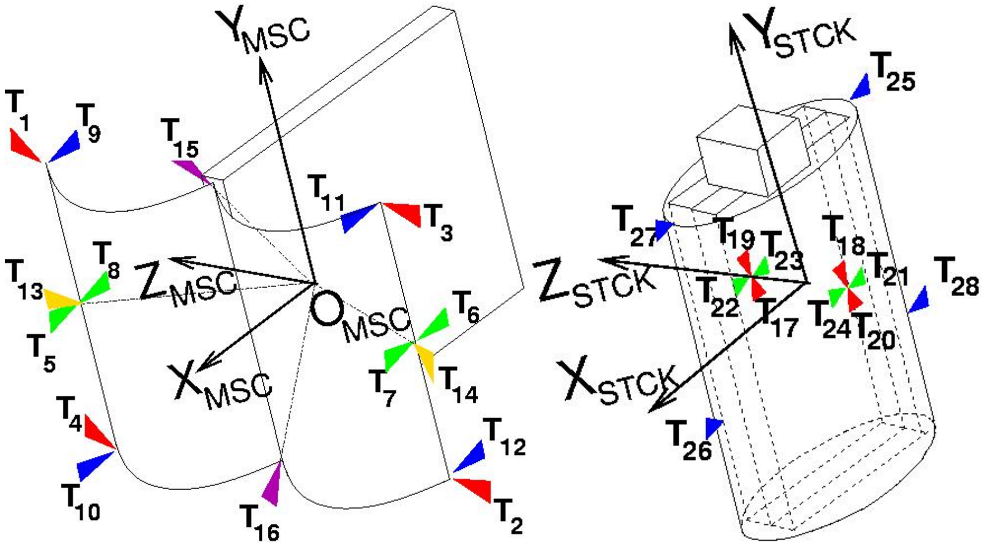

Figure 8-1: Placement of the thrusters for observation mode (left) and cruise or stack mode (right)

The hydrazine thrusters are not shown in the cruise configuration. They provide thrust in the +YSTCK axis. Note that the MSC will provide the control torques and forces for the stack during cruise and pre-deployment as explained in section 15.1.

During the cruise, the stack will roll, at a slow rate, about the Y_{STCK} axis. The STRs mounted on the Y+ face of the spacecraft on the MSC determine the attitude of the stack. During this part of the mission the attitude profile of the stack has to be such that the STR does not point towards the Sun, Earth, or the Moon taking into account that the STRs can be baffled to about 15°. (Only one STR is employed - the second STR is in a cold standby state.) The gyros are used to determine a departure from the slow roll rate of the stack. An uncommanded departure from the slow roll rate will trigger a stack emergency Sun acquisition manoeuvre. The CSSs might also be used to determine the departure of the stack from the slow roll rate.

The RWs are employed during cruise to reject perturbations and to control the attitude manoeuvres needed prior to the trajectory corrections. The angular momentum of the RWs should be dumped before the hydrazine thrusters are switched on to prevent triggering a momentum dump manoeuvre during the TCM.

It is assumed that during cruise, standby, and nominal modes the AOCS of the MSC has to counteract the effect of the torque generated by the SRP. For this purpose the MSC employs a set of three RWs. A fourth RW wheel is in a cold standby state. The angular momentum accumulated in the RWs is dumped using the cold gas RCS. The RWs are also used for the MSC slew manoeuvre, in the target acquisition mode.

8.3.2 Reaction wheel sizing

A comparison between the angular momentum accumulated during a slew manoeuvre and that accumulated to counteract the SRP torque has been performed.

The assumptions were:

- MSC mass properties:
  - $m_{MSC} = 4880$ kg
  - $I_{xx} = 31460$ kg m^2
  - $I_{yy} = 19550$ kg m^2
  - $I_{zz} = 15580$ kg m^2
- MSC cross sectional area $A_c = 49$ m^2
- MSC reflectivity coefficient k = 1.0
- Moment arm of the SRP torque $l_{SRP} = 0.3$ m
- Moment arm of the thrusters torque $l_f = 4.0$ m
- Maximum continuous observation time $t_{obs} = 3.5$ days
- Duration of the telescope slew manoeuvre $t_{slew} = 45$ min
- Slew angle $\theta_{slew} = 90°$
- Axis of the slew manoeuvre X

The telescope slew manoeuvre is performed using a *bang-bang* command of the reaction wheels. The fastest manoeuvre is performed such that the MSC slews half the angle in half of the time. During the slew manoeuvre the MSC RWs will accumulate zero or very little angular momentum. The maximum angular momentum, reached at the middle of the slew manoeuvre, is compared to that accumulated during the 3.5 days of observation.

The formula for the SRP force is $F_{SRP} = (k+1)\Phi A_c/c$, where k is the reflectivity coefficient, $\Phi = 1340$ W/m^2 is the solar radiation flux at L2, A_c is the cross-sectional area of the spacecraft, and c is the speed of light in vacuum.

With these assumptions the angular momentum accumulated during observation is estimated at $h_{SRP} = 39.7$ Nms and the maximum angular momentum reached during the telescope slew manoeuvre is $h_{slew} = 36.6$ Nms. Thus the RWs on the MSC were sized with a slight safety factor to have the capacity to accumulate an angular momentum of h_{RW}=40 Nms. A mid capacity RW from Teldix, with a momentum storage capability of 50 Nms, has been selected for this purpose. A detailed mission study should give accurate estimates on the SRP torque lever arm and moments of inertia. It is possible that the assumptions made, especially with regards to the lever arm of the SRP are rather pessimistic.

The total impulse, needed to dump the angular momentum, is needed to calculate the propellant mass. Assuming that 5% of the mission life of 20 years is dedicated to RW momentum dumping the total impulse is approximately 2.0×10^4 Ns. The number of momentum dumps is N=1982. It has been assumed that the duration of a momentum dump is \$10s\$ which gave a thruster force of 1 N.

8.3.3 Error budget allocation and performance analysis

The results of a error budget allocation and performance analysis are presented in Table 8-1 to Table 8-4. Table 8-1 presents the results of the MSC inertial pointing error budget allocation. Table 8-2 presents the results of the telescope (DSC to MSC) displacement error budget allocation. Note that the results in Table 8-2 are based on preliminary best engineering guesses since no test results are available for the optical lateral metrology packages. A proportional-integral-derivative (PID) controller was studied for both cases. In the tables S stands for systematic errors, LT for long-term errors and ST for short term or random errors.

	S(as)	LT(as)	ST(as)	Overall	Comments
Calibration method error	4/20	-	-	-	Allocated to ground operations to eliminate the 1 g to 0 g, ageing, testing and launch loads
Thermoelastic (STR to P/L)	-	20/20	-	-	Budgeted to configuration and structures
STR bias and drift	2/10	-	-	-	Manufacturer specs
Control system errors	-	-	0.5/2.0	-	From noise transmission (linear covariance) analysis
High freq. jitter	-	-	0.25/0.5	-	RW quantisation errors
Total	4.47/22.36	20/20	0.56/2.06	**25.03/44.42**	Algebraic sum on the row / RMS on the columns
Requirement				60/3600	Achievable

Table 8-1: MSC Pointing error budget (x,y/z)

	S(as)	LT(as)	ST(as)	Overall	Comments
Calibration method error	4/20	-	-	-	Allocated to ground operations to eliminate the 1 g to 0 g, ageing, testing and launch loads
Thermoelastic (STR to P/L)	-	-	-	-	Budgeted to configuration and structures
STR bias and drift	2/10	-	-	-	Manufacturer specs
Processing error	-	-	2/5	-	From noise transmission (linear covariance) analysis
Total	4.47/22.36	-	2/5	**6.37/27.36**	Algebraic sum on the row / RMS on the columns
Requirement				10/60	Achievable

Table 8-2: MSC Measurement error budget (x,y/z)

	S (mm)	LT (mm)	ST(mm)	Overall	Comments
Calibration method error	0.05/0.05/0.1	-	-	-	Allocated to ground operations to eliminate the 1 g to 0 g, ageing, testing and launch loads
Thermoelastic (MSC)	-	0.1/0.1/0.1	-	-	Budgeted to configuration and structures
Thermoelastic (DSC)	-	0.1/0.1/0.1	-	-	Budgeted to configuration and structures
Laser metrology bias and drift	0.05/0.05/0.1	-	-	-	Specs
Control system errors	-	-	0.1/0.1/0.1	-	From noise transmission (linear covariance) analysis
High freq. jitter	-	-	0.05/0.05/0.05	-	RW quantisation errors
Total	0.071/0.071/0.14	0.14/0.14/0.14	0.14/0.14/0.14	**0.35/0.35/0.42**	Algebraic sum on the row / RMS on the columns
Requirement				1/1/5	Achievable

Table 8-3: Telescope displacement error (x/y/z)

	S (mm)	LT (mm)	ST(mm)	Overall	Comments
Calibration method error	0.05/0.05/0.1	-	-	-	Allocated to ground operations to eliminate the 1 g to 0 g, ageing, testing and launch loads
Thermoelastic (MSC)	-	0.1/0.1/0.1	-	-	Budgeted to configuration and structures
Thermoelastic (DSC)	-	0.1/0.1/0.1	-	-	Budgeted to configuration and structures
Laser metrology bias and drift	0.05/0.05/0.1	-	-	-	Specs
Processing error	-	-	0.05/0.05/0.05	-	From noise transmission (linear covariance) analysis
Total	0.071/0.071/0.14	0.14/0.14/0.14	0.05/0.05/0.05	**0.26/0.26/0.33**	Algebraic sum on the row / RMS on the columns
Requirement				0.33/0.33/0.75	Achievable

Table 8-4: Telescope displacement error (x/y/z)

8.4 AOCS equipment list and mass and power budgets

This section presents the mass and power budgets of the AOCS units. Table 8-5 shows the MSC AOCS part list, and mass and power budget. The mass and the power are listed per unit and the power value listed for the RWs is that at the nominal level. The peak power level for the RWs is 100W.

AOCS equipment	# of units	Mass/unit (kg)	Power (W)	Supplier
Autonomous star tracker	2	7.5	15	Officine Galileo
Rate sensor	4	1.0	1	Laben
Course Sun sensor or attitude anomaly detector (AAD)	6	0.15	-	TNO-TPD
Reaction wheel	4	12	10	Teldix
RF navigation	Included in communication subsystem			
AOCS interface unit	Included in CDandH subsystem			
Failure detection and correction electronics uint (FDCE)	Included in the CDandH subsystem			

Table 8-5: MSC AOCS part list, and mass and power budget

8.5 DSC propellant use during telescope slew

This section presents the derivation of the formulas used to compute the propellant needed by the DSC to perform a translation on a circular arc during the XEUS telescope slew manoeuvres. The formulas are derived from basic curvilinear motion equations so they are applicable to any spacecraft moving on a circular arc in force-free environment.

8.5.1 Assumptions and problem set up

The main assumption made is that the spacecraft moves in a force-free environment, typical of the halo orbit at L2. The other assumption is that the motion is planar, i.e. there is no motion in the direction perpendicular to the plane of the slew. The motion of the DSC is on a circular arc of angle θ_f and radius d_f. The DSC translates from the initial to the final position on the arc over the time interval $t_{f,}$ i.e. the telescope slew time is $t_{f,}$. The initial and final angular velocities of the DSC are null. The control is bang-on bang-off for the fastest possible manoeuvre. This results in the DSC translating over the first half of the arc in half the time.

8.5.1.1 Equations of motion

The equations of motion of the point mass in a cylindrical reference frame Hibbler are:

$$\boxed{\begin{aligned} a_r &= \ddot{r} - r\dot{\theta}^2 \\ a_\theta &= r\ddot{\theta} + 2\dot{r}\dot{\theta} \\ a_z &= \ddot{z}, \end{aligned}}$$

Equation 1

where a_r, a_θ, and a_z are the components of the acceleration vector in the cylindrical reference frame, *r* is the distance from the point mass to the origin of the reference frame, θ is the azimuth angle, and *z* is the height measured from the origin of the reference frame.

Since the assumption is that the motion is on a circular arc the radius, $r = d_f$ = const and z=0 in Equation 1 become:

$$\boxed{\begin{aligned} a_r &= -d_f\dot{\theta}^2 \\ a_\theta &= d_f\ddot{\theta} \\ a_z &= 0. \end{aligned}}$$

Equation 2

For the sake of brevity Equation 2 is not carried further.

8.5.1.2 Translation commands

The translation of the DSC on a circular arc will be commanded in terms of accelerations (thrusts) given by Equation 2. This study proposes that the angular acceleration is kept at its maximum value for the first half of the arc and then it is reversed for the second half of the arc. The value of the angular acceleration is thus

$$\boxed{\ddot{\theta} = \begin{cases} 4\frac{\theta_f}{t_f^2} & \text{when } 0 \leq t < t_f/2, \\ -4\frac{\theta_f}{t_f^2} & \text{when } t_f/2 \leq t \leq t_f, \end{cases}}$$

Equation 3

which gives Equation 4.

$$\boxed{a_\theta = \begin{cases} 4d_f\frac{\theta_f}{t_f^2} & \text{when } 0 \leq t < t_f/2, \\ -4d_f\frac{\theta_f}{t_f^2} & \text{when } t_f/2 \leq t \leq t_f. \end{cases}}$$

Equation 4

To obtain the acceleration profile in the radial direction the value of the angular rate θ. This is obtained from integration of Equation 2 with the following initial conditions:

$$\boxed{\begin{aligned} &\dot{\theta} = 0, \text{ at } t = 0 \\ &\dot{\theta} = 2\theta_f/t_f, \text{ at } t = t_f/2. \end{aligned}}$$

Equation 5

The integration of Equation 2 with the ICs in Equation 5 gives:

$$\dot{\theta}(t) = \begin{cases} 4\frac{\theta_f}{t_f^2}t & \text{when } 0 \le t < t_f/2, \\ 4\frac{\theta_f}{t_f}\left(1 - \frac{t}{t_f}\right) & \text{when } t_f/2 \le t \le t_f. \end{cases}$$

Equation 6

Replacing Equation 6 in Equation 2 gives the expression of the radial acceleration as a function of time:

$$a_r(t) = \begin{cases} -16d_f\left(\frac{\theta_f}{t_f^2}t\right)^2 & \text{when } 0 \le t < t_f/2, \\ -16d_f\left[\frac{\theta_f}{t_f}\left(1 - \frac{t}{t_f}\right)\right]^2 & \text{when } t_f/2 \le t \le t_f. \end{cases}$$

Equation 7

8.5.1.3 Total impulse and propellant use

The forces needed to move the DSC on the circular are obtained by multiplying Equation 4 and Equation 7 with the mass of the DSC. To calculate the total impulse the value of the force is integrated over the manoeuvre time $\boxed{I_{tot} = \int_0^{t_f} F(t)dt.}$ The propellant mass is then calculated with the formula given by $\boxed{m_{prop} = \frac{I_{tot}}{I_{sp}g},}$ where I_{sp} is the specific impulse of the propulsion system and g = 9.81 m/s^2 is the average gravitational acceleration on Earth.

The forces obtained from Equation 4 and Equation 7 are integrated over the duration of the manoeuvre to give the following total impulses:

$$I_{tot,\,\theta} = 4md_f\frac{\theta_f}{t_f},$$
$$I_{tot,\,r} = \frac{4}{3}md_f\frac{\theta_f^2}{t_f},$$

Equation 8

where $I_{tot,\theta}$ is the total impulse of F_θ and $I_{tot,r}$ is the total impulse of F_r. The total impulse for the manoeuvre is then:

$$I_{tot} = 4md_f\frac{\theta_f}{t_f}\left(\frac{\theta_f}{3} + 1\right)$$

Equation 9

8.5.1.4 Results

For a DSC mass m = 1750 kg, a manoeuvre time t_f = 2700 s (=45min), a slew angle θ_f = 90º, and a focal length d_f = 50 m the total impulse is I_{tot} = 310.2 Ns. Assuming that a cold gas reaction control system (RCS), with I_{sp}= 50 s, then the mass used for the manoeuvre is m_{prop} = 0.632 kg.

The peak forces applied by the RCS are $F_{r,max}$ = 118.25 mN and $F_{\theta,max}$ = 75.4 mN. The time variation of the radial F_r and angular F_θ command forces is shown in Figure 8-2.

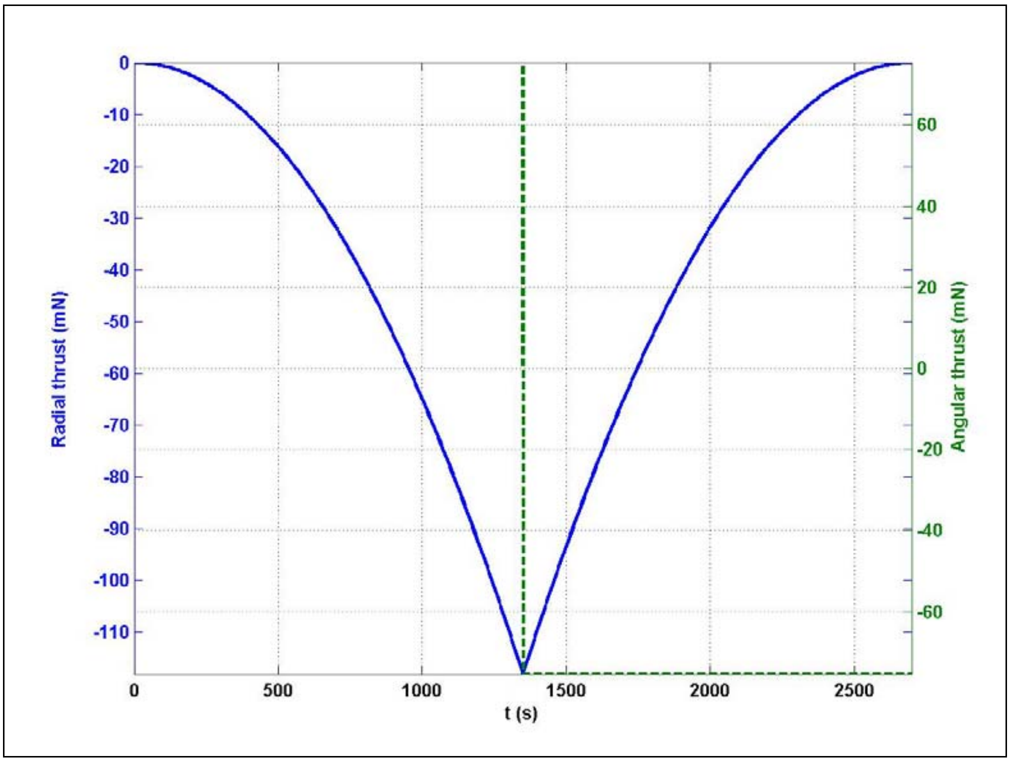

Figure 8-2: Variation of the radial and angular command forces of the DSC

8.5.1.5 Linear translation manoeuvre

In this section the translation along a straight line is compared to that on the circular arc studied above. The line stretches the circular arc of angle θ_f, i.e., the line and the arc start and end points coincide. The length of the line is 70.71 m. Assuming the same type of manoeuvre, half of the distance in half the time, the acceleration is $a_{lin} = 4\ l_f / t_f^2$. The total impulse for this manoeuvre is then $I_{tot,\ lin} = 4\ m\ l_f / t_f$.

For the same conditions as above the linear manoeuvre for the DSC has a total impulse I_{tot} = 183.3Ns and the propellant mass used is m_{prop} = 0.374 kg. The peak force for the linear manoeuvre is $F_{l,max}$ = 68mN.

8.5.1.6 Conclusions

The analysis of two types of manoeuvre shows that the translation manoeuvre on a straight line is more propellant efficient than a translation on a circular arc. The propellant saving is of the order of 40%. The advantages and disadvantages of each type of manoeuvre should be analysed in a further study.

8.6 FDIR approach

The FDIR approach for the MSC is typical. During the nominal observation mode the CSSs, also called attitude anomaly detectors (ADDs), detect any uncommanded departure from the set attitude. Once the anomaly is detected the MSC performs an emergency Sun acquisition manoeuvre and enters a spacecraft safe mode. It is assumed that during this manoeuvre the R/F subsystem is on all the time and the MSC to DSC relative distances are known. A formation safe mode should be entered at the exit of the spacecraft safe mode and prior to reinitialising the formation. It is important that the FDIR at the spacecraft and formation levels are thoroughly analysed and simulated in a further study.

8.7 Conclusions and recommendations

The architecture of the AOCS for the MSC is presented together with an estimation of the level of the noise transmitted through the closed loop attitude control system for one axis. It is shown that the AOCS units employed for the design of the AOCS satisfy the requirements and leave ample margins.

Further analysis of the entire AOCS should be performed to consolidate the preliminary architecture proposed in this study. Of particular importance are the formation initialisation and acquisition manoeuvres, the transition from the coarse (RF) to fine (laser) metrology, and the analysis of the formation keeping during the observation mode.

Calibration of the instrument made of two spacecraft is an issue that needs to be addressed by a detailed analysis of the metrology chain involved. The location of the cold gas thrusters for both the stack and deployed configuration should be optimised to reduce the number and to provide redundancy.

9. OPTICAL METROLOGY

The XEUS mission calls for two optical metrology systems with, in both cases, most of the hardware flown on the Detector Spacecraft (DSC) and minimum equipment on the Mirror Spacecraft (MSC). The first is a position metrology system, which is used to lock and maintain the position of the DSC to that of the MSC in a formation flying mode. This system will be used during the majority of the mission and it requires high precision to ensure that the X-ray focus from the MSC is maintained on a small detector flown on the DSC. If gratings are also flown on the DSC or MSC, the requirements placed on the optical position metrology system are even tighter.

The second optical metrology system is used to measure alignment of the mirror petals of the MSC, so that actuators on each petal can be used to correct their misalignments.

9.1 Optical metrology requirements and design drivers

9.1.1 Position metrology

The position metrology system on the DSC will be used to acquire and lock the DSC to the MSC, after the RF and AOCS systems bring the two spacecraft into a stand-off position at 120 m. The system provides attitude and position sensing data to allow formation flying and is used during all imaging modes, which are at 50 m spacecraft separation. In addition it is used during alignment of the mirror petals of the MSC.

To lock onto the MSC and maintain the detectors in the focus plane of the X-ray mirror, the system needs to meet the following requirements:

- Acquire and lock DSC to MSC after RF metrology brings DSC to:
  - ±12 cm lateral± 5 mm longitudinal
- Longitudinal metrology to 750 μm (15 ppm at 50 m) (maintain focus)
- Lateral metrology to 330 μm (6 ppm at 50 m) (position data to control X-ray focus point on a 5 mm detector carried on the DSC).
- Continuous pitch and yaw measurement to ±10 arcseconds, which allows ±1 arcminute attitude control to avoid vignetting

The metrology for the gratings has the following requirements:

- 10-m configuration:
  - 1 arcsecond pitch, 3.9 arcseconds yaw, 50 μm(x), 50 μm(y) (1 ppm)
- 50-m configuration:
  - 60 μm (x) (1 ppm), 289 μm (y)

9.1.2 Petal alignment metrology

During the commissioning phase, after the orbit of the DSC has been locked to the MSC and the MSC bought into its correct imaging position, a metrology system is required to measure the alignment of the petals that make up the MSC, X-ray mirror. The X-ray mirror will be formed from an 8x8 matrix containing 48 mirror petals (and 16 empty slots in the centre) and the metrology system needs to be able to measure the alignment of each petal, including both lateral shifts and tilts up to ±15 arcseconds with 1 arcsecond accuracy.

9.1.3 Optical metrology assumptions

The optical position metrology system assumes that the RF metrology system brings the DSC into the correct position for formation flying to within limits ±12 cm lateral, ±5 mm longitudinal, which defines that the beam size needs to be approximately 30 cm at 120 m. It is assumed that at 120 m range between DSC and MSC, as measured by the RF system, the DSC will hold position and the coarse optical metrology will be turned on. Once a position lock has been established with this system the DSC will approach to the focal length of the MSC (baseline 50 m) where the fine optical metrology system will additionally be turned on. The DSC will then operate as a slave to the MSC position with attitude monitoring by the optical metrology systems and maintenance by the AOCS.

Only one instrument will be placed at the X-ray mirror focus at one time. The position metrology system must therefore be capable of maintaining the X-ray focus on the smallest detector.

It is assumed that the petal alignment system will be operated once during the commissioning phase of the mission. However it is possible that the system could be turned on and operated again to realign the petals should further alignment be necessary. In the latter case the realignment process is infrequent, perhaps once per year.

9.2 Trade-offs

Several metrology systems were investigated. Many, such as fringe projection methods, coherent lidar scanning or imaging lidar, could not provide the necessary accuracy (RD[9], RD[10], RD[11]).

The use of a telescope on the DSC to measure lateral position, via three Light Emitting Diodes LEDs) on the MSC, was considered in combination with a Time of Flight (ToF) laser rangefinder to provide the required longitudinal accuracy. However an impulse ToF laser rangefinder cannot provide the required submillimetre accuracy. In addition this system could provide no measurement of pitch and yaw and it was decided to try and ease requirements placed on the DSC AOCS, particularly a ≤1 arcsecond pointing requirement, by seeing what could be achieved with optical metrology.

Trilateration systems have been shown to provide accuracies down to about 5 ppm (RD[9]) and require that the range from three DSC to MSC positions is measured. Their advantage is their relative simplicity over multilateration systems and lack of moving, mechanical components. However a trilateration system can only just accommodate the position metrology requirements for the baseline system and cannot reach the accuracies required if gratings are flown.

Multilateration systems have been shown to provide accuracies down to state of the art at 1 ppm (RD[9]). One advantage is that such systems can be made self-calibrating. Their disadvantage is their complexity and the requirement to accommodate four base stations (five with redundancy for self-calibration) with scanning, dual-λ interferometers to measure base station distances to all the target locations. The baseline provided by the DSC was considered feasible, although extending it via booms could be considered. The addition of a large set of corner reflector targets, distributed over the MSC petals and structure, could perform both the position and the petal alignment metrology (three corner reflectors per petal would be required). Therefore a multilateration is the preferred metrology system.

9.3 Optical metrology baseline design

9.3.1 Position metrology

The optical position metrology is provided using a coarse and a fine sensor. A laser rangefinder with Absolute Distance Meter (ADM) provides the coarse range measurement with submillimetric accuracy. A dual-λ interferometer provides more accurate range measurements to a precision of ±3.5 µm, so that the AOCS can control the DSC position with respect to the MSC. Both the coarse and the fine measurement systems use optical heads, located at four points on the DSC, which measure the distance to four corner cube reflectors on the MSC (see Figure 9-3). The measurements are made with pulsed laser systems and consequently are sequenced to each of the laser heads in turn. An analysis of the stray light from the system is beyond the scope of this report. However the wavelength of the system can be chosen to minimise effects, the system is pulsed and the position of the pulsed beam is known and can be accounted for during X-ray data analysis.

The AOCS system provides only 60 arcseconds measurement accuracy in pitch and yaw (tilt) which is ambiguous with a lateral shift of 9 mm if measurements are made to only 1 corner cube from each laser head. A 2 dimensional representation of this ambiguity is demonstrated in Figure 9-1 which shows that, for equal range measurements d1 and d2, two positions of the MSC are possible with respect to the DSC. At a range of 50 m, and using a 2.4 m baseline across the diagonal of the front face of the DSC, the ±3.5 µm fine range resolution provided by the metrology system is ambiguous with approximately 300 µm lateral, 10 µm longitudinal (focus) displacements and 1 arcsecond pitch or yaw. These position measurements are just within the requirements for the configuration without gratings and outside the requirements for both grating configurations.

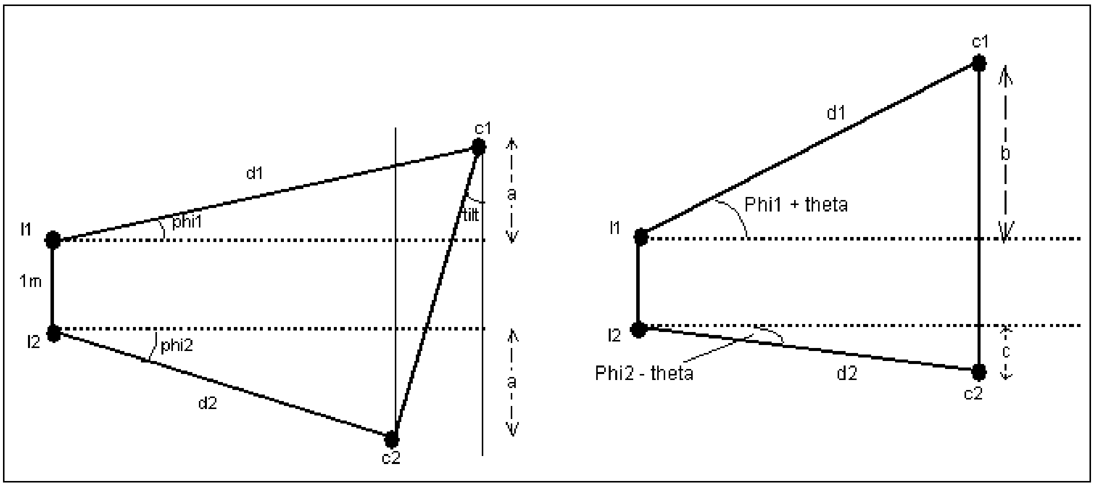

Figure 9-1: Position measurement ambiguity (l1 and l2 are laser heads on the DSC, c1 and c2 are corner cubes on the MSC)

Range measurements to at least three corner cubes, from each laser head of the position metrology system, are therefore needed to resolve ambiguities to a level below that of the system requirements (see Figure 9-2 for a 2-D representation). Multilateration is then used to calculate the position of the DSC, relative to the MSC, from the measured corner cube distances from each laser head site. A full analysis of the cumulative errors that can be expected from a multilateration measurement are a complex problem that is beyond the scope of this report, but a full analysis needs to assess the required number of measurements accounting for both range measurement accuracy and the stability and size of the baseline on the DSC. This is, in turn, affected by the stability that can be provided by the optical bench on the DSC.

9.3.1.1 Meeting grating requirements

The requirements for both the 50-m and the 10-m grating configurations are very demanding and require optical metrology to 1 ppm. A full simulation of the multilateration problem needs to be made to assess the probability that these requirements can be met. An additional analysis needs to be carried out to assess the feasibility of measuring the grating position relative to the DSC if the grating is in the 10-m configuration. This may be achieved by making range measurements between the laser head locations and corner cube reflectors placed on the outer ring of the grating structure. These measurements would allow the position of the grating to be measured to at least 80 μm lateral, 8 μm longitudinal and 1 arcsecond pitch and yaw. However they would require that the dual-λ interferometer could be tuned to operate at both 10-m and 50-m range with subsecond separations between measurements.

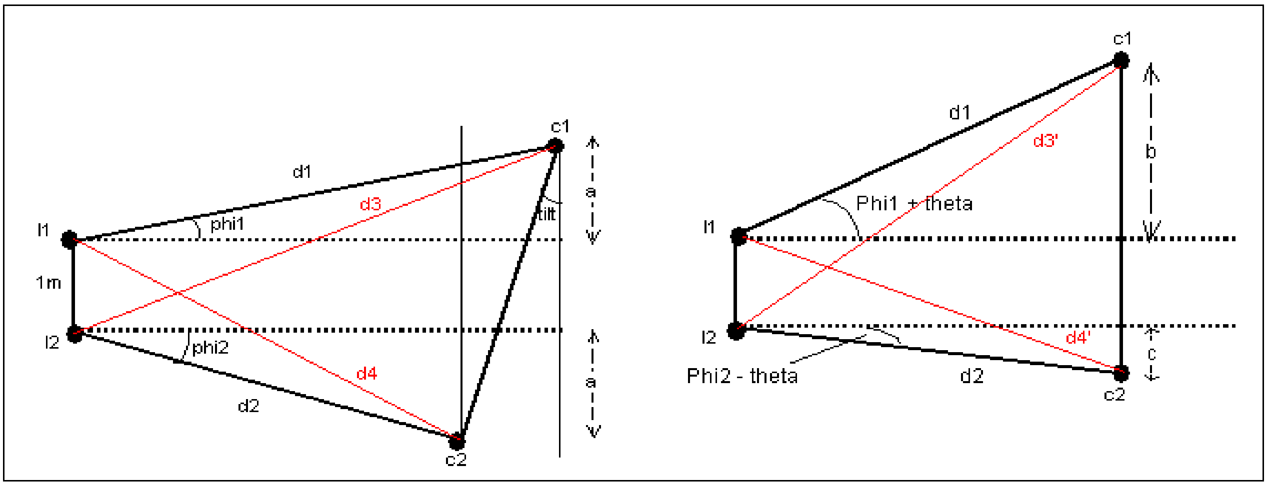

Figure 9-2: Additional measurements to reduce position measurement ambiguity

With regard to this report, a first iteration scheme has been designed with four laser head locations, from each of which range measurements are made (coarse then fine) to three corner cubes on the MSC (see Figure 9-3). The three measurements, at each location, could be implemented via one of two methods:

- Individual laser heads, aligned to point at each corner cube
- Single laser heads behind tip-tilt scan mirrors to allow access to any corner cube

The use of a tip-tilt scan mirror, at each laser head location, introduces four mechanisms with an associated increase in the power, complexity and risk of the design. For this reason the baseline is to use separate laser heads at each location and sequence range measurements between each of the heads in turn. Redundancy is therefore implemented via gradually decreasing position measurement accuracy for failure of separate laser heads. In the event that additional measurements are required, for example if a full multilateration analysis shows that this is necessary, or if alignment measurements of each mirror petal are included in the multilateration, then a change to a design using a scan mirror at each laser head location will be necessary. In this case five laser head locations may be necessary to provide adequate redundancy.

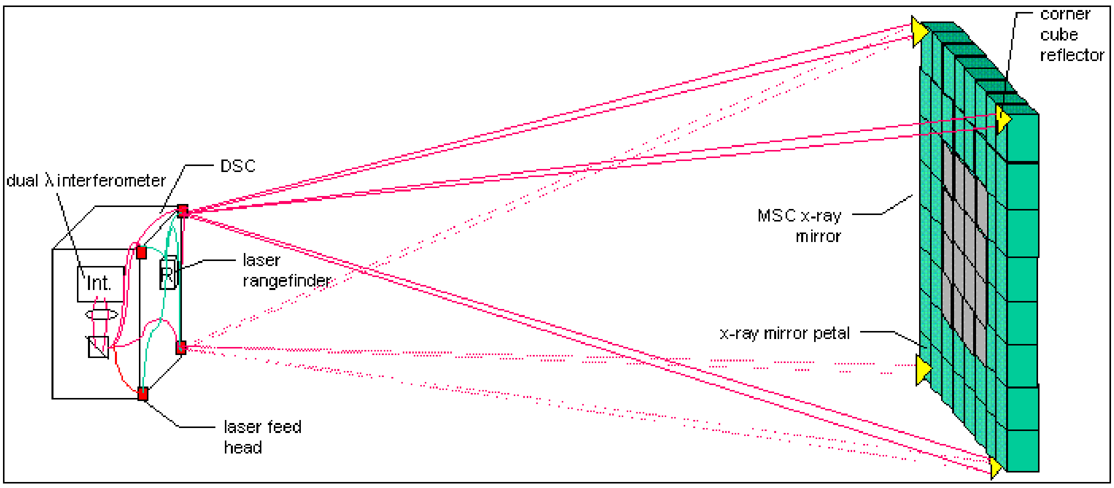

Figure 9-3: Position metrology

During imagining operations it is envisaged that the system will use optical fibre links between optical laser heads, mounted at four corner locations on the DSC front face, linked to both the laser rangefinder and the dual-λ interferometer. Measurements will be sequenced between each of the optical heads, using first the laser rangefinder and then the dual-λ interferometer, to produce a series of fine accuracy range measurements. The fine accuracy range measurements will be used in a multilateration algorithm to deduce the three dimensional position of each corner cube reflector.

9.3.1.2 Coarse range measurement system

At the hold, acquire and lock point range of 120 m, with the position and tilt accuracy provided by the RF system, it will be necessary to expand the laser rangefinder beams of the coarse system to at least 300 mm diameters. This expansion will not have an impact on the laser rangefinder accuracy, and since cooperative targets are used there is little power constraint.

To achieve a submillimetric accuracy the laser rangefinder principle has to be based on the modulation (intensity or frequency) of a continuous laser beam. Systems based on the measurement of the time of flight of a laser impulse are typically more simple than continuous modulated rangefinders, but at the moment only achieve accuracies of approximately 1 cm. Future ESA activities are foreseen to improve beyond this accuracy limit but are not yet proven technology. On the other hand, several continuous modulated laser radars exist and have demonstrated that accuracies much better than 1mm can be obtained. These systems are frequently used for applications with maximum range bellow 60 m, but the proper arrangement of the modulation wavelength can extend this to 120 m with minor impact on range accuracy for XEUS.

9.3.1.3 Fine range measurement system

The dual-λ interferometer is based on a breadboard already in development for the Darwin mission. Two Nd:YAG lasers are locked to a differential frequency by controlling the temperature of one of the lasers (see Figure 9-4). The Darwin breadboard will be used on spacecraft with formation flying separations of approximately 250 m. The breadboard works at 3 GHz, providing a 10 cm beat λ, which gives an unambiguity range of ±25 mm. The demonstrated range resolution with these parameters is ±35 μm and the breadboard is currently undergoing vacuum testing. By adjusting the beat frequency to 30 GHz it should be possible to obtain ±2.5 mm unambiguity range with a range resolution of ±3.5μm. To achieve this result temperature control of the stabilised laser will need to be much better than 1°. The unambiguity range means that the coarse optical metrology system must provide the range resolution within these limits, which is within the capability of the laser rangefinder.

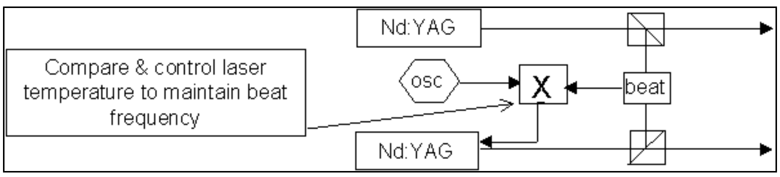

Figure 9-4: Dual λ interferometer

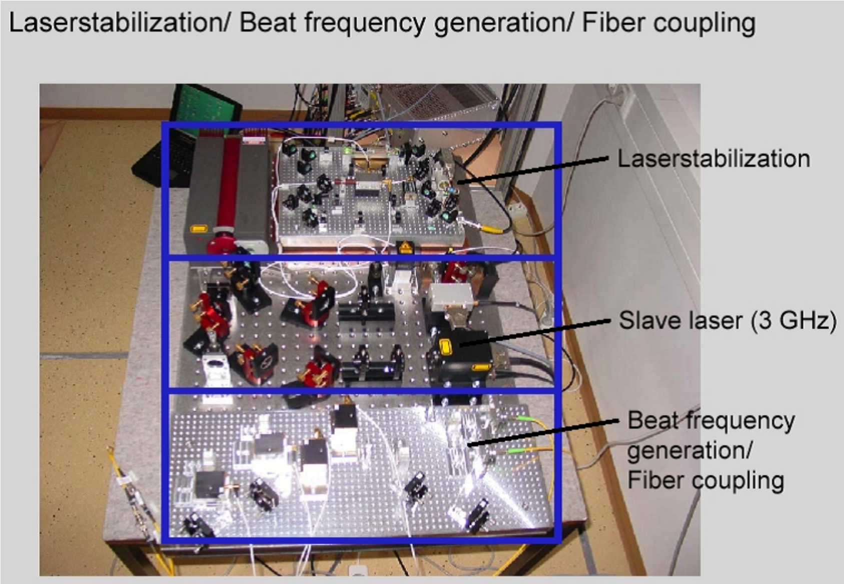

Figure 9-5: Darwin breadboard dual λ interferometer (see RD[12])

9.3.2 Position metrology performance

The coarse optical metrology, provided by the laser rangefinder with ADM system, supplies range measurements to submillimetric values. At 60 m range these are currently demonstrated to be 50 µm; at 120 m range these are estimated to be approximately 0.1 mm.

The fine optical metrology is provided by the dual-λ interferometer. A breadboard currently demonstrates ±35 µm range resolution over an unambiguity range ±25 mm. It is projected that the system can be retuned to supply range measurements to ±3.5 µm, within an unambiguity range of ±2.5 mm, for which <1° temperature stabilisation of the lasers will be necessary.

Using multilateration, between multiple points on the DSC and multiple points on the MSC, lateral position of the DSC relative to the MSC will be measured to <300 µm laterally, <10 µm longitudinally (focus) and <1 arcsecond tilt (pitch and yaw). A full analysis of the complex multilateration problem is needed to estimate the final performance of the position measurements provided by a multilateration algorithm. However state-of-the-art systems are shown to provide best accuracies of 1 ppm (RD[9]). This limit is at the requirement to fly gratings and requires careful consideration of the implementation of the gratings and the associated optical metrology.

9.3.3 Petal alignment metrology

There was no time to perform a full design of a petal alignment metrology system during this activity as the position metrology was considered more important to verify. However the alignment of each mirror petal on the MSC could be measured using the multilateration system of the position metrology system. In a calibration mode the system could be commanded to scan the pulsed coarse/fine measurement lasers to corner cube reflectors placed on each mirror petal; obviously it is necessary that scan mirrors are used at the laser head locations in this scenario (see Figure 9-6). The multilateration algorithm can then calculate the 3-D position of each corner cube reflector and from this the lateral shift and tilt of each petal can be inferred.

To view the entire MSC mirror from the DSC requires a 7° field of view, which is not demanding for a scan mirror system. However the scan mechanism will need to be verified for continuous operation over 4 years (the lifetime of the DSC).

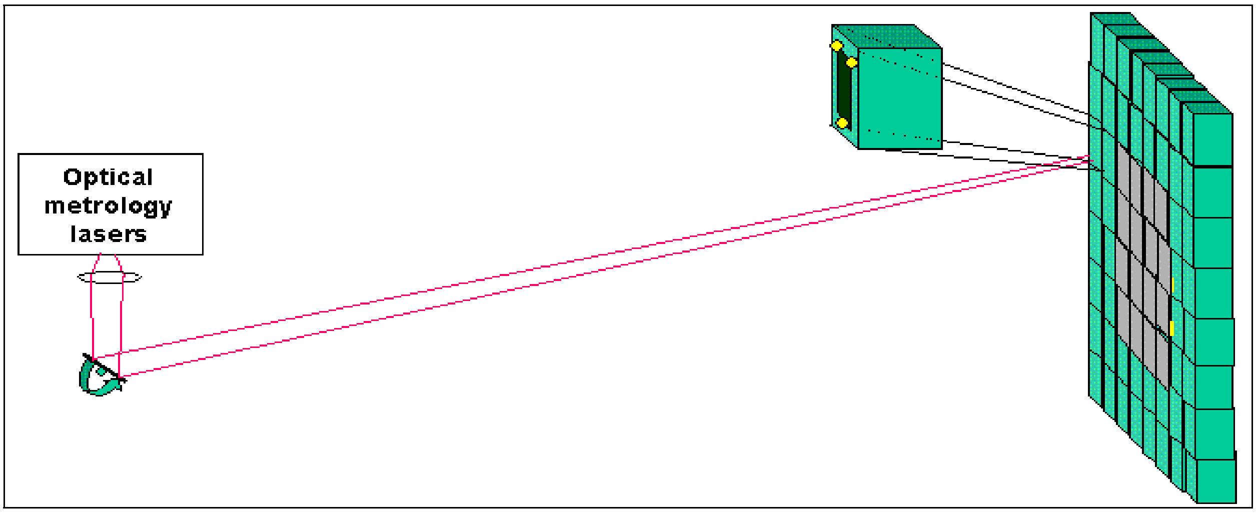

Figure 9-6: Optical petal alignment metrology

9.4 Budgets

Mass and power budgets are shown in Table 9-1 and Table 9-2 (figures include margin):

	No redundancy		Redundancy	
Item	**Mass (kg)**	**Power (W)**	**Mass (kg)**	**Power (W)**
Laser rangefinder	3.6	5	7.2	5
Dual λ interferometer	22.3	50	31.3	50
Petal tilt metrology	2.5	25	5	25

Table 9-1: Detector spacecraft budgets

	No redundancy		Redundancy	
Item	**Mass (kg)**	**Power (W)**	**Mass (kg)**	**Power (W)**
4 Corner cube reflectors	2.1	0	2.1	0
144 petal corner cubes	7.6	0	7.6	0

Table 9-2: Mirror spacecraft budgets

9.5 List of equipment

Laser rangefinder			
Item	**With no redundancy**	**With redundancy**	**TRP development (Automated Rendezvous and Docking)**
Stabilised laser with Absolute Distance Meter (ADM)	1	2	TRL 3
Electronics	1	2	TRL 3
Optical heads	3	3	
Dual-λ interferometer			In development for Darwin
Nd:YAG laser	2	3	TRL 3/4
Pump module	2	3	TRL 3/4
Stabilisation hardware	1	2	TRL 3/4
Modulation bench	1	1	TRL 3/4
Electronics	1	1	TRL 3/4
Optical heads	9	12	
Optical bench	1	1	
Tilt metrology			
Optics	1	2	
Electronics	1	2	

Table 9-3: List of optical metrology equipment on the DSC

Item	**With no redundancy**	**With redundancy**	**TRL**
Corner cube reflectors	4	4	8
Petal alignment corner cubes	144	144	8

Table 9-4: List of optical metrology equipment on the MSC

10. COMMUNICATIONS

10.1 Requirements and design drivers

- TT & C communications during all mission phases, any mode and near any attitude are required.
- Design should be kept as simple as possible to maximise the mission duration and reduce cost.
- Two-way ranging and Doppler capabilities are required during all mission phases.
- Only HK data are transmitted from MSC.
- Data rates shall be optimised by making realistic assumptions about on-board equipment and ground segment availability.
- RF metrology is required for relative position calculation MSC-DSC.
- Bi-directional MSC to DSC data transmission is required, with omni-directional coverage, after MSC deployment.
- Before deployment phase (stack separation) all DSC HK data are transmitted to Earth through MSC. Since no cable connection is allowed between both, wireless inter-spacecraft link is required.
- The angle between MSC axis facing to the Sun and the Earth has a maximum of 30 degrees during operational.
- Maximum distance supported for data transmission is equal to the maximum MSC-Earth distance. It is 0.0116 AU for the whole mission, and it happens during operational phase.

10.2 Assumptions and trade-offs

10.2.1 Data transmission assumptions

- Only HK data are to be transmitted to the Ground Station with a supposed data rate of 1 kbps.
- DSC HK data rate is 4 kbps.
- The maximum distance MSC-Earth is 0.0116 AU (see Figure 10-1). All transmission data rates are calculated for that distance.

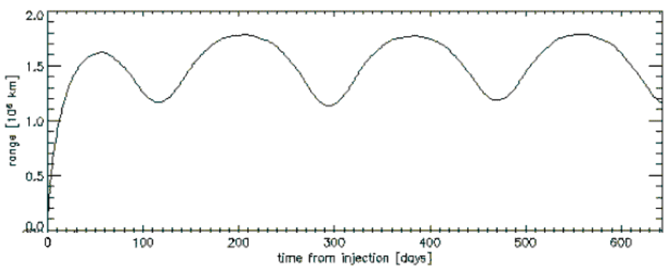

Figure 10-1: Halo orbit type 2 range (millions of km)

10.2.2 Antenna trade-off

The following considerations are important:

- The angular distance between MSC axis (pointing to the Sun) and the Earth is lower than 30 degrees for operational phase. See Figure 10-2.
- Steering mechanisms should be avoided to reduce system complexity, risk and mass.
- To reduce the operation costs, HK data should not be transmitted in real time. It should be transmitted at a high data rate to minimise the transmission time.

Traded-off antennas:

- *Dish*: discarded because the necessity of pointing steering mechanisms due its low beam-width (in the order of few degrees).
- *Helix*: discarded because its big sizes, weight, and difficulties of accommodation respect patch antennas.
- *Patch*: small, light and easy to accommodate. Its problem is the low gains (respect helicoidal antennas) close to 90 degrees from boresight.

The selected antenna is LGA patch with approximately a dimension of 90 x 90 x 20 mm and 100 g weight (*Surrey Satellite Technology Ltd. SPA_Series* X-band patch). Its 3dB beamwidth will be higher than 30 degrees (approximately ±35 degrees), so no steering mechanism or MSC attitude change is required during operational mode because the Earth will always be inside the beamwidth.

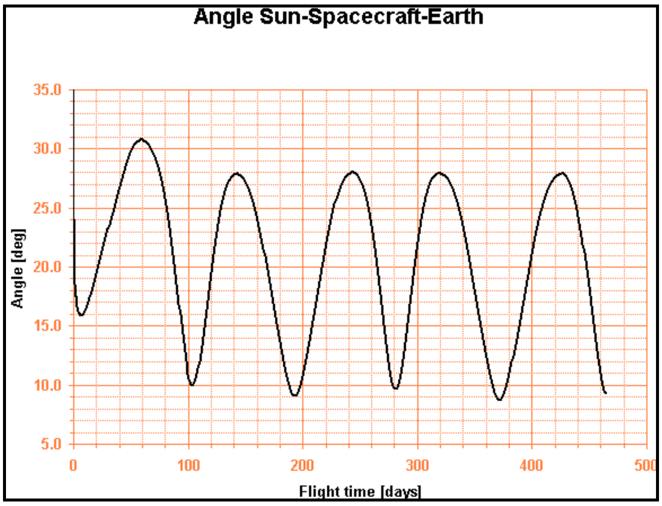

Figure 10-2: Angular separation Sun-MSC-Sun (degrees)

10.2.3 Ground station MSC communications band selection

The present situation of S-band (which is shared by Space Research (SR) Cat. A, Space Operation (SO) and Earth observation Services, plus high density mobile systems) is that high congestion and sharing difficulties with fixed systems have already appeared. Therefore S-band will be noisy. For this reasons, it is expected that ESA will reduce support to that band in the long term.

Considering X-band versus S-band, the most favourable frequency of operation depends on the kind of antenna used at both ends of the link (ground and space). In this case, assuming constant aperture at the Ground Station and a LGA on board (e.g. communications via LGA), the communications performances of S- and X-bands are similar in clear sky conditions (atmospheric absorption and rain losses are higher in X-band).

Ka-band is not used because its main advantage, the high data rate achieved using dish antennas, is not needed. In conclusion, X-band has been selected for both uplink and downlink.

10.2.4 Ground station diameter selection

Due to the low data rate requirements, a 15-m antenna would be sufficient. Nevertheless, a 35-m ground station antenna has been selected for operation reasons (see Chapter 20, Ground Segment and Operations). A 15-m ground station has been included as an option.

10.2.5 RF metrology

RF MSC-DSC data communication and RF metrology, used for rendezvous and FF, are required. Both requirements can be fulfilled using a similar system that is foreseen for ESA-Darwin mission that works in S-band. See RD[24] and RD[25]. Darwin consists of eight or four spacecraft in a flight formation acquired and maintained thanks to a similar RF system as coarse metrology to complement the laser one. XEUS's formation flying will comprise two spacecraft, therefore some modifications will be necessary.

RF metrology is a symmetrical system from hardware point of view, so both MSC and DSC will have the same on-board equipment working in S-band: set of antennas, a Navigation Processing unit and a Receiver/Transmitter unit (Rx/Tx). Two groups of three antennas are required, so six in total in each spacecraft.

The precision depends on the geometry of the antennas, so that value will be calculated for the location of XEUS's antennas. The three antennas of Table 10-1 have been considered for trade-off. Patch antennas have been selected.

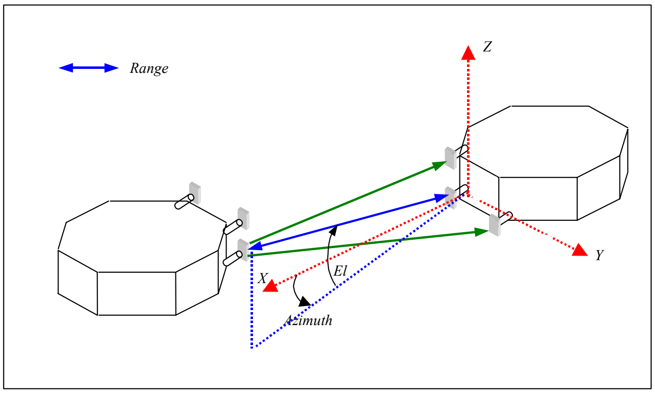

Figure 10-3: RF metrology coordinates system

Kind of antenna	Size	Mass	Gain at boresight	Gain at 90°
Cross dipole	D=10cm H=4cm	0.2 kg	4 dBi	-5 dBi
Quadrifilar helix antenna	D=10cm H=20cm	0.4 kg	3 dBi	-3 dBi
Patch antenna	D=8cm H=1cm	0.1 kg	4 dBi	-3 dBi

Table 10-1: Trade-off for antenna selection

10.2.6 Inter-spacecraft data transmission subsystem trade-off

Two considered options for bidirectional communications between MSC-DSC are RF and optical subsystems are shown in Table 10-2. Output of the trade-off is the RF subsystem.

	RF	Optical
Capacity	Bidirectional link Maximum distance: 60 m (**) Beamwidth: *hemispherical* BER=10^{-6} Data Rate = 20 kbps-200 kbps Low complexity and cost	Bidirectional link Maximum distance: 20 m (***) Beamwidth=±15 degrees BER=10^{-6} Data Rate = 100 kbps - Mbps Medium complexity and cost
Features	EMC with on-board equipment shall be certified Technology no space qualified Size: 4 cm x 3 cm x 1 cm (*) Mass: 30 g (*) Power consumption: 25mW	No EMC problems Technology no space qualified Size: 2 cm x 3 cm x 1.5 cm (*) Mass: 50 g (*) Power consumption: 100mW
(*) Approximate values for a non-space qualified prototype (**) 3 dB margin in link budget (***) 6 dB margin in link budget		

Table 10-2: Trade-off for inter-spacecraft communications subsystem

10.3 Baseline design

10.3.1 Summary depending on the mission phase

All provided links are bi-directional.

10.3.1.1 Initialisation till commissioning phase

- *Link with Earth*: quasi omni-directional coverage is provided using two low-gain antenna(s) in X-band for data transmission to the ground station.
- *Inter-spacecraft RF link*: DSC TT & C is transmitted through the MSC. One antenna in MSC and another in DSC.

10.3.1.2 After commissioning phase

Two links will be available for MSC:

- *Link with Earth*:
  - o Nominal: using X-band and the LGA that is over the solar panel.
  - o Contingency: X-band and any of the switched three LGAs, there will be omnidirectional coverage.
- *MSC-DSC data and RF metrology link*, in S-band. DSC will be the master and MSC the free flyer. To avoid collisions in case of optical metrology failure, this system will be always on.
  - o Data: using one of the two tx/rx S-band patch antennas. Omnidirectional coverage is provided for data transmission and reception.
  - o Metrology: based in two groups of three antennas each.
- *Inter-spacecraft RF link*: it is switched off.

10.3.2 Modulations and coding

The used modulations have been chosen from ECSS standard (RD[13]) considering that this is a CCSDS category-A mission. The used modulations are for uplink NRZ/PSK/PM and for downlink PCM-NRZ/BPSK(SINUS)/PM and GMSK with BTb=0.25. The first modulation will be used when ranging is required because with GMSK no ranging signal can be included.

A simple concatenated code is used for X-band communications with the Earth (downlink). See [RD[12]].

10.3.3 Contingency

Since LGAs are used, a 35-m ground station is required when using RG closed-loop techniques in PCM-NRZ/BPSK(SINUS)/PM. See Table 10-6. For open-loop techniques usage, a 15-m ground station is sufficient and GMSK modulation is used with a TC data rate of 2 kbps and a TM data rate of 21 kbps. See Table 10-8. In case of communications contingencies as regards MSC or DSC – Ground Station, the MSC-DSC data link could be used to link one spacecraft to the ground station using the other spacecraft communications link with Earth.

10.3.4 Ground station

Baseline is the New Norcia 35-m ground station (see Chapter 20, Ground Segment and Operations). RG is supported while using PCM-NRZ/BPSK(SINUS)/PM modulation. When using GMSK, only RG Doppler and Doppler rate measurements can be done.

Transmission		***Reception***	
Frequency band	**EIRP**	**Frequency band**	**Effective G/T at 10º elevation**
7145 – 7190 MHz	89.31 dBW (1995W RF)	8400 - 8450 MHz	42.52 dB/K

Table 10-3: Ground station main characteristics for Perth 15-m antenna

10.3.5 Mass memory

Since all HK data are stored on board until transmission begins, a first approximation for the mass memory is equal (pessimistic) to the HK data. All data are transmitted during the day, therefore a very minimum of 86 Mbps of memory is required.

10.3.6 MSC-DSC RF link: metrology and data transmission

Satellite configuration consists of one master (DSC) and one free-flyer (MSC). The system is based in TDMA/CDMA with chip rates of 1 Mcps. S-band is used.

The precision depends on the distance between the antennas. In this study, they are distributed in a L shape with distances of 7.3 m and 10.6 m. Considering the precision proportional to inverse of longitude RD[33] and taking as a reference Alcatel results RD[32], Table 10-4 is obtained.

The most important situation is when the MSC-DSC distance is 120 m, just when the optical metrology system begins to work. The precision given in that case is [±0.52 cm, Azimuth direction: ± 4 cm, Elevation direction: ±7.9 cm]. See an explanation of the coordinate system in Figure 10-3. For the Azimuth case, the case of 'line of sight >30 degrees' is used because the distribution of the antennas, the two used for azimuth have an angle of 35° with the mirror.

The maximum range is 30 km, obtained by modifying the transmitted TDMA frame of Darwin system RD[24] by increasing the slot duration two times (for Darwin, a four-spacecraft configuration), but maintaining the frame duration. Therefore, the Darwin frame duration is 20 ms and new slot duration 10 ms.

Coordinate	Interval	Angular Precision	Range precision
Range			±0.52 cm
Azimuth	Line of sight < 30º Line of sight > 30º	0.31º 0.075º	±16.2 cm ± 4 cm
Elevation	Elevation < 60º 60º < Elevation < 80º 80º < Elevation < 90º	0.15º 0.34º NA	±7.9 cm ±17.8 cm NA

Table 10-4: RF metrology precision for XEUS 2

With the proposed frame modifications, data communication is only possible below 16 km (8 km in the original system, so with frame modification the maximum range will be just the double). Data transmitted rates will be 9 kbps bidirectional, since instead of four spacecraft like in Darwin, there will be just two.

One antenna transmits and three (including the transmitting one) receive. Only three antennas work simultaneously for this purpose: the three of one side of MSC or the three of the other side. One group is selected using switches. The same applies to DSC.

The RF metrology system can be a communications back-up link with Earth for TT & C of MSC or DSC in case of contingency with the X-band system. DSC or MSC would then act as a relay.

	Forward link (DSC ->MSC)	Return link (MSC ->DSC)
Frequency	2100.00 MHz	2210 MHz
Tx power	1.3mW (distance <1 km), 1.2W (distance >1 km)	
Modulation	PCM-NRZ/BPSK/PM	
Coding	no coding	
FER	10^{-3}	
Bit rate	9 kbps	

Table 10-5: Communications link MSC-DSC in S-band

10.3.7 Inter-spacecraft communications before separation

An inter-satellite RF link is provided while MSC and DSC are stacked and for the first 60 metres after separation. Afterwards, it will be switched off.

In addition to the trade-offs already shown in Table 10-2, the following points apply:

- Based on ZIG-BEE and 802.14.5 protocols. See RD[27] till RD[31].
- Data rate: fixed at 20 kbps for XEUS's purposes.
- Emitted power: 0.5mW
- Standby power consumption is close to 0mW.
- Spread spectrum is used, so EMC is easy to comply because of the very low signal PSD.
- Antenna: helix with dimensions diameter = 5 mm, longitude = 40 mm
- Frequency band: unlicensed band at 2.4 GHz. It does not interfere with the RF metrology system since both work in different frequencies and also because the inter-spacecraft link uses a spread spectrum.

See Figure 10-5 for antenna location.

10.3.8 Antenna selection and location

Surrey Satellite Technology Ltd. SPA_Series S-band patch antennas are considered as baseline (RD[26]). The requirements for the antennas' location are:

- *TT & C antennas*: communications during all mission phases and any attitude and mode are required:
  - o Before mirror deployment, there is an antenna in the front part (over the solar panel) and another in the backside.
  - o After mirror deployment: one in the front (over the solar panel) whose boresight is aligned with the mirror direction will be used for nominal communications. For contingencies and operations requiring close to omnidirectional coverage there will be another antenna in the back of the mirror.
- *RF metrology system*: omni-directional coverage for data transmission. High coverage of the receiving antennas (including the transmission ones).
  - o The combination of the two groups of antennas shall have omnidirectional coverage to comply with the omnidirectionality for data transmission.
  - o The reception (that include the transmitter/receiver antenna) antennas do not need omnidirectional coverage, but in order to perform the metrology, the three of them

(one group of the two groups of three antennas) should see the other spacecraft (or the orange or the green antennas in Figure 10-3).

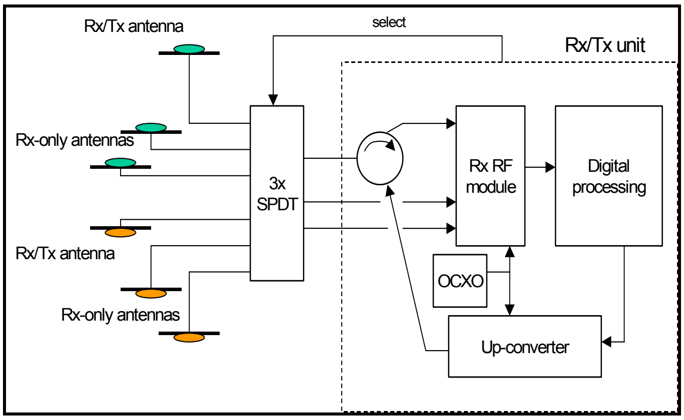

Figure 10-4: Block diagram for FF RF metrology

- *Inter-spacecraft wireless communications*: there will be one antenna in MSC and another in DSC. They should be directly visible to each other. An omnidirectional helix has been selected. See section 10.3.7.

10.3.9 Model

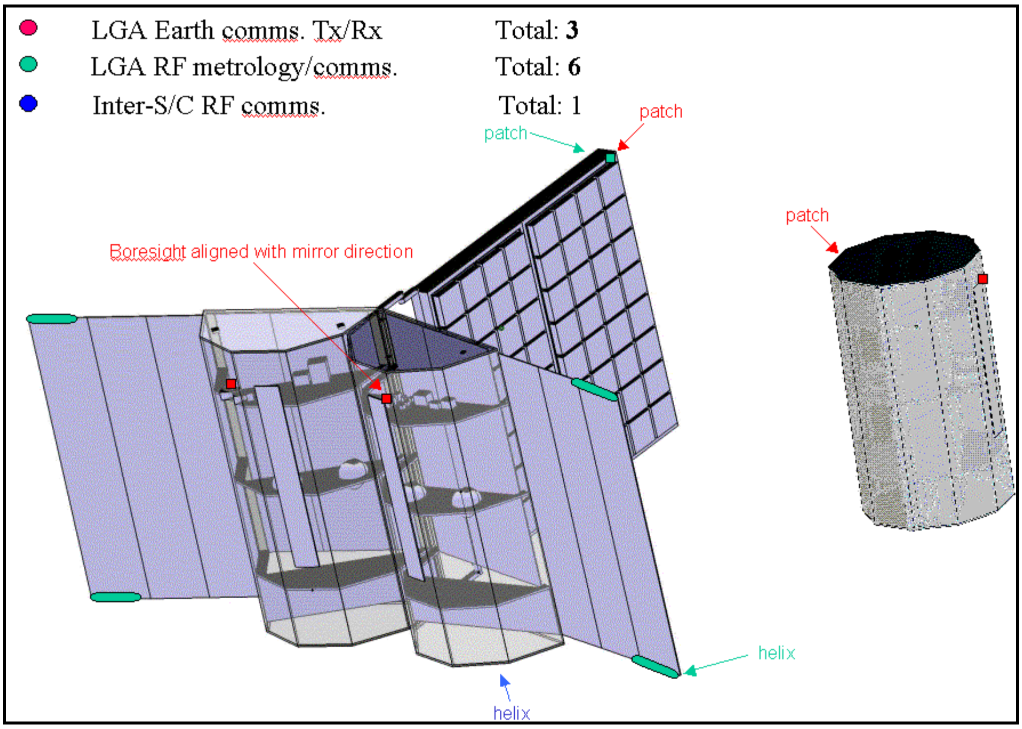

Figure 10-5: RF metrology and communications antenna location (deployed and stowed configuration)

10.3.10MSC - Ground Station link budget

The details for the standard link MSC- Ground Station are shown in Table 10-6 (see RD[13] till RD[20]). Standards will define the link. The baselined 35-m ground station antenna is used.

The MSC HK transmission time is 0.3 h considering 86 Mbits of data and a transmission rate of 95 kbps. If GMSK is used, the time is 0.24 h (but RG is not possible with this modulation).

	Uplink	**Downlink**
Frequency	7.15 GHz	8.4005 GHz
Tx power	1995W	15W
Modulation	NRZ/PSK/PM	PCM-NRZ/BPSK(SINUS)/PM GMSK with BTb=0.25
Coding	No coding	Concatenated, Interleaving=5 [convolutional ½ and Reed Solomon (223, 255)]
FER	10^{-5}	10^{-5}
Bit rate (operations)	2 kbps	95 kbps BPSK/PM 120 kbps GMSK
Bit rate (contingency or not Earth pointing, for example, manoeuvres)	2 kbps	24 kbps BPSK/PM 32 kbps GMSK

Table 10-6: X-band link Ground Station -MSC

10.4 List of equipment

Table 10-7 shows a summary of communications equipment and their masses. The total mass is 18.8 kg; in addition harness mass is 2 kg.

Element 1: Mirror S/C			**MASS [kg]**			
Unit	**Element 1 Unit Name** Click on button below to **insert new unit**	**Quantity**	Mass per quantity excl. margin	Maturity Level	Margin	Total Mass incl. margin
1	X-band LGA	3.00	0.10	Fully developed	5	0.3
2	X-band transponder	2.00	3.45	To be modified	10	7.6
3	X-band SSPA	2.00	1.30	Fully developed	5	2.7
4	X-band RFDU	1.00	1.50	To be modified	10	1.7
5	S-band transponder-metrology	2.00	3.00	To be developed	20	7.2
6	S-band omni antenna helix	4.00	0.20	Fully developed	5	0.8
7	S-band RFDU	1.00	0.30	To be modified	10	0.3
8	S-band omni antenna patch	2.00	0.10	To be modified	10	0.2
9	RF inter-S/C link	2.00	0.07	Fully developed	5	0.1
10	RF inter-S/C link antenna	1.00	0.01	Fully developed	5	0.0
-			0.0	To be developed	20	0.0
ELEMENT 1 **SUBSYSTEM TOTAL**		**10**	**18.8**		**12.2**	**21.0**

Table 10-7: Communications and RF metrology equipment

10.5 Options

10.5.1 Coding

Use of turbo codes ¼ for TM would allow a theoretical data rate increase of about a factor of 1.6 by reducing required telemetry data Eb/N0 in 2.3 dB. This code is not baselined because:

- It would add complexity to the MSC and ground station.
- The time to transmit the MSC (0.3 h) is low enough.
- Almost double the frequency bandwidth would be used with respect to concatenated codes. In future, when X-band may begin to show saturation problems, this would be important.

10.5.2 Ground Station

If a 35-m ground station is not usable, a 15-m ground station could be used for MSC. Another ground station should be used for DSC due its higher transmission data requirements. See Table 10-8 for link information. The time to transmit the 86 Mbits/day at 14 kbps is 2 hours, while the time to transmit at 21 kbps is 1.4 hours.

	Uplink	**Downlink**
Frequency	7.15 GHz	8.4005 GHz
Tx power	1995W	15 W
Modulation	NRZ/PSK/PM	PCM-NRZ/BPSK(SINUS)/PM GMSK with BTb=0.25
Coding	No coding	Concatenated, Interleaving=5
FER	10^{-5}	10^{-5}
Bit rate (operations)	2 kbps	14 kbps BPSK/PM 21 kbps GMSK
Bit rate (contingency or not Earth pointing, e.g. manoeuvres)	2 kbps	No ranging is possible 5 kbps GMSK

Table 10-8: X-band link Ground Station - MSC

11. THERMAL CONTROL

11.1 Requirements and design drivers

The design drivers and requirements for the XEUS mirror spacecraft's thermal control are in the following order of priority:

1. Minimisation of temperature variations across the mirror and along the optical axis of the mirror petals.
2. Minimum absolute mirror petal temperature around –160˚C
3. Radiation of heat dissipated by on-board equipment into deep space
4. Accommodation of all subsystems according to their operating temperature range during all expected mission phases and operative modes with their specific system and subsystem requirements on appropriate locations

11.2 Thermal design baseline

Optimisation of the thermal design could benefit from the work done in the context of XEUS 1. Accordingly, the XEUS part 2 activities could focus on finding the best design within the available mass limits.

The key results from the trades performed are as follows:

- The larger the opening angle of the canister halves, the lower the temperature difference across the mirror
- The smaller the temperature variations across the mirror, the lower the absolute petal temperature
- The lower the temperature gradient across the mirror, the higher the mass impact from the sun shield size

These three main parameters resulted in the MSC thermal design described hereafter (see also Figure 11-1). It is believed that the proposed solution provides a thermally optimised system configuration for the MSC and a good basis for a more detailed thermal design study at payload and subsystem level. It is not expected that any other configuration will significantly improve the mirror temperature gradients by keeping the lower petal temperatures above about –160˚C and having a lower MSC mass.

The proposed baseline solution is summarised as follows:

- Thermal design philosophy used for XEUS mirror spacecraft is based on the use of passive techniques. Heaters are foreseen for special tasks locally applied to some S/C bus units.
- The need to minimise gradients within the mirror petals i.e. along the optical axis and the fact that no active thermal control on the optical bench shall be applied led to a system design requirement for a MSC configuration that would be as symmetric as possible. What the mirror sees from the rest of the S/C should be the same on both sides of the mirror and should present the same thermal environment.

- When stowed, the canister halves have to accommodate the folded mirror. When deployed, this cavity does not provide a homogeneous and symmetric radiative area towards the mirror which is essential to minimise the temperature gradients in the mirror petals along the optical axis. To reduce the temperature gradient in the mirror plane, the radiative input from the canister halves shall be as low as possible. The solution to this is to close the canister cavities with a flat "cold" plate. This is accomplished by deployable panels stowed during launch on one of each canister sidewalls and deployed after the mirror is in its operating configuration (See Figure 12-12). To keep these panels at a low temperature, they could be equipped with a thermal shield/plate on the bus equipment side of the canister, for example, limiting the thermal input from the electronic boxes. The details of this particular shielding concept for the cold plate have not been studied during the CDF study but it is essential to consider them for the next phase of the project.
- The last part in the MSC deployment sequence is the deployment of symmetric sun shields or "hot plates" at each end of the canister (See Figure 11-1). The purpose of these hot plates is to further decrease the temperature gradient in the mirror plane and at the same time to increase the absolute temperature of the mirror. The sun shield design is based on deployable solar array panel technology with both front and read sides of the panels coated with black paint (See Figure 12-14).
- For the radiative and conductive parts of dissipating bus units along the canister length to distribute temperature homogeneously, heat pipes are mounted in the canister corners (See Figure 11-1). S/C internal surfaces have high emittance finishes to improve radiative heat transfer and to minimise the temperature gradients within the closed S/C. Therefore, all aluminium internal surfaces and internal equipment need to be black painted.
- The external Sun-oriented panels of the canister halves are covered with MLI. At two specific locations the solar array panels are mounted thermally decoupled on top of the MLI covered panels.
- During the cruise phase, when the MSC is in its BBQ configuration, two of the ten canister panels have no MLI insulation (when deployed these two panels are facing each other, seeFigure 11-1) ensuring that the stowed MSC stays in its required temperature range. The required thermo-optical properties of these two panels have to be studied in the next phase of the project.
- To minimise the thermal conductance from the canister to the mirror, all structural element in the conductive path are made from glass fibre.
- Subsystem equipment should be mounted on the floors of the top and bottom segment of the canister. Here also, symmetric heat dissipation will reduce the temperature gradients in the mirror.
- Interface fillers are used as necessary to help heat rejection from dissipating equipment.
- To maintain low temperatures on the batteries, they are thermally isolated from the S/C structure and internal environment and treated independently. Heaters controlled by thermostats will provide thermal control of the minimum temperature.
- The XEUS mirror S/C uses heaters to provide temperature control during all operational modes. For this mission it is important to consider all on-board equipment and in particular thermal control ("high" dissipating) units, which are not permanently operating by compensating their temperature as well as providing substitution heat according to the operating modes. Flight standard types are thermofoil flat (redundant, single layer), linear thermofoil heaters (UPS pipelines).

11.3 Thermal results

11.3.1 Nominal case

The hereafter-presented configuration is the nominal thermal case as reference. The XEUS mirror spacecraft has an open "T"-Shape, see Figure 11-1. Results of the thermal analysis are summarised in this chapter. The nominal case is defined as a fully symmetric configuration with the Sun coming from the X direction. To cover a wider observation field at any point in time, a thermally acceptable Sun angle around the Y-axis shall be defined. This angle is called the Sun inclination angle. For the nominal case, the Sun inclination angle is zero.

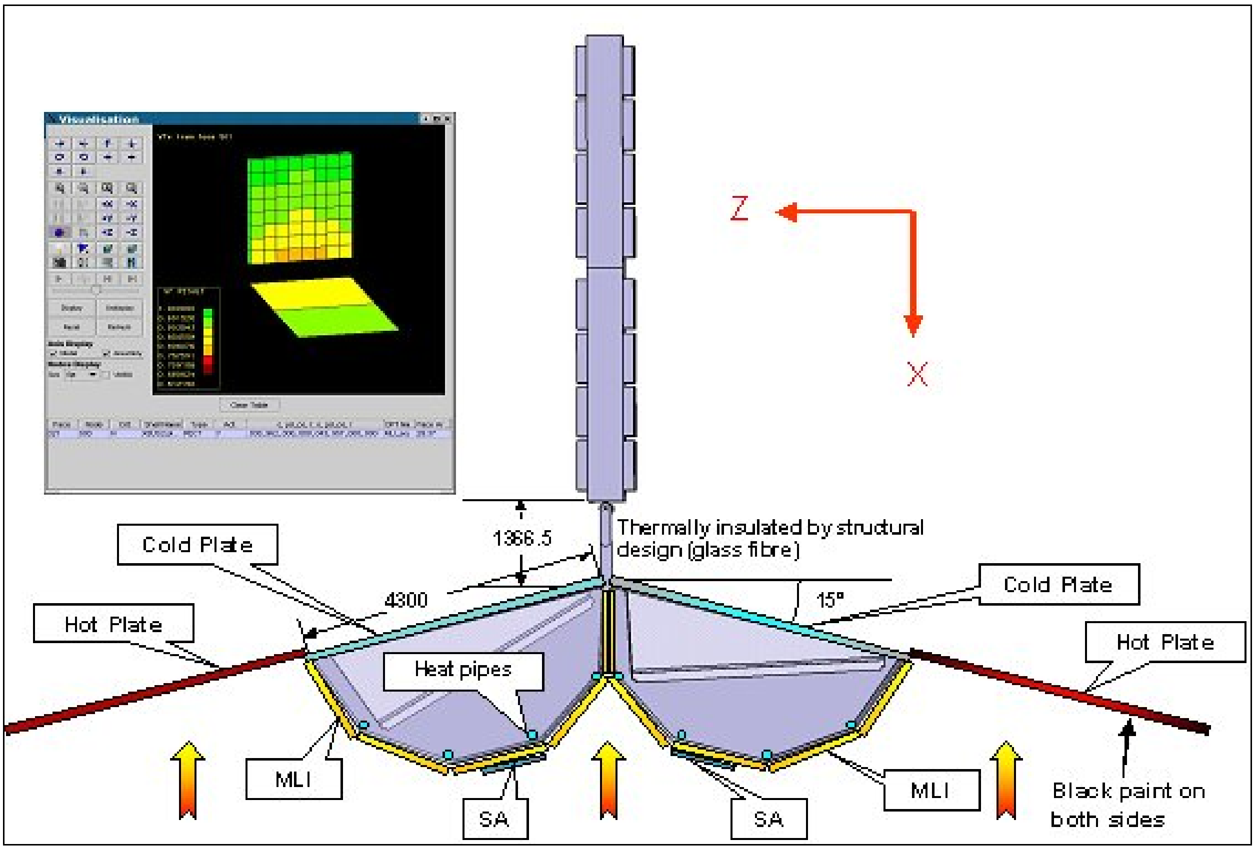

Figure 11-1: Principle of MSC thermal design

The main assumptions for this configuration are:

- External side of the canister covered with MLI
- Internal side of the canister covered with black or white paint (TBC)
- Mirror considered as black without conductive links between them
- Mirror decoupled conductively from the canister
- Internal dissipation of 172W in the canister
- Heat pipes in corners of cylinder to improve homogeneity/symmetry of thermal radiative source in the y direction
- Assumed conduction along the optical path of 0.21 WmK

- Deployable sun shield (hot plate) to increase thermal input on petals most distant from canister halves
- Deployable canister closure panels (cold plate) to minimise thermal input from S/C bus halves on petals closest to canister halves

With this configuration, the following thermal results can be derived:

- Solar array temperature in observation phase: 127.9˚C
- Solar array temperature in barbecue mode: 28.1˚C
- Canister temperature in observation phase: -13.5˚C +/- 4 ˚C

The results from mirror temperature distribution analysis are given for the nominal case in Table 11-1. A graphical visualisation of the results is given in Figure 11-3. The coordinate system for mirror petal location and definitions used for all thermal analysis tables are explained in Figure 11-3.

The key results for the mirror/optical bench are as follows:

- Maximum temperature variation across mirror: 37.7˚C
- Maximum temperature variation in mirror petals along the optical axis: negligible
- Minimum petal temperature: -161.2˚C
- Cold plate temperature: -45.0˚C
- Hotplate temperature: 61.2˚C

Mirror Cells Equilibrium Temperature								
T [C]	1	2	3	4	5	6	7	8
1	-130.2	-128.0	-125.7	-124.6	-124.6	-125.7	-128.0	-130.2
2	-127.6	-127.0	-125.9	-125.0	-125.0	-125.9	-127.0	-127.6
3	-129.1	-129.7	-129.7	-129.4	-129.4	-129.7	-129.7	-129.1
4	-132.8	-134.3	-135.2	-135.6	-135.6	-135.2	-134.3	-132.8
5	-137.8	-139.8	-141.4	-142.2	-142.2	-141.4	-139.8	-137.8
6	-143.2	-145.7	-147.8	-148.9	-148.9	-147.8	-145.7	-143.2
7	-148.9	-151.6	-153.9	-155.3	-155.3	-153.9	-151.6	-148.9
8	-154.4	-157.3	-159.8	-161.2	-161.2	-159.8	-157.3	-154.4
							-161.2	-124.6
							36.6	

Table 11-1: Mirror petal equilibrium temperature distribution for nominal case (˚C)

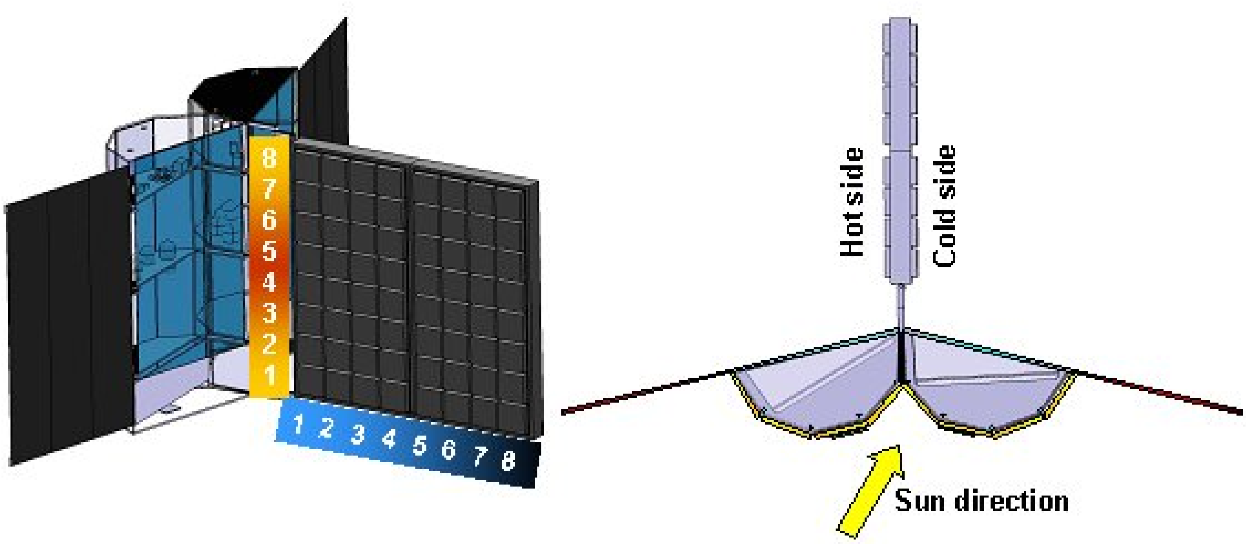

Figure 11-2: Coordinates and definitions for mirror thermal analysis tables

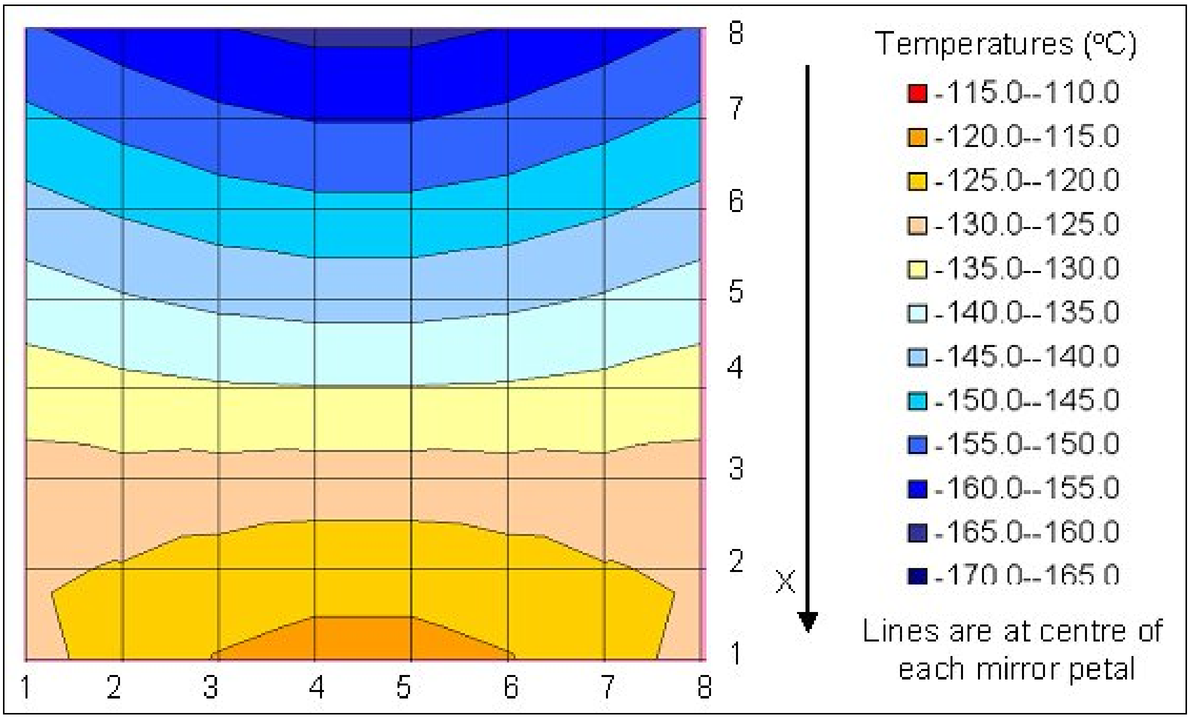

Figure 11-3: Mirror petal equilibrium temperatures for nominal case (˚C)

Since the maximum temperature difference between and within the mirror petals along the optical axis is important for the petal design itself, the internal in-plane petal temperature variations have been assessed and are presented in Table 11-2. The key results for in-plane temperature variations are:

- Maximum difference of temperature between two mirror elements: 6.7ºC
- Maximum difference of temperature within one mirror element: 8.3ºC derived from:
  - Maximum temperature difference in X direction of 6.7ºC and

- Maximum temperature difference in Y direction of 2.9ºC

T & Grad.	1		2		3		4		5		6		7		8
1	-130.2	2.3	-128.0	2.2	-125.7	1.2	-124.6	0.0	-124.6	1.2	-125.7	2.2	-128.0	2.3	-130.2
	2.7	3.2	0.9	2.1	0.2	1.3	0.4	0.4	0.4	1.3	0.2	2.1	0.9	3.2	2.7
2	-127.6	0.5	-127.0	1.2	-125.9	0.9	-125.0	0.0	-125.0	0.9	-125.9	1.2	-127.0	0.5	-127.6
	1.5	2.1	2.6	3.8	3.8	4.7	4.4	4.4	4.4	4.7	3.8	3.8	2.6	2.1	1.5
3	-129.1	0.6	-129.7	0.0	-129.7	0.3	-129.4	0.0	-129.4	0.3	-129.7	0.0	-129.7	0.6	-129.1
	3.8	5.2	4.6	5.5	5.5	5.9	6.1	6.1	6.1	5.9	5.5	5.5	4.6	5.2	3.8
4	-132.8	1.4	-134.3	0.9	-135.2	0.4	-135.6	0.0	-135.6	0.4	-135.2	0.9	-134.3	1.4	-132.8
	4.9	7.0	5.5	7.1	6.2	7.0	6.7	6.7	6.7	7.0	6.2	7.1	5.5	7.0	4.9
5	-137.8	2.0	-139.8	1.6	-141.4	0.8	-142.2	0.0	-142.2	0.8	-141.4	1.6	-139.8	2.0	-137.8
	5.5	7.9	5.9	7.9	6.3	7.5	6.7	6.7	6.7	7.5	6.3	7.9	5.9	7.9	5.5
6	-143.2	2.5	-145.7	2.1	-147.8	1.1	-148.9	0.0	-148.9	1.1	-147.8	2.1	-145.7	2.5	-143.2
	5.6	8.4	5.9	8.2	6.2	7.5	6.4	6.4	6.4	7.5	6.2	8.2	5.9	8.4	5.6
7	-148.9	2.7	-151.6	2.3	-153.9	1.3	-155.3	0.0	-155.3	1.3	-153.9	2.3	-151.6	2.7	-148.9
	5.6	8.5	5.7	8.2	5.9	7.3	6.0	6.0	6.0	7.3	5.9	8.2	5.7	8.5	5.6
8	-154.4	2.9	-157.3	2.5	-159.8	1.4	-161.2	0.0	-161.2	1.4	-159.8	2.5	-157.3	2.9	-154.4

X

Table 11-2: Difference of temperature distribution between and within mirror petals

11.3.2 Sensitivity analysis

The opening angles of the canisters have been studied during XEUS 1 activities. The general conclusion was that the greater the opening angle, the lower the temperature gradient. For XEUS 2 this has been taken into account so the maximum possible opening angle has been traded from a configuration and mass point of view. An opening angle of 105 degrees was found to be the best compromise for the MSC.

The sensitivity of the mirror temperature variation as a function of the Sun inclination has been studied in detail for the angles 5, 10 and 15°. The results are summarised in Table 11-3 to Table 11-5. For the location of the "hot" and "cold" sides, see Figure 11-2.
Figure 11-4 shows the results.

The key results for the sensitivity of the mirror temperature variations as a function of the Sun inclination angle is as follows:

- Sun inclination angle 0º: Maximum temperature variation across mirror: 37.7˚C
  - Minimum petal temperature: -161.2˚C
  - Maximum temperature variation in mirror petals along optical axis: negligible
- Sun inclination angle 5º: Maximum temperature variation across mirror: 36.8˚C
  - Minimum petal temperature: -162.0˚C
  - Maximum temperature variation in mirror petals along the optical axis: 1.8 ˚Sun inclination angle 10º: Maximum temperature variation across mirror: 36.9˚C
  - Minimum petal temperature: -163.3˚C
  - Maximum temperature variation in mirror petals along the optical axis: 3.5˚
- Sun inclination angle 15º: Maximum temperature variation across mirror: 37.0˚C
  - Minimum petal temperature: -164.2˚C
  - Maximum temperature variation in mirror petals along the optical axis: 5.3˚

'Cold Side' Mirror Cells Equilibrium Temperature								
T [C]	1	2	3	4	5	6	7	8
1	-131.2	-129.0	-126.7	-125.6	-125.6	-126.7	-129.0	-131.2
2	-128.6	-128.0	-126.9	-126.0	-126.0	-126.9	-128.0	-128.6
3	-130.1	-130.7	-130.7	-130.4	-130.4	-130.7	-130.7	-130.1
4	-133.8	-135.2	-136.2	-136.5	-136.5	-136.2	-135.2	-133.8
5	-138.7	-140.7	-142.3	-143.1	-143.1	-142.3	-140.7	-138.7
6	-144.1	-146.6	-148.6	-149.8	-149.8	-148.6	-146.6	-144.1
7	-149.7	-152.4	-154.7	-156.1	-156.1	-154.7	-152.4	-149.7
8	-155.2	-158.1	-160.6	-162.0	-162.0	-160.6	-158.1	-155.2
							-162.0	-125.6
							36.4	

'Hot Side' Mirror Cells Equilibrium Temperature								
T [C]	1	2	3	4	5	6	7	8
1	-129.5	-127.3	-125.0	-123.9	-123.9	-125.0	-127.3	-129.5
2	-126.9	-126.3	-125.2	-124.3	-124.3	-125.2	-126.3	-126.9
3	-128.4	-129.0	-129.0	-128.7	-128.7	-129.0	-129.0	-128.4
4	-132.2	-133.6	-134.5	-134.9	-134.9	-134.5	-133.6	-132.2
5	-137.1	-139.2	-140.8	-141.6	-141.6	-140.8	-139.2	-137.1
6	-142.6	-145.1	-147.1	-148.3	-148.3	-147.1	-145.1	-142.6
7	-148.3	-151.0	-153.3	-154.7	-154.7	-153.3	-151.0	-148.3
8	-153.9	-156.8	-159.2	-160.7	-160.7	-159.2	-156.8	-153.9
							-160.7	-123.9
							36.8	

Table 11-3: Mirror equilibrium temperature distribution for 5° Sun inclination

'Cold Side' Mirror Cells Equilibrium Temperature								
T [C]	1	2	3	4	5	6	7	8
1	-132.5	-130.3	-128.1	-126.9	-126.9	-128.1	-130.3	-132.5
2	-129.9	-129.4	-128.2	-127.3	-127.3	-128.2	-129.4	-129.9
3	-131.3	-132.0	-132.0	-131.7	-131.7	-132.0	-132.0	-131.3
4	-135.1	-136.5	-137.4	-137.7	-137.7	-137.4	-136.5	-135.1
5	-139.9	-141.9	-143.5	-144.3	-144.3	-143.5	-141.9	-139.9
6	-145.3	-147.7	-149.7	-150.9	-150.9	-149.7	-147.7	-145.3
7	-150.8	-153.5	-155.8	-157.1	-157.1	-155.8	-153.5	-150.8
8	-156.3	-159.1	-161.6	-163.0	-163.0	-161.6	-159.1	-156.3
							-163.0	-126.9
							36.1	

'Hot Side' Mirror Cells Equilibrium Temperature								
T [C]	1	2	3	4	5	6	7	8
1	-129.1	-126.8	-124.6	-123.4	-123.4	-124.6	-126.8	-129.1
2	-126.4	-125.9	-124.8	-123.8	-123.8	-124.8	-125.9	-126.4
3	-128.0	-128.6	-128.6	-128.3	-128.3	-128.6	-128.6	-128.0
4	-131.8	-133.2	-134.1	-134.5	-134.5	-134.1	-133.2	-131.8
5	-136.7	-138.8	-140.4	-141.2	-141.2	-140.4	-138.8	-136.7
6	-142.2	-144.7	-146.8	-147.9	-147.9	-146.8	-144.7	-142.2
7	-147.9	-150.7	-153.0	-154.3	-154.3	-153.0	-150.7	-147.9
8	-153.5	-156.4	-158.9	-160.3	-160.3	-158.9	-156.4	-153.5
							-160.3	-123.4
							36.9	

Table 11-4: Mirror equilibrium temperature distribution for 10° Sun inclination

'Cold Side' Mirror Cells Equilibrium Temperature								
T [C]	1	2	3	4	5	6	7	8
1	-134.1	-131.9	-129.7	-128.6	-128.6	-129.7	-131.9	-134.1
2	-131.5	-131.0	-129.9	-129.0	-129.0	-129.9	-131.0	-131.5
3	-132.9	-133.5	-133.5	-133.3	-133.3	-133.5	-133.5	-132.9
4	-136.6	-138.0	-138.9	-139.3	-139.3	-138.9	-138.0	-136.6
5	-141.4	-143.4	-145.0	-145.8	-145.8	-145.0	-143.4	-141.4
6	-146.7	-149.1	-151.1	-152.2	-152.2	-151.1	-149.1	-146.7
7	-152.2	-154.9	-157.1	-158.4	-158.4	-157.1	-154.9	-152.2
8	-157.6	-160.4	-162.8	-164.2	-164.2	-162.8	-160.4	-157.6
							-164.2	-128.6
							35.7	

'Hot Side' Mirror Cells Equilibrium Temperature								
T [C]	1	2	3	4	5	6	7	8
1	-129.0	-126.7	-124.4	-123.3	-123.3	-124.4	-126.7	-129.0
2	-126.3	-125.8	-124.6	-123.7	-123.7	-124.6	-125.8	-126.3
3	-127.8	-128.4	-128.4	-128.2	-128.2	-128.4	-128.4	-127.8
4	-131.6	-133.1	-134.0	-134.4	-134.4	-134.0	-133.1	-131.6
5	-136.6	-138.7	-140.3	-141.1	-141.1	-140.3	-138.7	-136.6
6	-142.1	-144.6	-146.7	-147.8	-147.8	-146.7	-144.6	-142.1
7	-147.8	-150.5	-152.9	-154.2	-154.2	-152.9	-150.5	-147.8
8	-153.4	-156.3	-158.8	-160.2	-160.2	-158.8	-156.3	-153.4
							-160.2	-123.3
							37.0	

Table 11-5: Mirror equilibrium temperature distribution for 5° Sun inclination

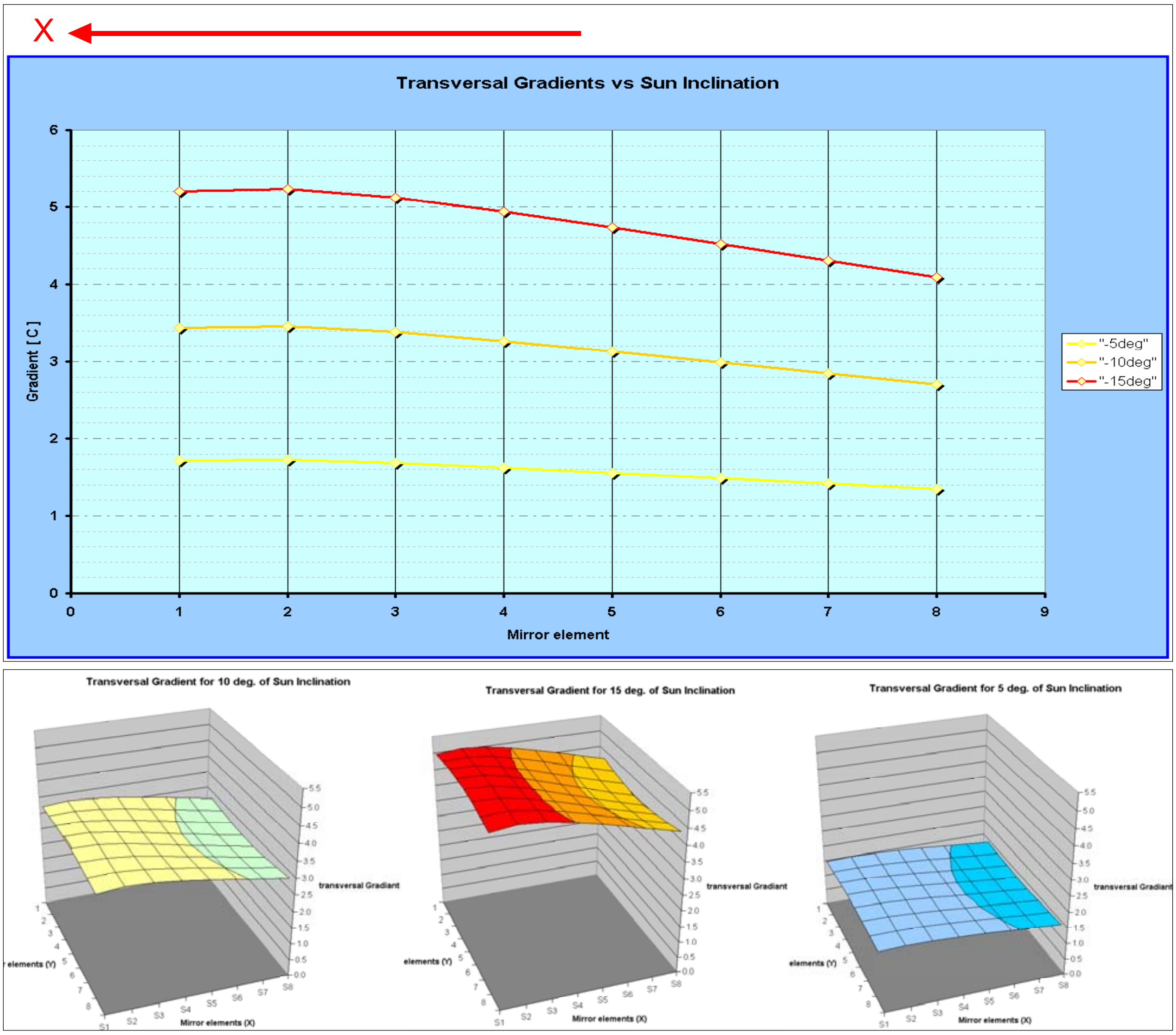

Figure 11-4: Mirror temperature variation as function of Sun inclination angle

11.4 Budgets

The mass and power budgets are summarised as follows:

<u>Mass:</u>

- MLI 84.63 kg
- Heaters 14.34 kg
- Heat pipes and other <u>25.95 kg</u>
- *Subtotal 124.92 kg*
- Margin 20% <u>24.98 kg</u>
- *Total 149.90 kg*

Note that the mass for the "hot plates" (sun shields) and "cold plates" (thermal closure panels) is part of the structure mass budget:

Power:
- Launch/LEOP 90W
- Cruise 75W
- Target acquisition 45W
- Observation mode 45W
- Safe mode 45W

11.5 Future work

The thermal analysis could only concentrate on the system design optimisation. The detailed local design still has to be optimised and it is important that it is properly reflected in the next steps of the project evolution. Some of the key thermal design analyses and recommendations to be addressed in future work are listed in section 11.5.1 and section 11.5.2.

11.5.1 Mirror related

- For a more reliable analysis of the mirror gradients (in-plane and along the optical axis), a detailed thermal model of the mirror petal is needed. Today the Sun inclination angle is limited to +/-15 degrees, however, it is expected that the highest local gradients are in the baffles system and that the crucial temperature gradient along the optical in the mirror petal itself allows for wider angular excursions and allowing more flexible science observation.
- Mirror leaf thermal model covering the interfaced between the mirror leaves (including hinges), to the mirror deployment mechanism and to the mirror petals

11.5.2 Mirror bus/service module related

To find the optimum location for each of the dissipating units, a detailed thermal model of the MSC service module is needed. The model shall encompass all radiative and conductive features and properly reflect the interaction with the mirror/optical bench. Some non-standard bus design optimisations that need to be done include:
- Detailed design of the thermal closure panels
- Optimisation of the thermal finish for the two non-MLI-coated canister panels

12. MECHANISMS

The following mechanisms of the MSC are important:

- At petal level:
  - Pointing actuators
  - Launch locks/HRM
- At shell level:
  - Deployment active hinge
  - Deployment passive hinge
  - Launch locks/HRM
  - Latches
- At shell radiating plate level:
  - Radiating plate deployment mechanisms
  - Radiating plate locking mechanism
  - Radiating plate HRM mechanisms
- At shell sun shield level:
  - Sun shield deployment hinges mechanisms
  - Sun shield locking mechanism
  - Sun shield HRM mechanisms
- At frame level:
  - Deployment active hinge
  - Deployment passive hinge
  - Launch locks/HRM
  - Latches
- At DSC level:
  - Grating platform booms deployment mechanism
  - Grating platform locking mechanism
  - Sun shield deployment mechanisms
  - DSC separation system
- At spacecraft stack level:
  - Stack separation system

12.1 Requirements and design drivers

12.1.1 Petal mechanisms (actuator and HRM)

Main drivers for the petals actuator mechanisms are:

- Number of actuator per petal: 3
- Actuator translating range: 5 mm
- Actuator translation resolution: 1 μm
- Restricted available volume: within the spacecraft sub-frame
- Requested duty cycle / life time: mainly beginning of life for some hundreds of cycles
- Thermal conditions at actuator level during operation: Cryo
- Main open point: mechanical fixation to the petal

The main drivers for the locking mechanisms at petal level are:

- HRM load capability at petal level: between 7000 and 10 000 N (assuming 5g on 70 kg of petal mass)
- Restricted available volume: within the spacecraft sub-frame
- Thermal conditions at HRM level during operation: cold to ambient T°
- Open points 1: resetability capability
- Open point 2: low shock design

12.2 Assumptions and trade-offs

12.2.1 Petals mechanisms

12.2.1.1 Petals pointing mechanisms

The main assumption is that mechanisms are needed for adjusting/pointing the petals toward the detector spacecraft mainly during the beginning of the mission (to cover the first months of the spacecraft's structure adaptation to space conditions). For reliability, it has been decided to use three actuators per petals (although two actuators plus a gimbal system could have been enough).

Three options can be envisaged for the petals mechanisms package (three actuators and locking mechanisms):

1. Specific "light" actuators associated with a specific launch locks (one launch lock for each actuator)
2. Strong actuator that does not need any specific launch lock to maintain the petal during the launch phase.
3. Smart self-locking actuator in launch configuration (once in orbit, first actuator movements are used to unlock the mechanism and the petal, and therefore, no additional launch lock is needed)

The main identified trade-off criteria for the identification of the best solution are:

- Pointing requirements
- Launch lock load performances/reliability
- Mass
- Power consumption
- Envelope (with respect to the small available volume)
- Development and qualification status
- Development risk

Each of the criteria has been evaluated and marked (from 0 to 10) in Table 12-1, with 10 corresponding to the best mark possible:

	Small Actuator + LL	Strong Actuator	Smart Actuator
Pointing requirement	9	3	9
Launch lock load perf.	9	8	8
Mass	8	4	6
Power	8	6	8
Envelope	8	3	6
Development status	10	10	3
Development Risk	8	8	4
TOTAL	**60**	**42**	**44**

Table 12-1: Actuator trade-offs

The option with the best total mark is the first one: use of a "small" actuator tune for the specific pointing requirements associated to a specific strong launch lock to off-load the actuator and hardly fix the petal to the structure, during the launch.

An example of possible actuator that can fulfil the requirements could be a European (to be developed) competitor to the Moog Rubicon:

- Resolution: < 1μm
- Stroke: 10 mm (with two stage/two motors)
- Operating T° range: 20° to 300°K
- Mass: 180 to 200g
- Outside diameter: 3.175 cm
- Length: < 10 cm
- Creep: 0.0 nm/day
- Power consumption: <0.1W (in Cryo)
- Axial stiffness: 1.06 N/μm

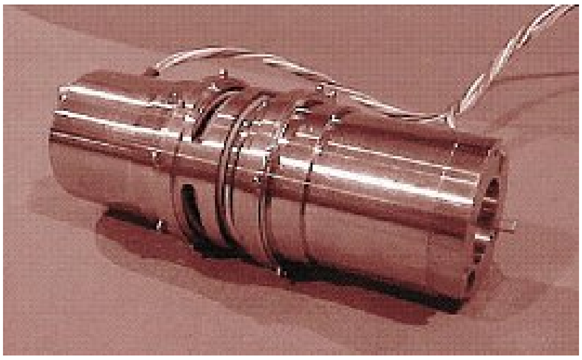

Figure 12-1: Potential actuator (Moog Rubicon)

The proposed implementation of the pointing actuators (in red) within the frame design (in black), at petal (in blue) level is the following:

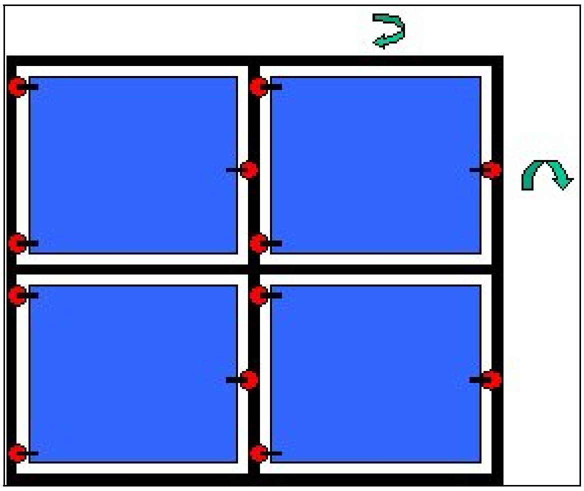

Figure 12-2: Actuator location

12.2.1.2 Petal Hold-down and Release Mechanism (HRM)

Two options are proposed for the HRM:

1. Use one common HRM command for eight petals of a same row
2. Use one HRM per actuator

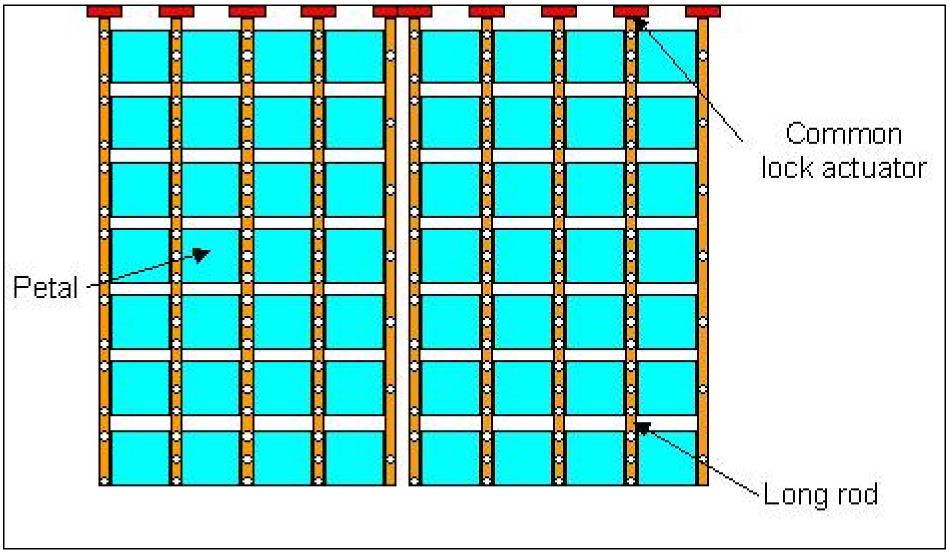

Figure 12-3: Common HRM principle

In this case, each HRM is located next to each actuator, therefore, three HRMs per petals are required to lock a petal. HRM location is similar to actuator location described in Figure 12-2.

A trade-off at HRM concept level has been performed to select the best concept with respect to mass, power consumption, and reliability.

	One HRM per actuator	Common HRM per row
Mass	4	6
Power consumption	4	6
Reliability	8	2
TOTAL	**16**	**14**

Table 12-2: HRM trade-offs

The reliability is the main criteria for the concept selection. Therefore, even if the two concepts are more or less similar in term of mass and power consumption, the preference is given to the design where each actuator is designed with an HRM.

The proposed selected concept design where a specific HRM is "attached" to each actuator is shown in Figure 12-4:

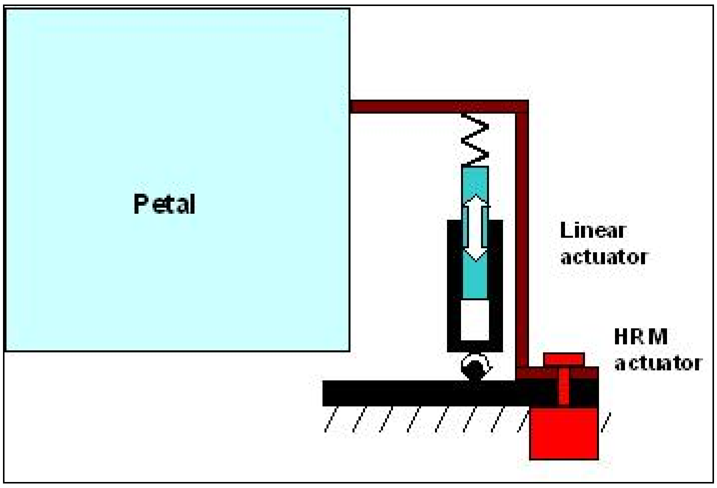

Figure 12-4: Proposed HRM concept

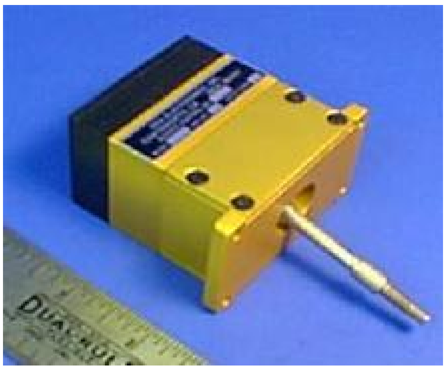

Figure 12-5: Potential HRM actuator (courtesy of NEA Electronics)

The desired features would be:

- Extremely Low Release Shock *
- Non-Redundant Actuation Circuit *
- Simultaneous Release of Multiple Hold-Down Points * Refurbishable by Replacing Initiator *
- Internal Torque Containment *
- Allows Angular Misalignment of Bolt or Rod (15°Cone)
- Extended Operating Temperature Range *
- Operates using Pyro Circuitry *
- Safe (Range Safety - friendly) *
- Space-Rated Materials *

•*Specifications:

- Ultimate Load: 6 200 pounds (28 000 N)
- Rated Release Load: 4 500 pounds (20 300 N)
- Source Shock: <50 g's at 2500 # preload
- Actuation Circuit: 4 Amps at 4 VDC during 25 ms
- Actuation Circuit: 2 Amps at 4 VDC during 100 ms
- Temperature Range: -80°C to 150°C
- (Could be extended to –135°C or more)
- Weight: 80 grams

12.2.2 Shell mechanisms

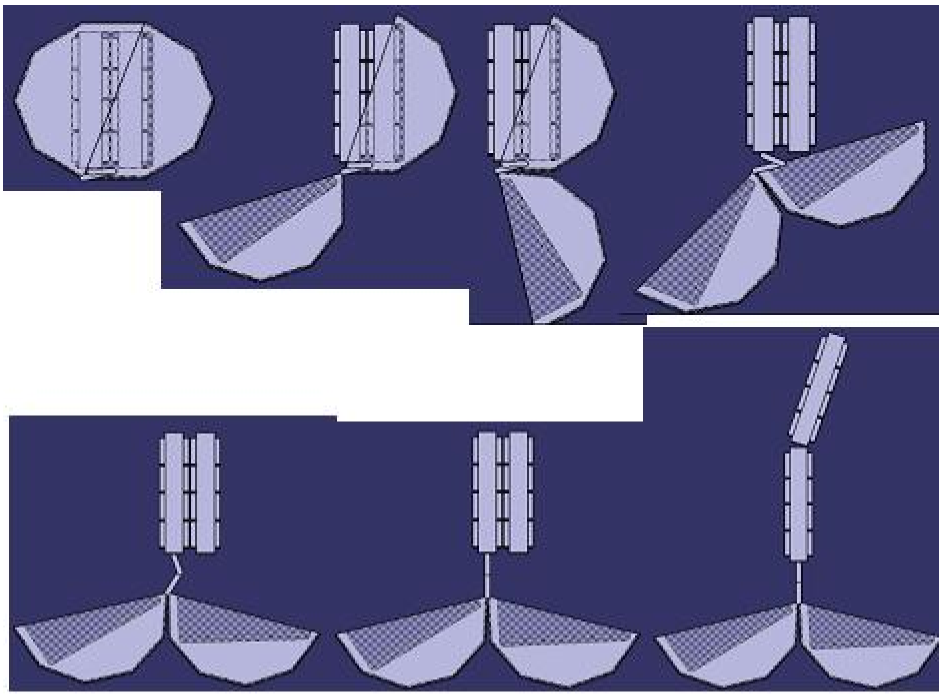

Figure 12-6: Deployment sequence

In the case of XEUS, the shells' deployment mechanisms have several functions. The first function is to deploy each half shell to reach the specific final angular position, but other mechanisms shall be used to move away the frames from the deployed shells. To achieve these complex deployments in a reliable way, the number of requested actuator is linked to the number of mechanical parts to be moves/deployed (no mechanical synchronisation is proposed). Therefore, a total of four actuators are requested. Two actuators will be used to deploy the two half shells, two others will be used to move away the two half shells from the frames.

In this case, a minimum number of four actuators, four passive hinges, eight latches and eight HRMs are requested.

The proposed design parameters are based on TerraSAR mechanism types where it has been proven that a large moving inertia required an inevitably relatively large actuator (torque and stiffness requirements mainly drive the actuator choice). Figure 12-7 shows the main elements of the mechanisms set for the two half frame deployment:

Active hinge layout:

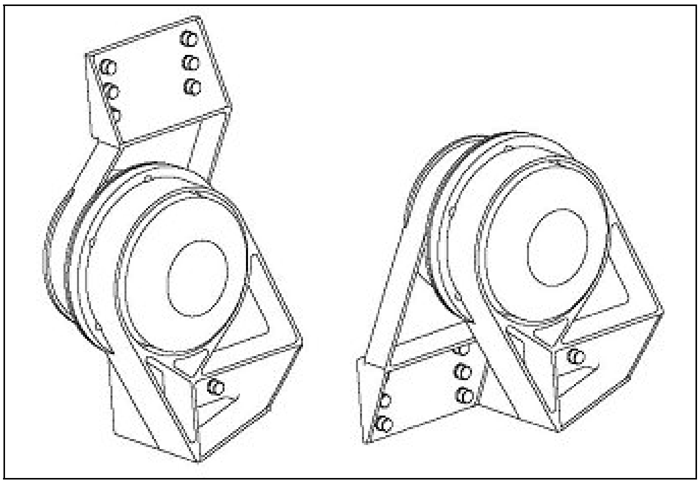

Figure 12-7: Open en closed potential active hinge design (courtesy of SENER)

Mass: 5 kg (including actuator)
Power consumption = 15W
Deployment angle <270°

An example of a possible rotary actuator that can fulfil the requirements could be a European (to be developed) competitor to the Moog Type 5 product:

Figure 12-8: Potential rotary actuator

Output step angle:	0.0075°
Tensional stiffness:	11 300 Nm/rad
Axial load capability:	13 400 N
Transverse load capability:	11 000 N
Moment load capability:	298 Nm
Output torque:	56 Nm
Holding torque (powered):	70 Nm
Holding torque (unpowered):	23 Nm
Mass:	2.2 kg

Passive hinge layout (integrating the cable wrap).

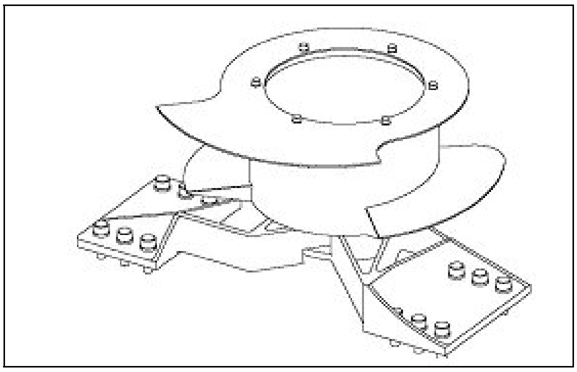

Figure 12-9: Potential passive hinge design (courtesy of SENER)

Mass:	2.5 kg
Power consumption:	0W
Deployment angle:	<270°

Latches layout

Mass:	1 kg
Stiffness:	<90 000 N/m
Applied preload:	1150 to 1350 N
Power consumption:	0W

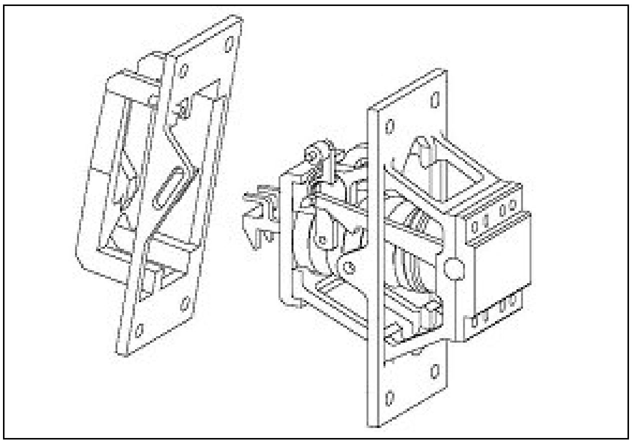

Figure 12-10: Latching mechanism (courtesy of SENER)

HRM layout

Mass: 1.5 kg (without pyro)
Power: 4A during 25ms
Preload: TBD

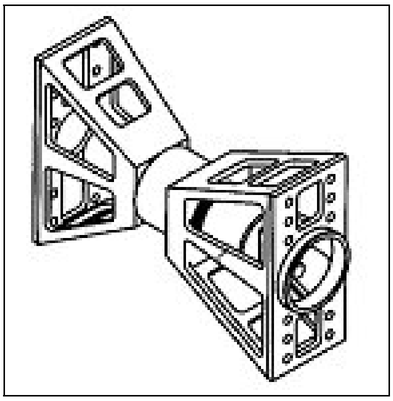

Figure 12-11: HRM mechanism (courtesy of SENER)

12.2.3 Radiating plate mechanisms

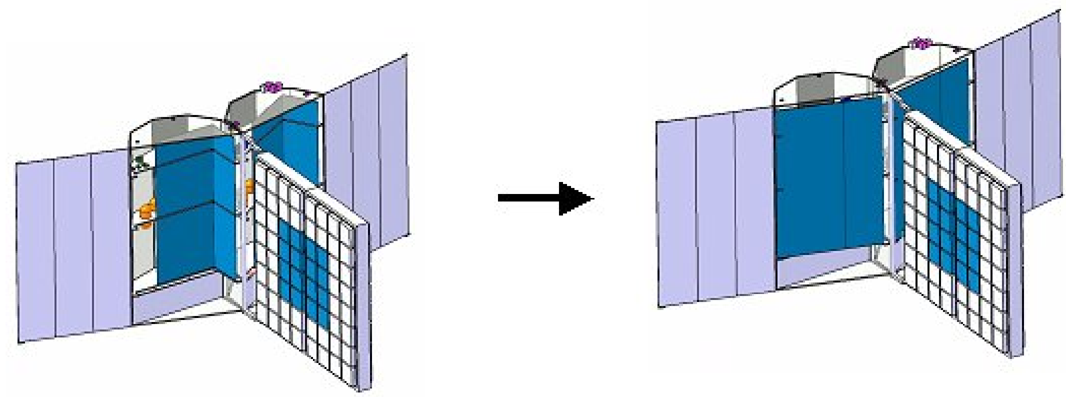

Figure 12-12: Radiating plate mechanism to deploy thermal closure panels

Each radiative plate is stowed (90° folded) inside each shell and then deployed "flat" to cover the shell. Therefore two lines of three hinges are requested per radiative plate. Due to the expected low mass and not very accurate final deployed position needed, "simple" damped spring-based hinges are proposed. The deployment speed of each of the radiative plate could be controlled to decrease or minimise the shock at the end of the deployment. The positive locking of each hinge in the requested deployed position will be achieved by the hinge itself. Several locking mechanisms (four per radiative panel) will be used to control and fix the deployed position. These specific foreseen hinges integrate a regulator that is based on fusible metal technology. Therefore, by simply heating the regulator with 10W or 15W, the deployment time could be tuned to 4 to 6 min (at 0°C starting temperature).

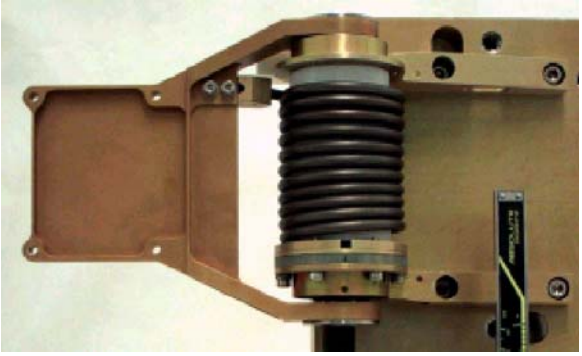

Figure 12-13: Hinge mechanism (courtesy of SENER)

To stow the thermal closure panels during launch, a minimum of nine HRM points will be needed (courtesy of SENER).

12.2.4 Sun shield mechanisms

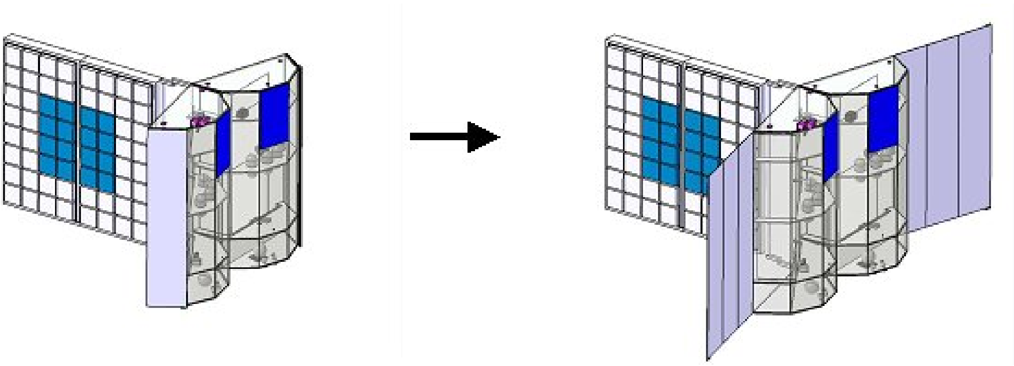

Figure 12-14: Sun shield mechanism principle to deploy "hot plates"

Each sun shield plate is considered similar to solar array panels that are folded (in three parts) and stowed on the side of the spacecraft during launch. Each can be deployed afterwards as soon as the HRM are released. Standard spring base hinges can be use for the sun shield deployment. Nine hinges are needed per sun shield. Locking mechanisms are used to maintain with the relevant stiffness the shield in the deployed position. Due to the large size of the sun shield, ten HRMs are needed to stow each shield on the side of the spacecraft during launch.

12.2.5 Mirror leaf mechanisms

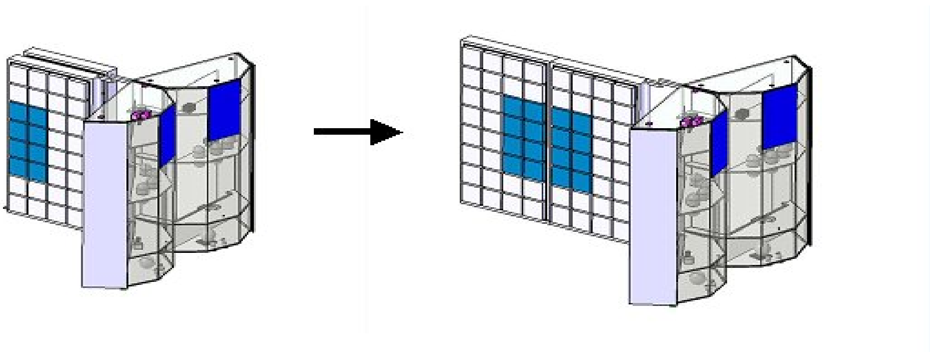

Figure 12-15: Mechanism principle to deploy mirror leaves

Several mechanism concepts can be used for the mirror leaf deployment. As first assumption, the simplest design is proposed for this CDF study. It consists of:

- One active hinge, powered by a rotary actuator and located between the two half parts to be deployed, close from a frame corner.
- Two passive hinges (simple hinges) located at the middle and at the opposite position/corner from the active hinge, and also located between the two half parts to be deployed.
- Six latches, to lock the two half frame in open/deployed position.
- Six launch lock devices, four located close to each corner and two located in the middle of the longer length of the two half frames (while in close position), to fix the two halves together during the launch and also offload the two hinges that should not be designed to withstand the launch loads.

As first assumption, the same type of actuators, passive hinges, latches and HRM as those used for the shell are proposed for the frame mechanisms.

12.2.6 DSC grating and sun shield mechanisms

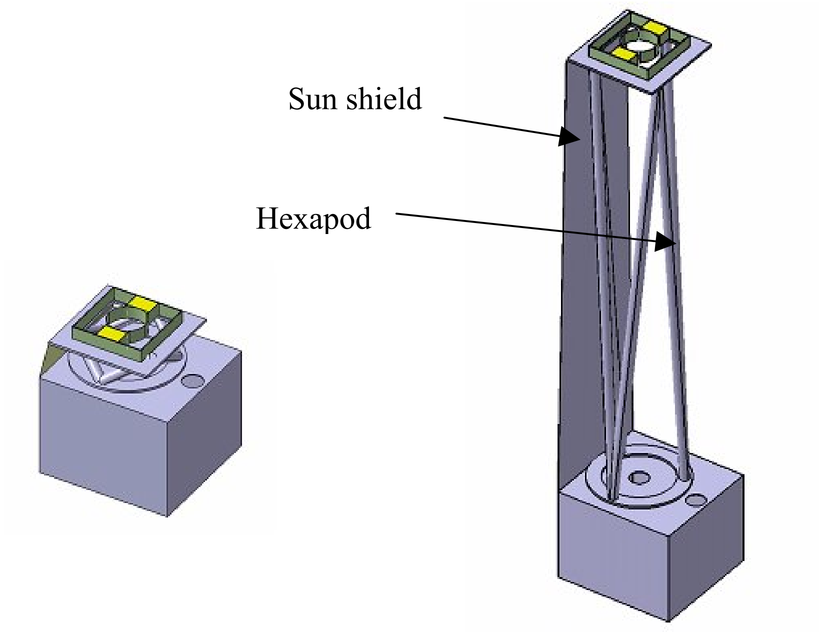

Figure 12-16: DSC grating panel (stowed and deployed configuration)

The proposed design of the deployable DSC grating and sun shield mechanisms is based on a hexapod made of six hollow deployable booms.

These types of booms are made of a biconvex tube mast that can be flattened and then rolled up around a drum into a small volume package. A drive system pulls the tube by the edge to deploy, and rotates the drum to retract. This approach leads to a mast fully operational and backlash free at any intermediary position, from zero to fully deployed. The mast can be manufactured in metal and composite (CRFP), in both cases a continuous manufacturing method is used, then, it provides tubes of unlimited length. A flat cable can be implemented also in the mast to provide signal and power to any payloads/experiments placed on the top.

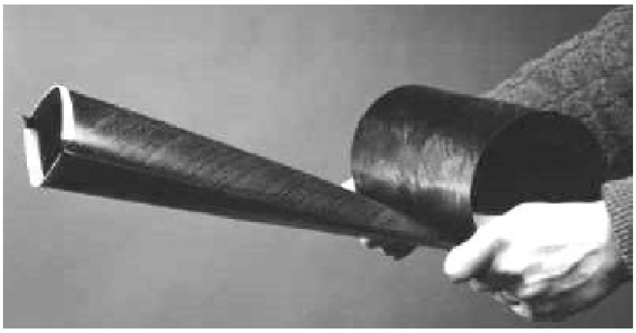

Figure 12-17: Collapsible tubular mast for grating panel deployment (courtesy of DLR)

Figure 12-18: Complete boom deployment mechanism example

The sun shield is made of an "rollable"/"unrollable" foil that is attached on one side to the DSC spacecraft and to the grating module on the opposite side and follow the booms deployment. In stowed position, the grating module is stowed on top of the DSC spacecraft thanks to six HRMs (one per boom).

12.2.7 DSC separation mechanisms set

The baseline is the spacecraft should be attached to the mirror spacecraft with four HRM points. The HRM points will be activated by pyro devices and will integrate each, a push-up device to eject the spacecraft from the launcher at the correct speed. Typical mass of such an HRM/Push up device is 2 kg (without the pyro element).

Figure 12-19: DSC separation mechanism (courtesy of SAAB)

12.2.8 Spacecraft stack separation mechanisms set

The baseline is the spacecraft should be attached to the launcher with ten HRM points. The HRM points will be activated by pyro devices and will integrate each, a push-up device to eject the spacecraft from the launcher at the correct speed. The typical mass of such an HRM/Push up device is 2 kg (without the pyro element).

12.3 Baseline design main budgets

12.3.1 Petals pointing and HRM mechanisms final budget

As seen in previous chapters, each petal needs three actuator and three HRMs.

The number of actuators and HRMs is 144 for the base line and 192 for the option with the frame equipped with 64 petals (8x8 petals with three actuators/HRM per petals):

- Mass per actuator = 200 g (single stage)
- Mass of each HRM = 200 g
- Mass of structure to link the HRM to the petal = 100 g (TBC with petal fixation)
- *BASELINE TOTAL MASS = 72 kg*
- *OPTION TOTAL MASS = 96 kg*

The power consumption for each HRM release is:

- 2A during 100 ms per point (0.216 Wh) or
- 4A during 25 ms per point (0.108 Wh)

Power consumption per actuator for pointing:

- <0.1W per actuator (under cryo)

12.3.2 Half frame mechanisms set

As seen in previous chapters, the petals half frame deployment requires a set of the following mechanisms:

- One active hinge
- Two passive hinges
- Six latches
- Six HRMs

The mass budget is the following:

- One active hinge = 5 kg
- Two passive hinges + cable-wrap = 2.5 kg
- Six HRMs = 6x1.5 = 9 kg
- Six latches = 6x1 = 6 kg
- *TOTAL = 25 kg*

The power consumption of the active hinge (actuator) is the following:

- For deployment = 15W during 20 or 40 minutes (depending on mot. margin calculation)
- For HRM firing = 6 times 4A during 25 ms

12.3.3 Shell mechanisms set

As seen in previous chapters, the shell mechanisms require a set of the following mechanisms:

- Four active hinges
- Four passive hinges
- Eight latches
- Eight HRMs

The mass budget is the following:

- Four active hinges = 4x5 = 20 kg
- Four passive hinges + cable-wrap = 4 x2.5 = 10 kg
- Eight HRMs = 8x1.5 = 12 kg
- Eight latches = 8x1 = 8 kg
- *TOTAL = 50 kg*

The power consumption of each active hinge (actuator) is the following:

- For deployment = 15W during 20 or 40 minutes (depending on mot. margin calculation)
- For HRM firing = 8 times 4A during 25 ms.

12.3.4 Radiating plate mechanisms

As seen in previous chapters, the two radiating plates mechanisms require a set of the following mechanisms:

- Four damped hinges
- Eight non-damped hinges
- 18 HRMs
- Six latches

The mass budget is the following:

- Four damped hinges = 4x 0.2 = 0.8 kg
- Eight non-damped hinges = 8 x 0.2 = 1.6 kg
- 18 HRMs = 18x0.5 = 9 kg
- Six latches = 6x0.2 = 1.2 kg
- *TOTAL = 12.6 kg*

The power consumption of each damped hinge (to regulated the deployment speed) is:

- For deployment = 30W during 15 minutes per shell side panels (depending on mot. margin calculation)
- For HRM firing = 18 times 4A during 25 ms

12.3.5 Sun shield mechanisms

As seen in previous chapters, the two sun shield mechanisms require a set of the following mechanisms:

- 18 deployment hinges
- 20 HRMs

The mass budget is the following:

- 18 deployment hinges = 18x 0.2 = 3.6 kg
- 20 HRMs = 20x1 = 20 kg
- *TOTAL = 23.6 kg*

For HRM firing = 20 times 4A during 25 ms.

12.3.6 DSC grating and sun shield mechanisms (optional)

As seen in previous chapters, the hexapod platform requires six deployment boom mechanisms and six HRMs. The deployable shield mechanisms are basically "unrollable" tubes:

- Six grating booms
- Six grating boom canisters
- Six grating booms and DSC launch lock
- One DSC and grating shield assembly

The mass budget is the following:

- Six grating booms = 6x 2 = 12 kg
- Six grating boom canisters = 6 x 12 = 72 kg
- Six grating boom and DSC launch locks = 6x1.5 = 9 kg
- One DSC and grating shield assembly = 1 x 15 = 15 kg
- *TOTAL = 108 kg*

The power consumption of a boom canister (to regulated the deployment speed) is the following:

- For deployment = 25Wx6 = 150W during 60 minutes (depending on mot. margin calculation)
- For HRM firing = 6 times 4A during 25 ms

12.3.7 DSC spacecraft separation mechanisms

As seen in previous chapters, the number of HRM points to rigidly attach the DSC spacecraft to the mirror spacecraft is 4. Each of the HRMs will integrate a push up device to eject the DSC spacecraft from the mirror spacecraft at the required speed. These four HRMs are the only pyro-based devices on the spacecraft.

Mass: 4 x 1.5 kg = 6 kg (not including pyro mass)
Power: 8 x 2A during 25 ms

12.3.8 Spacecraft stack separation mechanisms

As seen in previous chapters, the number of HRM points to rigidly attach the spacecraft to the launcher is 8. Each of the HRM will integrate a push up device to eject the spacecraft from the launcher at the required speed. These eight HRMs are the only pyro-based devices on the spacecraft.

Mass: 10 x 2 kg = 20 kg (not including pyro mass)
Power: 10 x 2A during 25ms

12.3.9 Summary

Baseline (144 petal actuators <u>without</u> grating deployment system)
Petal mechanisms mass = 72 kg
Shell mechanisms mass = 50 kg
Half frame mechanisms mass = 25 kg
Radiating plate mechanisms = 12.6 kg
Sun shield mechanisms = 23.6 kg
Spacecraft stack separation mechanisms = 20 kg
Total mass = 203.2 kg

Option (192 petal actuators and grating deployment system)
Petal mechanisms mass = 96 kg
Shell mechanisms mass = 50 kg
Half Frame mechanisms mass = 25 kg
Radiating plate mechanisms = 12.6 kg
Sun shield mechanisms = 23.6 kg
DSC grating and sun shield mechanisms = 108 kg
DSC spacecraft separation mechanisms = 6 kg
Spacecraft stack separation mechanisms = 20 kg
Total mass = 341.2 kg

Options and open areas
Number of actuators/HRM per petals
Deployment concept of the frames and shells

Note that the as-yet unknown fixation interfaces with the petals may significantly impact the mass of the mechanisms. Also, the volume available for the mechanisms implementation may impact the design choice and performances. Last concern is about the provided stiffness interfaces for the mechanisms fixation.

13. DATA HANDLING

This chapter describes the basic requirements, design drivers and baseline design description for the Data Handling System (DHS) of the mirror spacecraft.

13.1 Requirements and design drivers

The reliability and availability are the major requirements for XEUS DHS. The XEUS DHS is perfectly in line with the current development path for highly integrated avionic data systems in ESA. The DHS shall provide the capability to perform the following functions for the mission lifetime (up to 20 years):

- AOCS/GNC. Interface the sensors equipment (Sun Sensor, gyro, Star Tracker, RW) and control the propulsive system during all the mission phases.
- Mirror actuators. Interface and command the 48 mirror actuators with the CDMU.
- Telecommands. Include a TC handler that demodulates, decodes, validates, distributes and executes both real-time and time-tagged ground commands. For this purpose, both a direct interface with the transponder unit or a transponder unit that sits on the main CandC bus are suitable. The first solution allows use of recurrent transponder units.
- Telemetry. Acquire housekeeping data for transmission to ground and/or internal processing to support the autonomous functions (During contingency phase, the spacecraft shall remain in current operating mode autonomously for at least 72 hours).
- Communication with DSC. Communicate with the detector spacecraft.
- Power control. Monitor the battery status (mainly the charge/discharge current and voltage) and the SAT solar arrays.
- Thermal control. Keep the vehicle temperature inside definite limits by reading thermal sensors and control heaters.
- On-board time. Provide on-board time reference generation and distribution to ensure synchronisation and time tagging of attitude data for post-processing.
- Failure detection and recovery. Does not provide any function: ground control centre executes the failure recovery. The DHS has the capability to put the spacecraft in a “safe” mode that can be tolerated (for power, thermal, attitude point of view) permanently.
- On-board storage. Provide capability to store all housekeeping data.

13.2 Assumptions and trade-offs

13.2.1 Use of BepiColombo DHS

Highly Integrated Control and Data System (HICDS) is a project aimed to define the avionics architecture of BepiColombo. The HICDS project is divided into several activities. One activity, entitled “Miniature Integrated Avionics Electronics” (MIAE), is funded under the TRP programme; all other activities are directly funded by the Science Core Technology Program in the context of the HICDS project.

The objective of the MIAE activity is to reduce mass, volume, developments schedule of control and data systems for the BepiColombo mission and to other science missions when applicable. In particular, a mass reduction of a factor of 4 and a power consumption of a factor of 2 are expected when comparing to the avionics mass and power of actual ESA planetary missions (e.g. Mars Express).

13.3 Baseline design

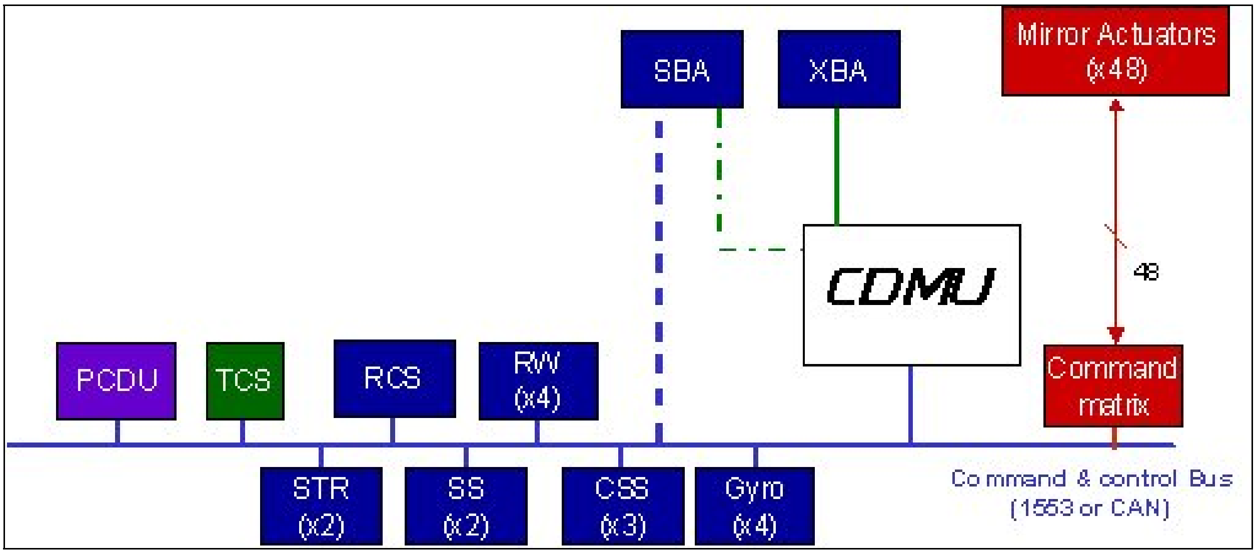

Figure 13-1: DHS baseline design

13.3.1 CDMU

The baseline design core of the CDMU is the avionics core of HICDS.
The avionics core is a complete internally redundant spacecraft controller incorporating the following functions:

- Telecommand Decoder with associated Command Pulse Distribution Unit
- Telemetry multiplexer and downlink formatter, including an essential TM data collector
- On-board Time manager
- Reconfiguration Module with associated Safeguard Memory
- Processor Module with external user interfaces

A view of the avionics core interfaces is shown in Figure 13-2:

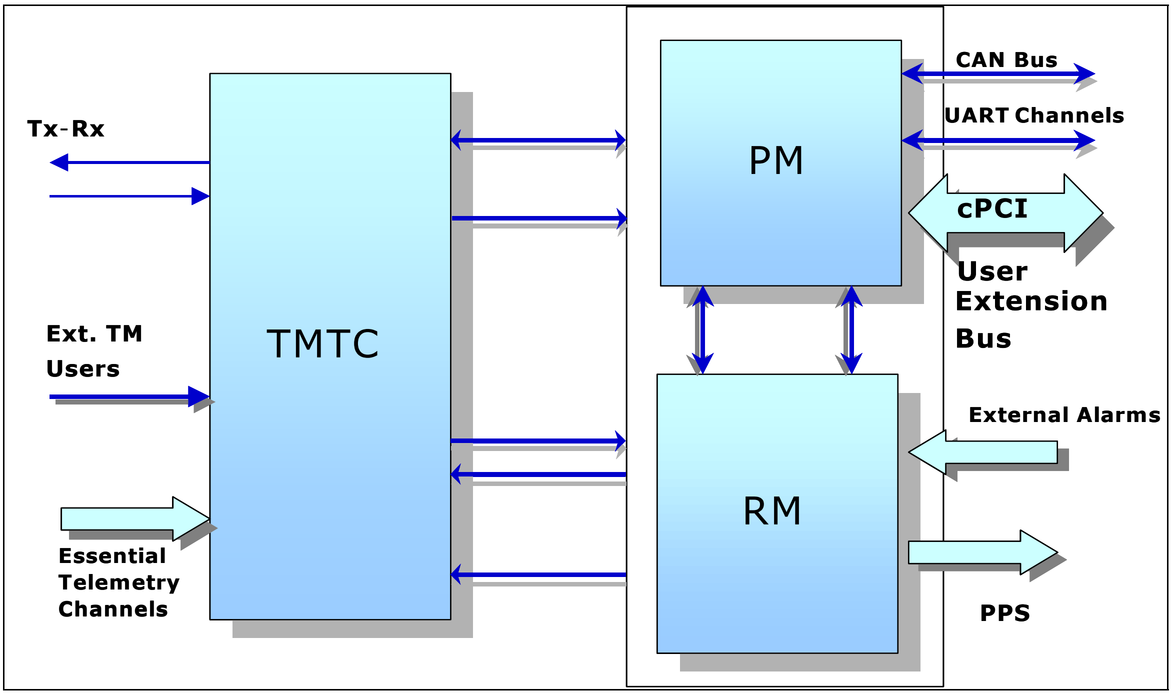

Figure 13-2: Block scheme of HICDS-MIAE avionics core architecture

13.3.1.1 Processor Module and Reconfiguration Module

The processor module is based on a LEON2-FT processor. It includes at least 128 kilobyte PROM, 3 Mbytes EEPROM, 6 Mbytes RAM (RAM and EEPROM EDAC protected) processor memories. It may also include CAN Bus Controller (HurriCANe-based, CANOpen compatible), four SpaceWire Links (for internal use), MAP interfaces, PCI Controller, four UARTS, Interrupt Controller, Timers and Service Signals.

The Reconfiguration Module includes all the hardware circuits devoted to internal and external alarm monitoring, and safeguard memory. The Safeguard Memory comprises at least 1 Mbyte RAM + 256 kilobyte EEPROM (EDAC) with autonomous scrubbing and write protections.

13.3.1.2 TM/TC module

The TM/TC module of the avionics core can be used for communication with the XEUS GS and DSC. The TM/TC module interfaces directly with the S-band and X-band assemblies.

13.3.1.3 Budget

Function	Mass (kg)	Power (W)
TC decoder and TM encoder function	2* 0.8	2* 1.5
Reconfiguration function and On-Board Time	2* 0.4	2* 1.0
Processing function	2* 0.4	5.0
Avionic core total	3.2	10

Table 13-1: Mass and power budget of the avionics core

A non-redundant TC decoder and TM encoder function fits on a double Eurocard size. A non-redundant Reconfiguration function, On-Board Time and procession function also fit on a double Eurocard size. The total number of boards in an avionics core is then four.

The budget including redundancy and DC/DC converters is:

- Mass: 4 kg
- Power: 12W
- Dimension: 5 double Eurocard size 165*233*160 mm^3 plus enclosure

13.3.2 Mass memory

Given the present available technologies the only feasible approach (without using expensive Honeywell Rad-Hard memories) for a SSMM to last 15 years in L2 is a gracefully degrading architecture that can guarantee EOL capabilities. It consists of memory module integrating multiple redundancy.

13.3.2.1 Memory array organisation

The proposed memory array has the following physical hierarchical structure:

- The memory device is a SDRAM device of 256 Mbits organised as 32M x 8 bits. Availability of these devices is still foreseen in the next 3-4 yrs. It may be necessary to replace them with 512 (64M x 8) MBit if phase C starts after 2008.
    - Optionally, if it is deemed necessary to reduce the power budget, SRAM devices may be used. SRAMs in general have a better behavior as regards lifetime and radiation effects but are one order of magnitude less dense than DRAMS. The final organisation of the memory will be the same, mass will be slightly higher, standby power consumption will be close to zero. In this case the use of chip stacks (like 3D packages) is unavoidable.
- The SDRAM packages are comprised of a stack of 1 SDRAM devices (256 Mbits per package). This approach offers more reliability and lower costs compared to a design using Multi chip carrier stack.
- The Memory block provides the minimum number of SDRAM packages required to build up the 20 bit-wide data word (16 bits user data + 4 bits EDAC). It is composed of 16 user SDRAM packages: 16 x 256 Mbits = 4 Gbits net capacity; four SDRAM packages are used for EDAC, which represents a total of 5 Gbits gross capacity.
- The Word Group provides the minimum number of 32 M x 8 bits organised SDRAM devices required to build up the 20 bit-wide data word. The word group is part of the memory block. It is composed of 16 SDRAM devices plus four for EDAC.
- The memory partition is composed of 1 word group. Each memory partition is powered and protected by an individual Latch-Up switch. The user capacity of a memory partition is 4 Gbits.
- The memory module contains up to four Memory Partitions. The user capacity of a memory module is up to 16 Gbits of net capacity or equivalently, 20 Gbits of gross capacity.
- The module array contains only one memory module.

The memory module is powered by two power supplies, responsible for partition 1 and 2, and partition 3 and 4, respectively. Only one partition is working at a time, the others remain switched off.

13.3.2.2 Module array internal redundancy

The module array is internally redundant and single point failure free. Redundancy is provided at several levels:

- Error correction and error detection provides the capability to:
  - Correct one SDRAM device error (SEU induced or loss of one device) within each word group of 20 SDRAM devices
  - Detect two SDRAM device failures (SEU induced or loss of two devices) within each word group of 20 SDRAM devices
- No redundancy at word group level. If the word group fails, the partition is lost.
- Spare partitions are used to replace totally failed memory partitions. Each memory partition is powered and protected by an individual Latch-Up switch.
- No redundancy at memory module level. If the memory module fails (which is the case if the power supply fail), the complete mass memory is lost.

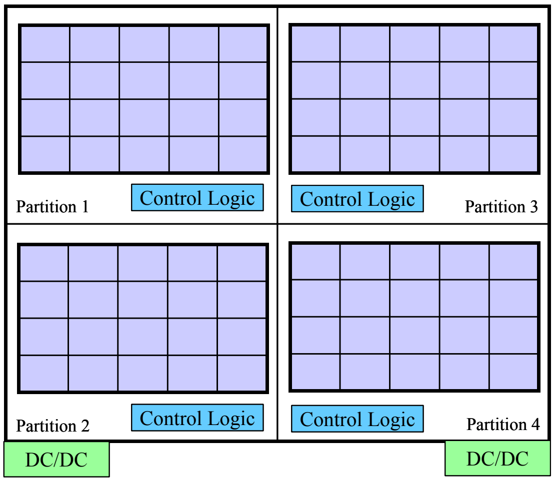

Figure 13-3: Mass memory- data storage architecture

The mass memory has a user capacity of 20 Gbits at the *beginning of life*. This may seem over-sized considering only 50 Mbits of memory are requested. Nevertheless it is not guaranteed that after 15 or 20 years of function the memory remaining will be sufficient. Up to now there is no example of any mission where a solid-state mass memory was used during such a long time. Even for a long mission like Rosetta, the mass memory remains switched off during the cruise (thus minimising the radiation effects) being operational only in the active phase of the mission.

Using memory devices of smaller capacity is not possible given that technology of memory devices is evolving continually and devices of smaller size will not be available any more at the time the mission enters phase C. The proposed design offers sufficient redundancy to expect a capacity End-of-life to be enough. Mass memory with such architecture will not be available off-the-shelf and has to be developed.

Budget:

- Mass: 1.5 kg
- Power: 4W operational, 3W Stby
- Embedded in the CDMU box

13.3.3 Decentralised system

The data handling system is in charge of interfacing the CDMU with the SVM's subsystems. This includes the PCDU, TCS, and all the sensors and actuators of AOCS (4 Reaction Weels, 2 Star Tracker, 2 Sun sensors, 3 coarse Sun sensors, 4 gyros and the propulsion subsystem). The use of a decentralised system is proposed, with proposel architectures for BepiColombo and SOLO.

In a decentralised system sensors and actuators integrate interface that allow communication with the CDMU through the command and control bus, unlike a centralised architecture that uses large RTU to interface sensors and actuators with the CDMU. Decentralised architecture uses micro RTU to interface equipment to the command and control bus.

The command and control bus may be either MIL-STD-1553B bus or CAN-bus.

13.3.4 Mirror actuators commanding

The data handling system is in charge of interfacing and controlling the 144 actuators that enable petals alignment. Three solutions were considered: *point-to-point*, command bus, and command matrix. The latter was retained. The description of the two others can be found in section 13.7.1. The linear actuators are bi-phase stepper motors, two wires are needed per phase (nominal and redundant).

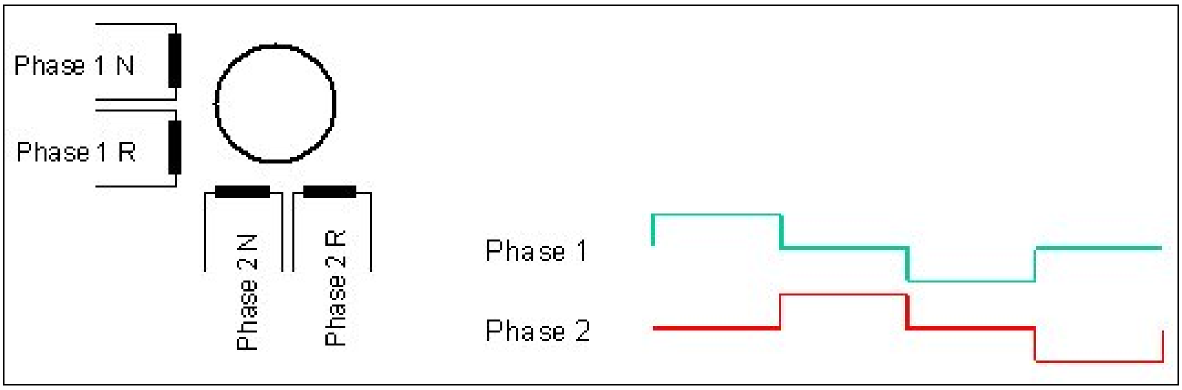

Figure 13-4: Linear actuator - motor control sequence

13.3.4.1 Command matrix

13.3.4.1.1 Principle

The actuators are connected in such a way that by activating one row and one column a single actuator is commanded. An example is given in Figure 13-5 for the nominal part of the first phase. The ground is connected to the column and the strobe is sent on the row.

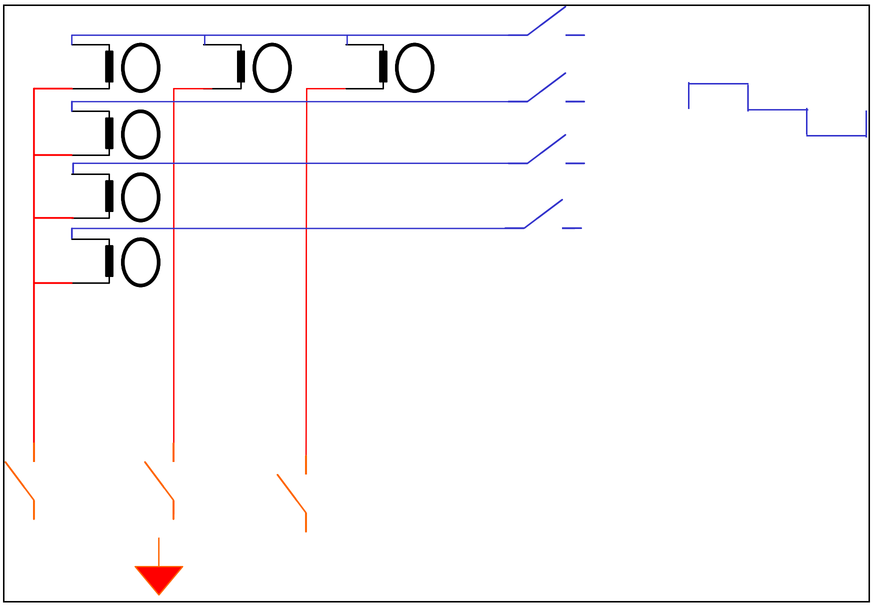

Figure 13-5: Command matrix principle for phase 1 nominal

13.3.4.1.2 Wiring

Figure 13-6 shows the wiring required for one phase (for a complete mirror). The matrix is 24 rows by 10 columns; there are 34 cables; each cable is doubled.

These are in total 144 lines to be routed to the actuators. Assuming the cables are AWG24 and weight 10 g/m, the total weight of cable is 13.5 kg. This total may be underestimated, mounting brackets, complex routings shall be taken into account.

Four matrixes of this type are needed to connect phase 1, phase 2, nominal and redundant.

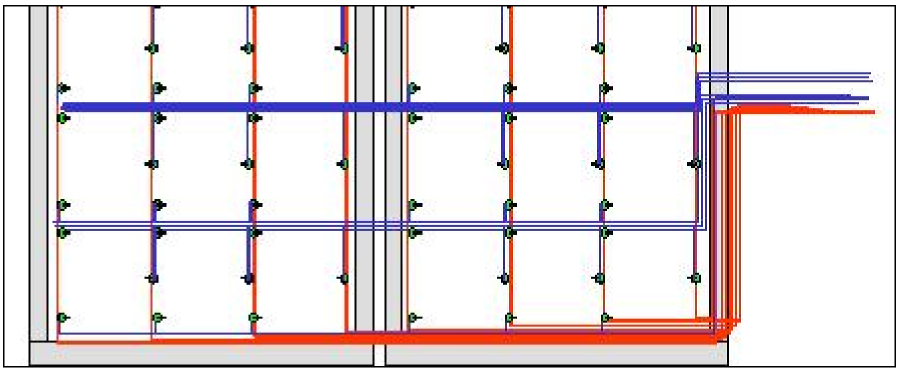

Figure 13-6: Wiring schematic for actuator triggering (see also Figure 14-13)

13.3.4.1.3 Command matrix board

A command matrix board is composed of a nominal and redundant control unit, the control unit is shown in Figure 13-7. The redundant unit is connected to the return line as shown in Figure 13-8. The board can be connected to the command and control bus. One row and one column are selected and the correct strobe is sent to control the phase.

The chosen command matrix board is capable of commanding a matrix of 16 by 36. Two of these boards are used, one for commanding phase 1 and phase 2 Nominal branches, the other for the redundant branches (see Figure 13-4).

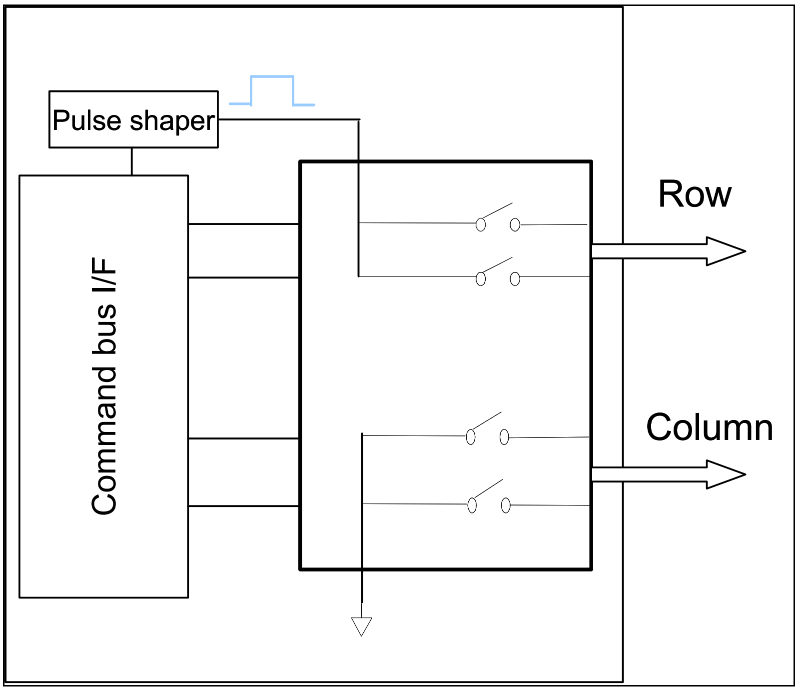

Figure 13-7: Functional block diagram

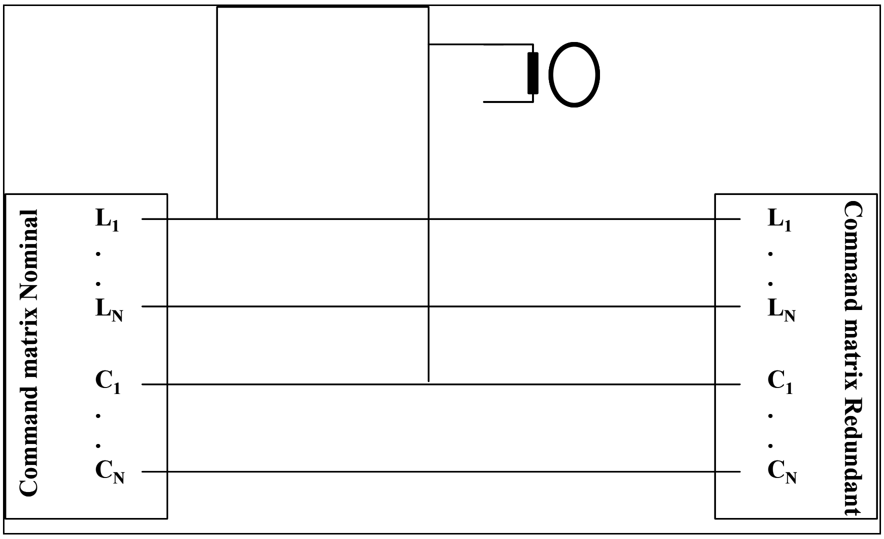

Figure 13-8: Command matrix, redundancy interconnection

13.3.4.1.4 Budget

A board weighs about 1 kg. The total mass (cable + boards) is 15.5 kg A board consumes 3.5W in stand-by and 12.5W when used.

13.4 Performance

13.5 Budgets

Unit	Mass	Power	Dimension
CDMU+MM	5.5 kg	16W	264 mm*278 mm*250 mm
9 bus I/F	1.8 kg	7W	Embedded
Command matrix box (for two boards)	2 kg	Stby 7W, peak 25w	60*260*280 mm
Actuators harness (not included in DHS budget)	12.1 kg		
total	9.3 kg	30W / 48W	

Table 13-2: Budgets

13.6 List of equipment

13.6.1 CDMU

The proposed CDMU will be developed for BepiColombo and SOLO. It is under development at the moment.

13.6.2 Mass memory

The mass memory is to be fully developed.

13.6.3 Decentralised system

MIL-STD-1553B and CAN bus are two standard command and control buses. The embedded interfaces that allow the connection of the units to the bus are of the same kind as the one proposed for BepiColombo and SOLO. They are currently under development.

13.6.4 Command matrix (for mirror actuators)

The command matrix boards are to be developed. Some suppliers provide boards of this type.

13.7 Options

13.7.1 Mirror actuators

Two other options were considered to command the mirror actuators. They are presented hereafter.

13.7.1.1 Point-to-point

This option consists of connecting each actuator to I/O boards using a point-to-point link. Each actuator comprises four twisted pair cables, giving a total of about 200 cables, 800 m of cable, and a total weight of 18 kg.

Assuming an I/O board that handles 32 HPC weighs 750 g, seven boards are needed which gives a weight of 5.25 kg. Some weight can be spared using ASIC or hybrid solutions that enable packing many more channels in a single board, anyway limiting factors will be the size of the connectors and the space needed for the cabling. Even if this solution introduces a lot of complexity in terms of cable routing, integration and testing, it seems the only possible due to the constraints of the mirror on electronics.

13.7.1.2 Command bus

This solution consists of connecting the actuators to a power bus and a command bus.
Switches (MOSFET) commanded by the command bus allow the production of the appropriate step to command the actuator. The principle is shown in Figure 13-9:

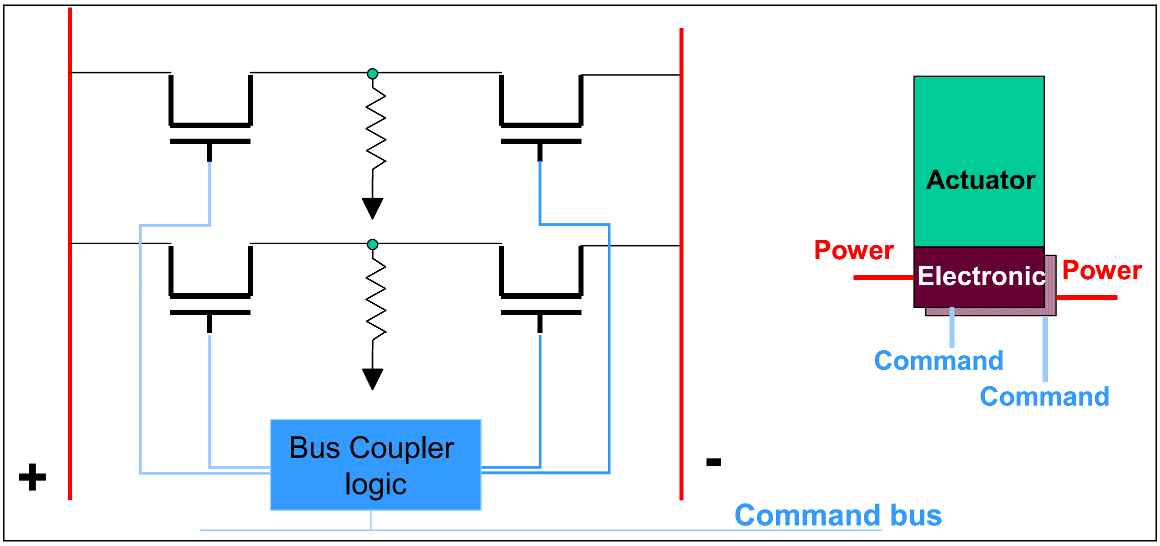

Figure 13-9: Command bus principle

This solution was discarded because of the non-operation of electronics at cryogenic temperature. Heating of the electronics with heaters or RHU was not accepted.

NASA Lewis Research Center is developing the enabling technologies for a cryogenic power system in conjunction with the NASA Jet Propulsion Laboratory (JPL) and universities. Demonstrations of two key technologies have been performed: high-temperature superconductor components and cryogenic compound semiconductor switch technology. A dc-dc converter for low-temperature operation was designed, built, and characterised with commercial, off-the-shelf components and a custom-built superconducting inductor. A High Electron Mobility Transistor switch was designed, fabricated, and characterised at low temperatures. High Electron Mobility Transistor structures have the potential to handle high current loads at cryogenic temperatures.

14. POWER

14.1 Requirements and design drivers

The requirements issued from the mission description applicable for the power subsystem are in line with capabilities of existing power subsystems: mission duration, radiation level, solar illumination and temperature range. Nevertheless, a recurrent power subsystem from another spacecraft is not possible for two main reasons:

1. The power subsystem has to cope with a spacecraft in a spin mode (barbecue mode) during the first part of the cruise and later with a Sun pointed attitude.
2. The specific cylindrical shape of the MSC is an important volume limitation for the implementation of the solar arrays

However, some recurrent modules could be implemented for the battery or the electronic modules. In addition to the mission timeline, the main design drivers of the power design are: cost, reliability and mass. Therefore, new technology developments are avoided as much as possible.

The rest of this chapter focuses on the power design, from the design requirements up to the performance evaluations of the final architecture. This design presented hereafter might not be the most optimised but it is viable. The goal of this short study was to demonstrate the feasibility of the mission, which has been achieved for the power subsystem.

14.1.1 Mission requirements

The launch shall take place in 2015. As baseline, the transfer is performed by a direct injection from Earth with the DSC and the MSC stacked together during the launch but also during the cruise.

After the 25 minutes corresponding to the launch phase, the initialisation of the spacecraft starts and will last around 48 hours. During this phase and for the rest of the cruise until the pre-deployment of the MSC, the spacecraft is stacked to the DSC in a spin-mode (rotation rate around one rpm). The AOCS subsystem will control the Sun pointing with an accuracy of around 15° compared to the rotation plane. However, during the propulsion manoeuvres (nominally shorter than two hours), this angle is not controlled anymore and the Sun will illuminate the bottom face of the MSC with a maximum angle of 20°.

The cruise phase is completely free of eclipse. But initially, an eclipse of maximum 75 minutes can occur during the 48 h of initialisation of the spacecraft. Consequently, the battery module shall be able to supply the power required during the launch followed immediately by a 75 minutes eclipse.

Prior to the deployment of the MSC and the separation of the DSC, the rotation rate is cancelled and one solar panel pointed at the Sun. During the deployment (and also during the safe mode when the DSC is deployed), a maximum Sun depointed angle of 15° is considered. An attitude failure more important does not have to be considered for the design, since it would imply the abortion of the mission due to the mirror being exposed to the Sun.

The power subsystem shall be compliant with a mission duration of 15 years with an extension of 5 years. The MSC is operating at the Lagrange point L2. The minimum solar illumination at this location is 1300 W/m^2.

Number	Mode Name	Definition	Acronym	Duration (min)
1	Launch Mode	***Lift-off to separation from launcher*** Only the essential S/S are on Battery fully charged	LM_STCK	25
2	Initialisation Mode	***Trajectory insertion*** Cancel tip-off rates and acquire Sun - the MSC provides the attitude estimation and the control torques and forces Turn-on cruise mode equipment (TTC, GNC) on MSC and ISL on both the MSC and DSC MSC power provided by MSC SA - battery as backup DSC power provided by DSC SA (DSC SA are stowed) Slow rotation about the longitudinal axis Launch dispersion correction 75 min eclipse (for the direct injection case)	IM_STCK	48 hours
3	Cruise Mode	***Cruise - from transfer trajectory insertion to L2 halo orbit*** Slow rotation about the longitudinal axis - the longitudinal axis is kept normal to the Sun vector except when trajectory correction maneuvers are performed Trajectory determinations by GS and corrections Data communication MSC - Earth via MSC LGA (HGA if compatible with orbit / attitude) DSC - MSC via the R/F metrology S/S MSC power provided by MSC SA - battery as backup DSC power provided by DSC SA (DSC SA are stowed) DSC systems check Stack is outgassing and stabilizing thermally	CM_STCK	100 days
4	Pre-deployment Mode	***Preparation for stack separation - in L2 halo orbit*** Wait for authorization to start preparation proceedures from GS Cancel angular rates Point the stack such that one panel the MSC and one of the stowed DSC SAs are normal to the Sun vector Wait for authorization to proceed with deployment (from GS)	PDM_STCK	60

Table 14-1: Mission mode of the MSC from the separation with the DSC

Number	Mode Name	Definition	Acronym	Duration (min)
1	Deployment Mode	***Stack separation and MSC deployment*** Activate separation mechanism on command from GS Cancel tip-off rates and acquire Sun Data communication MSC - Earth via LGA DSC - MSC via R/F metrology S/S Deploy Sun shield Unfold leaves Power generation (SA; battery as backup) and distribution to all S/S Mirror stabilises thermally Acquire and maintain a TBD attitude	DM_MSC	120
2	Commisioning Mode	***Initial formation acquisiton and telescope check-out and test*** MSC is target for Initial Formation Acquisition Data communication MSC - Earth via LGA MSC - DSC via R/F metrology S/S Relative position metrology S/S check-out Calibration	CM_MSC	120960
3	Target Acquisiton Mode	***Maneuver to obtain a rigid body-like rotation of the telescope*** The MSC receives an attitude profile from GS for the slew maneuver towards a new target star The MSC performs a "pure" slew maneuver Settling phase (cancel rates) and stabilize the attitude loop	TAM_MSC	30
4	Nominal Observatio	***Science operations*** Maintain the commanded attitude (counteract SRP torques, μmet impacts, gravity gradients) Collect photons Time tag attitude data for post-processing (and send it to the DSC?)	NOM_MSC	360 to 17,280 (6hrs to 12 days)
5	Orbit Maintenance I	***Halo orbit maintenance*** Orbit determination by GS Orbit maintenace profile uploaded from GS to MSC Maneuvers to maintain halo orbit - the maneuver profile is uploaded from the GS	OMM_MSC	120
6	MSC Safe Mode	***MSC safe mode: hibernation, Formation standby and failure recovery mode*** Emergency sun acquisition maneuver - triggered by detection of the Sun moving more than TBD° by one of the CSS Non-essential S/S on standby (or switched off?) Non-essential functions are halted. TM/TC access to DHS is guaranteed to enable failure detection and reconfiguration. Data communication MSC - Earth via LGA MSC - DSC via R/F metrology S/S - if possible Failure identification and recovery are executed partially on board and by the GS Trigger a formation safe mode	SM_MSC	TBD
7	MSC Collision Avoidance Mode	***Collision Avoidance Mode*** Collision avoidance maneuver - triggered by: 1. Detection of a relative velocity vector higher than TBDm/s inside of a cone of half angle of TBD°. 2. Failure of the RF metrology S/S. 3. Etc… Based on the last known state vector try to avoid the collision and attempt to maintain the 8km relative distance	CAM_MSC	TBD

Table 14-2: Mission modes of stacked configuration

The sizing mission modes are:

- For the energy storage module:
  - The launch and initialisation phase of 25 minutes followed by a possible eclipse of 75 minutes.
  - Prior to the separation of the spacecraft, the energy storage shall be able to cope with an autonomy of two hours (loss of altitude control…).
  - After the separation from the DSC and the deployment of the mirror, a loss of Sun pointing results in a mission abortion anyway. Therefore, the energy storage module

is no longer useful, except for possible peak power supply at the end of the mission when the power photovoltaic generation is low.
    - Also, if the power generation is not sized for the peak power requirements during the mission, the energy storage module will have to compensate for the lack of power on the bus.
- For the power generation module:
    - The initialisation and cruise modes: barbecue mode with an optimal illumination.
    - The propulsion phases with the Sun illuminating only the bottom part of the MSC.
    - The pre-deployment mode in which the power generation increases due to the fact that the rotation motion is stopped with one solar panel directly exposed to the Sun.
    - The commissioning, the orbit maintenance, the nominal modes with the spacecraft perfectly Sun pointed.
    - The deployment and the safe modes in which as a worst case, a deployment of 15° can occur.

14.1.2 Power requirements

Each unit of the MSC has an associated power profile for each mode that is defined by three values:

- A peak power
- A standby power
- A duty cycle value (duration of the peak power compared to the total duration)

For every mode, the peak and standby values have been summed to get the values at system level. An equivalent duty cycle is also computed to keep the same level of energy. Note that the peak power does not reflect a transient peak power, but typically the power consumption when the unit is *on*.

	Mode 1				Mode 2				Mode 3				Mode 4			
	Launch Mode				Initialisation Mode				Cruise Mode				Pre-deployment Mode			
	Pon	PstdBy	Dc	Wh	Pon	PstdBy	Dc	Wh	Pon	PstdBy	Dc	Wh	Pon	PstdBy	Dc	Wh
Thermal																
TOTAL	12	12	0	12	12	12	0	12	12	12	0	12	12	12	0	12
AOCS																
Star tracker (Jena Optronik)	24	5	0	5	24	5	1	5	24	5	100	24	24	5	100	24
Gyros (Systron Donner)	1	0	0	0	1	0	1	0	1	2	0	2	1	0	0	0
Reaction wheels (Honeywell)	60	15	0	15	60	15	0	15	60	15	20	24	60	15	10	20
Optical metrology	0	0	0	0	0	0	0	0	0	0	0	0	0	0	0	0
Fine sun sensor (Jena Optronik)	0	0	0	0	0	0	1	0	0	0	100	0	0	0	100	0
Medium sun sensor (Aero Astro)	0	0	0	0	0	0	1	0	0	0	100	0	0	0	100	0
TOTAL	86	20	0	20	86	20	0	20	86	22	44	50	86	20	36	44
Comms																
X-band LGA	0	0	0	0	0	0	0	0	0	0	0	0	0	0	0	0
X-band transponder	20	5	0	5	20	5	50	13	20	5	5	6	20	5	20	8
X-band SSPA	59	0	0	0	59	0	50	30	59	0	5	3	59	0	20	12
X-band RFDU	0	0	0	0	0	0	0	0	0	0	0	0	0	0	0	0
S-band transponder-metrology	20	20	0	20	20	2	0	2	20	2	0	2	20	2	0	2
S-band omni antenna helix	0	0	0	0	0	0	0	0	0	0	0	0	0	0	0	0
S-band RFDU	0	0	0	0	0	0	0	0	0	0	0	0	0	0	0	0
S-band omni antenna patch	0	0	0	0	0	0	0	0	0	0	0	0	0	0	0	0
RF inter-S/C link	0	0	40	0	0	0	40	0	0	0	40	0	0	0	40	0
RF inter-S/C link antenna	0	0	0	0	0	0	0	0	0	0	0	0	0	0	0	0
TOTAL	99	25	0	25	99	7	40	44	99	7	4	11	99	7	16	22
Propulsion																
Thruster (MP)	0	0	0	0	69	0	1	1	69	0	1	1	0	0	0	0
Filter (MP)	0	0	0	0	0	0	0	0	0	0	0	0	0	0	0	0
Latch valve (MP)	0	0	0	0	0	0	0	0	0	0	0	0	0	0	0	0
Pipe work (MP)	0	0	0	0	0	0	0	0	0	0	0	0	0	0	0	0
FVV(MP)	0	0	0	0	0	0	0	0	0	0	0	0	0	0	0	0
FDV(MP	0	0	0	0	0	0	0	0	0	0	0	0	0	0	0	0
PT(MP)	6	6	100	6	6	6	100	6	6	6	100	6	6	6	100	6
TC(MP)	6	6	100	6	6	6	100	6	6	6	100	6	6	6	100	6
Propellant tank(MP)	0	0	0	0	0	0	0	0	0	0	0	0	0	0	0	0
Thruster (CG)	4	4	100	4	4	4	100	4	4	4	100	4	4	4	100	4
Filter (CG)	0	0	0	0	0	0	0	0	0	0	0	0	0	0	0	0
Latch Valve (CG)	0	0	0	0	0	0	0	0	0	0	0	0	0	0	0	0
Pipe work (CG)	0	0	0	0	0	0	0	0	0	0	0	0	0	0	0	0
HP regulator (CG)	0	0	0	0	0	0	0	0	0	0	0	0	0	0	0	0
FVV (CG)	0	0	0	0	0	0	0	0	0	0	0	0	0	0	0	0
TC (CG)	28	28	100	28	28	28	100	28	28	28	100	28	28	28	100	28
PT(CG)	24	24	100	24	24	24	100	24	24	24	100	24	24	24	100	24
Propellant Tank (CG)	0	0	0	0	0	0	0	0	0	0	0	0	0	0	0	0
TOTAL	68	68	0	68	137	68	1	69	137	68	1	69	68	68	0	68
DHS																
CDMU (proc+TM/TC+MM)	14	11	100	14	14	11	100	14	14	11	100	14	14	11	100	14
bus I/F	5	1	100	5	5	1	100	5	5	1	100	5	5	1	100	5
command matrix unit	7	2	100	7	7	2	100	7	7	2	100	7	7	2	100	7
TOTAL	26	13	100	26	26	13	100	26	26	13	100	26	26	13	100	26
Mechanisms																
TOTAL	0	0	0	0	0	0	0	0	0	0	0	0	0	0	0	0

	Mode 1				Mode 2				Mode 3				Mode 4				Mode 5				Mode 6				Mode 7			
	Deployment Mode				Commissioning Mode				Target Acquisition Mode				Nominal Observation Mode				Orbit Maintenance Mode				MSC Safe Mode				MSC Collision Avoidance Mode			
	Pon	PstdBy	Dc	Wh	Pon	PstdBy	Dc	Wh	Pon	PstdBy	Dc	Wh	Pon	PstdBy	Dc	Wh	Pon	PstdBy	Dc	Wh	Pon	PstdBy	Dc	Wh	Pon	PstdBy	Dc	Wh
Thermal																												
TOTAL	45	0	100	45	45	0	100	45	45	0	100	45	45	0	100	45	45	0	100	45	45	0	100	45	45	0	100	45
AOCS																												
Star tracker (Jena Optronik)	24	5	100	24	24	5	100	24	24	5	100	24	24	5	100	24	24	5	100	24	24	5	100	24	24	5	100	24
Gyros (Systron Donner)	1	1	100	1	1	0	100	1	1	0	0	0	1	0	0	0	1	0	100	1	1	0	0	0	1	0	100	1
Reaction wheels (Honeywell)	75	15	30	33	60	15	10	20	75	15	100	75	60	15	10	20	60	15	10	20	60	15	20	24	60	15	10	20
Optical metrology	0	0	0	0	0	0	0	0	0	0	0	0	0	0	0	0	0	0	0	0	0	0	0	0	0	0	0	0
Fine sun sensor (Jena Optron	0	0	100	0	0	0	100	0	0	0	100	0	0	0	100	0	0	0	100	0	0	0	100	0	0	0	100	0
Medium sun sensor (Aero As	0	0	100	0	0	0	100	0	0	0	100	0	0	0	100	0	0	0	100	0	0	0	100	0	0	0	100	0
TOTAL	100	21	47	58	86	20	38	45	101	20	99	100	85	20	36	44	85	20	38	45	86	20	43	48	86	20	38	45
Comms																												
X-band LGA	0	0	0	0	0	0	0	0	0	0	0	0	0	0	0	0	0	0	0	0	0	0	0	0	0	0	0	0
X-band transponder	20	5	100	20	20	5	100	20	20	5	5	6	20	5	5	6	20	5	5	6	20	5	20	8	20	5	5	6
X-band SSPA	59	0	100	59	59	0	100	59	59	0	5	3	59	0	5	3	59	0	5	3	59	0	20	12	59	0	5	3
X-band RFDU	0	0	0	0	0	0	0	0	0	0	0	0	0	0	0	0	0	0	0	0	0	0	0	0	0	0	0	0
S-band transponder-metrolog	20	2	0	2	20	2	100	20	20	2	100	20	20	2	100	20	20	2	100	20	20	2	100	20	20	2	100	20
S-band omni antenna helix	0	0	0	0	0	0	0	0	0	0	0	0	0	0	0	0	0	0	0	0	0	0	0	0	0	0	0	0
S-band RFDU	0	0	0	0	0	0	0	0	0	0	0	0	0	0	0	0	0	0	0	0	0	0	0	0	0	0	0	0
S-band omni antenna patch	0	0	0	0	0	0	0	0	0	0	0	0	0	0	0	0	0	0	0	0	0	0	0	0	0	0	0	0
RF inter-S/C link	0	0	0	0	0	0	0	0	0	0	0	0	0	0	0	0	0	0	0	0	0	0	0	0	0	0	0	0
RF inter-S/C link antenna	0	0	0	0	0	0	0	0	0	0	0	0	0	0	0	0	0	0	0	0	0	0	0	0	0	0	0	0
TOTAL	99	7	80	81	99	7	100	99	99	7	24	29	99	7	24	29	99	7	24	29	99	7	36	40	99	7	24	29
Propulsion																												
4.00	0	0	0	0	0	0	0	0	0	0	0	0	0	0	0	0	0	0	0	0	0	0	0	0	0	0	0	0
Filter (MP)	0	0	0	0	0	0	0	0	0	0	0	0	0	0	0	0	0	0	0	0	0	0	0	0	0	0	0	0
Latch valve (MP)	0	0	0	0	0	0	0	0	0	0	0	0	0	0	0	0	0	0	0	0	0	0	0	0	0	0	0	0
Pipe work (MP)	0	0	0	0	0	0	0	0	0	0	0	0	0	0	0	0	0	0	0	0	0	0	0	0	0	0	0	0
FVV(MP)	0	0	0	0	0	0	0	0	0	0	0	0	0	0	0	0	0	0	0	0	0	0	0	0	0	0	0	0
FDV(MP	0	0	0	0	0	0	0	0	0	0	0	0	0	0	0	0	0	0	0	0	0	0	0	0	0	0	0	0
PT(MP)	6	6	100	6	6	6	100	6	6	6	100	6	6	6	100	6	6	6	100	6	6	6	100	6	0	0	0	0
TC(MP)	6	6	100	6	6	6	100	6	6	6	100	6	6	6	100	6	6	6	100	6	6	6	100	6	0	0	0	0
Propellant tank(MP)	0	0	0	0	0	0	0	0	0	0	0	0	0	0	0	0	0	0	0	0	0	0	0	0	0	0	0	0
Thruster (CG)	4	0	100	4	4	4	100	4	4	4	100	4	4	4	100	4	4	4	100	4	4	4	100	4	0	0	0	0
Filter (CG)	0	0	0	0	0	0	0	0	0	0	0	0	0	0	0	0	0	0	0	0	0	0	0	0	0	0	0	0
Latch Valve (CG)	0	0	0	0	0	0	0	0	0	0	0	0	0	0	0	0	0	0	0	0	0	0	0	0	0	0	0	0
Pipe work (CG)	0	0	0	0	0	0	0	0	0	0	0	0	0	0	0	0	0	0	0	0	0	0	0	0	0	0	0	0
HP regulator (CG)	0	0	0	0	0	0	0	0	0	0	0	0	0	0	0	0	0	0	0	0	0	0	0	0	0	0	0	0
FVV (CG)	0	0	0	0	0	0	0	0	0	0	0	0	0	0	0	0	0	0	0	0	0	0	0	0	0	0	0	0
TC (CG)	28	28	100	28	28	28	100	28	28	28	100	28	28	28	100	28	28	28	100	28	28	28	100	28	0	0	0	0
PT(CG)	24	24	100	24	24	24	100	24	24	24	100	24	24	24	100	24	24	24	100	24	24	24	100	24	0	0	0	0
Propellant Tank (CG)	0	0	0	0	0	0	0	0	0	0	0	0	0	0	0	0	0	0	0	0	0	0	0	0	0	0	0	0
TOTAL	68	64	100	68	68	68	0	68	68	68	0	68	68	68	0	68	68	68	0	68	68	68	0	68	0	0	0	0
DHS																												
CDMU (proc+TM/TC+MM)	14	11	100	14	14	11	100	14	14	11	100	14	14	11	100	14	14	11	100	14	14	11	100	14	14	11	100	14
bus I/F	5	1	80	4	5	1	80	4	5	1	100	5	5	1	100	5	5	1	100	5	5	1	100	5	5	1	100	5
command matrix unit	7	2	20	3	7	2	20	3	7	2	100	7	7	2	100	7	7	2	100	7	7	2	100	7	7	2	100	7
TOTAL	26	13	60	21	26	13	60	21	26	13	100	26	26	13	100	26	26	13	100	26	26	13	100	26	26	13	100	26
Mechanisms																												
Petal Actuator	0	0	0	0	0	0	0	0	0	0	0	0	0	0	0	0	7	0	5	0	0	0	0	0	0	0	0	0
Petal Locking Mechanism	0	0	0	0	0	0	0	0	0	0	0	0	0	0	0	0	0	0	0	0	0	0	0	0	0	0	0	0
Frame deployment active hing	15	0	30	5	0	0	0	0	0	0	0	0	0	0	0	0	0	0	0	0	0	0	0	0	0	0	0	0
Frame deployment passive hi	0	0	0	0	0	0	0	0	0	0	0	0	0	0	0	0	0	0	0	0	0	0	0	0	0	0	0	0
Frame latches	0	0	0	0	0	0	0	0	0	0	0	0	0	0	0	0	0	0	0	0	0	0	0	0	0	0	0	0
Frame HRM	0	0	0	0	0	0	0	0	0	0	0	0	0	0	0	0	0	0	0	0	0	0	0	0	0	0	0	0
Shell deployment active hinge	30	0	60	18	0	0	0	0	0	0	0	0	0	0	0	0	0	0	0	0	0	0	0	0	0	0	0	0
Shell deployment passive hin	0	0	0	0	0	0	0	0	0	0	0	0	0	0	0	0	0	0	0	0	0	0	0	0	0	0	0	0
Shell latches	-	-	-	0	-	-	-	0	-	-	-	0	-	-	-	0	-	-	-	0	-	-	-	0	-	-	-	0
Shell HRM	0	0	0	0	0	0	0	0	0	0	0	0	0	0	0	0	0	0	0	0	0	0	0	0	0	0	0	0
Sun shield deployment mecha	0	0	0	0	0	0	0	0	0	0	0	0	0	0	0	0	0	0	0	0	0	0	0	0	0	0	0	0
Sun shield locking mechanism	0	0	0	0	0	0	0	0	0	0	0	0	0	0	0	0	0	0	0	0	0	0	0	0	0	0	0	0
Sun shield HRM mechanism	0	0	0	0	0	0	0	0	0	0	0	0	0	0	0	0	0	0	0	0	0	0	0	0	0	0	0	0
Radiating plate deployment m	0	0	0	0	0	0	0	0	0	0	0	0	0	0	0	0	0	0	0	0	0	0	0	0	0	0	0	0
Radiating plate locking mecha	0	0	0	0	0	0	0	0	0	0	0	0	0	0	0	0	0	0	0	0	0	0	0	0	0	0	0	0
Radiating platre HRM mechan	0	0	0	0	0	0	0	0	0	0	0	0	0	0	0	0	0	0	0	0	0	0	0	0	0	0	0	0
Stack separation mechanism	0	0	0	0	0	0	0	0	0	0	0	0	0	0	0	0	0	0	0	0	0	0	0	0	0	0	0	0
DSC separation mechanism	0	0	0	0	0	0	0	0	0	0	0	0	0	0	0	0	0	0	0	0	0	0	0	0	0	0	0	0
Electronic petal actuator drive	0	0	0	0	0	0	0	0	0	0	0	0	0	0	0	0	0	0	0	0	0	0	0	0	0	0	0	0
Electronic frame and shell act	50	25	100	50	0	0	0	0	0	0	0	0	0	0	0	0	0	0	0	0	0	0	0	0	0	0	0	0
TOTAL	95	25	68	73	0	0	0	0	0	0	0	0	0	0	0	0	7	0	5	0	0	0	0	0	0	0	0	0

Table 14-3: Detailed power inputs

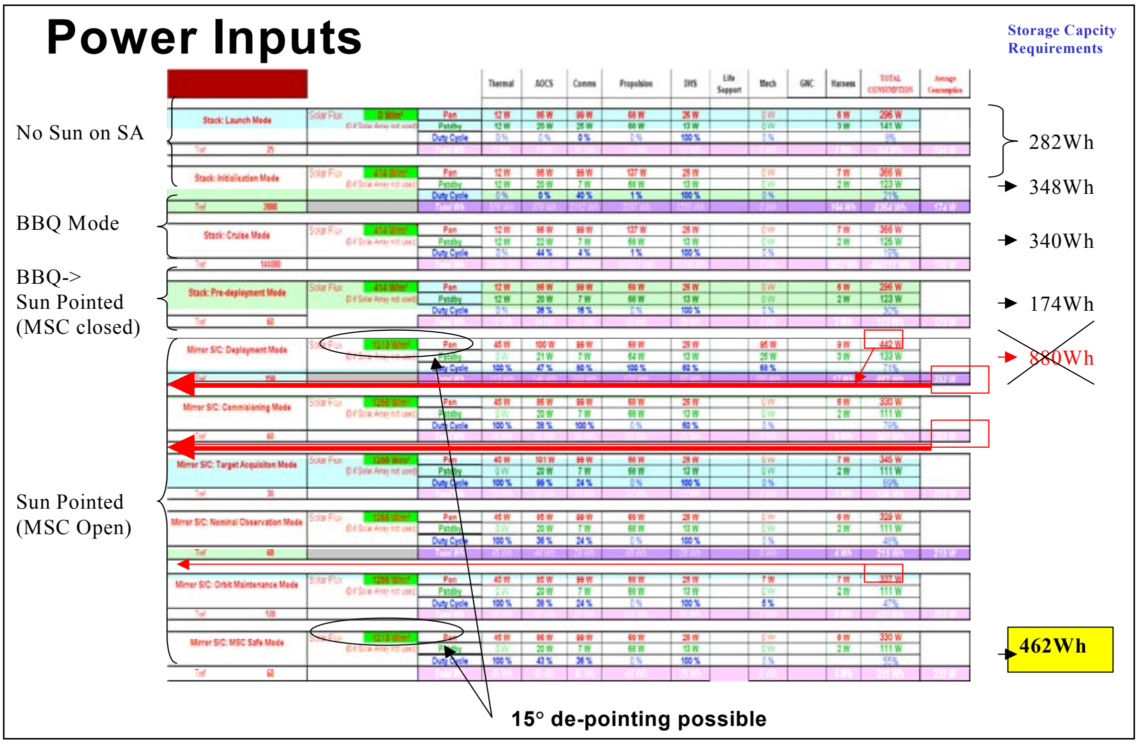

Table 14-4: Computation of all the power requirements on the bus

On top of the power requirements (Table 14-3), 2% of power loss has been taken into account for the harness. Table 14-4 shows the overall power requirements on the bus. For each mode a maximum power value and an average power value are assessed.

14.1.3 Configuration limitations

As shown in Figure 14-1, the mounting of fixed flat Sun-pointed solar panels during the observation mode is limited by the shape of the MSC. 37.2 m^2 maximum can be allocated for solar panels. Note that solar cells mounted on these panels would be always nominally tilted by 15° or 21°, depending on their location. If the area required is higher, a design with deployable solar panels has to be envisaged, but this solution would have a large impact in terms of mass, complexity and therefore reliability.

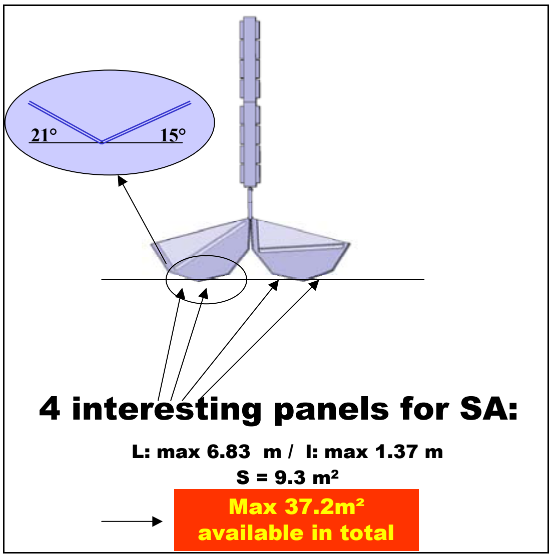

Figure 14-1: Panel location suitable for solar array mounting solar array

Thermal analysis concludes that solar cells mounted on such panels would have to cope with maximum temperatures of:

- 28.1ºC when in barbecue mode
- 127.9ºC when the panels are facing the Sun

14.2 Assumptions and trade-offs

14.2.1 Solar arrays configuration selection

The 37.2 m^2 area available for the mounting of photovoltaic cells exceeds by far the required area: Out of the four faces, one or maximum two could support all the solar cells. Since there is no advantage in spreading the solar cells across three or four panels, three options have been considered (see Figure 14-2):

- Option 1: mounting on all the cells on one face
- Option 2: mounting all the photovoltaic cells on one shell but spread equally between the two adjacent faces
- Option 3: mounting of the cells equally on two faces with one face per shell

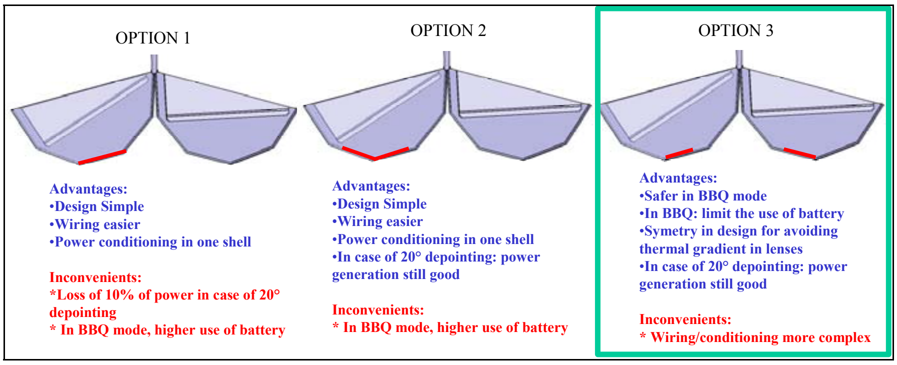

Figure 14-2: Solar array location trade-off (best configuration shown in green)

In addition to the mirror thermal gradient considerations, to the wiring complexity and to the loss of power when the Sun illumination is tilted, the efficiency of the power conditioning system was also assessed (see Figure 14-3). In spin mode, during one revolution, the power generated profiles are completely different between these three options: for the option 3, power generation almost always takes place; in option 1, during 50% of the time, no solar cell is illuminated. Therefore, in each option, the battery needs to compensate in different proportions for supplying the power required on the bus.

By taking into account the associated loss issued from the use of the battery (round trip efficiency and also when applicable the battery regulator efficiencies), the power conditioning will have different performances losses compared to a design with a 360° circular solar cells configuration. In the worst case, the efficiency should decrease by 21% in case of a regulated bus for the option 1.

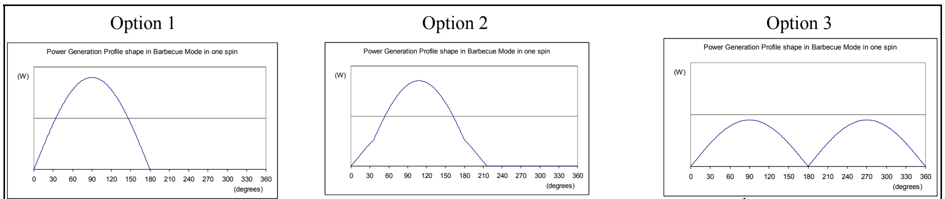

Factor SA sizing	360 deg panels	1 panel	2 panels next	2 panels opposite
regulated bus	0%	21%	19%	7%
unregulated bus	0%	4%	4%	2%

Figure 14-3: Spin mode: influence of the three options on solar array sizing

Out of all these parameters, the best solar array configuration candidate for the MSC is the option 3 also represented in Figure 14-4. To limit the internal wiring of the solar arrays and also the wiring to the power conditioning module, the solar cells only cover the top part of the external faces (the PCU like most of the equipment is located in the top part of the MSC).

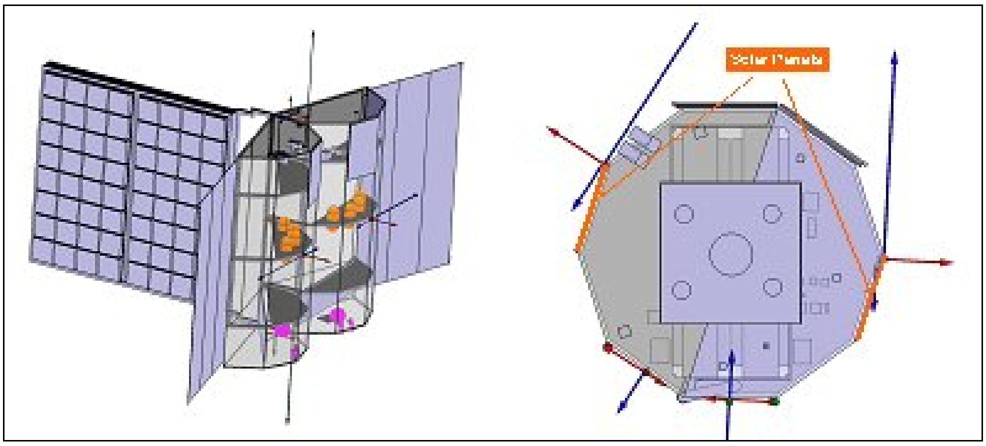

Figure 14-4: Location of the solar cell panels in deployed (left) and stowed (right) configuration

14.2.2 Solar cells selection

In addition to the system mass margin and the equipment mass margin, a margin of 20% has been considered for the power budget. As regards the power generation, a solution with solar cells is selected.

Batteries are mounted for three purposes:

1. To supply the power during the launch and initialisation phase
2. To provide the power in case of a temporally failure of the generation of solar arrays
3. If necessary, to complement the solar arrays, the transient peak power demands

The solar arrays are sized to provide maximum power and not the average power.

Compared to a typical GEO commercial spacecraft, on one hand, the mission duration is here slightly longer; on the other hand, the L2 location has a lower level of radiation. Therefore, the same level of degradation is assumed due to radiation on solar cells as for a GEO spacecraft.

Existing qualified solar cells are:

- Si cells: cheap and lighter but lower efficiency cells
- AsGa cells: expensive but higher efficiency especially for high temperature

A trade-off has been performed between solar array designs with:

- Si cells
- AsGa TJ (Triple Junction) cells: the most efficient and space qualified cells

Table 14-5 shows the masses and areas assessed for these two options in the four sizing modes for power generation:

	AsGa	Si	
Efficiency BOL	27,00	16,50	%
Radiation 20 Years	12,00	35,00	%
Temperature Factor on Pmax	-0,23	-0,40	%/degree
Filling Factor	90,00	90,00	%
Coverglass	0,95	0,95	
Mismatch + Calibration	0,97	0,97	
UV + Micrometeorites	0,99	0,99	
Random failure	0,98	0,98	
Pointing error	1,00	1,00	
Efficiency Array EOL	**19,12**	**8,63**	**%**
Efficiency Array EOL (at 127.9 deg C)	**14,50**	**5,01**	**%**
Efficiency Array EOL (at 28.1 deg C)	**18,89**	**8,45**	**%**
Mass Budget			
PV cells	0,72	0,56	kg/m2
150 um coverglass	0,40	0,40	kg/m2
Coverglass adhesive	0,07	0,07	kg/m2
Interconnects	0,01	0,01	kg/m2
Cell adhesive	0,23	0,23	kg/m2
Bus/wire/diodes	0,31	0,31	kg/m2
50 um Kapton	0,09	0,09	kg/m2
Total	**1,82**	**1,66**	**kg/m2**

Table 14-5: Solar arrays' efficiencies and mass budget for AsGa TJ and Si cells

Sizing done for maximum power

Sizing Case

	15 deg	15deg	0deg	0deg
Area Required	Initialisation/C	Deployment	Commisioning	Orbit Maintenance
AsGa	9.50	4.73	3.41	3.48
Si	21.04	13.44	9.69	9.90
		20deg	0deg	0deg
Mass Required	Initialisation/C	Deployment	Cominsioning	Orbit Maintenance
AsGa	19.0	9.5	6.8	7.0
Si	38.4	24.5	17.7	18.1

Table 14-6: Solar array sizing trade-off for maximum power considering Si and AsGa base TJ cells

In both cases, the sizing case is the barbecue phase of the cruise. To size the solar panels for supplying the power requirements of the spacecraft, an area of 21.04 m^2 would be necessary with Si cells compared to only 9.5 m^2 for the AsGa TJ cells option. Hence, Si option is not kept for the baseline even if these cells could be directly mounted on the half cylinders structure directly (AsGa cells can only be mounted on a flat surface).

14.2.3 Power subsystem modules configuration selection

The design of the MSC power subsystem has to take into account the spread of the power generation and the power users between the two distinct shells. Since the two shells are articulated through hinges, one of the main design drivers for the power subsystem is the limitation of the harness between these two structures. Also, due to the important size of the shells, the equipments location should also be optimised in terms of mass. Consequently, four architectures have been identified (Figure 14-5):

- Option 1: two autonomous power subsystems; one per shell.
- Option 2: one centralised power subsystem (conditioning + storage + distribution) located in one shell.
- Option 3: one centralised power conditioning and storage located in one shell. The distribution of the bus power is spread over the two elements.
- Option 4: two power conditioning units: one per solar array delivering a common bus shared between the two shells (This power bus can be a concept with redundant lines). The power of the bus is then distributed to each equipment by the mean of the PDU located in the same shell (one PDU per shell). The power storage can be located either only in one shell or either in both shells.

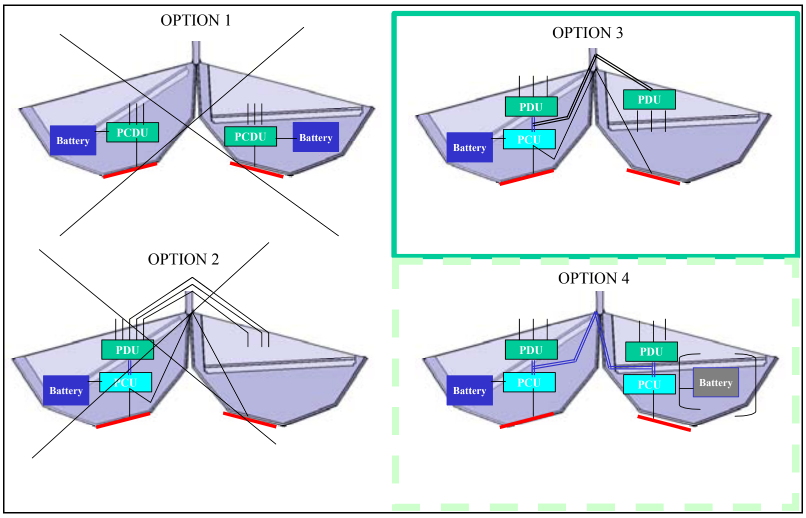

Figure 14-5: Power subsystem module configuration trade-off

In option 1, there is absolutely no power wiring need between the two shells. For the power subsystem, it is like having two separate spacecraft. Therefore, such an architecture has the following disadvantages:

- More complex management: two power subsystems instead of one
- Two battery modules and conditioning units instead of one
- The power balance has to be reached independently for each shell, which leads to increases of the total battery capacity and of the total solar array size.

Even if option 2 is the optimised concept for the number of modules, it has been discarded due to the important wiring required between the two structures. Option 3 seems a good design from all points of view. Moreover, the technology and architecture concept are already qualified for this configuration. Option 4 seems promising but needs further work in terms of management of the bus:

- How to perform the conditioning of a single bus with two autonomous units?
- How to implement the redundancy in case of a single point failure?
- Is such an architecture possible with only one battery module?

Therefore, option 3 is selected for the baseline and option 4 should be looked into in more details during the next study phases. In option 3, to limit the number of modules, the PCU and the PDU of the left shell are combined in one single module called PCDU. For limiting the harness asymmetry between the PCDU and the two solar arrays, the PCDU is located the closest from the hinges. Also for harness optimisation, the PDU of the right shell (called PDU2) is located closed to the hinges.

14.3 Baseline design

14.3.1 Architecture

Following the solar cells trade-off study, it was noted that the sizing mode is the barbecue mode during the cruise. The power subsystem architecture has to be optimised for this phase while keeping in mind that it has also to be compatible with the Sun pointed mode. An MPPT design seems the most efficient architecture: such a regulator always optimises the power generated from the SA. The only inconvenience is that there is always a constant loss between the power generated and the power available on the bus: the loss of the MPPT regulator. In this study, the efficiency of an MPPT is assumed to be 90%.

As shown in Figure 14-6, two architectures are possible using an MPPT:

- A fully regulated bus with BCR and BDR modules: for example, Mars Express
- A battery bus: the bus voltage varies with the battery voltage: when the battery is charged (tapervoltage mode), the bus is then also regulated. In all other cases, the bus follows the battery voltage.

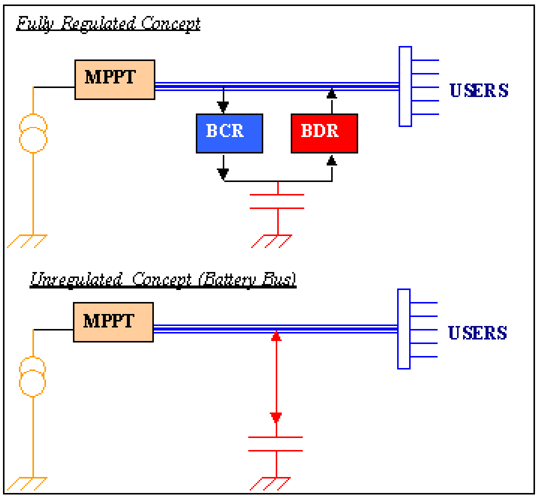

Figure 14-6: Regulated/unregulated MPPT topologies

The fully regulated concept is clearly heavier, but the voltage delivered is regulated in any cases. The users power data available in this phase of the study are too limited to perform a proper trade-off between these two options.

Nevertheless, *the battery bus architecture is therefore selected as the baseline architecture.* Indeed, the battery is only requested for the launch/initialisation phases and later on in the mission for failure cases. Therefore, by implementing undervoltage protections, the equipments that are *switched off* during launch and in failure mode do not required dedicated EPCs since the bus is always regulated when they are in use. Another possible option would be a design including:

- Primary batteries for supplying during the launch and initialisation phases
- Solar arrays for the rest of the mission

Such a design is really optimised for mass and volume purposes, but does not cover all the failure cases. Consequently, it has been decided to always have rechargeable batteries as backup.

14.3.2 Battery module

Compared to other existing technologies, Li Ion cells are the most attractive cells because of their reliability, efficiency, thermal, cost, mass and volume aspects. For the battery design, the data are extrapolated from a solution using Sony 18650 cells (RD[37]), but concurrent batteries (SAFT…) would also fulfil the requirements.

Sony 18650 Hard Carbon cells have been in production for nearly 10 years, and have been used by AEA, in conjunction with COM DEV, to produce the battery launched aboard the United Kingdom's Space Technology Research Vehicle (STRB) 1D. The technology was later also adopted for use on Beagle 2 Mars Lander and Mars Express Orbiter.

14.3.2.1 SONY 18650 hard carbon cell characteristics

Fully charged, the Sony 18650 cells have a cell voltage around 4.2 V and a capacity of 5.4 Whr. At discharge, the voltage drops to around 2.5 V. Built-in cell safety mechanisms include a cell disconnect mechanism if the cell is overcharged, overcurrent protection, and emergency cell vents. See Figure 14-7.

These cells have a wide operating temperature range from -25ºC to 60ºC. The battery can even be exposed to short term temperatures of up to 80ºC while maintaining performance, but this should be avoided as it will gradually shorten the battery life. It is recommended that the batteries be operated at around 10ºC, with higher temperatures applied during charge to increase the efficiency. Another advantage of these cells is that their degradation over life is predictable: the cells do not fail suddenly, but rather experience gradual fading of capacity.

These small capacity cells are connected in series to provide the required voltage, and a number of those strings are connected in parallel to provide the required capacity. Such a topology is highly tolerant to failure; cells fail open circuit causing only that string to fail, rather than propagating through the array of cells. Using this topology, redundant strings can be added to the battery, rather than having a second battery for back up.

14.3.2.2 Battery sizing calculation

During the launch and initialisation phase: 463 Wh are required on the power bus (566 Wh with 20% power margin).

For covering the capacity fading due to aging and cycling losses, assuming 1 year ground activities prior to launch, a DoD limitation of 80% was assessed for the battery sizing. Therefore, the capacity BOL of the battery has to be at least 694 Wh.

To have a bus voltage around 28 V, string lengths of seven cells must be used. To fulfill the 694 Wh required, 19 strings in parallel must be implemented. One extra string is added for covering the cells failures.

Figure 14-7: Battery module with Sony 18650HC cells

The mode sizing the storage device capacity is the safe mode that could occur in the first days after the deployment of the mirror in which two hours of power autonomy has to be supplied. A refining of the safe modes definitions would imply important changes in the battery design.

Battery		
Techno	AEA 18650HC	
Nb Batteries	1,00	
Mass Battery	7,79	kg
Energy Battery	756	Wh
Capacity Battery	30,02	Ah
Cell: Vmin	2,50	V
Cell: Vmax	4,20	V
Battery Configuration		
cells in a string	7	
number of strings	19 (+1)	
total cells	140	
Bat: Vmin	17,50	V
Bat: Vmax	29,40	V
Volume	6,86	l
Length	0,24	m
Width	0,19	m
Height	0,15	m

Table 14-7: MSC battery description

14.3.3 Main solar arrays

In the solar cells trade-off presented in section 14.2, all the data about the solar arrays are presented. The cells used are GaAs triple junction cells with 27% BOL efficiency. They are mounted on two fixed panels (3.47 m x 1.37 m) and have a total estimated weight of 19 kg.

Solar Array		
Techno	AsGa TJ	
Nb Arrays	2	
Size Total	9.5	m2
Length	1.368	m
Height	3.47	m
Mass Total	19	kg

Table 14-8: Mass and dimensions of the main solar panels

14.3.4 Additional solar array

During the propulsion phases, the MSC is still in a spin mode but the Sun will illuminate the bottom face of the MSC (with a maximum angle of 20°) instead of the sides where the solar arrays are located. Therefore, no power generation can be expected from the two main solar arrays during this phase. Nominally, this phase should last less than two hours and the battery module is anyway able to supply power during at least three hours. Nevertheless, to be tolerant to a severe failure that would result in a loss of attitude longer than three hours, an extra solar panel is added at the bottom of the spacecraft.

The selection of the same TJ cells as for the main solar arrays leads to the following results:

- Area: 1.28 m^2
- Mass: 2.33 kg

14.3.5 PCDU and PDU2

The PCDU is divided into:

- The power conditioning part
- The power distribution part (for the equipments located on the same shell)

The power conditioning is mainly composed of the MPPT regulators and the management of the recharge of the battery. A preliminary architecture is shown in Table 14-9:

Module	Number of modules	Power per module [W]	Specific power [Kg/W]	Weight per module [Kg]	Total Weight [Kg]
MPPT	3	286	1.33E-03	0.4	1.1
Cbank	0	1.0 mF	6.67E-01	0.6	0.0
MPPT control	1			0.25	0.25
MEA+MVL	1			0.75	0.75
TM/TC & AUX	1			0.75	0.75
battmgm	1			0.75	0.75
Total modules	7				3.6443142
Structure		Equal to	25%	of total weight	1.2
TOTAL PCU	7				4.9

Table 14-9: Power conditioning

The power distribution includes three types of protection:

- LCL for non essential loads
- FCL for essential loads
- Pyro protections

The total mass of this function is estimated to 9.64 kg and equally shared between the PCDU and the PDU2.

14.3.5.1 Non-essential loads

The non-essential power line is switched and protected by means of Latching Current Limiter (LCL). A LCL is a device that also acts as a protection device in case of overcurrent. Should the current through the LCL exceed the nominal current rating by (typically) 120%, the device will enter into current limitation mode. If current limitation continues for more than a given trip-off time (of the order of 10 ms), the LCL will open, to isolate the failed unit from the spacecraft bus. 35 LCLs are included in this unit.

14.3.5.2 Essential loads

The essential users shall never be switched off and shall be able to recover autonomously in case of return to normal conditions. Primary power is distributed to them through Foldback Current Limiters (FCLs): these are devices similar to LCLs, except that they do not feature *on/off* switching capability and overcurrent will never lead to disconnection when the trip-off time is exceeded. Four FCLs are included in this equipment.

14.3.5.3 Pyros actuation

The pyro function is included in the PCDU and is fully redundant at both actuation electronics and initiator level. The purpose of this electronics is to provide the necessary means to select a particular firing input power source and firing outlet, to fire, monitor and control the pyro outlet current to the actual pyro devices. The whole pyro function is enabled by a Select command, which powers the Current Limiter used for current control of pyro commands. Arm commands (one per group) allow the generation of the command pulse to any line which is part of the group to which the Arm command is dedicated. Finally, the Fire command (one per line) triggers the pyro device command pulse generation.

The harness of the 192 pyro actuators from the PCDU to the mirror is assessed in section 14.3.6.1. The total mass of the PCDU is 9.7.kg and 4.8 kg for the PDU2 module.

14.3.6 Mirror harness

Since the mirror is a completely new module for space application, an assessment has been performed of the mass of the harness. The harness of the mirror comprises two parts: the commands of the actuators and the pyro lines. The values presented here correspond only to the wires themselves: connectors and others additional harness elements have not been assessed in this study. The remaining harness (outside of the mirror itself) is also not assessed in this chapter, but it is taken into account at the system level based on extrapolation from existing spacecraft.

14.3.6.1 Mirror pyro harness

Three motors are mounted on each mirror. Therefore, 192 actuators require a connection with dedicated pyro lines. As shown in Figure 14-8, there are two possible electrical pulse requirements for firing the selected pyros. To optimise the harness mass, the option selected is 2 A at 4 V DC during 100 ms.

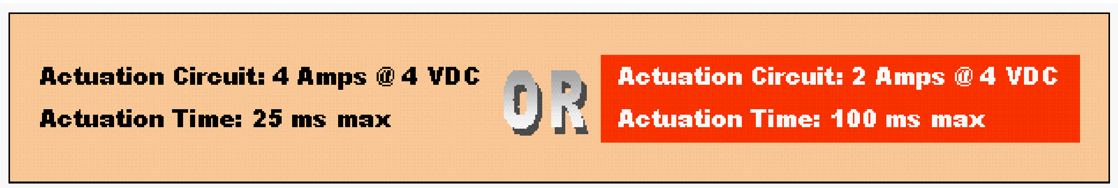

Figure 14-8: Electrical requirements for pyros of the mirror

By considering a derating of 50% and assuming a point-to-point architecture from the PCDU to the actuators, the harness length would be 2.02 km and the mass estimated to be 8.88 kg (without mass margin). Another approach kept in the baseline design is to have a point-to-point harness architecture only for the positive lines. The return lines would be common to all the actuators with a double wiring for redundancy purposes (see Figure 14-9). The harness length inside the mirror is then reduced to 1.16 km with a corresponding mass of 5.11 kg.

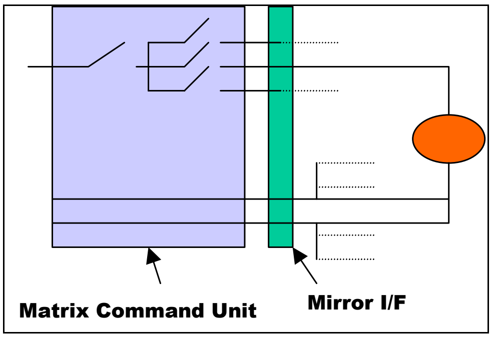

Figure 14-9: Wiring concept for the pyro lines

A concept with actuations performed simultaneously has also been assessed. However, the increase in harness gauge does not compensate the decrease in harness length: the total wiring mass is still higher.

14.3.6.2 Actuator command harness

The motors of the petals are commanded and powered by the same signal. These bi-phase motors can be commanded by supplying on the phases 1 and 2 the signals described in Figure 14-10:

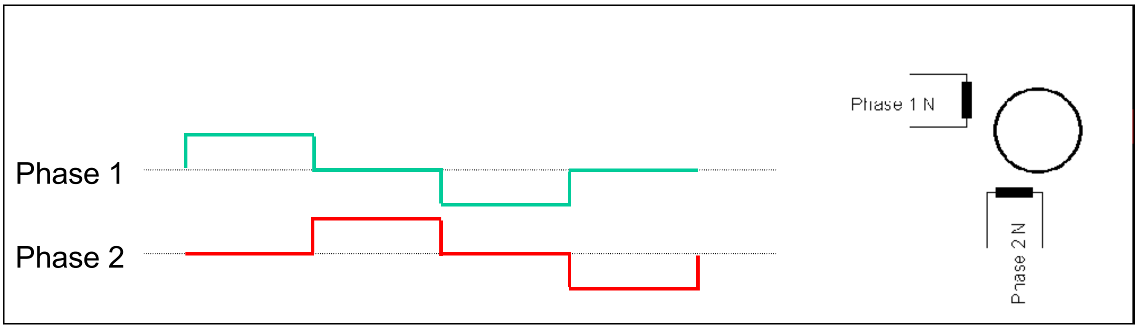

Figure 14-10: Motor control sequence

Three motors are installed on each petal: two are required and one is added as a backup. Hence, the same redundancy concept is taken into account for the harness: a single point failure can lead to the loss of a motor since two others are also available:

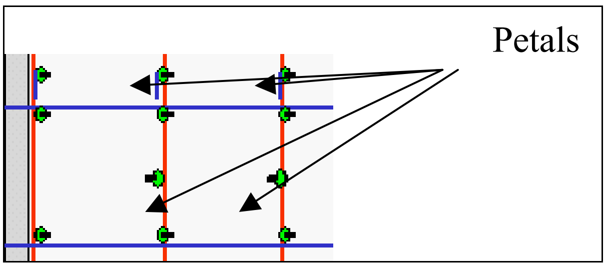

Figure 14-11: Locations of the motors around the petals

To optimise the harness mass, a matrix command concept has been selected based on existing matrix commands already existing for others applications.

14.3.6.2.1 Matrix command principle

The actuators are connected in such a way that by activating one row and one column a single actuator is commanded. An example is given in Figure 14-12 for the first phase. The ground is connected to the column and the strobe is sent on the row.

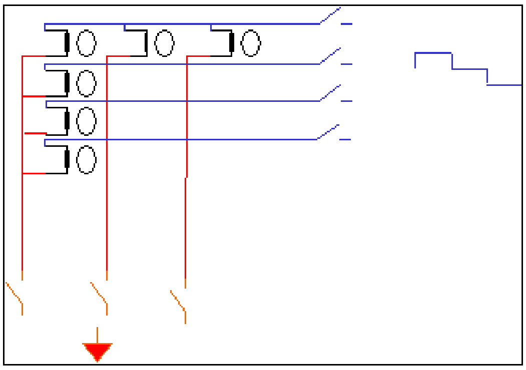

Figure 14-12: Command matrix principle for phase 1

14.3.6.2.2 Matrix command wiring

Figure 14-12 shows the wiring required for one phase. The matrix is 16 rows by 12 columns. One row (blue in Figure 14-13) is a serial connection of 12 motors with the first and the last ones connected to the command unit. One column (red in Figure 14-13) is a serial connection of 16 motors with the first and the last ones connected to the command unit.

Figure 14-13 shows the routing principle selected for the columns and the rows. For clarity only the routing of two columns and one row are shown. For the baseline only 48 petals out of 64 segments are mounted and connected.

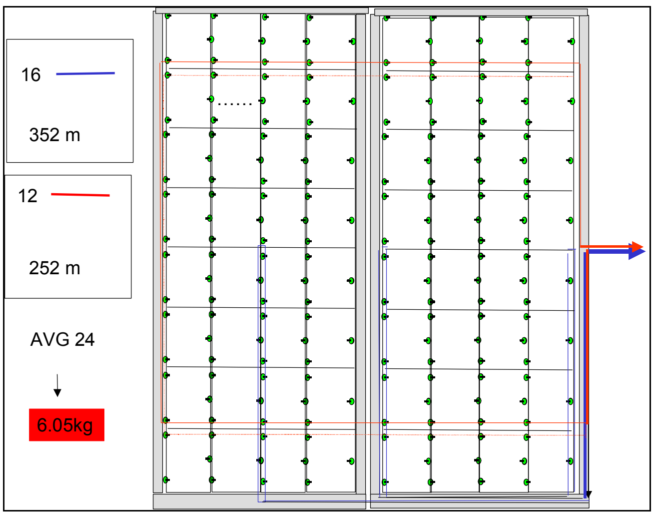

Figure 14-13: Harness actuator routing description

Assuming an AWG24 cable with a weight of 10 g/m, the total weight for a matrix is 6.05 kg. Since there is one matrix per phase, the total mass is 12.1 kg.

14.4 Performance and budgets

14.4.1 Role of the power subsystem in the grating option

The power consumption of the users is not dependant on the selection nor the grating principle. Consequently, the presented power architecture fulfils the mission requirements also in the grating option.

14.4.2 Role of the power subsystem in other launch considerations

This power architecture is compatible as long as the duration from the launch until the moment when the attitude of the spacecraft towards the Sun is locked (and without further eclipses) is shorter than 100 minutes. For a launch including HEO phases, the power subsystem capabilities should be reviewed.

14.4.3 Performances

During the cruise, the solar panels generated at least 440W on the bus. The power budget illustrated in Table 14-11 shows clearly that the solar panels are the sizing case for the cruise mode (in barbecue mode). However, when located at L2, a margin of more than 500W is available on the bus.

	15 deg	*15deg*	*0deg*	*0deg*
	Initialisation / Cruise	**Deployment**	**Commisioning**	**Orbit Maintenance**
Thermal	12 W	45 W	45 W	45 W
AOCS	86 W	100 W	86 W	85 W
Propulsion	137 W	68 W	68 W	68 W
DHS	26 W	26 W	26 W	26 W
Comms	99 W	99 W	99 W	99 W
Mechanism	0 W	95 W	0 W	7 W
Harness	7 W	9 W	6 W	7 W
Total	366 W	442 W	330 W	337 W
Total with 20% Margin	440 W	530 W	396 W	404 W
Power Available	439 W	1014 W	1102 W	1276 W
Power Margin	**0 W**	**484 W**	**707 W**	**872 W**

Table 14-10: Power budget

14.5 List of equipments

Including margins, the total mirror harness is expected to weigh around 20.6 kg. The modules related to the power subsystem itself (power generation, conditioning, storage and distribution) have a total contribution of 47.8 kg. For all the equipments, a mass margin of 10% is applied. In this proposed power architecture, the units are newly designed but use known and qualified technologies. For covering the uncertainties of the mirror harness, 20% is assumed in the total mass budget (see Table 14-11).

Element 1: Mirror S/C			MASS [kg]			
Unit	Element 1 Unit Name Click on button below to insert new unit	Quantity	Mass per quantity excl. margin	Maturity Level	Margin	Total Mass incl. margin
1	Battery LiIon	1	7.5	To be modified	10	8.2
2	PCDU	1	9.8	To be modified	10	10.8
3	Solar Panel	2	9.5	To be modified	10	20.9
4	PDU2	1	4.8	To be modified	10	5.3
5	Additional Solar Panel	1	2.3	To be modified	10	2.6
6	Harness Pyro Mirror	1	5.1	To be developed	20	6.1
7	Harness Command Motors Mirrors	1	12.1	To be developed	20	14.5
-	Click on button below to insert new unit		0.0	To be developed	20	0.0
ELEMENT 1 SUBSYSTEM TOTAL		7	60.6		12.8	68.4

Table 14-11: List of equipments for power subsystem

14.6 Options

14.6.1 Peak power supplied by both solar cells and battery module

In the baseline design, the solar array is sized to be able to provide the power requirements on the bus entirely during the nominal mission (except for possible transient on the bus). The battery is used only in the following cases:

- High transients on the bus
- Launch and eclipse during initialisation mode
- As a backup source of energy if failures affect the power generation.

Another approach would be to consider that the solar array is sized to provide a lower level of power. In that case, the battery module has to compensate for the lack of power on the bus. In the best case, the solar array can be designed to provide only the average bus power requirements. Table 14-6 has been computed again accordingly:

Sizing done for average power

Sizing Case

	15 deg	15deg	0deg	0deg
Area Required	Initialisation/C	Deployment	Commisioning	Orbit Maintenance
AsGa	5.75	4.57	3.38	2.93
Si	12.74	13.00	9.51	8.32
		20deg	0deg	0deg
Mass Required	Initialisation/C	Deployment	Cominsioning	Orbit Maintenance
AsGa	11.5	9.2	6.8	5.9
Si	23.2	23.7	17.5	15.2

Table 14-12: Solar array sizing trade-off for average bus power requirement

The solar array could decrease to 40% of its size. Nevertheless, this concept has not been kept as a baseline for three main reasons:

1. To compensate the use of the battery during this peak power periods and to keep a autonomy of two hours in case of any failure, the battery has to be increased.

2. The knowledge of the power consumption of the units and the corresponding timelines is not accurate enough in this stage of the study to assess the worst-case scenario.
3. The implementation of 9.5 m^2 of solar area instead of 5.75 m^2 does not have any major impact or limitation. Moreover, since the cells are mounted directly on the structure of the MSC, the mass increase is also moderated.

Such a design should be investigated in the next phase of this mission when more consolidated data on the bus power requirements are present. The study will need to consider:

- The efficiency trip of the battery (in addition to the efficiency of the battery regulators in case of a regulated bus)
- A worst case timeline including also a more realistic maximum power level reached on the bus (in this study, all the units active in the same time was considered as the maximum power level reachable)
- The increase of the battery module

14.6.2 Topology without an MPPT

Other power topologies that might also be good candidates for this mission are:

- S3R regulated
- S3R unregulated
- S4R regulated

Compared to the baseline design (battery bus), the possible benefits are relatively limited. Finer analyses are needed to derive the merits of such topologies in the several illumination cases encountered during this mission.

15. FORMATION FLYING

This chapter provides an overview of the formation flying strategy selected for the mission. It briefly describes all the mission modes, and it provides details for the mission modes during which the spacecraft fly in formation.

The mission has been divided into three elements. One element is the stack (STCK), the second element is the MSC, and the third element is the DSC. The two spacecraft are held together by an adaptor ring.

15.1 Requirements and design drivers

The mission scenario put forward calls for the MSC to have a lifetime of 15 to 20 years and for the DSC to have a lifetime of five years. It is envisioned that the DSC is replaced at least two times during the XEUS mission. Consequently a concept of operations is proposed such that the DSC performs the manoeuvres requiring the most propellant. For example, the translation manoeuvres for formation initialisation and acquisition (FIA) and formation keeping (FK), are performed by the DSC. The MSC thus takes a passive role, that of a cooperating target.

For the collective manoeuvre required to slew towards a new target it is proposed that the MSC performs a classical slew manoeuvre, i.e. rotation about its CoM. The DSC autonomously follows the MSC, performing a translation on a circular arc and a slew manoeuvre simultaneously. Thus the formation emulates a rigid body-like rotation. From an operations point of view the GS commands only one spacecraft with a relatively simple slew command.

Following the same logic, the orbit correction manoeuvres of the formation are uploaded to the MSC only. The DSC will follow the MSC maintaining the formation. Operations are again simplified. The GS commands a single spacecraft with relatively simple orbit correction manoeuvres.

The following sections describe the various mission modes for each of the elements.

15.2 Stack modes

The spacecraft are launched as a stack, with the DSC mounted on “top” of the MSC, on the +Y face of the MSC. After application of the final trajectory correction manoeuvre (TCM) the stack will separate and the two spacecraft will be deployed. It is estimated that the final TCM is applied, at the latest, during day 50 (see section 3.3.2).

During the stack modes the DSC and MSC communicate through the radio frequency (RF) navigation subsystem. The following modes have been identified for the stack.

15.2.1 Launch mode

The launch mode lasts from the lift-off to separation from launcher. The expected duration is at maximum 30 minutes. During the launch mode only the essential subsystems are on. These systems might include heaters and other environmental and thermal control equipment. It is envisioned that all of the GNC equipment and communications equipment will be switched off during the launch mode.

15.2.2 Initialisation mode

The initialisation mode commences at the end of the launch mode, immediately after the separation from the launcher. The duration of the initialisation mode is two days.

At the end of the initialisation mode the launch dispersions are corrected, the stack has acquired the attitude for the cruise, and a slow rotation of 1 rpm about the Y-axis. The proposed sequence of events for the initialisation mode is:

1. Switch on the subsystems needed for the mode.
2. Cancel the tip-off rates.
3. Perform launch dispersion corrections according to commands received from GS.
4. Acquire an attitude such that the STCK XZ plane and the Sun vector are at an angle which avoids the STR looking into the Sun.
5. Start rotating the stack slowly at 1 rpm about the Y-axis.

It is proposed that during the initialisation mode the attitude determination is performed with the STR of the MSC and the attitude control is performed with the MSC RWs. The cruise mode cold gas RCS can be used instead of the RWs if the torques produced by the RWs are not sufficient.

15.2.3 Cruise mode

During the cruise mode the stack rotates at 1 rpm about the Y axis and the orientation of the XZ plane is such that the Sun, Earth, and Moon are out of the field of view of the STR. Some manoeuvres might be necessary to keep the three celestial bodies out of the field of view of the STR. The cruise mode can last from 90 to 150 days.

During the cruise the stack might have to perform correction manoeuvres. If any correction manoeuvres are necessary they are applied during day 10 and day 50. The RWs of the MSC are used to orient the stack prior to the switching on of the monopropellant OCS thrusters. The cold gas RCS thrusters will be used during the correction manoeuvres to maintain the required attitude of the stack. The attitude determination will be provided by the STR of the MSC.

15.2.4 Pre-deployment mode

At the end of the cruise mode the stack enters the pre-deployment mode. The pre-deployment mode is expected to last a few hours. The stack pre-deployment mode prepares both spacecraft for deployment. In this mode the angular rate of 1 rpm is cancelled and the stack acquires the attitude convenient for the separation and deployment. The DSC systems are switched on or awakened from hibernation. It is proposed that the attitude of the stack during the pre-deployment mode is such that one of the MSC's solar arrays is normal to the Sun vector.

During the pre-deployment manoeuvres, the Sun, Earth and Moon must be kept out of the STR field of view.

15.3 Single spacecraft modes

The following sections describe the individual spacecraft modes. The names of the modes are the same for the MSC and the DSC. However, there are differences between the operations of the two spacecraft as outlined in the concept of operations at the beginning of the chapter. The differences are explained in the following sections.

The separation of the spacecraft is performed after a command issued from the GS. The control of the sequences leading to FIA is semi-autonomous. The GS will be in the loop only to issue the “go ahead” before critical manoeuvres. For example, there is a go ahead for the manoeuvre leading to the formation acquisition, during which the DSC approaches the MSC from a safe holding distance to the focal length of the telescope of 50 m.

15.3.1 Deployment mode

During the deployment mode the spacecraft separate and acquire a stable and safe relative position. At the end of the deployment mode the spacecraft will have null relative velocity and will be oriented such that they have a maximum area of the solar arrays exposed to the Sun. It is expected that the deployment mode lasts a few hours.

The following sequence of events is proposed for the MSC after the separation from the stack:
1. Cancel the angular rates resulting from the separation
2. Orient such that the X axis of the nominal mode points towards the Sun. This means the solar arrays of the MSC are normal to the Sun vector after deployment and the leaves of the mirror are in the shade of the shells
3. Deploy the (two) shells and the (two) mirror leaves
4. Maintain the X axis orientation towards the Sun
5. If needed re-establish communications with the DSC and GS

For the DSC a similar sequence of events is proposed, only that the DSC will perform additional manoeuvreing:
1. Deploy the solar arrays
2. Cancel the angular rates resulting from the separation
3. Orient such that the X axis points towards the Sun
4. Cancel the translation rates between the DSC and the MSC
5. Maintain the X axis orientation towards the Sun
6. If needed re-establish communications with the MSC and GS

Note that the DSC shall cancel the relative translational rates with respect to the MSC before it reaches the 4 km range of the RF navigation subsystem. Thus the separation mechanism has to be designed to minimise angular rates and provide a relatively small separation velocity. If the DSC moves beyond the operational radius of the RF navigation subsystem it can be brought back within range with intervention from the GS. However this would result in increasing the complexity of the operations since it requires highly accurate orbit determination for both spacecraft. See Chapter 20, Ground Segment and Operations.

15.3.2 Commissioning mode

The commissioning mode has two phases. The first phase is the FIA phase. It begins with a command from GS and it ends when the DSC is at 50 m from the MSC and the formation is locked using the fine metrology system. The second phase is the instrument checkout and calibration phase.

During the FIA phase the DSC performs three manoeuvres to reach the focal distance. The first manoeuvre starts at the waypoint WP0 in Figure 15-1. (At WP0 the relative velocity is null.)

1. The DSC moves from WP0 to WP1 where its CoM is on the negative side of the MSC Z axis. The attitude of the DSC is such that its Z axis is parallel to the Z axis of the MSC. During this manoeuvre the distance between spacecraft shall stay within the range of the R/F navigation subsystem (4 km). At the end of the manoeuvre (WP2) the relative velocity between spacecraft is null and the DSC is awaiting a go ahead from GS to proceed with the second manoeuvre. To reduce the collision risk during this manoeuvre the DSC will move such that the relative velocity vector does not point inside the safety sphere of the MSC.
2. After receiving the go ahead from the GS the DSC moves in the positive along the Z axis of the MSC in the positive direction. The DSC stops at a safe hold distance from the MSC. The attitude of the DSC is the same as during the first manoeuvre. To increase the safety of the approach operations the DSC moves at an angle with respect to the MSC Z axis such that the relative velocity vector does not point inside the safety sphere around the MSC. Once arrived at the safe hold distance, the DSC moves back to the Z axis. The safe hold distance is determined by the maximum operating distance of the laser range-finder system which is baselined at 120 m. The laser rangefinder is turned on and its nominal operation is checked. After the rangefinder check, assumed to give an OK status, the DSC awaits a go ahead from the GS to proceed with the third and final manoeuvre of the FIA.
3. The DSC moves from the safe hold distance towards the MSC and it stops at the focal distance of 50 m. The lateral metrology package is switched on and the fine relative position control loops are closed and stabilised.

The manoeuvres shown in Figure 15-1 are the most conservative. The relative velocity vectors during the first two manoeuvres, from WP0 and from WP1/WP2, point outside of the MSC safety sphere.

Note that WP2 can overlap WP3 so that the manoeuvreing from WP1 to WP2 is along the MSC Z axis. This would reduce the propellant used for the commissioning mode. For the same reason a direct approach from WP0 to WP2 (=WP3) is feasible. All the scenarios should be considered and simulation should be performed to assess the collision risks and determine which is the most efficient way to manoeuvre to acquire the formation.

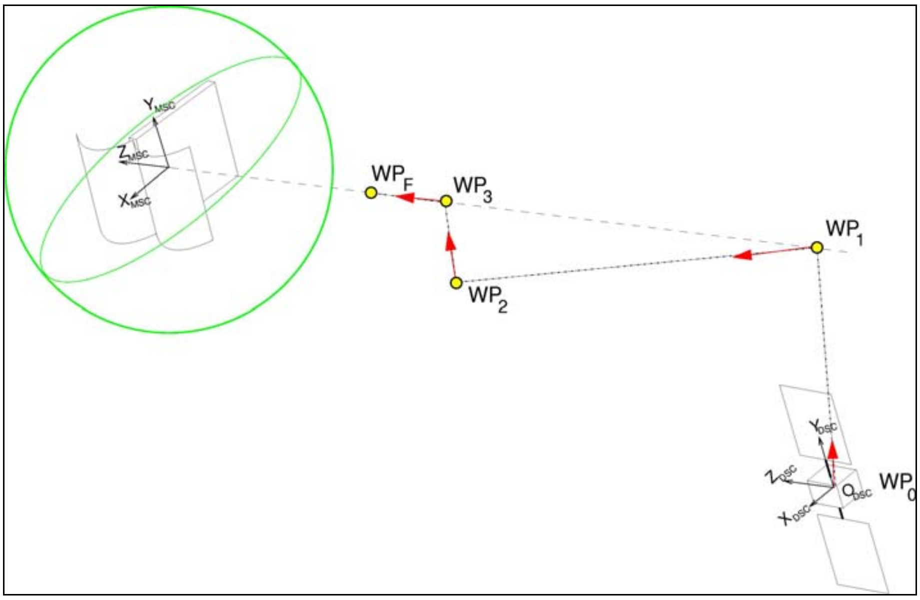

Figure 15-1: Manoeuvres leading to formation acquisition

The first two manoeuvres of the FIA phase are grouped under the formation initialisation subphase. The third part of the FIA phase is called the formation acquisition phase.

The R/F navigation subsystem is employed for the determination of the relative position and velocity during the formation initialisation subphase. During the formation acquisition subphase both the R/F and the laser rangefinder are used to determine the relative position and velocity. (Note that the laser rangefinder can only provide relative distance determination and possibly relative distance rates.)

The attitude determination of both spacecraft is provided by their respective STRs and the attitude is controlled with RWs. At the end of the FIA phase the lateral (laser) metrology package is switched on and the position control loops are closed and stabilised. The instrument checkout and calibration (ICC) phase follows the FIA. This phase is out of the scope of the present study and it should be analysed in a subsequent study.

15.3.3 Target acquisition mode

During the Target Acquisition Mode (TAM) the telescope is repointed at a new target. The MSC moves about its CoM only, i.e., it performs a “classical” slew manoeuvre. At the begining of this mode the MSC receives an attitude profile from the GS. The MSC follows the attitude profile using the STR as sensors and the RWs as actuators.

As the MSC slews, the DSC CoM translates on a circular arc (with a radius equal to the focal length) and it also rotates about its CoM so that the telescope made of the two spacecraft performs a rigid body-like rotation. The DSC control during slew is performed by its FK loop. Note that from the point of view of operations a single spacecraft is directly commanded. The telescope slew manoeuvre is shown in Figure 15-2.

The MSC performs a "classical" slew rotation (a rigid body rotation about its CoM.) The DSC translates and also slews. Only the MSC is commanded by the GS. The DSC maintains relative distance and attitude with respect to the MSC using its formation-keeping loop.

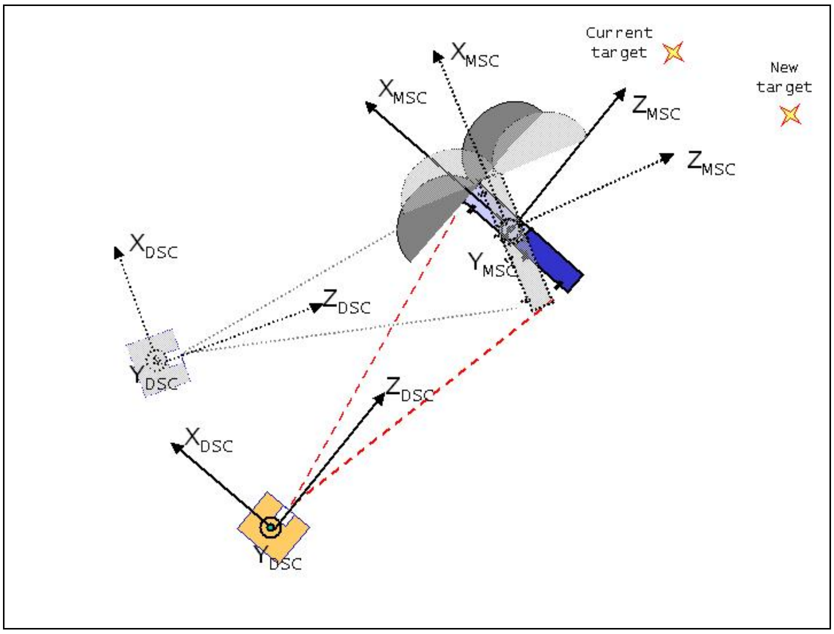

Figure 15-2: Slew manoeuvre of the telescope

15.3.4 Orbit maintenance mode

The orbit maintenance mode is entered upon command from GS. The command is uploaded to the MSC only. The MSC performs its correction manoeuvres with its cold gas nominal RCS thrusters. The DSC follows the MSC using the relative position control loops to keep the formation. The actuators of the MSC are its cold gas RCS thrusters.

Prior to the start of the orbit maintenance mode both spacecraft should dump the angular momentum in their RWs to avoid triggering a momentum dump during the manoeuvre. Similarly to the slew manoeuvre, only one spacecraft is commanded from the point of view of operations.

15.3.5 Spacecraft safe mode

A spacecraft safe mode is triggered by the coarse Sun sensors detecting an angular rate of a certain magnitude when none is commanded. The detection of the angular rate triggers an emergency Sun acquisition manoeuvre (SAM) and activates a collision monitoring routine. The SAM of the MSC should be designed such that the mirror petals are not exposed to the Sun.

The spacecraft should be in contact with the GS and a minimal DH capability should be maintained. Thus, the GS has access to the most recent valid state of the spacecraft and can perform fault identification and upload recovery commands. Due to the complexity of the mission, some fault identification and recovery should be performed on board to speed up the process of recovery.

15.3.6 Formation safe mode

The formation safe mode is entered at the end of a collision avoidance mode. At the exit from this mode the two spacecraft should be in a state similar to that at the end of the formation initialisation phase of the commissioning mode.

A detailed analysis is required for the definition of the entry and exit conditions from the formation safe mode. Since this is beyond the scope of the present study it should be revisited in future studies of the mission.

15.3.7 Collision avoidance mode

As regards baseline design, the collision avoidance mode is entered upon the detection of a possibility of collision. The collision flag is raised, for example, if the R/F navigation subsystem fails or if the safety sphere around one spacecraft is penetrated by the other spacecraft.

Since the DSC only has the capability to measure the relative position and velocity with respect to the MSC most of the collision avoidance tasks will be performed by the DSC. A detailed analysis of the collision avoidance mode and the recovery scenarios is beyond the scope of this study. It is recommended that a further study and simulations be performed to assess the collision risks and to determine the most appropriate procedures to reduce them.

16. RISK

The scope of this chapter is to identify the major risk contributors to the XEUS mission. For this purpose, requirements for mission success criteria and associated project safety requirements have been defined. For evaluating the XEUS risk contributors, XEUS modes and subsystems have been screened and associated with Failure Sensitivity Risk Indexes (FSIs) and Technology Risk Indexes.

16.1 Mission success requirements

The following mission success requirements have been defined for the XEUS mission.

16.1.1 For full mission success

16.1.1.1 Performance

1. The mission must deliver angular resolution of not less than 5 arcseconds to be classed 100% successful.
2. The mission must deliver an effective area of not less than 90% mirror petals correctly deployed and aligned.
3. 90% of achievable science data are correctly delivered to the end users.
4. The MSC-DSC position stability is maintained with +/- 5 mm (x- and y-axes) and +/- 1 mm (z-axis) at 50-m distance per maximum 3-day periods.

16.1.1.2 Mission duration

The mission duration of 3 years will allow the main science goals to be achieved.

16.1.1.3 Spacecraft delivery

As regards spacecraft delivery, both spacecraft must be delivered successfully into orbit and correctly functioning for full success criteria to be met.

16.1.2 For partial mission success

16.1.2.1 Performance

1. If the angular resolution is better than 12 arcseconds half energy width, the mission is considered partially successful
2. If at least 50% of mirror petals are correctly deployed and aligned, the mission is considered partially successful
3. 50% of achievable science data are correctly delivered to the end users

16.1.2.2 Mission duration

The mission is considered partially successful if science data are returned for 1.5 years duration.

16.2 Severity categories

16.2.1 Criticality level 1

This level will be associated to events jeopardising full mission success or causing the loss of both spacecraft or the permanent loss of one of the two spacecraft.

16.2.2 Criticality level 2

This level will be associated with events leading from full mission success to partial mission success.

16.3 Risk ranking

Table 16-1 shows the risk levels that have been used to rank the risk of failure and the risk associated with the mission modes.

Failure sensitivity risk index	Score
Maximum	5
High	4
Medium	3
Low	2
Minimum	1

Table 16-1: Failure sensitivity risk index

Table 16-2 shows the risk level that has been used to rank the technological risk:

Technology risk index	Score
Totally new	5
Under development	4
Known but in new application or new design but consolidated engineering experience	3
Known but in partially new application	2
Consolidated experience	1

Table 16-2: Technology risk index

The engineering judgement performed to allocate the risks values to the modes and to the subsystems has helped establish further criticalities and sensitivity indexes as shown in Table 16-3 to Table 16-12.

ELEMENT 1: Mirror spacecraft			
Number	Mode Name	Mode Criticality	Subsystems Required to operate for each Mode
1	Launch Mode	4	Power DHS
2	Initialisation Mode	3	AOCS Propulsion (hydrazine) Power Mechanism (leaf deployment) DHS
3	Cruise Mode	3	AOCS Propulsion(hydrazine + cold gas) Power DHS
4	Pre-deployment mode	2	AOCS Propulsion Power DHS
5	Stack Separation Mode	4	AOCS Propulsion Power DHS
6	Commissioning Mode	4	AOCS Propulsion Power Mechanism (mirror alignment) DHS
7	Formation Acquisition Mode	4	AOCS Propulsion Power DHS
8	Target Acquisition Mode	2	AOCS Power DHS
9	Nominal Observation Mode	2	AOCS Power DHS
10	Safe Mode	4	AOCS Power DHS
11	Collision Avoidance Mode	5	AOCS Propulsion Power DHS
12	Orbit Maintenance Mode	3	AOCS Propulsion Power DHS

Table 16-3: Mirror spacecraft modes w.r.t criticality index

And to the following tables for the subsystems:

Subsystem: AOCS		**Element 1, Mirror spacecraft**		
Equipment	**Equipment Total N^0**	**Equipment N^0 without redundancy**	**Technological Risk**	**Failure sensitivity index**
Star tracker (Jena Optronik)	2	1	1	3
Gyros (Systron Donner)	4	3	1	3
Reaction wheels (Honeywell)	4	3	1	3
Fine Sun sensor (Jena Optronik)	2	1	1	3
Medium Sun sensor (Aero Astro)	4	4	1	2

Table 16-4: Mirror spacecraft AOCS FSI

Subsystem: Communications		**Element 1, Mirror spacecraft**		
Equipment	**Total N^0**	**N^0 without redundancy**	**Technological Risk**	**Failure sensitivity index**
X-band LGA	3	2	1	1
X-band transponder	2	1	2	2
X-band SSPA	2	1	2	2
X-band RFDU	1	1	2	2
S-band transponder-metrology	2	1	3	3
S-band omni antenna helix	9	9	1	1
S-band RFDU	1	1	2	2
S-band omni antenna patch	2	2	1	1
RF inter-spacecraft link	2	1	1	1
RF inter-spacecraft link antenna	1	1	1	1

Table 16-5: MSC communications FSI

Subsystem: Data Handling		**Element 1, Mirror spacecraft**		
Equipment	**N^0**	**N^0 with redundancy**	**Technological Risk**	**Failure sensitivity index**
CDMU (proc+TM/TC)	2 boards	5 boards	2	2
Mass Memory	1 board	1 board	3	3
bus I/F	9	9	2	2
command matrix unit	2	2	2	2

Table 16-6: MSC data handling FSI

Subsystem: Thermal		**Element 1, Mirror spacecraft**		
Equipment	**Total N^0**	**N^0 without redundancy**	**Technological Risk**	**Failure sensitivity index**
MLI	2	0	1	1
Heaters and related equipment	1	0	1	2

Table 16-7: Mirror spacecraft thermal subsystem FSI

Subsystem: Mechanisms		**Element 1, Mirror spacecraft**		
Equipment	**Total N^0**	**N^0 without redundancy**	**Technological Risk**	**Failure sensitivity index**
Petal Actuators	192	At actuator winding level	5	3
Actuator Locking Mechanisms	192	No	2	1
Frame deployment active hinge	1	At actuator winding level	2	3
Frame deployment passive hinge	2	N.A.	2	1
Frame latches	6	Fail safe (for 1 failure)	2	1
Frame HRM	6	Two initiators	2	1
Shell deployment active hinge	4	At actuator winding level	2	3
Shell deployment passive hinge	4	N.A.	2	1
Shell latches	8	Fail safe (for 1 failure)	2	1
Shell HRM	8	Two initiators	2	1
Sun shield deployment mechanism	9	Redundant (Spring based)	2	1
Sun shield locking mechanism	9	Partially redundant	2	1
Sun shield HRM mechanism	10	Two initiators	2	1
Radiating plate deployment mechanism	6	Redundant (Spring based)	2	1
Radiating plate locking mechanism	6	Partially redundant	2	1
Radiating plate HRM mechanism	15	Two initiators	2	1
Stack separation mechanism	10	Two initiators per separation actuator	2	1
DSC separation mechanism	4	Two initiators per separation actuator	2	1

Table 16-8: MSC mechanics FSI

Subsystem: Propulsion		**Element 1, Mirror spacecraft**		
Equipment	**Total N^0**	**N^0 without redundancy**	**Technological Risk**	**Failure sensitivity index**
Thruster (MP)	4		2	1
Filter (MP)	2		2	1
Latch valve (MP)	2		2	1
Pipe work (MP)	2		2	1
FVV(MP)	2		2	1
FDV(MP	2		2	1
PT(MP)	2		2	1
TC(MP)	2		2	1
Propellant tank(MP)	2		2	1
Thruster (CG)	20		2	1
Filter (CG)	2		2	1
Latch Valve (CG)	4		2	1
Pipe work (CG)	2		2	1
HP regulator (CG)	4		2	1
FVV (CG)	8		2	1
TC (CG)	12		2	1
PT(CG)	6		2	1
Propellant Tank (CG)	8		1	1

Table 16-9: MSC propulsion FSI

Subsystem: Power		**Element 1, Mirror spacecraft**		
Equipment	**Total N^0**	**N^0 without redundancy**	**Technological Risk**	**Failure sensitivity index**
Battery LiIon	1	1	1	3
PCDU	1	1	2	3
Solar Panel	2	2	2	3
PDU2	1	1	2	3
Additional Solar Panel	1	1	2	3

Table 16-10: MSC power subsystem FSI

A brief description of the equipment follows:

- Battery: Battery cells are completely generic from existing/qualified missions (SMART-1, Mars Express, and so on). The battery arrangement may be optimised for this mission. The battery is considered for the moment as being one single battery but submodules could also be possible. By adding an extra string of cells, the failure of any cell is taken into account.

- PCDU/PDU2: Known and qualified technology is used (MPPT converters, battery regulators, and so on). However, the module will be newly designed for this project.
- Solar panels/additional solar panels: Existing technology will be used but the panel is new and needs to be designed and developed. There are 5% spare solar cells for redundancy purposes.

Subsystem: Optic-Metrology		**Element 1, Mirror spacecraft**		
Equipment	**N^0**	**N^0 with redundancy**	**Technological Risk**	**Failure sensitivity index**
Corner cube reflectors	3	3	1	3
Mirror strips (tilt measure)	36	36	1	3
>100 m length ground alignment facility	1	1		

Table 16-11: Optical metrology FSI

Subsystem: Structures		**Element 1, Mirror spacecraft**		
Equipment	**Total N^0**		**Technological Risk**	**Failure sensitivity index**
Mirrors inner frames	2		3	3
Mirrors outer frames	2		3	3
Top shell	2		1	1
Bottom shell	2		1	1
Horizontal platforms	4		1	1
Tank platforms	2		1	1
Closure panels	4		1	1
Bottom support panels	2		2	2
Thermal panels	2		1	1
Thermal flaps	2		1	1
Torsion bars	2		2	2

Table 16-12: Structure FSI

16.4 Major risk contributors

The major risk contributors are identified in Table 16-13:

Major Risk Contributors				
Subsystem	**Tech. Risk**	**Failure Risk**	**MAX Risk**	
			Technological	Failure
OPTICS	1	3		3
DATA HANDLING	3	3		3
MECHANISMS	5	3	5	3
COMMUNICATIONS	3	3		3
STRUCTURE	3	3		3
POWER	2	3		3
PROPULSION	2	1		
THERMAL	1	2		
AOCS	1	3		3

Table 16-13: Major risk contributors

16.5 Conclusions

The most critical mode identified is the collision avoidance with a criticality value of 5.

Many subsystems have been identified with the same failure risk value, equal to 3 (medium). They include Optics (included in the AOCS), Data Handling, Mechanisms, Communication, Structure, Power, AOCS. It is possible to highlight the subsystems among them that will be required to operate in the more critical mode, for example, for the Collision Avoidance Mode, AOCS, Power, DHS and Structure.

Those subsystems that will be required to operate more frequently are:

- Data Handling, Power and Structure they are required to operate in all modes
- Communication and, AOCS, are required in 11 Modes

For these also, mechanisms have been identified that are more critical, as regards technological risk.

17. PROGRAMMATICS/AIV

17.1 Requirements and design drivers

As regards programmatics and AIV issues, the requirements are separate for both of the spacecraft, but focussed on the Mirror Spacecraft (MSC), which is provided by ESA. The launch of the MSC is scheduled to 2015. The operational orbit will be the Lagrange point L2. A very long lifetime of 15 years is required, additionally the lifetime will be extended by 5 years. Regarding to consumables and radiation requirements a 10% margin on the nominal lifetime will be added (extended lifetime no margin).

The SVM of MSC shall be as simple as possible and require very few consumables. The MSC will be three-axis stabilised and no rotation during the observation phase will be carried out. The Detector Spacecraft (DSC), which is not ESA provided, requires a lifetime of 5 years with an extended lifetime of additional 2 years. As regards consumables and radiation requirements, a 10% margin on the nominal lifetime will be added (extended lifetime no margin). It is planned to replace the DSC if DSC-1 is at its EOL or more sophisticated detector systems become available.

17.2 Assumptions and trade-offs

The model philosophy is based on a proto-flight concept as proposed in other low-cost programmes. Unlike in the XEUS 1 study, a separate mirror module will be added to the model philosophy. A single launch with an Ariane-5 rocket in 2015 is planned.

All assumptions and trade-offs are limited to MSC only. As regards the AIV process, a separate payload (mirror) module and service module (SA/Canister) are proposed to ensure separate module environmental testing. In this way, well-separated MSC and DSC environmental testing has to be carried out. To ensure functional/alignment verifications combined measurements/tests with MSC and DSCTB are necessary. The DSC responsible shall do the investigations regarding the RF compatibility between spacecraft and Ground Stations. The mirror AIT process will be carried out in a cleanliness class 100 environment and the chemical particles will be controlled to avoid contamination. Therefore the separate mirror module will be built for the module qualification and training of the assembly, handling and integration procedures.

17.3 Baseline design

17.3.1 Performance (model philosophy)

A modular proto-flight model philosophy approach for MSC is proposed. The following models are necessary to ensure the AIV process:

STM: Structural and Thermal Model

MM: Mirror Module, real structure, mass and size, only one leaf will be equipped with three (low, medium and maximum mass) real mirror petals, after mirror module qualification the MM will be upgraded and used for the EOM

EOM: Engineering and Optical Model

PFM: Proto-Flight Model fully equipped
DSCTB: Detector Spacecraft Test Bench for combined functional and alignment verification

17.3.2 Model and test matrix

Test description	STM	DSCTB	MM	EOM	PFM
Handling/Integration	T		T	T	
Mech. Interface	R, T	-	To	R, T	T
Mass Property	A, T	-	To	Tv	Tv
Electr. Perform.	-	T*1)		T	T
Functional Test	-	TA*2)	To	T*4*1)	TA
Deployment Test	A, T	-	To	To	TA
Telecom. Link	-	T*1)		T*2)	A, T
Strength Load	A, To	-		To*5)	TA
Shock	To	-	To	To*5)	TA
Sine Vibration	A, To	-	To	To*5)	TA
Modal Survey	A, T	-	To	-	-
Acoustic Noise	To	-	To	To*5)	TA
Outgassing	-	-		To	I(TA)
Thermal balance	A, To	-		To*5)	TA
Thermal vacuum	To	-	To	To	TA
Grounding/Bonding	R, Tv	-		R, To	R, Tv
EMC cond. interf.	-	-		Tv	Tv
EMC rad. interf.	-	-		Tv	Tv
DC magnetic ?	-	-		Tv	Tv

Table Abbreviations:

A: Analysis
E: Equipment Level
I: Inspection
R: Review of design
TA: Test at acceptance level
TD: Development Tests
TQ: Test at qualification level
TV: Verification by Measurement

Table 1: MSC Verification Matrix

*1) = DSCTB link with MSC, as far as testable on S/C PFM level
*2) = Operational function tests and verification
*3) = MSC I/F verification
*4) = End-to-End link test
*5) = These tests have to be done for the mechanical and thermal qualification of the STM with a mirror dummy

This test matrix for MSC are recommended to ensure mission success and should harmonise with respect to verification requirements and the planning of the provider/customer.

Table 17-1: MSC verification matrix

17.3.3 XEUS master plan

ID	Task Name	Duration	Start	Finish
1	**XEUS Project**	**7676 days**	**Mon 06-07-03**	**Fri 35-11-30**
2	Phase A	220 days	Mon 06-07-03	Fri 07-05-04
3	Phase B	360 days	Mon 07-05-07	Fri 08-09-19
4	Negotiation Period	120 days	Mon 08-09-22	Fri 09-03-06
5	Phase C/D	1480 days	Mon 09-03-09	Fri 14-11-07
6	Shipment	60 days	Mon 14-11-10	Fri 15-01-30
7	Launch campaign	100 days	Mon 15-02-02	Fri 15-06-19
8	Launch MSC	0 days	Fri 15-06-19	Fri 15-06-19
9	Launch DSC	0 days	Tue 15-12-15	Tue 15-12-15
10	Transfer phase MSC	120 days	Sat 15-06-20	Thu 15-12-03
11	Transfer Phase DSC	120 days	Wed 15-12-16	Tue 16-05-31
12	Operational phase MSC	3911 days	Fri 15-12-04	Fri 30-11-29
13	Operatioanl phase DSC	1305 days	Wed 16-06-01	Tue 21-06-01
14	Extended phase MSC	1305 days	Mon 30-12-02	Fri 35-11-30
15	Extended phase DSC	523 days	Wed 21-06-02	Fri 23-06-02

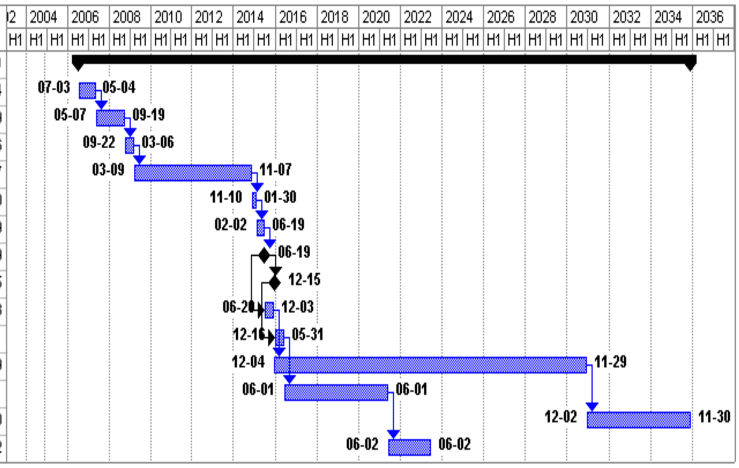

Table 17-2: XEUS mission schedule

It is assumed that a proper development programme for the optics is running almost in parallel.

17.3.4 XEUS AIV plan

ID	Task Name	Duration	Start	Finish
1	**Xeus 2 AIV Phase**	**7675 days**	**Mon 06-07-03**	**Fri 35-11-30**
2	**Spacecraft Reviews**	**405 days**	**Mon 07-03-05**	**Fri 08-09-19**
3	SRR	2 days	Mon 07-03-05	Tue 07-03-06
4	SDR	2 days	Wed 07-11-07	Thu 07-11-08
5	PDR	2 days	Thu 08-06-19	Fri 08-06-20
6	CDR	3 days	Wed 08-09-17	Fri 08-09-19
7	**Spacecraft Design&Development**	**7675 days**	**Mon 06-07-03**	**Fri 35-11-30**
8	Phase A	220 days	Mon 06-07-03	Fri 07-05-04
9	Phase B	360 days	Mon 07-05-07	Fri 08-09-19
10	Negotiation Period	120 days	Mon 08-09-22	Fri 09-03-06
11	Phase C/D	1480 days	Mon 09-03-09	Fri 14-11-07
12	Shipment	60 days	Mon 14-11-10	Fri 15-01-30
13	Phase E/F	5435 days	Mon 15-02-02	Fri 35-11-30
14	**Mirror Assembly Delivery**	**868 days**	**Tue 10-03-09**	**Thu 13-07-04**
15	STM	3 days	Tue 10-03-09	Thu 10-03-11
16	MM	5 days	Mon 11-01-03	Fri 11-01-07
17	EOM	5 days	Thu 12-03-01	Wed 12-03-07
18	PFM	5 days	Fri 13-06-28	Thu 13-07-04
19	**Mirror Assembly PFM + DSCTB Test's**	**350 days**	**Fri 13-07-05**	**Thu 14-11-06**
20	Optical Bench AIV	120 days	Fri 13-07-05	Thu 13-12-19
21	Vibration + TV/TB + UV colimation	75 days	Fri 13-12-20	Thu 14-04-03
22	Mirror Assembly AIT	75 days	Fri 14-04-04	Thu 14-07-17
23	Mirror Assembly Calibration	80 days	Fri 14-07-18	Thu 14-11-06
24	**Ground Segment**	**1304 days**	**Mon 07-02-05**	**Thu 12-02-02**
25	Ground Segment Requirement Review	2 days	Mon 07-02-05	Tue 07-02-06
26	Ground Segment Design Review	2 days	Mon 07-10-08	Tue 07-10-09
27	Ground Segment Critical Design Review	2 days	Thu 08-07-17	Fri 08-07-18
28	Ground Segment Readiness Review	2 days	Wed 12-02-01	Thu 12-02-02

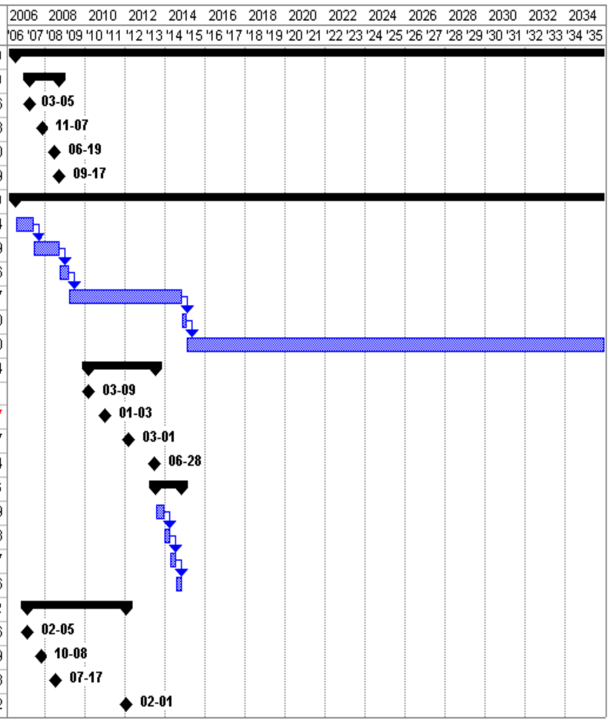

Table 17-3: AIV plan

17.4 Conclusions

At this stage of the requirements specifications, the AIV process cannot be assessed in detail. This is not unusual, given the technical challenges of the mission. Note that the mirror contamination and degradation over a period of 15+5 years cannot be verified experimentally. This is so because test methods for items for long-term exposure in space are unknown, other than for solar arrays.

Due to the particularity of having one instrument shared across two spacecraft, the instrument function verification needs particular attention. Using a separate mirror module and DSCTB for the qualification and verification process is strongly recommended.

18. COST

18.1 Assumptions

To perform an independent estimate of the industrial costs it was necessary to make a series of assumptions hereafter reported.

General methods and assumptions basic to the ESA TEC-ICE independent estimates are fully described in RD[42]; in particular, the detailed industrial cost estimates include:

- Provisions for pre-developments, Phase A and B costs;
- Phase C/D Industrial hardware and software development and production costs detailed down to equipment level; Ground Support Equipment and AIV (including Payload Integration) costs; Phase C/D Industrial Subsystem- and System-level Management and Control, Engineering, Product Assurance;
- Design Maturity Margin;

The Design Maturity Cost Margin takes into account expected cost growths resulting from unseen complexities, which emerge from higher design maturity and level of detail. It does not include stochastic events, which are only taken into account in an ad-hoc cost-risk analysis. The provision applies to the total Phase A, B and C/D cost.

Not included in the industrial cost estimates are:

- Ground segment and operations costs including LEOP and IOT
- Insurance for loss of mission
- Geographical distribution constraints cost impacts
- ESA internal costs and contingencies
- Scientists and PIs

The assumptions specific to the XEUS mission are:

Models Philosophy: according to the programmatics/AIV report, the programme needs STM, mirror EOM (Engineering and Optical Model) and PFM. Additionally there will be the need of a Detector Spacecraft Test Bench (DSCTB) for performing combined functional and alignment verification. It is assumed that this model will be provided by the partner Agency responsible for the DSC.

Payload: Mirror petals are part of a separate procurement and are delivered to the mirror assembler as ESA furnished equipment. The mirror petals, as requested by the customer, are not part of the estimate, but they are present in the product tree for remarking the interfaces.

Equipments: the product tree and design status of the equipments are shown in Table 18-1:

Space Segment Cost Breakdown	Number of Units	Performance characteristic (unit)	value	TRL (Today / Ph. C/D start)	DESTAT ECPLX	SM	STM	EM	EQM	QM	PFM	FM	Sp
Mirror Spacecraft													
Equipments													
AOCS													
Sun Acquisition Sensors	4	Accuracy (arcsec) =		6	OTS	4				1		4	
Fine Sun Sensor	0	Accuracy (arcsec) =			OTS								
Metrology mirrors and cubes	*1*			5	MoEq	1		1			1		
Star Trackers	2	Accuracy (arcsec) =	10	6	OTS	2					1	1	
IMU	1	FOG IMU (deg/sqrt(h)) =	2*10^-4	4	ModD	1		1			1		
Reaction Wheels	4	Momentum (Ns) =	0.2	6	OTS	4				1		4	
Cold Gas Propulsion		N2 Mass (kg) =	232										
Thrusters	28	Thrust (mN) =	55	4	OTS	28					1	27	2
Tanks	8	Volume (l) =	91	5	OTS	8					1	7	1
Valves and Piping	*2*	Total Mass =	41.8	5	MoEq	*2*					*2*		
PCUs + Electronics	1	Number of Boards =		4	OTS	1					1		
Hydrazine Propulsion		N2H4. Mass (kg) =	105										
Thrusters	4	Thrust (N) =	5	7	OTS	4					1	3	1
Tank	2	Volume (l) =	50	4	ModD	2				1		2	
Valves and Piping	*2*	Total Mass =	12.9	5	MoEq	1					1		
Electrical Power Subsystem													
Solar Panels (TJ GaAs)	3	Total Area (m2) =	10.8	6	MoEq		2				2		
PCDU	1	Max Power (W) =	317	4	ModD	1			1		1		
PDU 2	1	Max Power (W) =	317	4	ModD	1			1		1		
Battery	1	Capacity (Ah) =	21.3	5	MoEq	1			1		1		
Harness	*1*	Mass incl. margin (kg) =	4.68	5	MoEq						*1*		
Communication Subsystem													
X-band System (Earth)													
LGAs	3	Type =	patch	7	OTS	3						3	
Transponders	2	Data Rate (kbps) =	95	7	OTS	2					1	1	
SSPA, RFDU, lines	*1*	Transm. Power (W) =	15	5	MoEq	*1*					*1*		*0.2*
S-band System (metr. + comm.)													
Antennas	4	Type =	helix	7	OTS	4						4	
Antennas	2	Type =	patch	7		2						2	
Transponders	2	Data Rate (kbps) =	20	6	MoEq	2					1	1	
S-band System (intersat comm.)													
Antennas	1	Type =	omni	7	OTS	1					1		
Transponders	2	Data Rate (kbps) =	200	4	ModD	2		1		1		2	
Data Handling Subsystem													
CDMU (includes MM)	1	Number of Boards =		4	ModD	1			1		1		0.5
Canister Assembly													
Structures (2 Shells)													
Canister (CFRP)	1	Primary material =	CFRP	2	NewD		1				1		
Thermal Flaps	2	Primary material =	CFRP	2			2				2		
Mechanisms Assemblies													
HD&R	8			3	ModD	8		1		1		8	1
Hinges	4	Power Consumption (W) =		3	ModD	4		2		2		4	2
Depl. Drive Electr.	1	Number of Boards =		3	NewD	1			1		1		0.3
Latches	8			3	ModD	8		1		1		8	1
Thermal Flaps Mech.	9			2	ModD	9		1		1		9	2
Radiating plate Mech.	6			2	ModD	6		1		1		6	2
Separation (DSC-MSC)	10			2	NewD	10		1		1		10	2
Mirrors Assembly													
Mirror Petals	48			3	NewP	45			3	X		48	X
Structures (2 Leaves)													
Inner Frame	2	Primary material =	CFRP	2	NewD		2				1	1	
Outer Frame	2	Primary material =	Alumin.	2	NewD		2				1	1	
Mechanisms													
HD&R	6			7	OTS	6						6	1
Latches	4			7	OTS	4						4	1
Hinges	2	Power Consumption (W) =		3	NewD	2		2		2		2	2
Tilt Drive Electr.	1	Number of Boards =		3	NewD	1			1		1		0.3
Petals Tilt actuator	192	Power Consumption (W) =		3	MoEq					3		192	10
Petals HD&R actuator	192	Power Consumption (W) =		3	MoEq					3		192	10
Tilting Syst. Harness	1	Mass incl. margin (kg) =	16.8	5	MoEq						2		
Thermal Control		Total Mass (kg) =	124	5	MoEq						*1*		
On-board Software		Code (SLOC) =									1		
Adapter				3	NewP		1		1			1	

Table 18-1: Assumed MSC product tree, TRL, design status and hardware matrix

Design status and TRL: OTS equipment (TRL 8) implies that no modification and no qualification are needed. Minor modifications (TRL 6-7) imply that there is no need for EM or QM, the qualification is done on the PFM. Other modified equipments or designs (TRL 4-5) might require EM and/or QM. Equipments below TRL 4 need breadboarding and pre-development. The TRL definitions are shown in Table 18-2 and described in RD[43]:

Technology Readiness Levels:		Development Models involved
1	No development performed	none
2	Conceptual design formulated	none
3	Conceptual design proven analytically or experimentally	none
4	Critical functions/characteristics demonstrated	BB
5	Breadboard or EM tested in relevant environment	EBB, EM
6	Prototype tested in relevant environment	STM, EQM, QM
7	Prototype tested in space	PFM
8	Full operational capability (Flight-proven)	FM

Table 18-2: Assumed TRL definitions

Industrial set-up: international collaboration together with the complexity of the system will force a heavier industrial consortium structure than a fully cost-effective one would recommend. The following has been assumed: an Industrial Team set up consisting of a Prime Contractor for the MSC system, a Prime Contractor for the mirrors petals development and manufacture, a Prime Contractor for the definition and coordination of the metrology systems development[1]. Additionally the MSC Prime will probably have a subcontractor for the development test and verification of the canister structure (which is an unconventional, one-of-a-kind product), plus a different integrator will probably be in charge of the mirror assembly, which certainly will be critical in the schedule. Figure 18-1 shows the assumed contractual set-up:

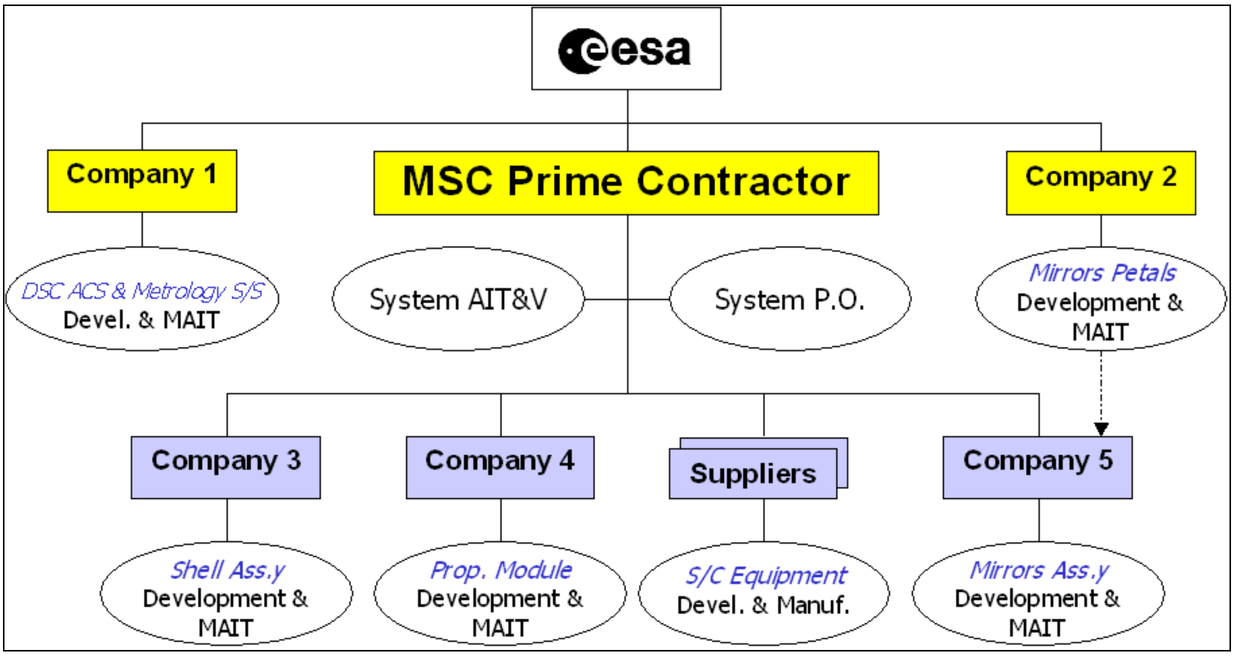

Figure 18-1: Assumed industrial set-up

[1] The assumption is defined as generally as possible and it does not exclude the possibility that the same company can act as Prime for all the systems. However, in any case a situation with three main Project Offices is envisaged.

A fully European development and production is assumed and also at component level it is assumed that European-qualified components will be available at the beginning of phase C/D.

Metrology: metrology and formation flight are assumed today at TRL 2-3, but currently there are development activities going on in the frame of other missions that aim at bringing the technologies at level 4. It is reasonable to expect heritage for the XEUS phase C/D when these systems are at a mature technology level and adaptation to the specific XEUS mission occurs.

DSC Equipments																	
ACS																	
Sun Acquisition Sensors (3)							7		**OTS**	3						3	
Fine Sun Sensor (2)							7		**OTS**	2						2	
Fine Star Trackers (2)							7		**OTS**	2						2	
IMU (1)							7		**OTS**	1						1	
Reaction Wheels							7		**OTS**	4						4	
Computer + S/W					5				**ModD**			1			1		
Cold Gas System							7		**OTS**	1						1	
Metrology S/S																	
Control Electronics + S/W		2										1			1		
RF Metrology (S-band system)									**OTS**	1						1	
Rangefinder (Axial)			3						**NewD**	1			1		1		
Interferometer (lateral)		2							**NewD**	1			1		1		
Scanner (tilt)		2							**NewD**	1			1		1		

Table 18-3: Assumed TRL, design status and hardware matrix for the DSC equipment supplied by ESA

The attitude control system of the DSC is supposed to employ the same hardware as the MSC. Additionally there will be a computer for the real-time orbit maintenance (the DSC adapts to maintain the nominal flight formation). The control electronics for the metrology subsystem will be implemented within the ACC; a specific software application evaluates the eventual tilting commands to be sent to the MSC.

18.2 Industrial cost estimate

The cost estimate performed is focussed on the MSC design, providing figures at subsystem level as sums of equipments cost estimates and system or subsystems level activities costs.

18.2.1 Class of estimate

The cost estimate for XEUS is identified, according to the Cost Engineering Chart of Services RD[44], as *Class 4* of a *Major Complexity* project, performed in a *Normal* time-frame. This classification gives an expected accuracy of 15-30%. Class 4 estimates are performed for projects at conceptual or feasibility stage, when the study defines the equipment level hardware.

The selected Design Maturity Margin, 20%, is the default for the Class 4 Major Complexity.

18.2.2 Estimate summary

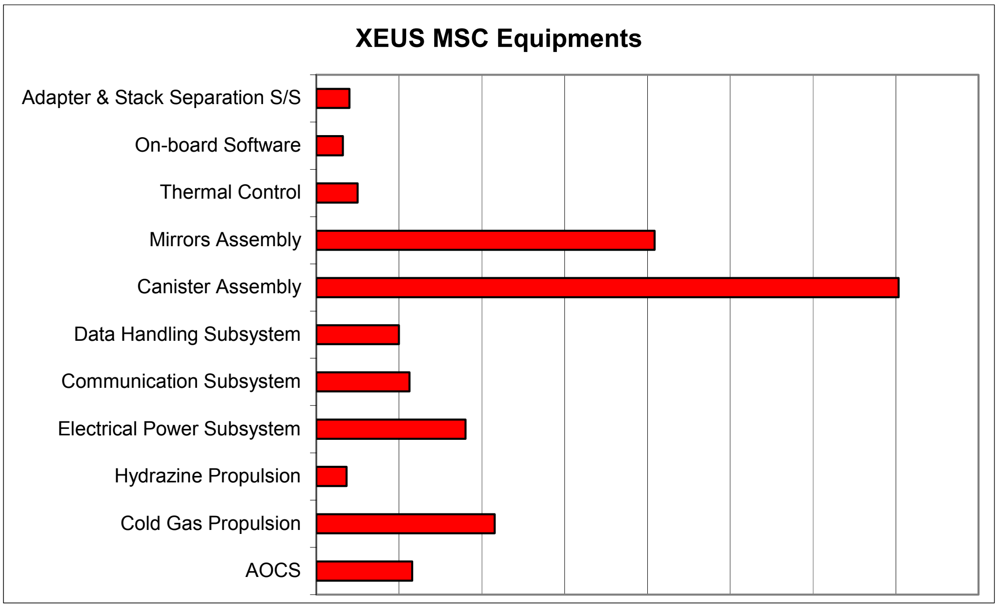

Figure 18-2: MSC equipments cost estimate

Figure 18-2 shows that the mirror and canister assemblies represent the highest project costs: the mirror because of the delicate and long assembly and test, while the canister's high cost is mainly due to the new structure which has to be specifically developed for this project. The estimate is shown in Figure 18-3:

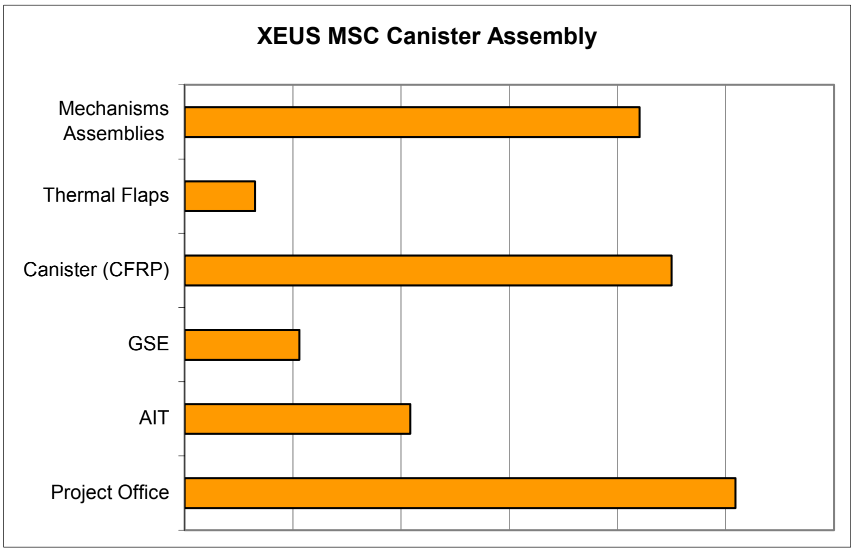

Figure 18-3: MSC canister cost estimate

18.2.3 The pre-developments

The estimate includes some pre-development provisions. They are not estimates, but provisions based on typical ESA pre-development contracts. Note that there is no provision for the metrology subsystem, nor for the mirror petals.

18.3 Justification of the cost estimate

- AOCS equipment cost is estimated analogous to other ESA science missions.
- The cold gas RCS equipment cost is assumed essentially recurring (being currently under development for LISA Pathfinder); and it is assumed that the components can be procured together with the DSC system, to lower the average unit cost.
- The hydrazine RCS equipment cost is assumed essentially recurring.
- Electrical Power, Data Handling, Communication subsystems are based on existing technologies flight proven with minor modifications or modified design. The only exception is the intersatellite link, proposed via a wireless system, currently under development; that estimate is based on the expert opinion.
- The breakdown of the canister assembly shows the highest cost in the engineering and manufacturing of the unconventional structure.
  The high cost of the project office is essentially related to the system engineering effort.
  The 700 kg structure is assumed as *extremely complex* in its interfaces, in particular when manufactured in composites.
- The mirror assembly is a structure that has very strict requirements. The main problem will be the integration and test. The estimate assumes that extensive tests are performed on the Mirror Module (MM) not fully representative of the flight model, with just three to four real mirrors and STM mirrors covering the rest. Two leaves are produced as PFMs. The high cost is also related with the early activities and the constraints to keep up the schedule deadlines. The project office has to be carried fully mobilised for a long time. Possible redesigns have to be foreseen for the structure and the interfaces.
- Thermal control is fully passive, but large radiators are necessary to get rid of the heat accumulated on the structure exposed to sunlight. Ingenious solutions are necessary to maintain the whole mirror at a temperature as homogeneous as possible. The thermal design foresees about 70 kg of MLI to cover the large canister.
- The MSC on-board software, essentially for data handling and housekeeping, will be tailored for the mission, but no particular efforts are envisaged. The tilting system software is implemented on the DSC.
- The MSC system costs do not include costs for building or refurbishing a new facility for AIT and V. The system validation is assumed performed in an ad-hoc facility, but already existing.
- The DSC costs relevant to ESA included in the estimate only cover up to the PFM. Additional recurring and non-recurring costs for additional missions are not included in that total.
- The DSCTB is assumed to be provided by the responsible of the DSC. This item should consist of a bench for transmitting and receiving the laser beam for the petals alignment.

A provision for three *additional spacecraft* supply, assuming that the equipment is not modified is given in Figure 18-4. It is assumed that the three spacecraft will not be produced as a series, so that no “learning” effect is introduced. No provision for storage and cocooning is included, as well. However, in that hypothesis, it is necessary to include a provision for early procurement of Hi-Rel parts and their storage to avoiding problems of obsolescence and loss of suppliers, which may lead to re-design (so additional non-recurring costs).

18.4 Cost risk analysis

Several sources of cost risk can be identified:

- *The industrial set-up*. The project, being developed in collaboration with other Agencies will include several activities of coordination and interface. A clear split between DSC and MSC activities, together with a clear and detailed definition of the interfaces, should be imposed to avoid ambiguities. However, there is a risk for an additional contractual layer, given that a company should be responsible for the whole mission to ensure the integrity of the overall concept.
- *The AIV of the mirror*. This has been recognised as a very long and delicate activity. Problems due to delays or redesign can cause high cost overruns because they impact the critical path.
- *Cleanliness requirements*. Since the mirror petals are very sensitive to contamination, it is highly probable that special precautions will be taken by the Prime. ESA requirements should be clearly stated in the ITT, to enable the most convenient selection of facilities and procedures.
- *Technical risk*. To evaluate the mission success, as well as the mission reliability, the admitted fault level of the mirror petals adjust system should be clearly defined. It is indeed also a source of cost risk, because the reliability assurance of such a system under strict requirements should require special efforts. Note that the product assurance of mechanisms that have to work in space for 15 years might prove to be unfeasible for high reliability at system level.
- *Mirror petals*. In the frame of the analysed study, the petals have been treated as black boxes. Nothing can be stated about these assemblies, but they might present a high level of cost risk being a new technology. The full qualification of three to four different types of petals will be necessary.
- *System tests and GSE*. There is a need for large infrastructures for system tests. For example, the infrastructure for the combined alignment and functional tests has not been identified yet. There is also a need to clarify who is responsible for the system level performances verification; this can be quite complex and highly risky.
- *Schedule and planning slippages*. The project is very sensitive to schedule slippages, which introduce a high cost-risk source due to the heavy industrial consortium, aggravated by the interagency coordination. Many items need full qualification, several phases need to be coordinated among different agencies.
- *DSC equipment*. The high cost-risk source is related to the integration of hardware and software into a spacecraft that is under responsibility of another agency. The estimates assume that the integration and tests are performed in Europe, but if that is not the case, that cost will be surely exceeded.

- *Metrology*. The high cost risk associated with the metrology subsystems is linked to their current low TRLs and to the fact that they are developed for a different, still unapproved mission.

During the CDF study, the subsystem specialists have contributed to the cost-risk analysis giving inputs to an ad-hoc table. They have been asked to identify the levels of confidence about their assumptions and to describe a worst-case scenario that might bring costs overrun, together with a score of the severity of the consequences with respect to the cost and to the schedule.

The inputs have been used to assign scores of Low (L), Medium (M) and High (H) cost-risk to the cost estimates at subsystem level, to derive a range between minimum (MIN) and maximum (MAX) values of the estimate. The range has fed a Monte Carlo simulation that gives a statistical summation of the different estimates, rather than a pure analytical sum, which tends to underestimate the correlation between the estimates.

The cost-risk analysis has been performed for the total MSC and for the ESA part of the DSC, separately. See Figure 18-4:

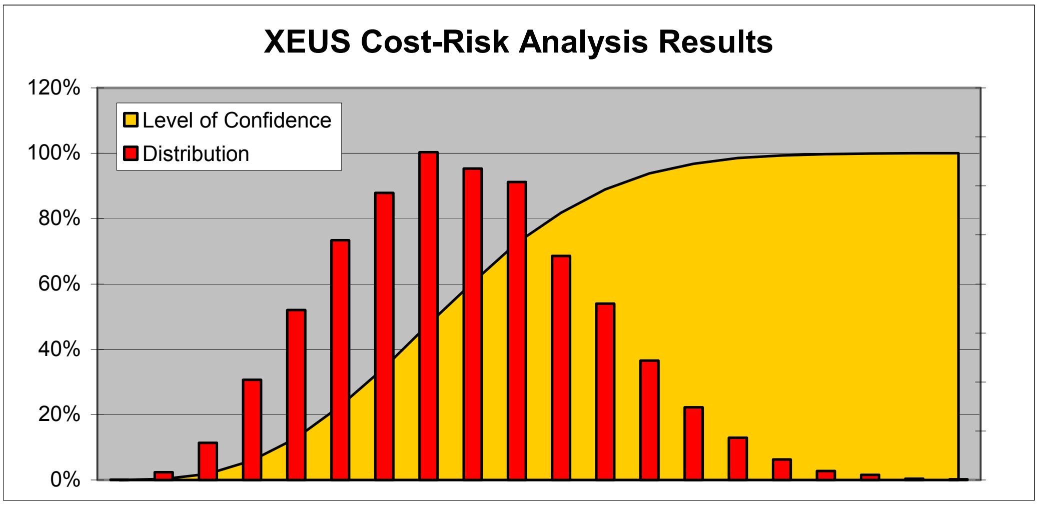

Figure 18-4: Cost-risk analysis results

19. GRATING OPTION: CONFIGURATION

The configuration is related to the option affecting the DSC. In this case, a deployable optical bench has to be placed on the DSC: a grating deployable to 10 m length is stowed on a face of the DSC by means of a hexapod, see Figure 19-1:

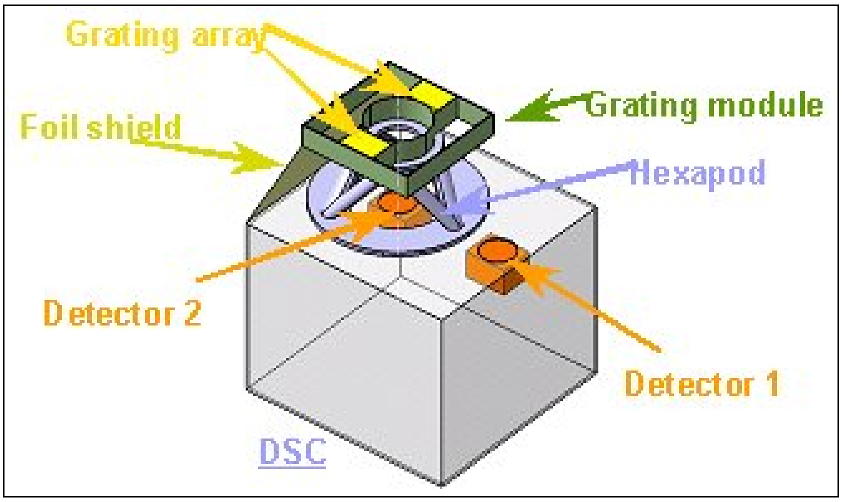

Figure 19-1: Configuration of 10-m grating lens stowed panel on the DSC box

Deploying the grating gives the final configuration panel shown in Figure 19-2:

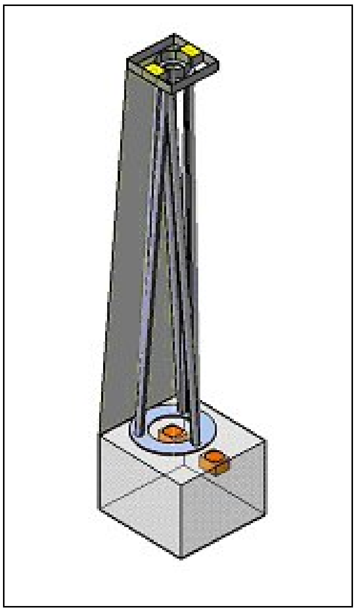

Figure 19-2: Deployed grating panel on the DSC

The deployed configuration dimensions are such that the two detectors both have free visibility on the mirrors leaves of the MSC.

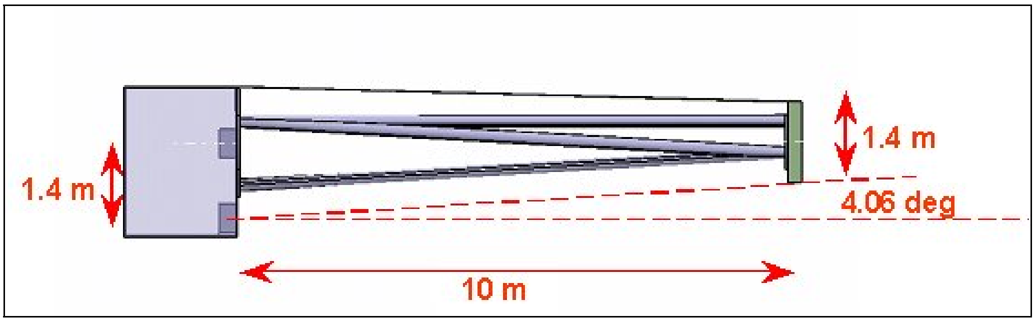

Figure 19-3: Characteristic dimensions of the deployed grating configuration on DSC

20. GROUND SEGMENT AND OPERATIONS

The ground segment and operations infrastructure for the Flight Operations Segement (FOS), of the XEUS mission will be set up by ESA/ESOC. This infrastructure will be based on extension of the existing ground segment infrastructure, customised to meet the mission-specific requirements. The concept for the establishment of the XEUS ground segment will be the maximum sharing and reuse of facilities and tools made available for other science observatory missions.

20.1 Requirements and design drivers

The preparation of the ground segment and operations concept for XEUS is mainly driven by the 'design to cost' concept. The approach considered has been the "family of mission concept" for science observatory missions for the ground segment and operations. Wherever possible, technical facilities and tools and manpower will be shared between other science observatory missions and XEUS.

Due to the characteristics of the mission, both the MSC and DSC will communicate with the ground station in X-band for uplink and downlink after separation.

Nominal spacecraft control during most of the cruise and the observation phase will be "off-line". Only one ground station will be allocated for communications with the spacecraft during these phases (15-m antenna for cruise, 35-m antenna for routine operations), providing a daily visibility duration of 3 hours on average during the routine phase. That implies that both XEUS spacecraft are assumed to provide on-board capabilities so that the satellites are able to perform corrective actions in the event of on-board anomalies and the ground segment does not need to monitor the spacecraft in real time. The "off-line" operations concept allows the possibility of sharing shifts with the science observatory mission Flight Control Team (FCT).

20.2 Assumptions and trade-offs

The main assumptions considered for the design of the ground segment for XEUS are the following:

- It is assumed that XEUS will be flying sharing the science observatory mission facilities with other flying science observatory missions (mainly software as MCS, Simulator, and the dedicated control room) and manpower (mainly in the areas of Quality Assurance, Project Control, Ground Segment Management, and Operations Management). However XEUS will have a separate core team for Flight Control and Flight Dynamics. Sharing SPACONS between missions will be considered at ESOC.
- A close link between the XEUS, GAIA and Darwin project teams is assumed.
- It is assumed that the XEUS operations can be performed by a team that is organisationally as close as possible/practical to the GAIA and Darwin Mission Operations and Satellite Control teams under OPS-OP.
- A launch in October 2015 is assumed.

- 15-year overall mission lifetime is assumed, including LEOP and commissioning during cruise, cruise itself, and observation. (3-5 months cruise, 15 years nominal Observation). Replacement of the DSC every 5 years, including de-orbiting the “old” DSC, LEOP, cruise and rendezvous of the replacement DSC.
- The spacecraft will be launched by an Ariane-5 from Kourou, and will be transferred directly to L2.
- The LEOP network will be composed of: Kourou, Vilspa, and Perth/New Norcia.
- No dedicated backup station will be considered for the routine mission (spacecraft emergency cases will be supported by the network as per priority rules).
- The maximum HKTM data rates are 1 kbps (MSC) and 4 kbps (DSC).
- It is assumed that all payload HKTM is included in the same virtual channel as the satellite HKTM and is therefore directly available to ESOC.
- Science data acquisition from New Norcia/Cebreros (X-band) is the ESOC baseline.
- The composition of the FCT during mission preparations and mission operations will be determined by the criticality of the operations and the possibilities of sharing the team with other missions.
- It is assumed that it will be possible to set up the LEOP timeline so that critical operations can be covered by the Main Flight Control Team (A-Team).
- It is assumed that it is sufficient that the LEOP Back-up Team (B-Team) is comprised of Flight Control Team members from another interplanetary exploration mission (such as GAIA) and that they will be involved mainly in monitoring activities.
- The provision, installation and validation of a mini-Mission Control System (mini-MCS) in the main ground station is part of the baseline.
- It is assumed that the structure and naming convention of the XEUS database (DB) will be identical to the GAIA DB.
- Use of the SCOS2000 Mission Control System is assumed. The same MCS is assumed to for MSC and DSC. The cost for the MCS development will mainly include the customisation for XEUS and the Mission Planning System.
- It is assumed that some automation will be available including: Initial Pass Operations/Establishing of Ground Station Link and some limited reporting capabilities.
- Hardware usage will be shared with GAIA/Darwin where possible (for example, MPS, back-up system for the DDS).
- The mission planning scenario will be divided into different levels, namely long-, medium-, and short-term planning. Months before each observation period a baseline planning will be established and this plan will be refined and prepared for uplink short before the observation period.
- Mission planning will be supported during normal working hours of the FCT.
- Real-time reaction will be of the order of 3 minutes during critical mission phases (for example, LEOP) provided there is ground station coverage, the problems are detected in the HKTM and Flight Control/Contingency Recovery Procedures are available.
- In routine phases under ground station visibility (approximately 3 hrs/day) operations will always be performed in near real time.
- Off-line operations are performed during nominal routine operations and during the periods when no there is no ground station contact.
- SPACON positions will be manned one 8-hour shift per day (5 days/week).

- Not all the duration of a ground station pass can be dedicated to science downlink.
- Spacecraft TM and TC service shall be compliant with the ECSS Standards.

20.3 Baseline design

The ESA/ESOC ground segment will consist of:

- The Ground Stations and the Communications Network.
- The Mission Control Centre (infrastructure and computer hardware)
- The Flight Control System (data processing and Flight Dynamics Software)
- Infrastructure (Mission Control System, Simulator, etc)

The XEUS ground segment shall provide X-band payload data acquisition during commissioning, observation and extension phase. The XEUS ground segment shall provide:

- A satellite monitoring and control chain, which includes:
  - An X-band housekeeping TM acquisition and processing functional chain
  - An X-band TC generation and uplink functional chain
  - Off-line performance analysis functions
- An orbit and attitude monitoring and control functional chain
- An overall mission planning function
- An OBSM facility
- Data archiving

20.3.1 Ground stations and communications network

The ground station network to be used for XEUS during LEOP will be composed of the 15-metre antennas in Kourou, Villafranca and Perth (or New Norcia). This network almost guarantees 24-hour coverage of the spacecraft during this critical period. For the cruise phase and the observation and extended phase, the 35-m antenna in New Norcia is the baseline.

In the spirit of the “family of missions” a detailed schedule could be set up to optimise the use of the ground stations sharing coverage time and ground station charges between XEUS and other missions. It can be assumed that at the beginning of the mission XEUS, GAIA and possibly Darwin can share the New Norcia/Cebreros 35-m ground station system.

The Ground Facilities Control Centre monitors and remotely controls all the ESTRACK ground tracking stations, using information provided by Flight Dynamics and the scheduling office. They are also responsible for the TM/TC links to and from the ground stations and any data retrieval of stored science from the TMPs or the ranging IFMS, CORTEX and MPTS equipment.

A station computer monitors and controls (locally, automatic or remotely from MSCE) all equipment on the station. It provides different backup modes (TM quicklook, backup commanding). A Front-End controller unit controls the antenna subsystem.

All ESA stations interface to the MSCE at ESOC in Darmstadt via the OPSNET communications network. OPSNET is a closed Wide Area Network for data (telecommand, telemetry, tracking data, station monitoring and control data) and voice. It is assumed that the communication system will support the LEOP and routine data exchanges between the Control Centre in Darmstadt and the ground stations identified in this section.

20.3.2 The Mission Control Centre

The XEUS mission (MSC and DSC) will be operated from ESA/ESOC and it will be controlled from the Mission Operations and Satellite Control Element (MSCE), which consists of the Main Control Room (MCR) augmented by the Flight Dynamics Room (FDR) and Dedicated Control Rooms (DCRs) and Project Support Rooms (PSRs). The MCR will be used for mission control during LEOP and possibly the Commissioning Phase in the event of serious anomaly. During cruise, and the observation phase the mission control will be conducted from a Dedicated Control Room shared with other observatory science missions, such as GAIA and Darwin.

The control centre is equipped with workstations giving access to the different computer systems used for different tasks of operational data processing. The control centre will be staffed by shared SPACONS from other observatory science missions with support from operations engineering staff, experts in spacecraft control, flight dynamics and network control, available on a part time basis for the full mission duration. Space and equipment for scientists, project and industry experts and public relations will be provided close to the MSCE as required, during the critical phases of the mission.

20.3.3 Computer facilities

The computer configuration used in the MSCE for XEUS will be derived from existing structures. The computer system consists of:

- A computer system used for the Flight Operations Plan generation in a form directly usable by the mission-dedicated computer
- A mission-dedicated computer system (including workstations hosting SCOS-2000) used for real-time telemetry processing and for command preparation and telemetry and command log archiving, and also for non real-time mission planning and mission evaluation
- Workstations hosting the flight dynamics system
- The simulation computer, providing an image of the spacecraft system during ground segment verification, for staff training and during operations

All computer systems in the control centre will be redundant with common access to data storage facilities and peripherals. Workstations of a similar type will preferably be used for all related computing, to maximise flexibility and to minimise maintenance costs. The workstations allowing privileged user access to the Flight Control System will be located in the different control rooms as necessary.

20.3.4 The flight control software system

The flight control system will be based on infrastructure development (SCOS2000), using a distributed architecture for all spacecraft monitoring and control activities. The flight control system includes the following facilities:

- Telemetry reception facilities for acquisition, quality checking, filing and distribution
- Telemetry analysis facilities for status/limit checking, trend evaluation

- Telecommand processing facilities for the generation of commands for control, master schedule updates, and on-board software maintenance. The facilities will also provide uplink and verification capabilities.
- Monitoring of instrument housekeeping telemetry for certain parameters that affect spacecraft safety and command acceptance and execution verification.
- Separation and forwarding of payload telemetry to Science Data Processing Centres
- Checking, reformatting, scheduling command request for payload.

Within the SCOS2000 system, mission-specific software will be developed wherever necessary.

20.4 Mission operations concept

20.4.1 Overview

The XEUS mission operations will comprise:

- Spacecraft operations, consisting of mission planning spacecraft monitoring and control and all orbit and attitude determination and control of the MSC
- Spacecraft operations, consisting of mission planning spacecraft monitoring and control and all orbit and attitude determination and control of the DSC
- DSC science instruments operations from the European Space Astronomy Centre (ESAC) in Villafranca, consisting of the implementation of the observation schedules and collection and data quality control of the science telemetry.

Mission operations will commence at the separation of the XEUS system from the launcher and will continue until the end of the mission, when ground contact to the spacecraft will be aborted. Mission operations will comprise the following tasks:

- Mission planning: long-term and short-term planning (24 hours to 1 week time frame)
- Spacecraft status monitoring
- Spacecraft control, based on monitoring and following the Flight Operations Plan and the short-term plan
- Orbit determination and control using tracking data and implementing orbit manoeuvres (MSC only – the DSC will follow automatically using RF metrology)
- Attitude determination and control based on the processed attitude sensors data in the spacecraft telemetry and by commanded updates of control parameters in the on-board attitude control system (MSC only – the DSC will adjust its attitude automatically using RF metrology)
- On-board software maintenance
- Operations support for the experimenters in terms of telemetry packet routing and command checking with respects to spacecraft safety, and telecommand uplink
- Maintenance of ESA ground facilities and network

20.4.2 Mission planning, spacecraft monitoring and control

The operations support activities for XEUS will be conducted according to the assumptions in section 20.2 and can be summarised as follows:

- All operations will be conducted by ESA/ESOC according to procedures contained in the Flight Operations Plan (FOP).

- Nominal spacecraft control during the routine mission phase will be ‘off-line’. The contacts between the Mission Control Centre and the spacecraft, except for collecting payload and housekeeping telemetry, will therefore primarily be used for pre-programming of autonomous operation functions on the spacecraft, and for data collection for off-line status assessment. Anomalies will be normally detected with delay.
- All XEUS operations (the XEUS system before MSC/DSC separation at L2 and both spacecraft post-separation) will be conducted by uplinking a master schedule of commands for later executions on the spacecraft. The master schedule will be prepared by a dedicated Mission Planning System, using inputs defined by the SOC. The master schedule shall be able to cover at least 30 days of nominal operations.
- The DSC payloads will be operated by the ESAC in Villafranca. The health of the scientific instruments will be monitored and necessary control actions will be taken following the same procedures as for the spacecraft subsystems. The telemetry data products received from the instruments on-board the orbiter will be monitored for its data quality before it is delivered to SOC. (From the SOC it is distributed to the science consortium performing the science data processing).
- During the LEOP phase for each spacecraft, 48 hours of TT & C X band operations will be conducted from the ESA/ESOC MCR.
- During the Cruise Phase, there will be low-key operations from an ESA/ESOC DCR.
- During observation and extended operations one-shift operations 8 hours per day 5 days/week will be maintained from the ESOC DCR, with TT & C in and Science downlink operations in X-band.

20.4.3 Orbit and attitude control

The flight dynamics support will consist of:

- Orbit determination of the spacecraft during the LEOP and Transfer phases using one ground station tracking, ranging and Doppler data.
- Orbit determination of the MSC during routine phases shall be done using one ground station tracking, ranging and Doppler data. It is assumed that no orbit determination of the DSC will be required, as it will follow the MSC using RF metrology.
- Manoeuvre optimisation: the manoeuvres performed for wheel de-saturation will be optimised to minimise propellant consumption and considering all operational conditions.
- Attitude Control System Monitoring: monitoring and verification of the on-board functions such as star tracker window and sensitivity setting.
- Antenna steering: preparation of attitude manoeuvres and antenna steering schedule.
- Manoeuvre command generation: preparation of command sequences or input to master schedule updates related to all orbit and attitude manoeuvres.
- Manoeuvre monitoring.
- Calibration of thrusters and sensors.

21. CONCLUSIONS

A new mission concept for XEUS has become available with the development of a new X-ray optics technology that significantly improves on current state-of-the-art XMM-Newton technology. Developing a lightweight X-ray mirror technology for XEUS has meant a 10-fold reduction in mass and 3-fold reduction in volume. Using new optics technology, new mission architectures were considered during the CDF study and these were no longer reliant on complex and expensive ISS deployment. The deployment directly to an L2 orbit has important advantages, such as a stable thermal environment, stable straylight configuration and long-duration observation periods.

The initial study assumed that the workhorse Soyuz-Fregat launcher would be used to launch separately the Mirror (MSC) and Detector (DSC) spacecraft. The conclusion was that a viable mission scenario was achievable, but even with optimistic mirror mass assumptions the overall collecting area does not meet the science requirements. A follow-up study assuming the launch of both spacecraft on a singe Ariane-5 conversely showed the potential that the improved mass capability allowed the requirement of 10 m^2 collecting area at 1 keV could be met. Extended payload element options were also studied for a wider range of science capabilities. The study showed that the ambitious science requirements of the XEUS mission can be met with the novel mission design and the application of new emerging technologies. The adequate further development and maturing of the optics and formation flying technologies is recommended.

22. REFERENCES

RD[1] Pavón S, XEUS Mission Analysis and Sky Coverage, *MAO WP-446*, ESA/ESOC, August 2002.

RD[2] Hechler M, Herschel/Planck CReMA, Draft issue 1.2, *FP-NA-RP-0010-OPS/GA*, ESA/ESOC/MAO, 2001-07-30.

RD[3] Hechler M, GAIA CReMA, Draft issue 0.0, ESA/ESOC/MAO, 2002-08-19.

RD[4] Delta IV Payload Planners Guide, Update-April 2002, *MDC 00H0043*, the Boeing Co., Huntington Beach, California, USA, April 2002.

RD[5] Soyuz for Exploration Missions, Presentation to ESA/Astrium, *Meeting ESA Horizons Mission Status 2005-2012 and Soyuz*, ESA-HQ, Paris, 2002-02-27.

RD[6] Yáñez A, Soyuz/Fregat 2-1b from Kourou: Estimated Performance for HEO and Escape Missions, *MAO WP-470*, Draft, ESA/ESOC, 2004-03-30.

RD[7] XEUS Detector Spacecraft (DSC) Spacecraft Definition Document, David Lumb and Marcos Bavdaz with contributions from JAXA-ISAS, May 2004, Issue 1.0.

RD[8] Hibbler, R.C., "Engineering Mechanics, Statics, and Dynamics" 4-th Ed.- 1986.

RD[9] '*Large Scale Metrology – An Update*', DH Parker et al, National Physics laboratory, Teddington, UK.

RD[10] 'A New Self-Calibrating 3D Interferometric Fringe-Based Imaging System for profiling, Positioning and Control in Space Use', Beverley T Meggitt et al, ESA Final Report #15787/02/NL/PA, December 2002.

RD[11] 'A compact 3D imaging laser radar system using Geiger-mode APD arrays: system and measurements', Conference on Laser Radar Technology and Applications VIII, SPIE, April 2003.

RD[12] '*Interferometer – HPOM Progress Mtg 8*', SIOS/ TU Ilmenau presentation, ESA Contract #15654/01/NL/PA, November 2003, Delft.

RD[13] ECSS-E-50-05A, Radio Frequency And Modulation Standard, published 24 Jan 2003.

RD[14] CCSDS 101.0-B-6. *Telemetry Channel Coding Standard*. Blue Book. Issue 6. October 2002.

RD[15] PSS-04-104, *Ranging Standard*, March 1991.

RD[16] CCSDS 102.0-B-5. *Packet Telemetry Standard*. Blue Book. Issue 5. November 2000.

RD[17] CCSDS 201.0-B-3. *Telecommand Part 1—Channel Service*. Blue Book. Issue 3. June 2000.

RD[18] CCSDS 202.1-B-2. *Telecommand Part 2.1—Command Operation Procedures*. Blue Book. Issue 2. June 2001.

RD[19] CCSDS 203.0-B-2. *Telecommand Part 3—Data Management Service*. Blue Book. Issue 2. June 2001.

RD[20] ECSS-E-70-41A, Telemetry And Telecommand Packet Utilization, published 30 January 2003.

RD[21] CCSDS 211.0-B-2. *Proximity-1 Space Link Protocol*—Data Link Layer. Blue Book. Issue 2. April 2003.

RD[22] CCSDS 211.1-B-1. *Proximity-1 Space Link Protocol*—Physical Layer. Blue Book. Issue 1. April 2003.

RD[23] CCSDS 211.2-B-1. *Proximity-1 Space Link Protocol*—Coding and Synchronization Sublayer. Blue Book. Issue 1. April 2003.

RD[24] Formation Flying RF Subsystem. *'RF Sub-System Architectural Design'*. 14 December 2002.

RD[25] Formation Flying RF Subsystem. *'TN on antenna accommodation'*. FFRF-ASPI-TN 4. 30 September 2002.

RD[26] http://centaur.sstl.co.uk/datasheets/Subsys_PATCH.pdf : S and X band patch antenna *Surrey Satellite Technology Ltd.* data sheet.

RD[27] IEEE 802.15.4 web site: http://www.ieee802.org/15/pub/TG4.html

RD[28] Institute of Electrical and Electronics Engineers, Inc., IEEE Std. 802.15.4-2003, IEEE Standard for Information Technology—Telecommunications and Information Exchange between Systems—Local and Metropolitan Area Networks—Specific Requirements—Part 15.4: Wireless Medium Access Control (MAC) and Physical Layer (PHY) Specifications for Low Rate Wireless Personal Area Networks (WPANs). New York: IEEE Press. 2003.

RD[29] 'Current Activities and Status of the ESA-ESTEC Sponsored Wireless Onboard Spacecraft Working Group'. DASIA 2004 Wireless Session paper.

RD[30] ESA Wireless Onboard Spacecraft Web Site : http://www.wireless.esa.int/

RD[31] Geraldine Artaud, Patrick Plancke, Rodger Magness, Dick Durrant, Chris Plummer. 'IEEE 802.15.4: Wireless Transducer Networks'. DASIA 2004.

RD[32] Parkinson and Spilker, Eds.'Global Positioning System: System and Applications I'. Progress in astronautics and aeronautics. Volume 163.

RD[33] 'Formation flying RF subsystem Final Report'. Contract number 15511/01/NL/EC. Alcatel Space.

RD[34] http://www.grc.nasa.gov/WWW/RT1996/5000/5480di.htm

RD[35] http://www.saftbatteries.com/130-Catalogue/PDF/space_lithium.pdf

RD[36] SMART-1 Battery Management Electronic (BME) J.O. Cabezas, F.H. Pedersen, P. Rueda, 6th European Space Conference, May 2002, Porto, Portugal.

RD[37] Low Temperature Cell: Summary Report, D. Curzon AEA Technology, LION-AEA-LT-RP-0008, 18/05/04.

RD[38] ECSS-E-10-02A, Space Engineering Verification.

RD[39] ECSS-E-10-03A, Space Engineering Testing.

RD[40] ESA bulletin 100, The Integration and Testing of XMM.

RD[41] ESA SP-1253, The XEUS Telescope.

RD[42] General Methods and Assumptions, TEC-ICE/GRE/HJ/2004/002_01.

RD[43] Technology Readiness Levels, TEC-ICE/GRE/HJ/2004/003_01.

RD[44] TEC-ICE Chart of Services, TEC-ICE/GRE/HJ/2004/001_03.

23. ACRONYMS AND ABBREVIATIONS

AOCS	Attitude and Orbit Control System
A5	Ariane-5
ADM	Absolute Distance Meter
AIV	Assembly, Integration and Verification
BDR	Battery Discharge Regulator
BER	Bit Error Rate
BOL	Beginning Of Life
CandC	Command and Control
CDMA	Code Division Multiple Access
CDR	Critical Design Review
CFRP	Carbon Fibre Reinforced Plastic
CoM	Centre of Mass
CReMA	Consolidated Report on Mission Analysis
DB	Data Base
DCR	Dedicated Control Room
DoD	Depth Of Discharge
DSA	Deep Space Antenna
DSC	Detector Spacecraft
DSCTB	Detector Spacecraft Test Bench
ΔV	Velocity increment (m/s)
ECA	Etage Cryogénique supérieur Ariane
ECC	Error Checking and Correction
EDAC	Error Detection And Correction
EMC	Electromagnetic Compatibility
EOL	End Of Life
ESA	European Space Agency
ESOC	European Space Operations Centre
FCL	Foldback Current Limiter
FCT	Flight Control Team
FCV	Flow Control Valve
FDR	Flight Dynamics Room
FER	Frame Error Rate
FF	Formation flying
FIA	Formation Initialisation and Acquisition
FK	Formation keeping
FOP	Flight Operations Plan
FOS	Flight Operations Segment
FSI	Failure Sensitivity Index
GRP	Glass Reinforced Plastic
GS	Ground Station
GTO	Geostationary Transfer Orbit
HEO	Highly Elliptical Orbit

HGA	High Gain Antenna
HK	Housekeeping data
HKTM	Housekeeping Telemetry
HPOM	High Precision Optical Metrology
HRM	Hold-down and Release Mechanism
I/F	Interface
ICC	Instrument checkout and calibration
IFMS	Intermediate Frequency and Modem System
JAXA	Japan Aerospace Exploration Agency
L_1, L_2	Libration or Lagrange point 1, 2
LCL	Latching Current Limiter
LD	Laser Diode
LEOP	Launch and Early Orbit Phase
LGA	Low Gain Antenna
MAO	Mission Analysis Office
MCR	Main Control Room
MCS	Mission Control System
MGA	Medium Gain Antenna
MM	Mirror Module
MPPT	Maximum Power Point Tracker
MSC	Mirror Spacecraft
MSCE	Mission Operations and Satellite Control Element
NASA	National Aeronautic and Space Administration
NNO	New Norcia
OBSM	On-Board Software Maintenance
OCS	Orbit Control System
PAF	Payload Attach Fitting
PCDU	Power Conditioning and Distribution Unit
PCU	Power Conditioning Unit
PDR	Preliminary Design Review
PDU	Power Distribution Unit
PSD	Power Spectral Density
PSR	Project Support Room
PV	Photovoltaic
RCS	Reaction control system
RD	Reference Document
RF	Radio frequency
RFDU	Radio Frequency Distribution Unit
RG	Ranging
RHU	Radioisotope Heater Units
RW	Reaction Wheels
S/C	Spacecraft
S/S	Subsystem
SA	Solar Arrays
SADM	Solar Array Drive Mechanism
SCOS	Satellite Control and Operations System

SDR	System Design Review
SEPM	Solar Electric Propulsion Module
SEU	Single Event Upset
SOC	Science Operations Centre
SPACON	Spacecraft Controller
SRR	System Requirement Review
SSPA	Solid State Power Amplifier
STCK	Stack
TBC	To Be Confirmed
TC	Telecommand
TCM	Trajectory correction manoeuvre
TDMA	Time Division Multiple Access
TM	Telemetry
TMP	Telemetry Processor
ToF	Time of Flight
TRL	Technology Readiness Level
TTandC	Tracking, Telemetry and Command
TV/TB	Thermal Vacuum/Thermal Balance
UV	Ultraviolet
WP	Waypoint
WSB	Weak Stability Boundary
XEUS	X-ray Evolving-Universe Spectroscopy

APPENDIX A: Reduced science option (XEUS 1)

Introduction and objectives

Introduction

The initial feasibility study for the XEUS mission using the ESA Concurrent Design Facility was requested by ESA/ESTEC/SCI-A in early 2004. The study began with a kick-off on 26th May 2004 and finished with an Internal Final Presentation on 18th June 2004. It consisted of eight technical half-day sessions of the interdisciplinary study team. For this initial study, Soyuz-Fregat launches from Kourou were requested (MSC and DSC launched separately into L2) and optimistic mirror mass assumptions were provided. The CDF team presented a viable solution for this scenario of which a summary is given in this Appendix.

Although the study was performed in the same depth as done for XEUS part 2, only an executive summary is reported here. If needed, more details can be requested from the CDF database via the XEUS study manager.

Objectives of XEUS 1

The objective of XEUS part 1 was to perform a feasibility study for the XEUS mission by using a “design-to-mass/volume” approach compatible with Soyuz-Fregat launches from Kourou and L2 as final orbit.

The demonstration of feasibility shall be reported by presenting the:

- Proposed mission architecture (DSC and MSC)
- System and subsystem conceptual design for the MSC
- Proposal for the mirror petal accommodation
- Optimal MSC spacecraft configuration
- Formation flying package (accommodation on DSC and MSC)
- Technical risk assessment
- Programmatics
- Costing

The baseline science mission objectives for XEUS 1 were the same as presented in detail for the XEUS part 2 report and concentrated mainly on the:

- Detection of massive black holes in earliest active galaxy nuclei
- Study of the formation of first gravitationally bound
- Study of evolution of metal synthesis
- Characterisation of intergalactic medium

The proposed payload consists of three X-ray primary imaging spectrometers on the DSC (for more information, see XEUS Payload Definition Document):

- WFI (Wide Field Imager)
- NFI2 (Narrow Field Imager 2)
- NFI1 (Narrow Field Imager 1) for low energy range

System requirements and design drivers

System requirements

- The system comprises two spacecraft flying in formation at L2:
  - Mirror spacecraft – MSC (Provided by ESA)
  - Detector spacecraft – DSC (JAXA design considered for this study)
  - DSC to be considered as "black box" based on JAXA configuration input (1753 kg with baseline instrument package)
  - MSC – DSC separation distance nominal 50 m (option 25 m, 75 m, 100 m)
  - MSC life time: 15 years + 5 years extension
  - DSC life time: ~5 years (replaceable at EOL and/or if more sophisticated detectors become available)
- Launch:
  - Launch date: 2015
  - MSC and DSC to be launched separately from Kourou
  - Launcher: Preferably Soyuz Fregat
- Operational orbit: L2
- Typical observation periods: 3×10^5 s (about 3.5 days)

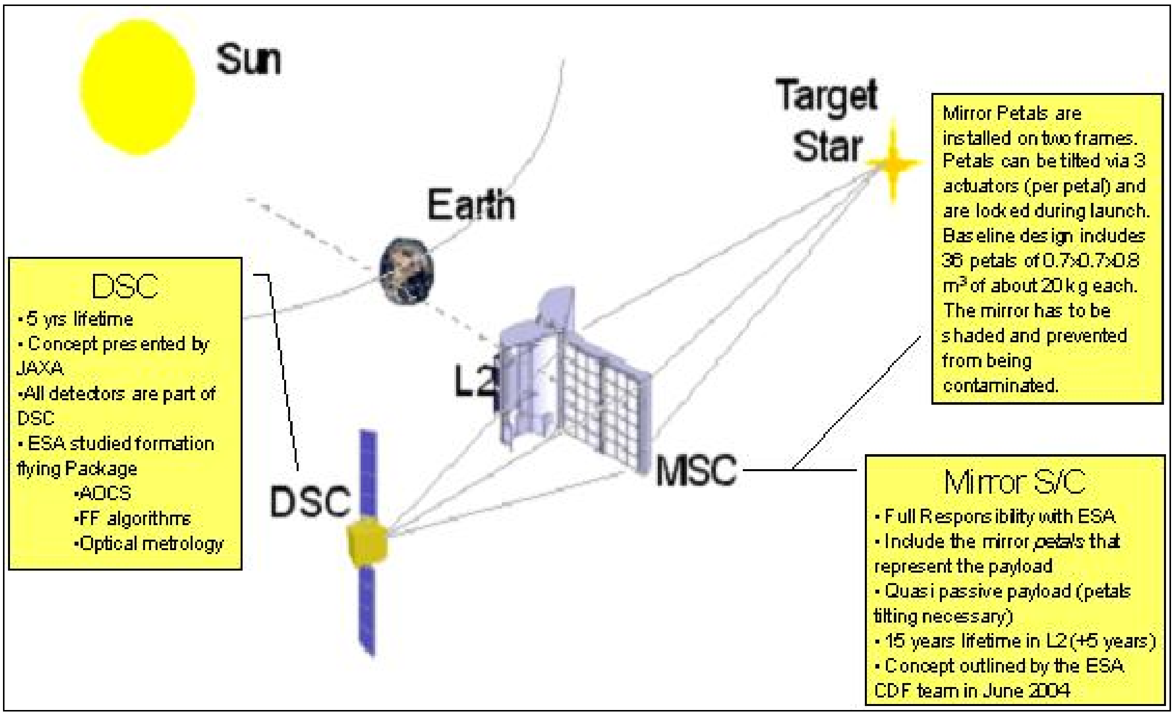

Figure A-1: Elements overview of the XEUS mission

Design drivers

The CDF study identified the following major design drivers for the mission:

- Formation Flying & Rendezvous:
    - Major issue for DSC AOCS: required relative range error during nominal formation keeping imposes autonomous control system
    - Ranging accuracy from ground segment → operations & rendezvous strategies
- MSC lifetime:
    - Imposes very low consumables, simple and reliable design for the SVM of MSC
- Launch vehicle and injection strategy:
    - Drives the maximum launch mass (effective available mirror surface), cost, programmatic
- Mirror petals:
    - Average petal mass of 40 kg/m^2 (applicable or all MSC-DSC separation distances)
    - Require a large number of actuators on MSC + optical detection system to compensate for initial mirror misalignment
    - Petals require locking during launch
- Temperature gradients in mirror plane:
    - Direct impact on MSC configuration.
- Temperature gradients within mirror petals in optical axis:
    - Off normal Sun angle to be limited to ± about 5°
- Mirror contamination prevention:
    - Specific strategies to avoid contamination. Stay in launch configuration (BBQ mode) until outgassing procedure is executed and completed
    - Configuration: Protect mirror during outgassing, protect from exhaust-plume impingement on mirror surface
    - Propulsion: choice of non-contaminating propellant. Hydrazine used during cruise and could be burnt off if necessary. Cold gas used for AOCS manoeuvres

MSC design summary

MSC requirements

From the system objectives and requirements a set of requirements was derived for the mirror spacecraft. They are as follows. The global MSC configuration is given in Figure A-2.

- Lifetime = 15 years+ 5 years extension
- No formation keeping (only target acquisition, orbit correction & maintenance)
- Three-axis stabilised (canister halves are Sun pointing)
- Payload: matrix of petals that constitute the mirror (≈700 kg)
- Mirror petals shall be kept clean from contamination
- The misalignment of the petals shall be corrected to 1 arcsec accuracy (1- 4 μm)
- Pointing accuracy toward target: 15 arcsec (half cone) during the observation time (Typical observation periods: $3x10^5$ s)

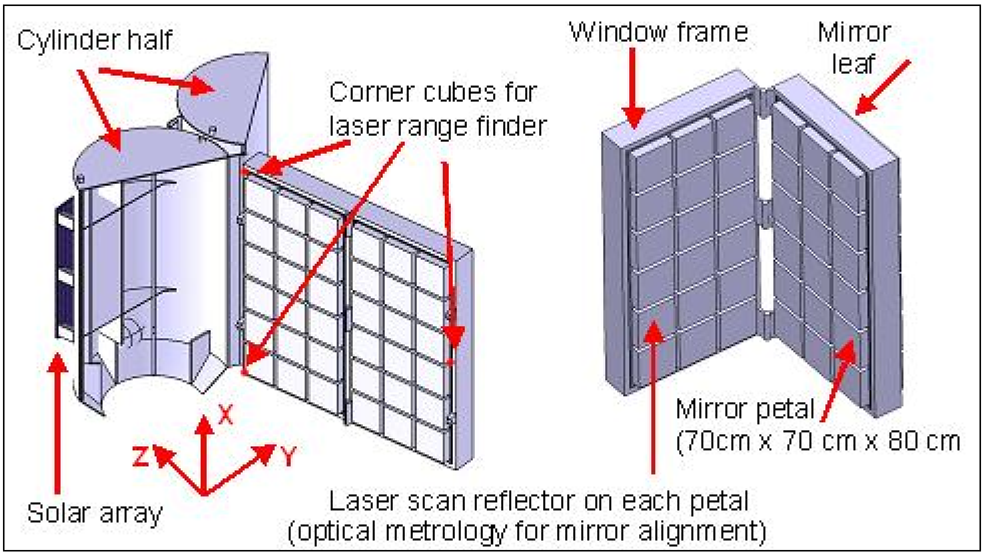

Figure A-2: MSC configuration

DSC requirements

No system requirements were derived for the detector spacecraft. However as both spacecraft have to fly in formation, formation flying-related requirements on the DSC have been derived:

- Lifetime: five years lifetime + 2 years extension
- The DSC performs the initial formation set-up, the formation keeping and reorientation (as flyer, chaser spacecraft)
- The DSC attitude pointing accuracy shall be maximum 1 arcsec (half cone) during the observation time

XEUS telescope requirements

The telescope requirements were found to be the following:

- Pointing direction = centre of detector to centre of optics
- The DSC – MSC distance shall be at 50 m (baseline), 25 m, 75 m, or 100 m as options: The four cases shall be studied and the system impact of changing the inter-satellite distance shall be assessed
- Mainly affected by DSC to MSC position error: +/-1 mm max (allowed formation flying error sideways to optical axis)
- Focal depth is +/-5 mm (allowed formation flying error along optical axis)

Launcher trade-offs

Four launcher options were evaluated:

1. "Soyuz-direct": a Soyuz-Fregat launches the MSC directly to L2; the DSC is to be launched after the MSC
2. "Soyuz-HEO": a Soyuz-Fregat launches the MSC into a Highly Elliptical Orbit (HEO). The MSC then uses its own propulsion module for the HEO to L2 transfer. The DSC is to be launched after the MSC

3. "Ariane-dedicated": both MSC & DSC are launched as a stack using a dedicated Ariane-5 directly to L2; upon arrival at L2 the two spacecraft undock
4. "Ariane-shared": both MSC & DSC are launched as a stack using an Ariane-5 (shared with another passenger) into the Geostationary Transfer Orbit (GTO). A propulsion system is used to escape from GTO to L2, using a transfer via L1; upon arrival at L2 the two spacecraft undock

The four options are traded off, as shown in Table A-1:

Trade-key:	A	Launcher trade-off											
System Option:		1			2			3			4		
Name		Soyuz-direct			Soyuz-HEO			Ariane-dedicated			Ariane-shared		
Notes													
Parameter	Weights	Option	Ranking	Value	Option	Ranking	Value	Option	Ranking	Value	Option	Ranking	Value
Launch costs	3.00		+	12.00		+	12.00		0	9.00		+	12.00
MSC wet mass	1.00	2050	-	2.00	3014	0	3.00	<7000	++	5.00	3000	0	3.00
DSC wet mass	0.50	2050	0	1.50	2050	0	1.50	<7000-MSC	0	1.50	2050	0	1.50
launch cost uncertaincy	1.00	30%	0	3.00	30%	0	3.00	10%	+	4.00	10%	+	4.00
Volume	1.00		0	3.00		0	3.00		++	5.00		--	1.00
Rendezvous	1.00	yes	-	2.00	yes	-	2.00	no	0	3.00	no	-	2.00
Propulsion system	1.00	No	0	3.00	Yes	-	2.00	No	0	3.00	No	0	3.00
Constraints on DSC	1.00	DSC 1/2 y later	0	3.00	DSC 1/2 y later	0	3.00	DSC+MSC same time	0	3.00	DSC+MSC same time Launch with co-passenger	--	1.00
Trajectory	1.00	Direct to L2	0	3.00	HEO	-	2.00	Direct to L2	0	3.00	L1->L2	--	1.00
Total Score:				32.5			31.5			36.5			28.5

Table A-1: System trade-off table

The conclusions from the trade-off are as follows. The decision which options to select as baseline and which options to study were not based on a score.

System option 1 was selected as baseline for the study, as it showed many technical, programmatic and cost advantages as well as independence in terms of launch and design for the MSC. The baseline is therefore a direct injection of the MSC into the L2 halo transfer orbit. System option 2 was selected as the option to be studied apart from the baseline; this option is different from the baseline in terms of a to-be-added propulsion system transfer from a HEO to the L2 halo transfer orbit. The baseline was chosen such that adding a large propulsion model has a relatively small effect. System option 3 was selected as the second option to be studied but in less detail, as the impact on the design is considered small.

System option 4 shows that the Ariane shared option (option 4) has more negative aspects than the other options. In particular, given the complicated and long transfer orbit, and constraints on programmatics in terms of delivering three spacecraft to Arianespace at the same time (MSC, DSC and the co-passenger), the study team decided not to study option 4.

MSC baseline design

The baseline design features a MSC launched in 2015, using a direct injection to L2. The DSC is launched later to join the MSC. Except for the cold gas system, the MSC is using only standard off-the shelf equipment for its bus design. All units are located in/on the two cylinder halves of the MSC. The MSC configuration and dimensions are shown in Figure A-3:

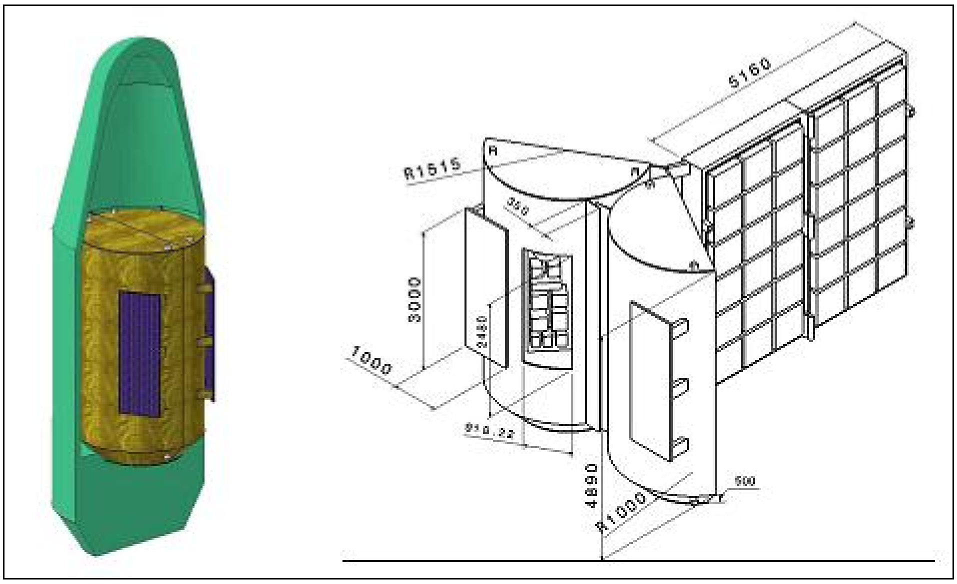

Figure A-3: XEUS launch configuration and MSC dimensions

Special strategies mission strategies and the usage of two different propulsion systems have been defined to prevent petal contamination:

- A BBQ mode is used during initialisation, and monopropellant (hydrazine) thrusters are used only in stowed configuration.
- Launcher dispersion and trajectory corrections of ~30 m/s are performed by hydrazine engines. The last manoeuvre is after about 50 days. For attitude corrections, cold gas thrusters are used for the remaining part of the cruise phase (when mirror is deployed)
- At L2, only the cold gas propulsion system is used
- Thruster orientation was chosen to minimise the effect of plume impingement on mirror petal baffles during orbit maintenance and attitude control.
- Reaction wheels are used for slew manoeuvres to acquire new targets
- Relative drift compensation between MSC and DSC is executed by the DSC only

Table A-2 shows an overview of the MSC modes of operations:

Number	Mode Name	Definition
1	Launch Mode	*Lift off to separation* - All subsys are off except for essential equipment Battery fully charged
2	Initialisation Mode	*Trajectory insertion* An automatic switch is used at separation to activate the equipment (incl. Transmitter) Coarse sun pointing provided by upper stage at separation Satellite capable of receiving and executing telecommands TT&C by LGA. Attitude acquisition in Sun Pointing Mode (SPM) Sun shield to be deployed, SA operational, and leaves unfold Launch dispertion correction and bbq mode
3	Cruise Mode	*Trajectory adjustment - up to L2 orbit "insertion"* Service Module Commissioning - all s/s in nominal working status Trajectory determinations and corrections Data communication S/C - Earth via LGA (via HGA if compatible with orbit / attitude) Power generation (SA; battery as backup) and distribution to all S/S with instruments in SAA TBD Mirror is stabilizing thermally
4	Stand By	*Stand By Mode - up to rendezvous with DSC* Mode similar to the cruise mode - the only difference is that the MSC is now in a halo orbi Orbit determinations and corrections Data communication S/C - Earth via LGA (via HGA if compatible with orbit / attitude) Power generation (SA; battery as backup) and distribution to all S/S with instruments in st
5	Rendezvous Mode	*Reduction of orbit dispersion* The MSC receives telemetry from GS with the location of the DSC Points -Y towards MSC with a constraint on SAA Communication between DSC and MSC established sequencies: 1) ground navigation 2) Local radio navigation - about 20 km distance **3) coarse optical navigation - 1 m from nominal DSC position** 4) Precision optical navigation - 1 mm from nominal DSC
6	Collision Avoidance Mode	*Collision Avoidance Mode* Emergency maneuver to get out of the way of the DSC if a threat is detected SAA maintained Telemetry downlink at "short" intervals ground station Attempt to keep communication with the DSC
7	Target Acquisiton Mode	*Maneuver to obtain a rigid body-like rotation with the MSC slew* The MSC receives an attitude profile from GS for the slew maneuver towards a new targe The MSC performs an open loop slew maneuver Setlling phase (cancelling rates) and switch to closed loop attitude lock
8	Nominal Observation Mode	*Science operations* Maintain the commanded attitude (counteract SRP torques, μmet impacts) Time tag attitude data for post-processing
9	Safe Mode	*Hibernation and Failure Recovery mode:* The spacecraft is kept SUN pointing. Accuracy determined by power system. Instruments are put on standby or switched off. Non-essential functions are halted. TM/TC access to DHS is guaranteed to enable failure detection and reconfiguration. TT&C by LGA. Failure detection and recovery are executed by the ground. *Emergency Sun Acquisition Maneuver*

Table A-2: MSC modes of operation

The DSC element has not been designed in this study. For the mission architecture and formation flying package design, the baseline design suggested by JAXA has been adopted (see RD[7]and Figure A-4).

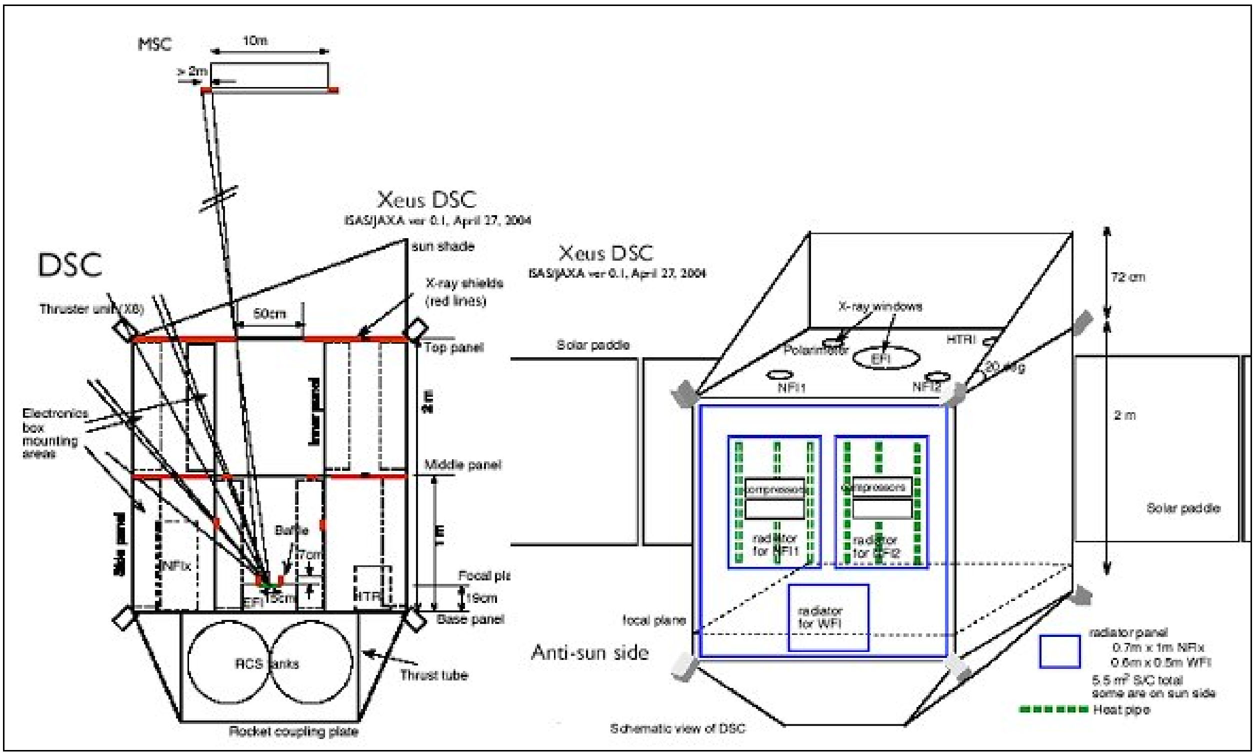

Figure A-4: DSC system overview

Schematic mission summary

A schematic mission summary of the XEUS mission and the MSC's main characteristics are presented hereafter.

Scientific objectives

- Detection of massive black holes in earliest active galaxy nuclei
- Study of the formation of first gravitationally bound
- Study of evolution of metal synthesis
- Characterisation of intergalactic medium

Payload

- MSC:
    - Two deployable mirror leaves with in total six by six segments of which all 64 are populated with mirror petals.
    - Petal dimension: length 70 cm, width 70 cm, height 80 cm
    - Average petal mass: 40 kg/m2
- DSC:
    - WFI (Wide Field Imager)
    - NFI2 (Narrow Field Imager 2)
    - NFI1 (Narrow Field Imager 1) for low energy range (0.1 – 2 keV)

Launcher

- MSC:
  - Soyuz-Fregat version 2B, ST fairing
  - Direct injection into L2 (2080 kg launch mass, including adapter)
  - Directly mounted on the eight available hard points (∅ 2000 mm) on the Fregat upper stage
- DSC:
  - Soyuz-Fregat version 2B
  - Injection into L2 via two intermediate HEO orbits (apogee 40 000 km and 90 000 km) or via L1 (Weak Stability Boundary travel trajectory)

Mirror spacecraft

- MSC nominal mission: 15 yrs, extended mission up to 20 yrs (Note that the DSC is expected to be designed for 5 years and planned to be replaced when required)
- Main spacecraft bus: Round cylinder 3030 mm x 4890 mm (stowed configuration).
- Dry mass = 1733 kg. Propellant mass 110 kg.
- System mass margin: 16%
- Three-axis stabilised with cylinder Sun pointing (cold gas system to prevent mirror contamination)
- Reaction wheels for re-pointing to acquire new target
- No formation keeping (only orbit correction & maintenance)
- Payload: Matrix of petals that constitute the mirror (~700 kg)
- Absolute point error 1 arcminute (X & Y-axes), 1 arcminute on Z-axis
- Absolute measurement error 1 arcsecond (X & Y-axes), 300 arcseconds on Z-axis
- Two body mounted solar arrays of in total 5.3 m^2 using triple junction cells with 28% BOL efficiency
- Two switchable X-band LGAs, omni coverage
- S-band inter S/C RF link
- Greater than 72 hrs full autonomy

Cruise phase and XEUS deployment

- Duration: 90 to 160 days
- Direct injection:
  - Launcher’s dispersion correction required, $\Delta V < 25$ m/s, to be performed with AOCS not later than 2 days after injection
  - Trimming manoeuvre: < 2 m/s at day 10
  - Mid-course manoeuvre: < 1 m/s at day 50
  - MSC - DSC separation after day 50
  - No ΔV required for L2 halo orbit insertion
- The proposed XEUS deployment scenario is as follows:
  - During the initial part of the cruise phase MSC remains in launch configuration and is spin stabilised (hydrazine thrusters)
  - MSC commissioning commences after stack separation and could be completed prior to target orbit (L2) being reached

Nominal Mission Phase

- Duration: 15 + 5 years extension
- Final orbit; L2 halo orbit:
  - No eclipses
  - Amplitude: > 670 000 km
  - Orbit period: 6 months
  - No insertion ΔV when using optimal transfer trajectory
  - Quasi-periodic: Every 20 days, small orbit maintenance manoeuvres needed (~ 5 cm/s)
  - Orbit maintenance budget: 1-2 m/s per year
  - Typical observation time: $3x10^5$ s (about 3.5 days)

Formation Flying Package

- Formation set-up and precision formation flying control performed by the DSC (MSC is free-flyer, DSC is follower). The same applies when slewing to a new target.
  - Both S/C move in purely inertial space
  - Both S/C perform absolute pointing control
  - Only the DSC performs relative distance control (including relative drift compensation)
  - DSC – MSC distance during science operations shall be 50 m
  - Allowed formation flying error along optical axis: +/- 5 mm
  - Allowed formation flying error sideways to optical axis: +/- 1 mm
- Metrology approach:
  - Inter S/C distance >10 km: Range and Doppler measurements from Ground station
    - Precision: Position error 400 m – 4.5 km,
Velocity error 2.35 mm/s – 6.8 mm/s
  - Six LGA antennas on MSC, six on DSC
  - Inter S/C distance <30 km: RF metrology (S-band)
    - Precision at 120 m: Elevation: ±12 cm, Azimuth: ± 6 cm, Range: ± 0.52cm
    - Six LGA antennas on MSC, six on DSC
  - Inter S/C distance <120 m: optical metrology
    - Three corner cube reflectors on MSC mirror
    - Laser rangefinder with absolute distance meter (submillimetric accuracy) on DSC
    - Dual λ interferometer (±3 µm range resolution)
    - Nine optical heads, max. ~2.5 m baseline:
    - Pulses sequenced to each head
    - Multilateration
  - Inter spacecraft link (S-band) allows data transfer (housekeeping) in the event of one of the two spacecraft losing communication with ground segment

Operations

- Only MSC housekeeping (per day: 0.3 hrs at 95 kbps)
- LEOP performed by ESA LEOP network stations Kourou, Vilspa and Perth/New Norcia

- Routine operations using the Perth 35-m ground station linked to XEUS mission control centre (or 2 hours down link for a 15-m antenna at 16 kbps)
- For initial MSC - DSC formation set up:
  - One ground station tracking
  - Range and Doppler measurements:
    - Range: Two measurements per pass
    - Doppler: One measurement per 10 minutes (measurements taken during 3-hour tracking pass)

Programmatics

- Model philosophy: STM, ATB & PFM.
- System Simulation Facility
- Formation flying test bed

Budgets

The mass budget for the MSC baseline design is shown in Table A-3. The instrument mass is based on a mirror surface area of 17.6 m^2 (36 petals of 70 cm x 70 cm) with a density of 40 kg/m^2, leading to 705 kg. No adapter is used; the cylinder is attached directly to launcher hard points.

Mirror S/C				
	Target Spacecraft Mass at Launch			2080.00
	Without Margin	Margin		Total
Dry mass contributions		%	kg	kg
Structure	531.32 kg	10.00	53.13	584.45
Thermal Control	33.70 kg	5.00	1.69	35.39
Mechanisms	88.64 kg	16.05	14.23	102.87
Pyrotechnics	5.00 kg	5.00	0.25	5.25
Communications	18.20 kg	10.44	1.90	20.10
Data Handling	9.30 kg	20.00	1.86	11.16
AOCS	35.19 kg	5.43	1.91	37.10
Propulsion	113.70 kg	5.74	6.53	120.23
Power	42.34 kg	10.00	4.23	46.57
Harness	63.00 kg	0.00	0.00	63.00
Instruments	705.00 kg	0.00	0.00	705.00
Optics	1.80 kg	5.00	0.09	1.89
Total Dry	1647.18			1733.00
System margin		13.69	%	237.29
Total Dry with margin				1970.28
Propellant	109.72 kg	0.00	0.00	109.72
Launch mass				2080.00

Table A-3: XEUS MSC mass summary

The overview shows a reduced MSC dry mass margin (14%) with respect to the system margins normally applied at pre-assessment level (20%). The main contributors to the dry mass are structures, mechanisms, instruments and propulsion.

The power budgets are shown in Table A-4:

		hermal	AOCS	Comms	Propulsion	DHS	Mech	harness (excl.	TOTAL CONSUMPTION
Launch Mode	Pon	90 W	5 W	99 W	5 W	30 W	0 W	5 W	234 W
	Pstdby	0 W	0 W	22 W	0 W	30 W	0 W	1 W	53 W
Eclipse Mode	Duty Cycle	100 %	100 %	4 %	100 %	0 %	0 %		58%
Tref 150 min	Total Wh	225 Wh	13 Wh	62 Wh	13 Wh	75 Wh	0 Wh	8 Wh	395 Wh
Cruise Mode	Pon	75 W	5 W	99 W	5 W	30 W	0 W	4 W	218 W
	Pstdby	0 W	0 W	22 W	0 W	30 W	0 W	1 W	53 W
	Duty Cycle	100 %	100 %	4 %	100 %	0 %	0 %		54%
Tref 60 min	Total Wh	75 Wh	5 Wh	25 Wh	5 Wh	30 Wh	0 Wh	3 Wh	143 Wh
Target Acquisiton Mode	Pon	45 W	50 W	69 W	5 W	30 W	0 W	4 W	223 W
	Pstdby	0 W	0 W	22 W	0 W	30 W	0 W	1 W	53 W
	Duty Cycle	100 %	100 %	16 %	100 %	0 %	0 %		66%
Tref 60 min	Total Wh	45 Wh	50 Wh	33 Wh	5 Wh	30 Wh	0 Wh	3 Wh	166 Wh
Nominal Observation Mode	Pon	45 W	15 W	69 W	5 W	30 W	0 W	4 W	188 W
	Pstdby	0 W	0 W	22 W	0 W	30 W	0 W	1 W	53 W
	Duty Cycle	100 %	100 %	16 %	100 %	0 %	0 %		58%
Tref 60 min	Total Wh	45 Wh	15 Wh	33 Wh	5 Wh	30 Wh	0 Wh	3 Wh	131 Wh
Safe Mode	Pon	45 W	15 W	69 W	5 W	30 W	0 W	4 W	168 W
	Pstdby	0 W	0 W	22 W	0 W	30 W	0 W	1 W	53 W
	Duty Cycle	100 %	100 %	16 %	100 %	0 %	0 %		58%
Tref 60 min	Total Wh	45 Wh	15 Wh	33 Wh	5 Wh	30 Wh	0 Wh	3 Wh	131 Wh

Table A-4: XEUS MSC power budget

More details on the mass distribution are shown in Table A-5 (MSC) and Table A-6 (DSC). The latter table lists only the equipment related to formation flying.

Element 1 - Mirror S/C						
FUNCTIONAL SUBSYSTEM	nr	Mass (kg) per unit	Total Mass (kg)	Margin (%)	Margin (kg)	Mass (kg) with Margin
Structure			**531.32**	**10.00**	**53.13**	**584.45**
Cylinder	1	178.24	178.24	10.00	17.82	196.07
Bottom cone	1	37.96	37.96	10.00	3.80	41.75
Closure bottom plate	1	18.14	18.14	10.00	1.81	19.96
Closure top plate	1	24.05	24.05	10.00	2.41	26.46
Mid shear wall	2	11.91	23.82	10.00	2.38	26.20
Outer frame	1	49.39	49.39	10.00	4.94	54.33
Inner frame	1	131.16	131.16	10.00	13.12	144.28
Horizontal plate	4	4.69	18.75	10.00	1.87	20.62
Small shear wall	4	5.10	20.39	10.00	2.04	22.43
Bottom cone stiffener	8	1.55	12.38	10.00	1.24	13.62
Equipment wall	2	8.51	17.02	10.00	1.70	18.73
Thermal Control			**33.70**	**5.00**	**1.69**	**35.39**
MLI	1	27.70	27.70	5.00	1.39	29.09
Heaters and related equipment	1	6.00	6.00	5.00	0.30	6.30
Mechanisms			**88.64**	**16.05**	**14.23**	**102.87**
Paddle Actuators	108	0.20	21.60	20.00	4.32	25.92
Actuator Locking Mechanisms	108	0.13	14.04	20.00	2.81	16.85
Frame deployment active hinge	1	5.00	5.00	10.00	0.50	5.50
Frame deployment passive hinge	1	2.50	2.50	10.00	0.25	2.75
Frame latches	4	1.00	4.00	10.00	0.40	4.40
Frame HRM	6	1.50	9.00	20.00	1.80	10.80
Shell deployment active hinge	1	5.00	5.00	10.00	0.50	5.50
Shell deployment passive hinge	1	2.50	2.50	10.00	0.25	2.75
Shell latches	4	1.00	4.00	10.00	0.40	4.40
Shell HRM	6	1.50	9.00	20.00	1.80	10.80
S/C Separation	8	1.50	12.00	10.00	1.20	13.20
Pyrotechnics			**5.00**	**5.00**	**0.25**	**5.25**
Communications			**18.20**	**10.44**	**1.90**	**20.10**
LGA	3	0.10	0.30	10.00	0.03	0.33
X-band transponder	2	3.50	7.00	10.00	0.70	7.70
X-band SSPA	2	1.30	2.60	5.00	0.13	2.73
X-band RFDU	1	1.50	1.50	10.00	0.15	1.65
S-band transponder-radar	2	1.50	3.00	20.00	0.60	3.60
S-band omni antenna	9	0.20	1.80	5.00	0.09	1.89
S-band RFDU	1	2.00	2.00	10.00	0.20	2.20
Data Handling			**9.30**	**20.00**	**1.86**	**11.16**
CDMU (proc+TM/TC+MM)	1	5.50	5.50	20.00	1.10	6.60
bus I/F	9	0.20	1.80	20.00	0.36	2.16
command matrix unit	1	2.00	2.00	20.00	0.40	2.40
AOCS			**35.19**	**5.43**	**1.91**	**37.10**
Star tracker (Jena Optronik)	2	4.30	8.60	5.00	0.43	9.03
Gyros (Systron Donner)	4	0.06	0.24	5.00	0.01	0.25
Reaction wheels (Honeywell)	4	6.00	24.00	5.00	1.20	25.20
Optical metrology	1	1.00	1.00	20.00	0.20	1.20
Fine sun sensor (Jena Optronik)	2	0.62	1.24	5.00	0.06	1.30
Medium sun sensor (Aero Astro)	3	0.04	0.11	5.00	0.01	0.11
Propulsion			**113.70**	**5.74**	**6.53**	**120.23**
Tank (N2H4)	1	1.50	1.50	5.00	0.08	1.58
Filter (N2H4)	2	0.30	0.60	5.00	0.03	0.63
Latch Valve (N2H4)	6	0.50	3.00	5.00	0.15	3.15
Thruster (N2H4)	12	0.30	3.60	5.00	0.18	3.78
Piping (N2H4)	1	4.00	4.00	5.00	0.20	4.20
Tank (N2)	1	85.00	85.00	5.00	4.25	89.25
Pyro Valve (N2)	4	0.50	2.00	5.00	0.10	2.10
Thruster (N2)	12	0.30	3.60	20.00	0.72	4.32
FCV (N2)	12	0.30	3.60	5.00	0.18	3.78
Piping (N2)	1	4.00	4.00	5.00	0.20	4.20
HP regulator (N2)	1	0.50	0.50	20.00	0.10	0.60
LP regulator (N2)	3	0.50	1.50	20.00	0.30	1.80
Pressure transducers (N2)	4	0.20	0.80	5.00	0.04	0.84
Power			**42.34**	**10.00**	**4.23**	**46.57**
Battery LiIon	1	10.81	10.81	10.00	1.08	11.89
PCDU	1	13.33	13.33	10.00	1.33	14.66
Solar Panel	2	9.10	18.20	10.00	1.82	20.02
Harness			**63.00**	**0.00**	**0.00**	**63.00**

Table A-5: Equipment list (MSC)

Element 2 - Detector S/C						
FUNCTIONAL SUBSYSTEM	nr	Mass (kg) per unit	Total Mass (kg)	Margin (%)	Margin (kg)	Mass (kg) with Margin
AOCS			**32.09**	**9.85**	**3.16**	**35.25**
Star tracker (Jena Optronik)	2	4.30	8.60	10.00	0.86	9.46
Gyros (Systron Donner)	4	0.06	0.24	5.00	0.01	0.25
Reaction wheels (Honeywell)	4	3.60	14.40	5.00	0.72	15.12
Optical metrology	1	7.50	7.50	20.00	1.50	9.00
Sun sensor (Jena Optronik)	2	0.62	1.24	5.00	0.06	1.30
Medium sun sensr (AeroAstro)	3	0.04	0.11	5.00	0.01	0.11
Optics			**4.00**	**10.00**	**0.40**	**4.40**
Tilt measurement system	2	2.00	4.00	10.00	0.40	4.40

Table A-6: Equipment list (DSC formation flying)

Options

Option 1: injection via HEO to L2

The major differences with respect to the baseline are:

- Mission: to reduce gravity losses a two-HEO-step injection is used, first the orbit is raised from 180x40 000 km to 180x90 000 km. Then, the injection to the L2 transfer orbit takes place.
- Propulsion: the escape from HEO requires a large propulsion module (700 m/s with bipropellant main engine) – cold gas thrusters are still used for the remaining part of the mission (no hydrazine)
- Structure: adapted to carry the propulsion module

An updated MSC system mass budget is shown in Table A-7. The DSC has no change in mass with respect to the baseline.

Mirror S/C				
		Target Spacecraft Mass at Launch		2944.00
	Without Margin	Margin		Total
Dry mass contributions		%	kg	kg
Structure	578.31 kg	10.00	57.83	636.14
Thermal Control	33.70 kg	20.00	6.74	40.44
Mechanisms	88.64 kg	16.05	14.23	102.87
Pyrotechnics	5.00 kg	5.00	0.25	5.25
Communications	18.20 kg	10.44	1.90	20.10
Data Handling	9.30 kg	20.00	1.86	11.16
AOCS	35.19 kg	5.43	1.91	37.10
Propulsion	167.58 kg	5.50	9.22	176.79
Power	42.34 kg	10.00	4.23	46.57
Harness	63.00 kg	0.00	0.00	63.00
Instruments	705.00 kg	0.00	0.00	705.00
Optics	1.80 kg	5.00	0.09	1.89
Total Dry	1748.05			1846.31
System margin		14.24	%	262.85
Total Dry with margin				2109.16
Propellant	834.84 kg		0.00	834.84
Launch mass				2944.00

Table A-7: MSC system mass for the HEO option

Option 2: launch using an Ariane-5. Launch mass: 6800 kg

The major differences with respect to the baseline are:

- Detailed design not available
- Expected mass budget
- Detector spacecraft has heavier structure if below the MSC in the Ariane-5 fairing (1700 kg)
- Mirror spacecraft mass is considered as in the baseline (2050 kg)
- Mass for two interfaces (adapters) (200 kg)

In total, 1700+2050+200= 3950 kg

It was concluded that the Ariane-5 launch offers a huge mass margin (>3000 kg). A large part of this mass could be allocated to significantly increase the mirror surface (by a factor greater than 2).

Conclusions

The conclusions from the XEUS 1 feasibility study are summarised in this chapter. They have been organised in three categories:

General

Based on the specific boundary conditions (i.e. reduced science approach, optimistic mirror mass) the XEUS reduced science mission is judged to be feasible from technical, programmatic and cost points of view and no obvious "showstoppers" have been identified

The baseline architecture is based on a Soyuz 2.1b - Fregat launch from Kourou with direct injection into a L2 halo orbit:

- Allows a system margin on dry mass of about 13.7%
- Mirror area is 17.64 m^2 (36 petals of 70 cm x 70 cm)
- A single Soyuz-Fregat launch via a HEO orbit to L2 allows a system margin on dry mass of about 14.2%
- Option: A combined MSC-DSC launch with Ariane-5 offers a huge mass margin (>3000 kg) allowing for a significant increase in mirror area (factor 2 to 2.5) and would simplify the operations and formation set-up. An alternative launcher for a combined MSC/DSC launch is Delta IV-H offering even more alternatives.

For setting up the MSC-DSC formation, it is recommended to launch the MSC first and make the DSC the chaser:

- MSC is designed for 15 years lifetime (+ 5 years extension)
- For a realistic launch window, the DSC has to be either launched via an intermediate orbit (HEO) to L2 or via L1 on a weak stability boundary travel trajectory. The launch window for a direct injection would be limited to 1 day per 6 months

The proposed baseline design for the MSC and AOCS/formation flying package allows flying in formation with the DSC at variable separation distances of 25 m, 50 m, 75 m, or 100 m without any redesign.

Inter-spacecraft link (S-band) allows data transfer (housekeeping) in the event of one of the two spacecraft losing communication with ground segments.

None of the payload options, such as the 10 m or 50-m grating or High-Energy Telescope option, can be implemented in this Soyuz Fregat-based low science option.

Design related

The biggest challenge during the study was the mass/configuration constraints and minimisation of the temperature gradients and absolute mirror temperature. The results from the thermal analysis related to the mirror are:

- Passive mirror temperature control (due to large mirror area and its open structure)
- Temperature variation across mirror is 71.5°
- Actual lowest absolute temperature is –162°C

Note that for the XEUS 1 study the thermal trades for the MSC configuration and mirror thermal analysis were less sophisticated than those done for XEUS part 2, but sufficient to define future work related to this issue. The XEUS part 2 study was a first step in improving the understanding of this most important design driver for the MSC.

Critical areas

The following key critical areas require more detailed assessment:

- Mirror temperature distribution:
    - Although no specific mirror in-plane (longitudinal) and transversal (petal front front to rear) have been specified, it is recognised that the gradients are critical and should be minimised.
    - Based on the simplified thermal analysis performed during the CDF study, the mirror in-plane gradient of about 70°C might not be acceptable:
        - A detailed optical analysis is required to define the limits at mirror/petal level to optimise the MSC configuration
        - A detailed thermal model of the mirror petals is required
        - To reliably predict the temperature distribution of the MSC mirror/petals a detailed trade-off and thermal analysis is required to optimise the MSC cylinder configuration and thermal subsystem
    - Alternative MSC configuration were outlined that have the potential to further reduce the mirror gradients (a maximum gradient of about 40°C seems to be achievable)
- Given the expected mirror petal mass of 40 kg/m^2, the maximum mirror size to be launched into L2 via a direction injection is 17.64 m^2 (36 petals of 70 cm x 70 cm):
    - Any increase in petal mass density or total mirror size requires a launch via a HEO orbit requiring an additional propulsion stage on the MSC. The limits for the HEO option is:
        - A maximum mirror area (considering 40 kg/m^2) of 19 m^2 or
        - If the mirror mass is 43 kg/m^2 the maximum mirror area is 17.64 m^2
- Contamination of X-ray mirror:
    - Although it is expected that the proposed outgassing approach (BBQ mode) during the initial cruise phase or HEO (prior mirror deployment) is a credible solution for preventing a mirror contamination, a detailed investigation of this scenario and its effectiveness is essential
- For environmental reasons, the launcher performance might have to be reduced in the future by about 5% due to the possible implementation of a de-orbit kit on the upper stage

- Stray light analysis:
  - Stray light is recognised to be critical but no detailed analysis has been done during this study
  - Acceptable solutions exist but it is essential that a detailed stray light analysis is performed to confirm impacts
- Mirror petal:
  - As the largest single payload mass component, suitable investments into the mirror technology are essential to keep the mass under control
  - The proposed baseline considers that each mirror petal is equipped with three actuators to allow for a potentially required mirror alignment. However due to the limited information on the petal interface, the actuator concept and mirror petal locking during launch has to be revisited when more detailed information of the final petal design is available

The optical bench design and its behaviour during launch and in the space environment (such as moisture loss) might allow the omission of the petal actuation systems.